

INSTRUMENTATION REQUIREMENTS FOR DIFFERENT ACCELERATOR TYPES

B.J. Holzer, CERN, Geneva, Switzerland

Abstract

At present more than 15000 particle accelerators exist worldwide, being built and optimised to handle a large variety of particle beams for basic research and applications in industry and medicine. Diagnostic tools have been developed and optimised according to the special requirements of these machines and to meet the demands of their users. Storage rings for ultra cooled heavy ion beams, third generation synchrotrons for the production of high brilliant radiation, super conducting protons machines working at the energy frontier and finally linear electron accelerators for FEL applications or high energy physics are just the most prominent representatives of the large variety of accelerators. Each of them needs highly sophisticated tools to measure and optimise the corresponding beam parameters. Accordingly the issue addressed here is not to cover in full detail the different diagnostic devices but rather to concentrate on the aspects and needs as seen by the accelerator physicists and machine designers.

GENERAL CONTEMPLATIONS

The considerations presented here try to give a general overview about the needs in beam diagnostics for quite different machines. Clear enough there are beam parameter “standards” as orbits, beam intensity and lifetime that have to be measured, controlled and displayed in any machine. But given the large variety of accelerators optimised for different purposes there are also quite special needs and beyond the standards we will mostly outline the requirements of these beam parameters that need highly sophisticated measurements devices.

The spectrum of up to date accelerators covers a wide range: Proton or heavy ion storage rings running at the energy frontier as HERA, TEVATRON, RHIC and clear enough the LHC, and on the other side the low energy proton or heavy ion machines that are optimised for medical therapy. Then clear enough there are the special requirements of the electron machines that are optimised for synchrotron light production - be it as 3rd generation light sources or as FEL linacs. And in the end the planned high energy linear colliders that are not yet in their construction phase but already now set requirements for beam stability and control that have not been reached yet. These examples represent the extremes at least concerning the diagnostic tools that had to be established and we hope that talking about these, the large variety of accelerators that exist today like betatrons, cyclotrons, proton linacs are automatically included.

01 Overview and Commissioning

HIGH ENERGY PROTON MACHINES

The most prominent one today is clearly the Large Hadron Collider LHC [1] at CERN whose main parameters are listed in Table 1.



Figure 1: The LHC storage ring at CERN, Geneva.

Beam Parameters: The Standards

As in any (circular) accelerator the standard beam parameters that have to be measured are first of all the orbit and the tune in the two transverse planes. The requirements here differ not too much from other proton or heavy ion machines: beam sizes in the order of a millimetre or a certain fraction of it, and the usual golden rule to measure and control the orbit on the level of a tenth of the transverse beam dimension does not impose strong conditions on the beam position monitor system.

Table 1: LHC Main Parameters

LHC	
proton energy	7 TeV
particles per bunch	$1.2 \cdot 10^{11}$
number of bunches	2808
beam current	0.582 A
stored beam energy	362 MJ
beam size (arc)	1.2mm ... 0.3 mm
bunch length	8 cm

Figure 2 shows one of the very first LHC beam orbits that were obtained during the beam commissioning in 2008. Before correction, the proton orbit in LHC in both planes was in the order of 5-10 mm, still to high for intense beams and clearly beyond the level that is required for high energy operation. After a few correction cycles however the required level of 1-2 mm rms had already been obtained.

PERFORMANCE OF AND FIRST EXPERIENCES WITH THE LHC BEAM DIAGNOSTICS

O. R. Jones*, CERN, Geneva, Switzerland

Abstract

During the 2008 LHC injection synchronisation tests and the subsequent days with circulating beam, the majority of the LHC beam instrumentation systems were capable of measuring their first beam parameters [1]. This included the two large, distributed, beam position and beam loss systems, as well as the scintillating and OTR screen systems, the fast and DC beam current transformer systems, the tune measurement system and the wire scanner system. The fast timing system was also extensively used to synchronise most of this instrumentation. This presentation will comment on the results to date, some of the issues observed and what remains to be done for the next LHC run.

THE LHC BTV SYSTEM

There are a total of 37 TV beam observation systems (BTV) of 7 different types installed in the LHC. Each BTV station is equipped with two screens; a 1mm thick alumina plate (scintillator) and a 12 μ m thick titanium foil to produce Optical Transition Radiation OTR. The alumina plates are very sensitive and can observe single bunches of well below 10^9 particles, but due to their thickness significantly perturb the beam. The number of photons emitted by the OTR is much less than that of the alumina screen, on the other hand the perturbation to the beam is minimal allowing multiple monitors to be used at the same time as well as multi-turn observation.

First Results from the LHC BTV System

During commissioning the beam was initially steered through the transfer lines and different sections of the machine using the alumina screens, producing very clear but completely saturated images (See Fig. 1).

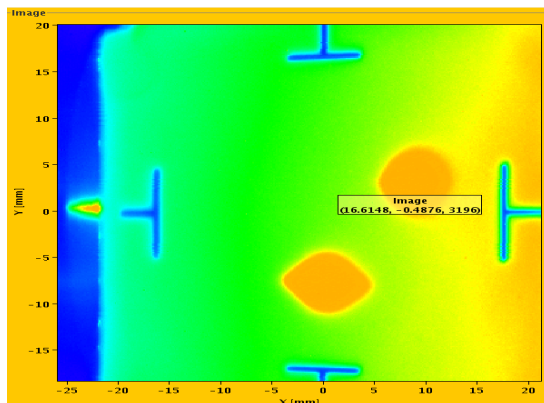


Figure 1 : The first full turn in the LHC as seen by the BTV system (10/9/2008).

After this first step the OTR screens replaced the alumina screens as they reduced the blow-up of the beam, reduced the radiation due to beam losses and produced images well suited for analysis with good linearity and no saturation. The possibility of observing OTR emission for even the lowest intensity pilot bunches (2×10^9 protons) was due to the high sensitivity of the standard CCD cameras.

The BTV monitors performed well and were extensively used during all the synchronization tests and for the first circulating beam in the LHC. They provided a quick, reliable tool for the operators in this initial commissioning phase.

Outlook for the LHC BTV System

Due to the expected radiation levels in the injection regions a gradual replacement of the standard CCD cameras with less sensitive radiation hard cameras is foreseen. This will result in losing the possibility to observe single pilot bunches in OTR mode.

THE LHC BLM SYSTEM

The purpose of the LHC BLM system is threefold: to protect the LHC equipment from damage; to avoid beam induced magnet quenches; to observe losses for machine parameter tuning such as the adjustment of collimators. The protection requirements led to the placement of detectors at all likely loss locations, resulting in over 4000 installed monitors mainly around the quadrupole magnets and in the collimator regions. These are either 1.5 litre N_2 filled ionisation chambers or 10cm long Secondary Emission Monitors (SEM). The signals of almost all monitors are compared with pre-defined threshold values which, if exceeded, result in a retraction of the beam permit signal and consequently a beam dump. The BLM monitor acquisition systems for both half sectors served by a given access point are concentrated on the surface, with a redundant link to the beam interlock system transmitting the beam permit signal to the dump system.

Early Performance of the LHC BLM System

Fig. 2 shows the readings of all ionisation chambers around the ring during single turn operation with Beam 1. The bias level of the acquisition is given by the current injected into each channel to continuously test their status. A variation in this test current can be seen for the individual channels as a result of different settings in the front-end electronics. This will have to be better adjusted in all front-end cards before the next running period. The large reading left of IP1 is due to the dump of the beam on the TCT collimator.

The signal to noise level can be better assessed if this bias current level is subtracted, giving a noise level two

*Rhodri.Jones@cern.ch

BEAM DIAGNOSTIC SYSTEM OF XFEL/SPring-8

H. Maesaka[#], S. Inoue, T. Ohshima, S. Matsubara, A. Higashiya, M. Yabashi, T. Shintake and Y. Otake,
RIKEN/SPring-8, 1-1-1, Kouto, Sayo, Hyogo, 679-5148, Japan
H. Ego, K. Yanagida and H. Tomizawa, JASRI/SPring-8, 1-1-1, Kouto, Sayo, Hyogo, 679-5198, Japan

Abstract

We present the design and the performance of the beam diagnostic system of XFEL/SPring-8. The XFEL facility requires sub- μm resolution beam position monitors (BPM), screen monitors with less than 10 μm resolution, high-speed beam-charge monitors and a temporal structure measurement system with less than 10 fs resolution. We developed an rf cavity BPM system that uses the TM110 mode at 4760 MHz. The estimated position resolution was 0.2 μm . For the screen monitor, we designed a custom lens system having 2.5 μm resolution and variable magnifications from 1 to 4. For the charge measurement, we developed a high-speed differential current transformer (CT). The rise time of the CT signal was 0.2 ns and common-mode noise was considerably reduced. To measure the temporal beam structure, we developed a C-band (5712 MHz) transverse deflecting cavity that has a disk-loaded backward traveling wave structure. This cavity can resolve a beam into a few fs fragments. Thus, the beam-diagnostic system satisfies the demands of the XFEL accelerator.

INTRODUCTION

An x-ray free-electron laser facility at SPring-8 (XFEL/SPring-8) [1] is under construction to generate coherent and extremely intense x-rays, where various new applications are expected in life sciences, material sciences, etc. The target wavelength is less than 0.1 nm. The XFEL light is generated by a self-amplified spontaneous emission (SASE) process.

A schematic layout of the XFEL facility is illustrated in Fig. 1. An electron beam with a normalized emittance of 0.6 π mm mrad is generated by a thermionic electron gun. The beam is accelerated to 8 GeV by the following series of rf accelerator cavities: 238 MHz pre-buncher, 476 MHz booster, L-band (1428 MHz), S-band (2856 MHz) and C-band (5712 MHz) accelerators. In the mean time, the bunch length is shortened from 1 ns to 30 fs by using a velocity bunching process of the sub-harmonic acceleration cavities and a bunch compression process of the three magnetic chicanes. Finally, the peak current becomes 3 kA without substantial emittance growth. The electron beam is finally fed into in-vacuum undulators, and an XFEL light is generated. The undulator period is 18 mm and the maximum K-value is 2.2.

In order to maintain the high gain SASE process at an x-ray wavelength, we need to monitor the beam position, the transverse beam profile, the beam charge, the beam arrival timing and the temporal bunch structure at each acceleration stage. The resolution of the beam-position

monitor in the undulator section is required to be less than 0.5 μm so as to maintain an overlap between the electron beam and radiated x-rays with 4 μm precision. The transverse beam profile should be measured with a spatial resolution of less than 10 μm . The required resolution of the temporal bunch structure is less than 10 fs.

In this paper, firstly we show an overview of the beam diagnostic system, and then we describe the design and the performance of each diagnostic device.

OVERVIEW OF THE BEAM DIAGNOSTIC SYSTEM

The diagnostic system of XFEL/SPring-8 [2,3] consists of high-resolution rf cavity beam position monitors (RF-BPM), precise screen monitors (SCM), high-speed differential current transformers (CT) and a transverse rf deflector system. The quantities of these monitors are summarized in Table 1, and are shown in Fig. 1. A detailed description of each monitor is given in the next section.

Table 1: Summary of the Number of Beam Monitors

	Number of Monitors
RF cavity BPM	56
Screen Monitor	43
Current Transformer	30
Transverse RF Deflector	1

DESIGN AND PERFORMANCE OF EACH DIAGNOSTIC DEVICE

RF Cavity BPM

Since the details of the RF-BPM are reported in Ref. [4], we summarize the performance of the RF-BPM. The RF-BPM cavity consists of two cylindrical cavity resonators: a TM110 dipole resonator for the position detection and a TM010 monopole resonator for the phase reference and the bunch charge measurement. We designed an RF-BPM cavity with a resonant frequency of 4760 MHz and a detection electronics equipped with an IQ (In-phase and Quadrature) demodulator. We tested the RF-BPM system in the SCSS test accelerator [5] with a 250 MeV electron beam and a 0.3 nC bunch charge. The position resolution was 0.2 μm and the beam arrival timing resolution of the TM010 cavity was 25 fs.

Screen Monitor

The transverse beam profile is monitored by a SCM. We use a fluorescent screen, such as Ce:YAG for a low-

[#]maesaka@spring8.or.jp

HIGHLIGHTS FROM BIW08

F. Sannibale, Lawrence Berkeley National Laboratory, Berkeley, CA 94720, U.S.A.

Abstract

The 13th edition of the Beam Instrumentation Workshop (BIW08) took place at the Granlibakken Conference Center on the beautiful shores of Lake Tahoe in California during the first week of May 2008. About 130 participants registered for the workshop. Included in the program during the three and a half days were three tutorials, eight invited and seven contributed oral presentations, and more than 50 poster contributions. A discussion group session and the vendor exhibition simultaneously held with the single day poster session, afforded many opportunities for informal discussion and idea exchange between attendees. During the workshop, the 2008 Faraday Cup Award that recognizes innovative achievements in beam diagnostics was also presented. In this talk, I will present the highlights from BIW08. The overall quality of the contributions was notably high, which made the selection of the topics for this talk quite difficult. Although I endeavoured to produce a balanced choice of highlights, the final list is surely incomplete due to time limitations of the talk, and also it unavoidably reflects my personal point of view and preferences.

INTRODUCTION

When the DIPAC09 Programme Committee proposed me to present a talk and write this contribution on the highlights of the 2008 edition of the Beam Instrumentation Workshop (BIW08), the first question I asked myself was: why a highlights talk?

Several answers came soon to my mind. First, it could be a good way to inform people in the community that did not attend BIW08 on what happened and on what interesting was presented during the workshop. Second, it could stimulate a tighter link between the two main international workshops on beam diagnostics and instrumentation that alternates every other year between Europe and USA. Last but not least (for me), the preparation of the talk and paper would give me a unique chance and opportunity to read and learn from the large number of contributions presented during the workshop.

So I decided to accept the challenge and soon started to work on it. Of course, as everything in this world, there are always drawbacks in every situation, and this one was not an exception. The quality of most of the contributions was significantly high and for obvious time and space limitations only a limited number of highlights could be picked. This made the selection process very difficult. Additionally, even for the selected contributions, only few slides and paragraphs could be used. The forced choice was to describe only general concepts without many details in the attempt of stimulating the reader interest and to refer to the BIW08 proceedings for deeper information.

The selection criteria used in the highlights choice included novelty, originality, broadness of interest, quality

of the work and so on. At the same time, when possible and reasonable, an attempt of spreading the choice over different fields, particle species, and geographical locations was done.

Unavoidably, personal interest and bias played a role in the selection as well, and I apologize in advance to the authors of those contributions that have been undeservedly excluded from this incomplete list of highlights.

OLD & NEW IN BIW08

With BIW08, the Beam Instrumentation workshop was at its 13th edition. The structure of the workshop gradually evolved over the years into the present shape that has been pretty much constant over the last editions. BIW08, during the three and half days included 3 tutorial talks, 8 invited and 7 contributed oral talks, plus two special talks. The single poster session included ~ 50 contributions and was held simultaneously with the vendor exhibition in order to facilitate informal discussion and information exchange. The workshop also included a more formal discussion session and the presentation of the 10th Faraday Cup Award, sponsored by Bergoz Instrumentation and assigned by the BIW Program Committee to the authors of innovative beam instrumentation [1].

BIW registered ~ 130 attendees and 9 vendor exhibitors and for the first time in this edition two new initiatives were introduced. Partial financial support for graduate and under-graduate students was offered, and the proceedings of the workshop were published on the JACoW open World Wide Web database [2]. With these initiatives, the BIW Program Committee tried to boost the interest to beam diagnostics in new generations of engineers and physicists, and to facilitate a free and wider diffusion of the workshop publications.

More information on BIW08 can be found elsewhere [3].

CONTRIBUTIONS HIGHLIGHTS

The selected highlights will be presented by loosely following the contribution category, starting with the Faraday Cup Award, going through tutorial, invited and oral contributions, and finishing with posters.

Faraday Cup Award

The 10th Faraday Cup Award was assigned to Suren Arutunian of the Yerevan Physics Institute of Armenia for the invention, construction and successful test of the diagnostic system "A Vibrating Wire Scanner" [4].

Figure 1 shows a 3D view of the core part of the instrument. A metallic wire is stretched through a region where the magnetic field due to a couple of permanent magnets situated on the wire support itself is present.

COMMISSIONING RESULTS OF BEAM DIAGNOSTICS FOR THE PETRA III LIGHT SOURCE

K. Balewski[#], G. Kube, K. Wittenburg, A. Brenger, H.-T. Duhme, V. Gharibyan, J. Klute, K. Knaack, I. Krouptchenkov, T. Lensch, J. Liebing, Re. Neumann, Ru. Neumann, G. Priebe, F. Schmidt-Föhre, H.-Ch. Schröder, R. Susen, S. Vilcins-Czvitkovits, M. Werner, Ch. Wiebers, Deutsches Elektronen Synchrotron DESY, Hamburg, Germany

Abstract

PETRA III is a new hard x-ray synchrotron radiation source which will be operated at 6 GeV with an extremely low horizontal emittance of 1 nmrad. This new facility is the result of a conversion of the existing storage ring PETRA II into a light source. The conversion comprises the complete rebuilding of one eighth of the 2304 m long storage ring, which will then house 14 undulator beam lines, the optical and experimental hutches, and the modernization and refurbishment of the remaining seven eighths. In addition two 100 m long damping wiggler sections have been installed which are required to achieve the small design emittance. Construction, installation and technical commissioning have been finished middle of March and then the commissioning with beam started. In this paper we present the results that have been achieved during commissioning with special emphasis on the role of diagnostic systems.

INTRODUCTION

At DESY the former storage ring PETRA II with a circumference of 2304 m has been converted into a dedicated light source PETRA III [1], [2]. This new source is a third generation, hard x-ray facility similar to APS, ESRF and SPRING8 and serves as a supplement to the X-FEL which will be build at DESY. The basic parameters are given in table 1.

Table 1: PETRA III parameters

Parameter	PETRA III	
Energy / GeV	6	
Circumference /m	2304	
Total current / mA	100	
Number of bunches	960	40
Lifetime / h	24	2
Emittance (horz. / vert.)/nm	1 / 0.01	
Number of insertion devices	14	

The emphasis of the conversion was on achieving a very small horizontal emittance and to solve the stability problems that are usually connected with high brightness beams.

The number of insertion devices is rather modest for a machine of this size but this due to the fact that the conversion should be cost effective.

PETRA II consisted of eight almost identical parts which are usually called octants. One of the octants has been completely removed and replaced by a new experimental hall of almost 300 m length and 30 m width (see Fig. 1).

Damping wiggler sections

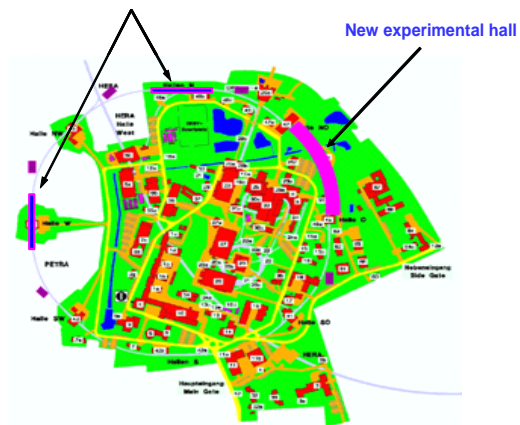


Figure 1: Ground Plan of the DESY site with the PETRA ring. The new experimental hall (purple) is situated between the PETRA halls North-East and East and the damping wiggler sections are in the North and West.

This new hall houses the experimental huts and supplies 9 straight sections in a DBA lattice to install insertion devices. The concept of canted undulators has been applied so that PETRA can be equipped with 14 undulators. Presently 3 two meter long undulators have been installed.

The geometry and the lattice of the remaining seven so called old octants have been kept. The existing hardware was reused if possible but refurbished and modernized to fulfil the high demands on reliability of a light source.

The emittance of the combination of the seven old octants and the new octant is roughly 4 nm rad, well above the design goal. Damping wigglers have been installed to enhance the radiation damping of the machine and thereby reduce the emittance to the required value [3]. These damping wigglers [4], [5] have been accommodated in the long straight sections in the North and West.

The conversion was finished middle of March and then the commissioning of PETRA III started.

[#]klaus.balewski@desy.de

SSRF BEAM DIAGNOSTICS SYSTEM COMMISSIONING*

Y.B. Leng[#], K.R. Ye, W.M. Zhou, Y.Z. Chen,
SSRF, SINAP, Jiading, Shanghai 201800, P.R. China

Abstract

SSRF is a 432 m-circumference synchrotron light source with a 150MeV linac, a 3.5GeV full energy booster, and a 3.5GeV storage ring. Principal diagnostics systems have been installed and nearly all have been commissioned during past two years. Data have been obtained on beam position, beam profile, current, and synchrotron radiation diagnostics beamline on the storage ring. Multi bunch transverse feedback system has been applied on the ring. Results for the 150MeV electron beams in the linac, up to 3.5GeV in the booster, and 3.5GeV in the ring will be presented.

INTRODUCTION

SSRF is a 3.5 GeV energy dedicated electron synchrotron radiation source. Recently the commissioning performance goals of the whole facility were met. Multi-bunch beam intensity of the ring has reached 200mA. At 200 mA, the lifetime is larger than 10 hour with all ID gaps closed. The commissioning process went very rapidly. Instrumentation played a critical role [1].

Table 1 shows the primary specification of the various diagnostics systems.

Table 1: SSRF Beam Instrumentation Specifications

Location	Measurement	Specification
Injector	Beam position	Resolution 100 μ m@1.67MHz
	Beam profile	Resolution 200 μ m@2Hz
	Bunch charge	Relative accuracy 2%
	Energy	Relative accuracy 0.1%
	Emittance	Relative accuracy 10%
	DC current	Resolution 50 μ A@10kHz
	Tune	Resolution 0.001@200Hz
Ring	Beam position	Resolution 10 μ m@694kHz Resolution 1 μ m@10Hz
	Beam profile	Resolution 10 μ m
	Beam length	Resolution 2ps
	DC current	Resolution 10 μ A@1Hz
	Tune	Resolution 0.0001

To meet above requirements a beam instrumentation system, consisting of 61 stripline BPMs, 152 button BPMs, 2 DCCTs, 11 Wall Current Monitors (WCM), 3 ICTs, 1 faraday cup, 18 screen monitors, 2 tune monitors,

3 transport line slits, 2 ring scrapers, 1 multi bunch feedback system and 1 dedicated diagnostics beam line, has been developed, implemented and commissioned during past 4 years.

The data acquisition system for beam instrumentation is designed on EPICS platform, which follows “standard model” architecture. Five kinds of IOCs were used in this system: VME bus IOC, Libera embedded IOC, PXI bus IOC, scope embedded IOCs, and soft IOC [2].

BEAM POSITION MONITORS

Position Measurement

Beam position monitor system fully equipped with Libera EBPM processors, which provides raw ADC data, turn by turn (694kHz @ ring, 1.67MHz @ booster) data, fast application (10kHz) data and close orbit (10Hz) data at the same time, is the most powerful tools during the commissioning and machine study of SSRF.

Beam position in the LINAC is calculated from raw ADC data of Libera. 40 μ m position resolution and 3pC bunch charge sensitivity have been reached during commissioning. Calibrated by ICT, the sum signal of BPM has been used to give a fast estimation of bunch charge and transport efficiency of LINAC during daily operation.

For the booster raw ADC data and turn by turn (1.67MHz) data are much useful than others. Synchronized by gun-shot trigger the raw ADC data could deliver first turn information. In this way 30 BPMs around the booster ring acted as beam arriving monitor to help operator tuning the machine to store injected beam during the day one commissioning. Decimated turn by turn data from all BPMs is used to present dynamic beam orbit during energy ramping.

For the Ring first turn information derived from raw ADC data help operator to determine beam loss location and tuning machine to store the first beam very quickly (few hours). SA data (10Hz), which position resolution reaches hundred nm level, resents precise closed orbit of the ring. Calibrated by DCCT the sum signal of SA data also could be used to present beam current and calculate beam lifetime. The beam spectrum (FFT of fast application data) is ideal tools to identify orbit noise source. With one million samples the frequency range of beam spectrum could cover from .1 Hz to 5 kHz. Current dependent instability has been observed with this tool. Global turn by turn capability and 3 μ m position resolution provides a powerful platform for accelerator physicists and operators to perform Response matrix measurement, Optics optimization, global and local phase advance measurement and phase space measurement.

*Work supported by Chinese Academy of Science

[#]leng@sinap.ac.cn

GLOBAL ORBIT FEEDBACK SYSTEMS DOWN TO DC USING FAST AND SLOW CORRECTORS

N. Hubert*, L. Cassinari, J-C. Denard, A. Nadji, L. Nadolski,
Synchrotron SOLEIL, Gif-sur-Yvette, France

Abstract

Beam orbit stability is a crucial parameter for 3rd generation light sources in order to achieve their optimum performance. Sub-micron stability is now a common requirement for vertical beam position. To reach such performance, Global Orbit Feedback Systems are mandatory. This paper describes the different design approaches for Global Orbit Feedback Systems. A few machines can use a single set of strong correctors. Most of them have their strong corrector bandwidth limited by eddy currents in aluminum vacuum chamber, or power-supply speed together with the required digitization granularity. Then, a second set of fast correctors is required for high frequency correction. But Fast and Slow Orbit Feedback Systems cannot work together with a common frequency range, they fight each other. An earlier solution has been to separate fast and slow systems by a frequency dead-band. This approach does not allow correcting efficiently the orbit shifts due to the gap movements of the increasingly sophisticated insertion devices that are installed on new machines. The different solutions that have been recently implemented are reviewed.

INTRODUCTION

Third generation light sources are built for producing high brilliance photon beams. Brilliance improvements have mainly been achieved by emittance reduction in both planes. The vertical emittance and beta functions define the beam size and divergence, which leads to the beam stability requirements. Commissioned in 1987, Super-ACO had a design vertical beam size of 230 μm in its straight sections. This parameter for NSLS II, to be commissioned in 2013, is $\sim 2 \mu\text{m}$, which is 100 times smaller. Position and angular stability requirements, usually one tenth the rms beam size σ_z and beam divergence σ'_z respectively, call for position stabilities of 20 μm for Super-ACO and 0.2 μm for NSLS II. Sub-micron stability is a formidable challenge that can only be achieved by implementing global orbit feedback systems. These systems are increasingly sophisticated in order to combine slow and fast corrections at the required speed and stability levels. Machines presently in operation with only a slow orbit feedback system should be able to profit at reasonable cost of the addition of a fast system using a set of cheap fast correctors that works together with the slow ones. The same scheme will also provide a cheaper solution to the new machines with very small beam sizes.

BEAM STABILITY REQUIREMENTS

For most beamlines, beam stability implies photon flux stability. They select the photon flux through a slit. The slit defines a beam size aperture for beamlines equipped with a focusing optics and an angular aperture for those equipped with a non-focusing optics. The flux variation is worse with smaller slits. Then the usual requirement $\Delta z/\sigma_z$ or $\Delta z'/\sigma'_z \leq 10\%$ leads to $\Delta I/I \leq 0.5\%$. Let's note that the photon beam size is diffraction limited and the beam divergence is that of the bending magnet or ID photon source; these effects convolved with the electron beam emittance gives the resulting photon beam an emittance larger than that of the electron beam, especially for low energy beamlines. However, for hard X-ray beamlines the electron beam dominates both beam size and divergence.

The effect of the beam position noise on the photon flux depends also on the integration time T_i of the experiment. The position noise components at frequencies higher than $1/T_i$ appear as an emittance growth, not as a photon flux fluctuation. Then the emittance ellipse ϵ_c describing the electron beam position and angle fluctuations can be added quadratically with the stable photon beam emittance ϵ_0 for obtaining an effective photon beam emittance ϵ_{eff} :

$$\epsilon_{\text{eff}}^2 = \epsilon_c^2 + \epsilon_0^2 \quad (1)$$

In this case, high frequencies instabilities do not really affect the stability of the photon flux; they only decrease its intensity in a stable way. One can consider as noise source only the part of the position spectrum that is at frequencies $F < 1/T_i$.

PERTURBATION SOURCES

To fulfil their tight stability requirements, great care is taken in the design and construction of the new machines. Nevertheless, there are still some remaining perturbations to be suppressed by global orbit feedback systems. Perturbation sources can be sorted in decreasing order of their time period [1].

Long Term

With time periods comprised between a few hours and a few minutes, air and cooling water temperatures are important [2]. Changes in air temperature affect the position of Beam Position Monitors (BPMs) and of magnets. In the first case, only the beam position readings are affected. In the latter one, there is an amplification of magnet movements on the beam orbit. Phenomena like sun and moon tides may have an impact of 10 to 30 μm .

*nicolas.hubert@synchrotron-soleil.fr

DIGITAL BPM SYSTEMS FOR HADRON ACCELERATORS*

J. Belleman[†], S. Bart-Pedersen, G. Kasrowicz, U. Raich, CERN, Geneva, Switzerland

Abstract

The CERN Proton Synchrotron has been fitted with a new trajectory measurement system (TMS) [2]. Analogue signals from forty beam position monitors are digitized at 125 MS/s, and then further treated entirely in the digital domain to derive the positions of all individual particle bunches on the fly. Large FPGAs handle all digital processing. The system fits in fourteen plug-in modules distributed over three half-width cPCI crates. Data are stored in circular buffers of large enough size to keep a few seconds-worth of position data. Multiple clients can then request selected portions of the data, possibly representing many thousands of consecutive turns, for display on operator consoles. The system uses digital phase-locked loops to derive its beam-locked timing reference. Programmable state machines, driven by accelerator timing pulses and information from the accelerator control system, direct the order of operations. The cPCI crates are connected to a standard Linux computer by means of a private Gigabit Ethernet segment. Dedicated server software, running under Linux, knits the system into a coherent whole.

INTRODUCTION

The CERN Proton Synchrotron (PS) is a 200 m diameter 26 GeV alternating-gradient synchrotron built in 1959. It is part of the injector complex that prepares protons and ^{208}Pb ions for the LHC.

The PS is equipped with forty electrostatic BPMs, each delivering three analogue signals: A horizontal and vertical displacement signal, Δ_x , Δ_y and an overall sum Σ . The 120 BPM signal channels are digitized using LTC2255, 14 bit, 125 MS/s ADCs, and the digital sample streams are then further processed into per-bunch positions using Xilinx Virtex-4 FPGAs. Results are stored into a memory large enough to store several seconds worth of data (Fig. 1).

Nine channels, corresponding to three BPMs, are combined on a single cPCI digitizer module. This module is the only board that has been custom designed for this application. Fourteen of these modules are distributed over three half-width cPCI crates (Fig. 2). Each crate also contains a standard, off-the-shelf Concurrent Technologies PP410 module controller. A private Gigabit Ethernet segment connects the module controllers to a Supermicro Core[™] i7,

* We acknowledge the support of the European Community-Research Infrastructure Action under the FP6 "Structuring the European Research Area" programme (DIRAC secondary-Beams, contract number 515873)

[†] Jeroen.Belleman@cern.ch

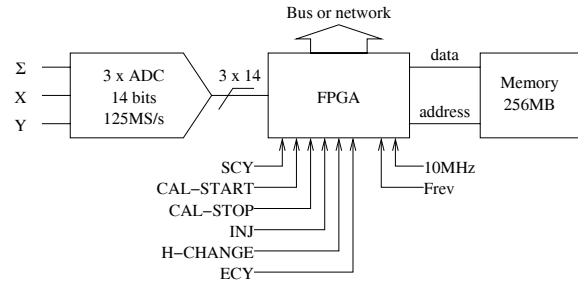


Figure 1: Signal processing block diagram for one BPM.

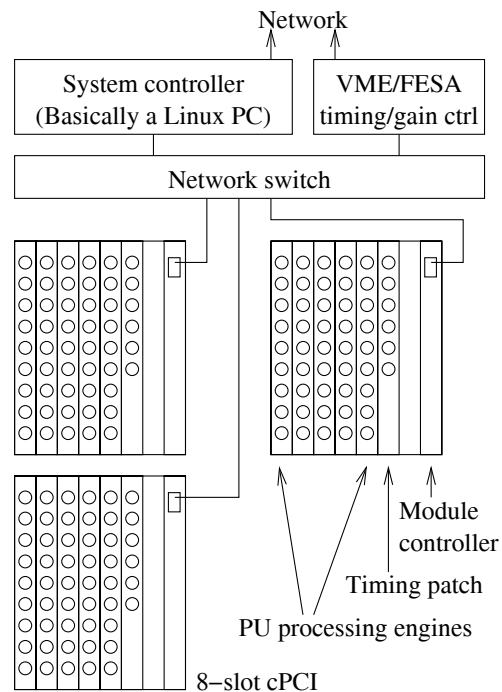


Figure 2: TMS block diagram.

model 5046-XB system controller. The system controller also acts as a BOOTP server and NFS file server for the cPCI processor boards. The three module controllers and the system controller all run Fedora Linux. A server daemon running on the system controller provides an RPC-based interface through which the whole system appears as a coherent single instrument. The server can handle multiple simultaneous independent clients. The system was built to CERN's specification by British industry [1].

For reasons of standardization and uniformity, a server based on CERN's Front-End Software Architecture (FESA) mediates between the TMS and control room ap-

FEM SIMULATIONS – A POWERFUL TOOL FOR BPM DESIGN

P. Kowina, P. Forck, W. Kaufmann, P. Moritz, GSI Darmstadt, Germany
 F. Wolfheimer, T. Weiland, TU Darmstadt, Germany

Abstract

This contribution focuses on extensive simulations based on Finite Element Methods (FEM) which were successfully applied for the design of several Beam Position Monitor (BPM) types. These simulations allow not only to reduce the time required for BPM prototyping but open up new possibilities for the determination of characteristic BPM features like signal strength, position sensitivity etc. Since a precise visualization of the signal propagation along the BPM structure is possible, effects like field inhomogeneities or cross-talks between adjacent electrodes can be controlled. Moreover, modern simulation programs enable to define a charge distribution moving at non relativistic velocities, which has an impact on the electromagnetic field propagation. It is shown that for slow ion beams the frequency spectrum of the BPM signal depends on the beam position. Simulation methods are discussed in the context of different BPM realizations applied in hadron accelerators. All simulations described in this paper were performed using CST Suite [®] [1].

LINEAR-CUT BPM

Proton and ion synchrotrons are usually operated at the bunching frequency f_{rf} in the order of few MHz. In these accelerators bunches typically have a length of a several meters. For such beam parameters linear-cut BPMs are preferred due to its excellent linearity of the position determination and the independence of the measurements in the orthogonal directions [3]. Moreover, the full transversal coverage by the electrodes allows precise position measurements even for the beams with transversal large and complex charge distribution. An example of such a BPM, sometimes called “shoe-box” due to its cuboid shape, is shown in Fig. 1. Also other geometrical realizations,

having e.g. elliptic cross section, show the same electromagnetic properties, see [4] and references therein.

The most important BPM parameter is its *position sensitivity*, defined as an response of the BPM on the beam displacement [3].

Assuming the bunches much longer than the BPM itself, the electric field propagation in the BPM can be well approximated with TEM wave traveling on a wire. The eventual influence of effects caused by non-relativistic beams is minor and can be neglected. Based on this assumption the BPM position sensitivity can be experimentally determined using so called stretched wire method, see e.g. [5]. In this method the amplitude changes of the signals induced in the electrodes are measured as a response on the changing wire position.

Similarly, position sensitivity can be obtained by means of FEM-based simulations that allow optimization of the BPM design entering in the time consuming prototyping phase. Since simulations enable three dimensional field visualization, the field inhomogeneities or distortions effecting BPM linearity caused by e.g. structure discontinuities can be found and eliminated.

The optimizations performed for linear-cut BPMs with rectangular as well as elliptic cross sections and different electrode arrangements are described in Refs. [2, 4, 6]. It was investigated how the presence of different BPM components like e.g. guard ring influence the position sensitivity and linearity of the position determination. In order to investigate the influence of the whole environment on the position readout, the complete BPM was modeled together with the surrounding vacuum chamber [7]. All components were defined with realistic material permittivity and conductivity. The volume was divided in 3-dimensional hexahedral meshes with typically 10^6 to 10^7 cells – depending on the model complexity. The number of meshes is mainly blown-up by small curved parts or elements oriented diagonally with respect to the main coordinates. The beam was simulated as a traveling wave on a wire using the CST Time Domain Solver and thus reproducing the stretched wire method. An excitation was defined as a Gaussian shaped pulse with length of $5 \mu s$ corresponding to the bandwidth of 200 MHz. The position sensitivity was calculated from S-parameters expressed in frequency domain as described in [2]. The goals in optimization of the BPM design were: i) enlarged position sensitivity, ii) linearity of the position determination, ii) reduction of the offset between electrical and geometrical center of the BPM and iv) independence of measurements with respect to the orthogonal directions.

Here we concentrate on the aspect of cross-talk between adjacent BPM electrodes that decreases the difference of

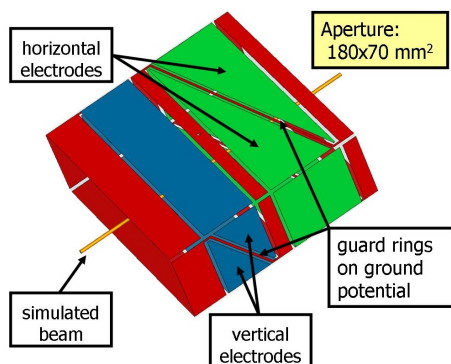


Figure 1: An example of the linear-cut BPM [2].

STATUS OF BEAM IMAGING DEVELOPMENTS FOR THE SNS TARGET

T. J. Shea, C. Maxey, T. J. McManamy, ORNL, Oak Ridge, Tennessee, USA
D. Feldman, R. Fiorito, A. Shkvarunets, UMD, College Park, Maryland, USA

Abstract

The Spallation Neutron Source (SNS) continues a ramp up in proton beam power toward the design goal of 1.4 MW on target. At Megawatt levels, US and Japanese studies have shown that cavitation in the Mercury target could lead to dramatically shortened target lifetime. Therefore, it will be critical to measure and control the proton beam distribution on the target, in a region of extremely high radiation and limited accessibility. Several sources of photons have been considered for imaging the beam on or near the target. These include a freestanding temporary screen, a scintillating coating, Helium gas scintillation, optical transition radiation, and a beam-heated wire mesh. This paper will outline the selection process that led to the current emphasis on coating development. In this harsh environment, the optics design presented significant challenges. The optical system has been constructed and characterized in preparation for installation. Optical test results will be described along with predictions of overall system performance.

MOTIVATION

The design of targets for megawatt class accelerators is generally limited by material issues such as radiation damage, the ability to adequately cool the structures and the stresses generated by thermal profiles, coolant pressures and short pulse effects. Performance usually improves with more compact targets, while the engineering challenges increase. A key parameter for design is the beam profile and peak current density for a given beam energy since this drives the peak radiation damage rate, the peak volumetric heating in the target and the peak heating in any window system the beam passes through. The containment structure for liquid metal targets are also subject to cavitation damage for short pulse operation and studies for SNS and JSNS mercury targets have shown this may be a sensitive function of peak current density [1]. Generally, targets that are designed for high performance are close to the engineering limits and subject to potential damage if the beam density or power increases. Development of diagnostic systems which give accurate beam profile information during full power operation would allow targets to be safely designed with less engineering margin and with improved lifetime estimates based on radiation damage. Rapid detection of high beam density could be used to trip the beam for target protection.

As shown in Fig. 1, the SNS will operate at beam powers exceeding 1 MW by late 2009. Currently, from a location 9.5 meters upstream of the target, a harp provides the last profile measurement. This multi-wire device and upstream instrumentation provide data that help predict the properties of the beam at the target. Unfortunately, the

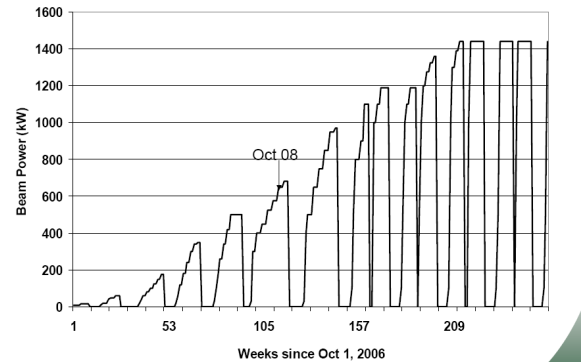


Figure 1: Ramp-up of SNS beam power.

estimated uncertainty of the current density prediction exceeds 25%. Assuming that the target's damage rate scales with the fourth power of the peak current density, a 30% increase in this parameter would reduce the target lifetime by over 60%. At J-PARC, another high power facility with a liquid metal target, the situation is significantly better. Their multiwire monitor sits much closer to the target and recent studies have demonstrated agreement between this device and image plate activation analysis [2]. During commissioning at the SNS, the situation was also better. A temporarily installed Al₂O₃:Cr screen provided a full 2 dimensional image of the beam at the target [3]. This uncooled device was removed in 2006 before high power operation began. Due to the valuable data provided by the temporary system, and in anticipation of high power levels, a new beam on target imaging system is being developed.

IMAGING OPTIONS

Several sources of photons were considered. Their relative yields were calculated and are summarized in Table 1. In this table, the screen refers to a typical Chromium doped alumina material that was used in the temporary target imaging system. For the future, one option is to install a similar screen for low power tune-up after each target replacement. Before the pulse repetition rate is ramped up to achieve full power, the target would have to be retracted, the screen robotically removed, and the target reinserted. This procedure could take over one week and therefore impact operations.

Since a water-cooled shroud surrounds the target, a second option is to coat this shroud with a thin luminescent material. Heating of the scintillator would be limited, and it could be used during full power operations. As this option was selected for the initial deployment, it receives a detailed treatment in the next section.

Optical transition radiation is produced at the unmodified target surface. For 1 GeV protons, photon

NON-DESTRUCTIVE BEAM POSITION MEASUREMENT IN A PROTON THERAPY BEAM LINE*

D.T. Fourie, L. Anthony, A.H. Botha, J.L. Conradie, J.L.G. Delsink, J.G. de Villiers, P.F. Rohwer, P.A. van Schalkwyk, iThemba LABS, P.O. Box 722, Somerset West 7129, South Africa
 J. Dietrich[#], Forschungszentrum Jülich, D-52425 Jülich, Germany

Abstract

Non-destructive beam position monitors (BPMs) have been in use at iThemba LABS for several years in the neutron therapy and radioisotope production beam lines, as well as in the transfer lines between the two K8 injector cyclotrons and the K200 separated-sector cyclotron. The sensitivity of these BPMs is limited by noise and pickup from the RF systems to about 300 nA in the high-energy beam lines. For proton therapy, using the scattering method, position measurements at beam currents as low as 20 nA have to be made. A new and more sensitive BPM as well as the electronic measuring equipment, using RF pickup cancellation and improved filtering, have been developed and installed in the proton therapy beam line. The BPM, the electronic equipment and the results of measurements at beam currents down to 10 nA for 200 MeV protons are described.

INTRODUCTION

Variable energy beams of light and heavy ions from ECR ion sources, as well as polarized protons, are used for nuclear physics research at iThemba LABS [1]. A high intensity 66 MeV proton beam can be switched between vaults for neutron therapy and radioisotope production for medical and industrial purposes. Proton therapy has been practised since 1993 with a 200 MeV beam at beam intensities of between 20 nA and 70 nA, using gas-filled multi-wire and segmented ionization chambers for beam position measurements. Non-destructive BPMs [2,3] that can fit in any of the standard beam diagnostic chambers together with other diagnostic elements were developed and installed in the high intensity beam lines. The sensitivity of these BPMs is not sufficient for use in the proton therapy line, owing to the dimensional restrictions on their length, noise in the solid state multiplexers and pickup from the main and the two flat-topping RF systems, that operate at the third and fifth harmonics, as well as from the rebunchers, that operate at the second and fourth harmonics.

The usefulness of the existing BPMs, not only for beam alignment and position monitoring, but also for detecting sources of beam instability, provided the incentive to investigate the possibility of building BPMs with greater sensitivity. Since beam phase measurements [4] in the separated-sector cyclotron could be made at beam currents in the nA range by cancellation of the relatively large pick-up signal, it seemed feasible that the same

technique could be used for BPMs in the beam lines, where the level of the pick-up signals is much lower, to improve the sensitivity to such an extent that they can be used in the proton therapy beam line and perhaps also in the nuclear physics beam lines, where low intensity beams with variable energy are used. Tuned BPMs [5] were not considered because of the variable frequency operation of the accelerators. A new BPM, and a test set-up for signal processing electronics, similar to that which is used for beam phase measurements, was designed and built from available amplifiers, filters and measuring equipment. From past experience with the BPMs it is known that the level of the pick-up is the lowest at the third harmonic, i.e. at 78 MHz, for the 200 MeV proton beam. At 66 MeV the pick-up signal that is caused by the flat-topping system of the light-ion injector cyclotron is the lowest at the fifth harmonic, i.e. at 81.8 MHz. The third harmonic flat-topping system of the separated-sector cyclotron causes a much larger disturbance. The signal processing equipment was therefore built to operate in a 10 MHz band centred at 80 MHz.

THE BPM

The influence of the electrode dimensions on the signal level and harmonic content for different beams was calculated according to the method described by Timmer et al. [6]. The BPM electrodes are considered as capacitors that are charged by the beam and discharged through a resistor connected to ground. To verify the order of magnitude of the calculated value, a simpler and less accurate method, which assumes that charge appears only on the inside of the electrodes when the beam enters the BPM, and similarly disappears from the inside when the beam leaves it, was used to calculate the beam pulses with Laplace transforms. With the second method the pulse form differs, as can be expected, significantly from those of the first, but there is good agreement between pulse and harmonic amplitudes. The main BPM dimensions are shown in Fig. 1. To obtain larger harmonic

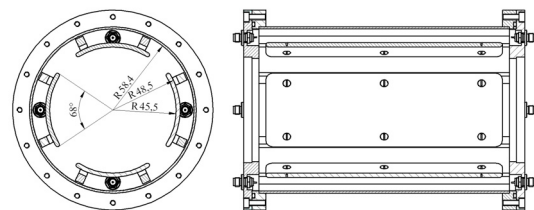


Figure 1: Cross-sectional views of the BPM.

*Work supported by BMBF and NRF, Project-codes: SUA 06/003 and GUN2075288.

[#]j.dietrich@fz-juelich.de

ORTHOGONAL COUPLING IN CAVITY BPM WITH SLOTS

D. Lipka*, D. Nölle, M. Siemens, S. Vilcins, DESY, Hamburg, Germany
 F. Caspers, CERN, Geneva, Switzerland
 M. Stadler, D. M. Treyer, PSI, Villigen, Switzerland
 H. Maesaka, T. Shintake, RIKEN/SPring-8, Hyogo, Japan

Abstract

XFELs require high precision orbit control in their long undulator sections. Due to the pulsed operation of drive linacs the high precision has to be reached by single bunch measurements. So far only cavity BPMs achieve the required performance and will be used at the European XFEL, one between each of the up to 116 undulators [1]. Coupling between the orthogonal planes limits the performance of beam position measurements. A first prototype build at DESY shows a coupling between orthogonal planes of about -20 dB, but the requirement is lower than -40 dB (1%). The next generation cavity BPM was build with tighter tolerances and mechanical changes, the orthogonal coupling is measured to be lower than -43 dB. This report discusses the various observations, measurements and improvements which were done.

INTRODUCTION

A cavity BPM consists of a coaxial dipole resonator with four symmetric arranged slots and a reference resonator, see Fig. 1. A charged particle beam excites electromag-

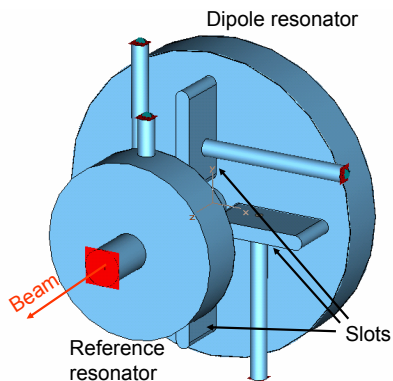


Figure 1: Design view of a cavity BPM, here only the vacuum parts are shown.

netic fields. Antennas in the slots and the reference resonator observe a voltage. The signal used from the dipole resonator is the TM_{11} mode (the dipole mode is spatial filtered due to the slots), which is proportional to the beam offset times charge. Charge and phase normalization are done with the signal from the reference resonator (TM_{01} mode which is proportional only to the charge), see Fig. 2, such that the beam position is observed. The phase relation

between dipole and reference resonator is used to determine the sign of the displacement.

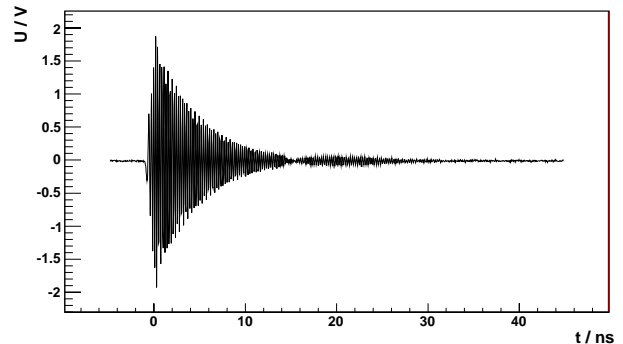


Figure 2: Time domain response signal from reference resonator with visible reflexion after about 14 ns.

Both transverse beam displacements are measured by using two orthogonal feedthroughs (ports) of the dipole resonator, the other two ports are terminated by $50\ \Omega$ loads. When the beam is only shifted in one direction with respect to the electromagnetic axis of the BPM only one port should show an offset. With a coupling of both planes the other port will give a signal too, see Fig. 3. If the resulting coupling is larger than requested this limits the BPM performance.

This paper shows the investigation of the coupling for two prototypes (one of the first and one of the second generation) with two methods. The reason of the coupling is evaluated and possible improvements are named.

FIRST CAVITY BPM GENERATION

Three prototypes have been produced at DESY. The design originally developed at SPring-8 [2] was changed according to the boundary conditions of the European XFEL with a resonance frequency of 4.4 GHz. One prototype was installed at FLASH in 2008, see Fig. 4. The BPM can be moved in both transverse directions by stepper motors. The ports are connected with 1.5 m long cables (H&S SUCOFORM SM141) followed with 120 m long cables (RFS LCF 78-50JA 7/8" CELLFLEX) each. The signals are taken with an oscilloscope, 20 GSamples/s. In Fig. 3 the signal from the orthogonal port shows a different decay time compared to the *correct* port. This leads to the assumption that the loaded quality factor is increased. The signals shown in Fig. 2 and Fig. 3 top indicates a reflexion

* dirk.lipka@desy.de

ALIGNMENT MONITORS FOR AN X BAND ACCELERATING STRUCTURE

M. Dehler, J.-Y. Raguin, A. Citterio, A. Falone, Paul Scherrer Institut, Switzerland
 W. Wuensch, G. Riddone, A. Grudiev, R. Zennaro, A. Samoshkin, D. Gudkov, CERN, Switzerland
 G. d’Auria, M. Elashmawy, Sincrotrone Trieste, Italy

Abstract

Currently an X band traveling wave accelerator structure is under development in a collaboration between CERN, PSI and ELETTRA. At PSI and ELETTRA, it will serve for longitudinal phase space compensation at the respective FEL projects, where CERN will use it to test break down limits and rates in the high gradient regime. The design employs a large iris, $5\pi/6$ phase advance geometry, which minimizes transverse wake field effects while still retaining a good efficiency. In addition, we plan to use an active monitoring of the beam to structure alignment and to include two wake field monitors coupling to the transverse higher order modes. These allow steering the beam to the structure axis giving a higher precision than mechanical alignment strategies. Of special interest is the time domain envelope of these monitor signals. Local offsets due to bends or tilts show up as distinct patterns, which should be easily detectable via basic measurements.

INTRODUCTION

Within the context of the GLC and NLC projects, a considerable effort has been going on in developing high power X band RF systems for high energy e^+e^- colliders[1]. After the conclusion of these projects, the recent decision by CLIC to change their principal RF frequency from 30 GHz to an European X band frequency near 12 GHz has given a renewed push to X band development. A big RF structure fabrication and testing program involving major laboratories around the world is under way.

A relatively new application for X band technology is in free electron lasers. LCLS compensates nonlinearities in the longitudinal phase space with an X band structure in order to improve bunch compression. The European FEL projects SPARC, FERMI@ELETTRA and PSI-XFEL also plan to employ it for the same purpose. In that context, a collaboration between CERN, PSI and ELETTRA has been set up to develop suitable structures. While being operated at the PSI-XFEL and the FERMI FEL, an ultra long performance test also important for CLIC, these are also going to be submitted to break down tests at CERN.

Looking at the PSI-XFEL, beam voltages up to 30 MeV are required using only a limited power in the order of 40 MW at the structure, which means a fairly efficient structure. On the other hand, the beam has a relatively modest energy of 250 MeV, so that we are relatively sensitive to transverse wakes. So we need to make a good compromise between a high shunt impedance, generally associated with low apertures, and a low transverse kick, demanding the

02 BPMs and Beam Stability

opposite. The structure will have no HOM damping. But two wake field monitors are foreseen to align the structure to the beam and to minimize transverse kicks.

The monitor use TE type coupling to the dipole modes in the structure to reject the fundamental as well as higher order longitudinal modes. A special feature is, that we also make use of the fact that wave propagation inside the RF structure is relatively slow at a few percent of the speed of light. The spread out pulse response of the wake monitors not only contains information about the offset but also about higher order misalignments as structure tilts. So basic measurement procedures using only the envelope of the output signal are possible.

FUNDAMENTAL MODE PROPERTIES

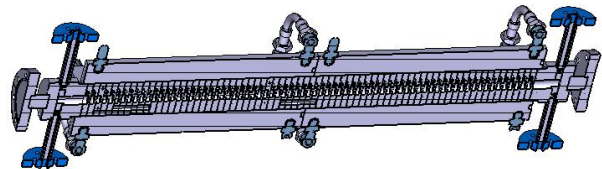


Figure 1: Cut through X band accelerating structure.

For both ELETTRA and PSI specifications, a single structure with 750 millimeter active length is the most appropriate solution. The NLC structure type H75 ($5\pi/6$ phase advance) has been chosen as the most suitable candidate for the testing program. The original H75 design, with all iris aperture, thickness and ellipticity of the iris varying along the structure, provides an accelerating gradient of 65 MV/m for 80 MW input power and was successfully tested up to 100 MV/m with a SLAC mode launcher [2, 3], which we also use here. The relevant parameters are summarized in Table 1.

Table 1: Structure Specifications

Beam Voltage	30 MeV
Max. Power	29 MW
Iris diameter	9.1 mm (avg.)
Wake field monitors	up/downstream
Operating temp.	40 deg. C
Fill time	100 ns
Repetition rate	100 Hz

WAKE FIELD MONITOR

To measure the beam offset inside the structure, we couple to the lowest dipole mode. Minimum perturbation of the fundamental mode and maximum information in the output signal, easily post processed, are the principal design criteria. Where and how to couple, what to expect as a signal is shown in the following.

INSTALLATION AND COMMISSIONING OF A COMPLETE UPGRADE OF THE BPM SYSTEM FOR THE ESRF STORAGE RING

B.K. Scheidt, F. Epaud, ESRF, Grenoble, France

Abstract

The ESRF Storage Ring has, over the last 3 winter months, been fully equipped with new electronics for its BPM system while causing a minimum disturbance to its large community of X-ray beam-line users. The Libera-Brilliance is now doing the treatment of the weak RF signals on all 224 BPM stations, and has replaced the old RF-Multiplexing system that had served reliably for 17 years. This paper describes the precautions that had been taken to make the whole transition as smooth as possible, with regards to the reliability for the SR operation and the positional stability of more than 40 X-ray beams. Information is given on the network & computer control, based on the Tango distributed control system and its device-servers and tools. Results will be presented to demonstrate the strongly improved performance and functionality in every field of application, and that will make this new BPM system the key component in the near future's upgraded orbit stabilization system.

HISTORY, MOTIVATION , CHOICE OF TECHNICAL SOLUTIONS

The agreed upgrade program of the ESRF light source, including that of the accelerator complex [1], has created an opportunity to modernize drastically the old BPM system of the SR. For its orbit control and beam stabilization (incl. feedbacks) the ESRF SR depended on 2 separate and independent systems, both of in-house design & conception : 1) The slow BPM system of 224 stations that had been conceived 20 years ago, and 2) the fast-BPMs with only 32 stations and 16 (vert.) & 32 (hor.) correctors for fast-feedback.

Both BPM types use blocks with 4 buttons for vacuum wall-current pick-up of the RF signal. At the time of conception (i.e. before 1990) of the slow system it was believed that fast & high-resolution beam position measurements would not be possible with the button-type of BPMs (and its RF electronics for signal treatment) and that instead X-BPMs, installed on numerous X-ray beam-lines would satisfy those fast needs. However, such X-BPMs suffered from intrinsic limitations and have never satisfied these requirements.

To overcome this, additional, independent BPM blocks were installed with electronics for fast measurements. Their purpose and usage has evolved progressively over the years, from first pure local fast feedbacks to finally a pure global SR ring feedback system to which very recent improvements were made to cover the full frequency band of the needed orbit stabilization [2].

The slow BPM system had an addition to its basic functionality with a high-resolution 'quasi' Turn-by-Turn measurement mode [3] that, with a stable & reproducible

synchronization to an orbit kicker, allows the precise measurement of the SR lattice parameters. But it does not have a genuine single turn capacity, and for injection studies or for coping with severe injection problems, this old system requires certain conditions (4 strong injection currents for a single measurement) that are today no longer compatible with operation needs, nor with restrictions imposed by radiation safety regulations.

The satisfaction of today's requirements on the performance and functionality of a BPM system is no longer realistic through an 'in-house' design because of the technical complexity of different fields inside such system like RF signal treatment, digital signal conditioning through FPGAs, and interfacing with computer networks. This argument applies also to the ability to exercise the rigorous quality-control that is needed for production of a large series of units.

A few years ago the BPM needs of the new synchrotron light sources DLS and Soleil [4,5] had been satisfied successfully, in collaboration with them, by a commercial product called 'Libera-Electron' of the Instrumentation Technologies company [6]. Subsequently this product has provided more light sources for their BPM needs. [7,8,9]

This original product, after being fully employed & analysed by the DLS and Soleil [10,11], was improved in 2007 by a successor called 'Libera-Brilliance'. A total of 8 units of this product were procured at the end of 2007 and tested at the ESRF, during the first half of 2008, for full compatibility with the ESRF needs and the ESRF particularity of (multiple-) single bunch fillings.

VERIFICATIONS ON PROTOTYPES

These single bunch fillings yield an electric signal from the pick-up buttons that reaches a high peak voltage (upto 100V), and is very rich in harmonics (at 355KHz revolution frequency) in the frequency spectral domain. Both aspects can pose a problem to the Libera in terms of degradation of its performance, notably its low noise characteristic and its reproducibility for different SR currents & filling patterns : a) the input electronics may not have fully linear transmission characteristics for such high peak voltage, and b) certain spectral lines of the input signal may mix in an un-expected way with some of the Liberas 'internal' frequencies (the rates of the ADC convertors and the RF 'cross-bar' switches for internal calibration purposes) or some of its harmonics.

The old ESRF system had employed, directly after the pick-up buttons , RF bandpass filters (352 MHz, 40MHz bandwidth) and our long experience of their robustness, reliability and stability is such that we rely on these same components, now employed just in front of the Libera RF inputs, i.e. after ~20m of RG223 RF cable.

DESIGN STATUS OF BEAM POSITION MONITORS FOR THE IFMIF-EVEDA ACCELERATOR

I. Podadera*, B. Brañas, A. Ibarra, CIEMAT, Madrid, Spain
 J. Marroncle, CEA-Saclay, Gif-sur-Yvette, France

Abstract

The IFMIF-EVEDA accelerator [1] will be a 9 MeV, 125 mA CW deuteron accelerator which aims to validate the technology that will be used in the future IFMIF accelerator. Non-interceptive Beam Position Monitors pickups (BPMs) will be installed to measure the transverse beam position in the vacuum chamber in order to correct the dipolar and tilt errors. Depending on the location, the response of the BPMs must be optimized for a beam with an energy range from 5 up to 9 MeV and an average current between 0.1 and 125 mA. Apart from the broadening of the electromagnetic field due to the low-beta beam, specific issues are affecting some of the BPMs: tiny space in the transport line between the RFQ and cryomodule (MEBT), cryogenic temperature inside the cryomodule, phase and energy measurement in the diagnostics plate (DP), and debunching and big vacuum pipe aperture at the end of the high energy beam transport line (HEBT). For this reason different types of BPMs are being designed for each location (MEBT, cryomodule, DP and HEBT). In this contribution, the present status of the design of each BPM will be presented, focusing on the electromagnetic response for high-current low-beta beams.

During the commissioning time the beam will be mostly pulsed with low duty factors. Therefore, both CW and pulsed operation has to be foreseen during the design phase. For a proper design of the monitors a first rough estimation can be done by implementing simple analytical models. However, powerful 3D electromagnetic software should be used for a more careful optimization of the geometry, the monitors response and the coupling to the beam. Presently these tools are being used for the design of the monitors all along the accelerator. The status of the design will be presented hereafter.

Table 1: Range (approx.) of the Beam Properties for the BPMs at IFMIF-EVEDA

Beam parameter	Min. Value	Max. Value
Energy E (MeV)	5	9
$\beta = v/c$	0.0727	0.0975
Peak current I_b (mA)	10	125
Average current $\langle I_0 \rangle$ (mA)	0.1	125
Pulse length T_p (ms)	1	CW
Duty factor (%)	0.1	CW
Bunch length σ_z (ns)	0.1	1.7
Transverse size $\sigma_{x,y}$ (mm)	1	20

INTRODUCTION

The design of the beam position monitors for the high-current low-energy accelerator IFMIF-EVEDA is facing important challenges due to the broadening of the electromagnetic detectors, the radiation environment and the debunching along the line, as described in [2]. The main use of the beam position monitors will be the monitoring of the transverse position of the beam centroid along the accelerator by calculating the differential signal from the vertical and horizontal pair of electrodes of the device. This parameter will be used to correct the dipole errors of the different elements and transport safely the beam along the accelerator. In addition, the bunch phase will be also measured in order to tune the rebuncher and the superconducting cavities. Last but not least the beam position monitors in the diagnostics plate will be in charge of measuring the mean energy of the particles by using the Time of Flight technique. The BPMs are expected to provide sufficient phase accuracy (using the sum signal) for this measurement.

The main beam parameters in which these monitors will work are summarized in Tab. 1. In normal operation, the accelerator will work with CW beams but during commis-

LAYOUT AND REQUIREMENTS

Global Layout

Figure 1 sketches the distribution of the different types of beam position monitors inside the accelerator. A total of 18 monitors will be placed on the accelerator, distributed in at least four types of monitors (see Tab. 2) due to the different requirements at each section as detailed hereafter.

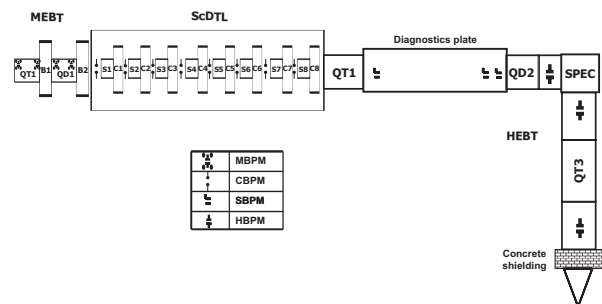


Figure 1: Distribution of the Beam Position Monitors along the accelerator.

*ivan.podadera@ciemat.es

DEVELOPMENT OF THE RF CAVITY BPM OF XFEL/SPRING-8

H. Maesaka[#], S. Inoue, T. Ohshima, S. Matsubara, T. Shintake and Y. Otake,
RIKEN/SPring-8, 1-1-1, Kouto, Sayo, Hyogo, 679-5148, Japan
H. Ego, JASRI/SPring-8, 1-1-1, Kouto, Sayo, Hyogo, 679-5198, Japan

Abstract

We describe the design and performance of the rf cavity beam position monitor (RF-BPM) for the x-ray free-electron laser project at SPring-8 (XFEL/SPring-8). The required position resolution is less than 0.5 μm . To achieve this demand, we designed an RF-BPM that has a TM110 cavity to detect the beam position and a TM010 cavity to obtain the beam charge and phase reference. The resonant frequency is 4760 MHz for both cavities. We designed a detection circuit equipped with IQ (In-phase and Quadrature) demodulators. We installed the BPM system into the SCSS test accelerator and performed a beam test. We observed a position sensitivity of approximately 0.1 μm and a position resolution of less than 0.2 μm at a 0.3 nC bunch charge. We evaluated the resolution of the beam arrival timing measurement with the phase being between the TM010 resonator and a reference rf signal. The temporal resolution was 25 fs. These results are sufficient for the beam tuning of XFEL/SPring-8.

INTRODUCTION

The x-ray free-electron laser project at SPring-8 (XFEL/SPring-8) [1] is underway to open a new era of life sciences, material sciences, etc. The XFEL/SPring-8 facility consists of an electron injector with a thermionic cathode, C-band high-gradient accelerators and short-period in-vacuum undulators. XFEL/SPring-8 is designed to generate a coherent x-ray beam at an angstrom wavelength by a self-amplified spontaneous emission (SASE) process.

One of the most important technical issues is to overlap the electron beam with radiated x-rays throughout the undulator section with high precision. The position difference between the electron beam and the x-rays must be less than 4 μm [2]. Therefore, we require the resolution of the beam position monitor (BPM) to be less than 0.5 μm . Among various types of BPMs, only an rf cavity BPM (RF-BPM) can achieve this demand, because of its high beam-cavity coupling. There exist some past experimental reports with nanometer-level resolutions [3-5].

It is also important to monitor the time difference between a beam and a reference rf signal. The temporal precision of the XFEL accelerator is demanded to be less than 50 fs [6]. An RF-BPM has a capability to detect beam arrival timing from the phase of an excited rf signal.

We designed a BPM system comprising an RF-BPM cavity and a detection circuit in order to achieve the required resolution. This system was installed into the SCSS test accelerator, which was built to demonstrate the

feasibility of XFEL/SPring-8, and has been operating as FEL at extreme ultraviolet (EUV) FEL since 2006. Our BPM system was tested with a 250 MeV electron beam. In this paper, we describe the design of this system and the results from beam tests.

DESIGN OF THE RF-BPM SYSTEM

The RF-BPM uses a TM110 dipole resonant mode in a cylindrical cavity to measure the beam position. The longitudinal electric field, E_z , of TM110 is expressed as

$$E_z = E_0 J_1\left(\frac{\chi_{11}r}{a}\right) \cos \varphi e^{j\omega t}, \quad (1)$$

where E_0 is a constant that represents the field amplitude, J_1 is a first-order Bessel function of the first kind, $\chi_{11} \approx 3.8$ is the first root of $J_1(r) = 0$, a is the cavity radius and ω is the resonant angular frequency. Since $J_1(r)$ can be approximated by a linear function near the axis, the amplitude of the TM110 field excited by an electron beam is proportional to beam displacement.

The voltage amplitude of the output signal from the TM110 cavity can be written as [7]

$$V = V_1qx + jV_2qx' + jV_3q + V_n, \quad (2)$$

where q , x and x' are the beam charge, the beam position and the slope of the beam trajectory, respectively. V_1qx is the in-phase component proportional to the beam position, jV_2qx' is the quadrature-phase component coming from the beam slope, jV_3q is also the quadrature-phase component due to leakage of the parasitic TM010 monopole mode and V_n are the other components, such as a thermal noise. To obtain beam position information, we have to scale the signal with the beam charge and determine the sign with a phase reference. Therefore, we prepared an additional TM010 mode cavity in the same cavity block to provide charge and phase information.

Based on concepts mentioned above, we designed the RF-BPM illustrated in Fig. 1. For the TM110 cavity, the rf signal is picked up through a coupling slot that is decoupled to the TM010 monopole mode in order to minimize the third term of Eq. 2 (jV_3q). The resonant

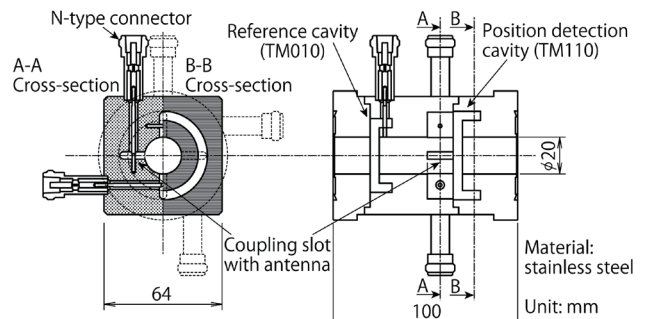


Figure 1: Drawing of the RF-BPM cavity.

[#]maesaka@spring8.or.jp

BUNCH BY BUNCH FEEDBACK SYSTEM USING iGp AT KEK-PF

R. Takai[#], M. Tobiyama, T. Obina, J. W. Flanagan, M. Tadano, T. Mitsuhashi,
 KEK, 1-1 Oho, Tsukuba, Ibaraki 305-0801, Japan

Abstract

A transverse bunch-by-bunch feedback system using iGp feedback signal processors has been tested at the KEK-PF. The system consists of a bunch position detection system using 1.5 GHz components of the beam ($3 \times f_{RF}$), iGp feedback signal processors, and a transverse feedback kicker with a high power amplifier. It shows sufficient performance to suppress instabilities completely up to a beam current of 450 mA. Results of the mode analysis of the instabilities using the grow-damp function of the iGp are also shown.

INTRODUCTION

Photon Factory electron storage ring (PF-ring) has been operated in a single- or multi-bunch mode of 2.5 GeV. In the multi-bunch operation, several coupled-bunch mode instabilities are observed in both transverse and longitudinal planes as a stored beam current increases. As for the transverse instabilities, we have suppressed them by using a bunch-by-bunch feedback system developed based on that of SPring-8 [1]. Although this feedback system had worked without major problems since the installation of 2005, we are now planning to replace it to that using “integrated General purpose signal processors (iGp)”, which have been developed by the collaboration of KEK, SLAC, and INFN-LNF [2]. The iGp is equipped with not only a greater flexibility for the change of tunes, but also many GUI panels that enable us to remotely change various parameters on digital processing such as coefficients of an FIR filter. It has already been used in the longitudinal bunch-by-bunch feedback system of PF-ring, and succeed in suppressing longitudinal dipole oscillations sufficiently [3]. In order to confirm its effectiveness for transverse instabilities, we have constructed the transverse feedback system using the iGp, and tested its basic performance. The details and some experimental results of the tentative feedback system are

presented herein.

The main parameters of PF-ring are listed in Table 1.

FEEDBACK SYSTEM

The transverse bunch-by-bunch feedback system is mainly composed of three sections, an analogue front-end detection, a digital signal processing, and a beam correction. The block diagram of the whole system is shown in Fig. 1.

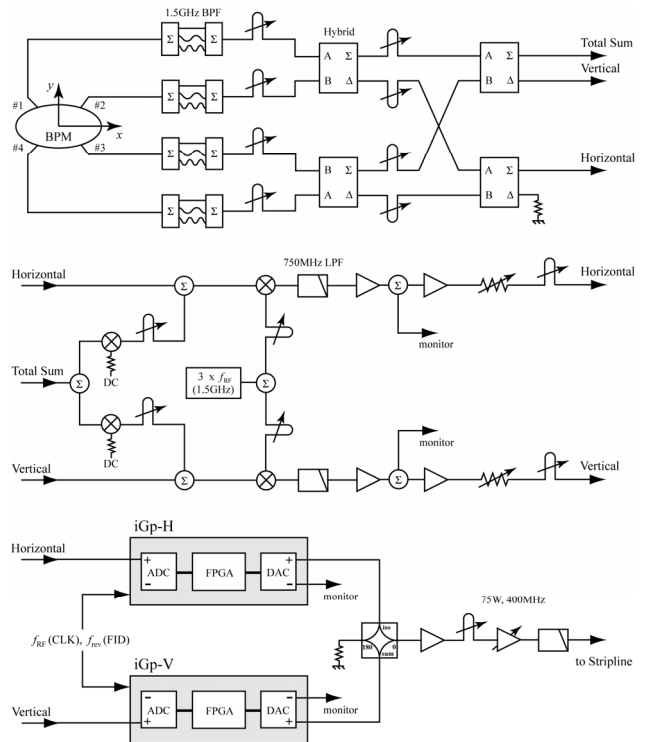


Figure 1: Block diagram of the transverse feedback system using the iGp.

Table 1: Main Parameters of PF-ring

Beam energy	2.5	GeV
Circumference	187	m
RF frequency f_{RF}	500.1	MHz
Harmonic number	312	
Revolution frequency f_{rev}	1.603	MHz
Betatron tune ν_x / ν_y	9.6 / 5.28	
Damping time τ_x / τ_y	7.8 / 7.8	ms
Stored current (single/multi)	50 / 450	mA

[#]ryota.takai@kek.jp

Front-end Detection Section

The beam signals picked up by a 4-button BPM are processed individually via a 1.5 GHz band-pass filter (BPF) which consists of a power combiner/splitter and three delay cables. The output signals are summed by hybrid circuits (M/A-COM, H-183-4) and converted into three signals, Horizontal, Vertical, and Total Sum. After offset components in Horizontal and Vertical are cancelled by using Total sum, the transverse position of each bunch is detected by a synchronous detection at the 3rd harmonic of the RF frequency ($3 \times f_{RF}$). The timing of the signal processing is precisely adjusted with line stretchers while a single bunch is stored.

THE MEASUREMENT OF BUNCH INTENSITY USING THE LHC BPM SYSTEM

J.L. Gonzalez*, E. Calvo, D. Cocq, R. Jones, CERN, Geneva, Switzerland

Abstract

A convenient way of having beam bunch intensity information available all around the LHC ring is to use the beam position monitor (BPM) system. The principle is to add the BPM signals, process them and make the result compatible with the time-modulation method used for transmitting the position over a fibre-optic link. In this way the same acquisition system can make both position and intensity data available. This paper describes the technique developed and presents the first intensity measurements performed on the CERN-SPS and LHC.

INTRODUCTION

The LHC beam position system is comprised of more than 1070 beam position monitors, the majority of which are electrostatic button electrode pick-ups. Each BPM provides both position and intensity information. The acquisition electronics is split into two parts, an analogue front-end, which sits in the tunnel, and an integrator/digitiser/processor VME module located on the surface [1]. Transmission from tunnel to surface is carried out using a time-encoded signal over a single mode fibre-optic link. A digital multiplexer, located in the position to time normaliser board [2], allows for either position or intensity selection, eliminating the need for a separate optical transmission system and digital acquisition boards for the intensity measurement. A WorldFIP fieldbus is used to control the tunnel stations.

THE LHC BPM SYSTEM

The LHC BPM system is foreseen to work with bunch intensities ranging from 1.5×10^9 to 2×10^{11} protons, using two sensitivity settings (low or high). Figure 1 shows the basic layout of the system. Each normaliser module gets the high frequency beam signals of the horizontal or the vertical electrodes and filters them using a pair of matched, 70 MHz, low-pass filters in order to significantly reduce any bunch length dependence due to the shortening of the bunch during acceleration. The filter is followed by a passive combiner, which makes the analogue sum of these signals available for further processing in the beam intensity board. Intensity information can actually be transmitted either directly using the optical output of the intensity module or via the normalisers, since the signal produced is compatible with the time-modulation method used for encoding the beam position.

Intensity Measurement Principle

Figure 2 depicts the intensity measurement principle. An analogue input multiplexer selects for which of the

* jose.luis.gonzalez@cern.ch

two counter-rotating beams the intensity will be measured. The input signal is the combination of the horizontal and vertical sum signals from the two associated normalisers. Detecting the zero crossing of the BPM signal triggers both the laser “Start” pulse and the constant current discharge source after a predefined delay.

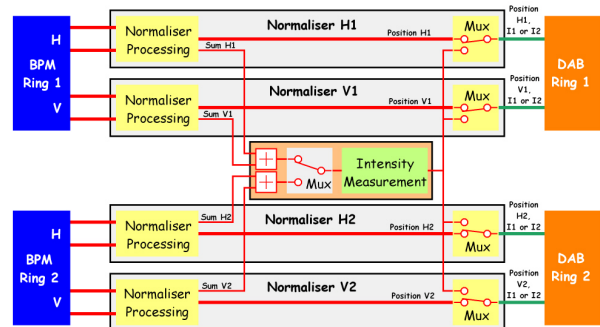


Figure 1: LHC position and intensity measurement system layout.

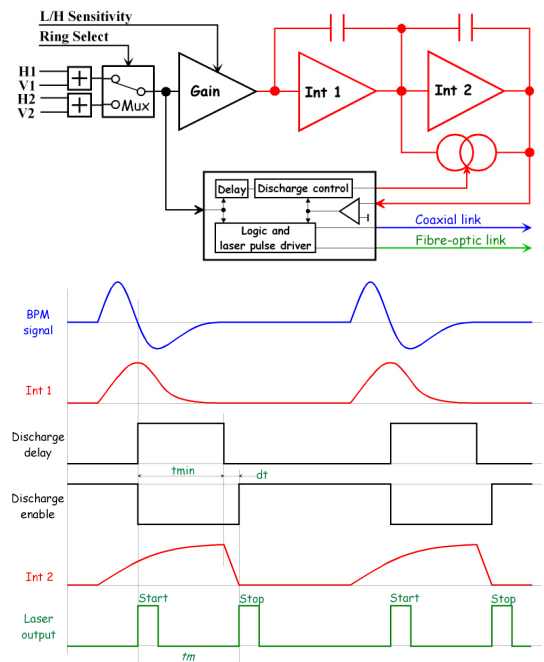


Figure 2: Intensity measurement principle and related waveforms.

The sensitivity control input adapts the gain to the beam dynamic range. The resulting signal is then integrated twice and a fast comparator produces the laser “Stop” pulse when the output voltage of the second integrator reaches zero, due to the constant current discharge. The Start and Stop pulses have a duration of 1ns and the

EXPERIMENTAL VERIFICATION OF PARTICLE-IN-CELL SIMULATION RESULTS CONCERNING CAPACITIVE PICKUP DEVICES*

M. Ruff[†], L.-P. Schmidt, University of Erlangen-Nuremberg, Germany
S. Setzer, Siemens AG, Healthcare Sector, Erlangen, Germany

Abstract

For beam position monitoring purposes, three different approaches have been applied to investigate and compare pickup button and electron beam spectrum characteristics. Results on this simulative approach are presented. Induced pickup currents have been calculated both with an analytical and a numerical method. An experimental validation of these simulation results has been conducted with the 6-MeV electron beam from a linear accelerator for medical purposes. The measurements were conducted under non-vacuum conditions. Good agreement between particle-in-cell simulation and experimental data was achieved concerning pickup power spectral distribution and dependence from beam current and beam displacements although non-negligible electron spread during air passage of the electron beam cannot be avoided.

INTRODUCTION

Multi-energy particle accelerators are widely used in cancer treatment facilities [1]. High efforts are being made to ensure precise generation of the beam as well as high precision irradiation and thus to minimize the risk of harming the patient. However, in a clinical environment, unavoidable effects can influence beam position. For multiple-angle treatment, medical accelerators usually comprise rotatable gantries, where the effects of mass and earth's magnetic field can cause beam displacements. Moreover the vicinity of magnetic resonance systems, even if positioned in a different treatment room, was found to be responsible for minor misalignments to the intended beam path. Besides other measures to monitor and stabilize the beam profile, position measurement and correction of the beam is advantageous for radiation stability.

In this paper, investigations on capacitive pickup devices are presented. A comparison between analytically calculated pickup characteristics and simulation results obtained with the software package CST PARTICLE STUDIO (CST PS) is given. Moreover, particle-in-cell (PIC) simulation results are compared to measurements conducted with test probes and the 6-MeV electron beam from a Siemens medical linear accelerator. In contrast to usual beam position

monitoring, these measurements have been conducted under non-vacuum conditions, as in therapy applications particles propagate through a certain distance in air before reaching the patient.

SIMULATIVE APPROACHES

To calculate the induced current on pickup probes and their spectral distribution, two alternative approaches based on different calculation methods have been applied:

Analytic Calculation in Matlab

An analytic approach for calculating the beam induced currents on capacitive pickups has been implemented in *Matlab* software. The developed tool is based on a numerical analysis given in [2]. The induced current on a pickup probe is calculated from the displacement current across the area of the pickup device. The influence of different bunch shapes is accounted for by the useage of weighted point charges. Therefore, the point charge is spread over a normalized distribution describing the bunch shape. The induced current on the button is then obtained by integration of the individual weighted point charge contributions at every sample of a given time interval. The total current can be calculated by considering the total number of particles and thus, the total charge in the bunch.

For spectral analysis of the pickup signals, the developed tool applies a Fast-Fourier-Transformation (FFT) to the signal in time domain which comprises the currents induced from a selectable number of bunches in a bunch train. The power levels contained in the beam spectrum fundamental and a number of bunch harmonics are then derived.

Particle-in-Cell Analysis in CST PS

To introduce pickup geometry parameters not covered by the Matlab analytic approach, like metal thickness and RF feed, PIC simulations [3] have been conducted in the full 3D electromagnetic solver software package *CST PARTICLE STUDIO*. Open boundaries have been chosen to avoid reflections of beam generated fields in the simulation volume. The induced currents are observed by mode selective time domain monitors in the vicinity of the waveguide ports. Further data processing is done in CST's postprocessing toolbox.

* Work supported by Bayerische Forschungsstiftung in the project "MEDieMAS - Effiziente Bestrahlungsgeräte für Krebstherapie (Efficient radiation systems for cancer therapy)", file number AZ-735-07

[†] marcel@lhft.eei.uni-erlangen.de

INVESTIGATION OF PRECISE PIPELINE-TYPE ADCS IN A BURST REGIME FOR A SINGLE-SHOT BPM*

A. Kalinin, ASTeC Daresbury Laboratory STFC, Warrington, UK
S. Artinian, Bergoz Instrumentation Ltd, Saint Genis Pouilly, France

Abstract

In the EMMA Accelerator turn-by-turn BPM, the ADC should execute several successive fast rate measurements with a clock burst triggered by the bunch on each turn. We investigated a work of some fast pipeline-type ADC ICs in a burst regime where a minimal burst length is decided by the ADC latency. The results show that pipeline-type ADCs a main merit of whose is a high precision are usable in a beam-triggered single-shot BPM as well as in other event-triggered systems. The set-up used for the investigation illustrates the measurement arrangement in the EMMA BPM. The employed technique described can be used for detailed investigation of a single shot BPM noise.

INTRODUCTION

On the EMMA Accelerator [1], the bunch trajectory is to be measured on each turn in 84 circumference points. The turn is $T = 55.2\text{ns}$. The bunch executes up to ten turns, and its trajectory is spirally enlarging in the horizontal plane, sweeping about a half of the pickup aperture. For machine tuning, the bunch can be made circulating larger number of turns on a stationary orbit.

Aiming at a compact and inexpensive EMMA BPM system, we, first of all, use in it a multiplexing of two pickup signals in each plane into a single channel where the second signal is delayed by $T/4 = 13.8\text{ns}$. The BPM synchronous detector output is a pair of spaced as above single polarity pulses about 5ns length each. On each turn, the ADC measures these two beam pulses and then makes two measurements of the DC pedestal.

Next, in the system, as a time reference signal for synchronous detection and clocking the ADC, the beam signal itself is used. [2] This approach allows first, to avoid a cumbersome network of external reference distribution from BPM to BPM, and second, to use a single synchronous detector (and a single ADC) instead of the I/Q scheme where a double set of each is required.

Trying to find optimal solutions for the EMMA BPMs in particular, and for the single shot BPMs that are now in demand, in general, we had tended towards ADC of the pipeline type. Being sufficiently fast, consuming low power, being comparatively inexpensive, a pipeline ADC has a solid advantage of high accuracy in comparison to a flash ADC.

We saw also that with ability to work in the burst regime, the pipeline ADCs could make possible precise measurements in any event-triggered system, for instance, in accelerator-based high energy particle detectors.

In this paper we report results of some initial burst regime investigation. Our investigation has not covered a broad range of modern ADC ICs available on market. We have not made chip-to-chip statistic measurements for that ADC that fits the purpose. Our immediate result is that an ADC has been identified for which the regime is feasible albeit with use of some additional facility.

TEST SET-UP

We used commercial ADC Evaluation Boards. A differential burst was directly fed into the ADC clock inputs. The burst was taken from a generator 81150A (Agilent Technologies). The clock period was 14ns.

At the ADC analog inputs, three circuits were used: (1) the ADC inputs were short to the ADC internal reference; (2) the inputs were connected to the differential outputs of an operational amplifier (differential gain $G_{2d} = 1$) whose inputs were short to GND; and (3) the ADC inputs were connected to the same amplifier one input of which was fed from a non-inverting preamplifier ($G_1 = 4$, 50Ohm input impedance). Amplifiers AD8000 and ADA4939 (both from Analog Devices) were used.

A preamplifier input pulse signal of about 13bit resolution was taken from another output of the 81150A generator. A DC pedestal that in the case of single polarity input pulse makes a full ADC range usable was introduced in the preamplifier.

The ADC output was observed using a logic oscilloscope DL9505L (from Yokogawa Electric Corp.). For each kind of measurements, a 64-shot array was recorded, using manual trigger. For the ADC latency of m clock periods, the readings of the samples of number $m + j$, $j = 1, 2, \dots, 4$ were recorded by setting the oscilloscope logic cursor at these samples.

ADC TEST

We tested two ADCs: MAX1427 (15bit, 80MHz, $m = 3$ cycles, from MAXIM) and AD6645ASQ (14bit, 105MHz, $m = 3$ cycles, from Analog Devices).

A response of the first ADC (with the inputs short to the ADC reference) to a clock burst is shown in Figure 1 where a full horizontal size is about $7\mu\text{s}$. The burst is shown on the upper trace DRY (it is the ADC's Data Ready signal). After the start, one can see that the ADC readings have a long transient: from big (negative) values through some ringing to a noise floor at four least bits (on the right from the cursor line which is distanced from the start by $4.4\mu\text{s}$). Obviously, this ADC is not suitable for a single shot BPM.

* The work was done within a BASROC/ CONFORM/ EMMA Project, and was supported by the UK Science and Technology Facilities Council, and by Bergoz Instrumentation Ltd.

DESIGN OF A RESONANT STRIPLINE BEAM POSITION PICKUP FOR THE 250 MEV PSI-XFEL TEST INJECTOR

A. Citterio, M. Dehler, D.M. Treyer, B. Keil, V. Schlott, L. Schultz, PSI, Villigen PSI, Switzerland

Abstract

The 250 MeV PSI X-FEL Test Injector will use resonant stripline beam position monitor (BPM) pickup as standard BPMs to reach the desired single bunch resolution in the order of 10 μm in a charge range of 10 to 200 pC. This paper presents the electromagnetic design of the pickup that was performed with Microwave Studio. The pickup was optimized in terms of the main radiofrequency (RF) characteristics - frequency, shunt impedance, unloaded and loaded Q s - of the resonant modes of interest, in order to obtain the signal characteristics required by the electronics, that samples the pickup signals directly at 5 GSamples/s [1]. Mechanical aspects of the design are also presented, with particular attention to the tuning pin solution for stripline alignment. Based on the simulated geometry, one pickup prototype was built and tested and the correct characteristics of the resonant modes were verified.

OVERVIEW

To provide the desired position resolution in the ten micrometer range along the 250 MeV PSI-XFEL injector, about 25 standard beam position monitors are foreseen to measure and stabilize the beam position within $\sim 10\%$ of the final beam size. The choice of a 500 MHz resonant stripline pickup and a 5 GSample/s direct sampling electronics [1] based on existing PSI designs [2] allowed a cost-efficient solution and fast prototyping of pickups and electronics as well as of the digital signal processing firmware and software. At the desired bunch charge range from 200 pC down to 10 pC, resonant striplines are superior e.g. to button pickups since they concentrate the output signal spectrally at a high signal-to-noise ratio, thus enabling higher position resolution with narrowband processing, even for single shot operation and low bunch charges [3]. The main advantage over cavity pickups is the significantly reduced cost and development time especially for the electronics, since the low Q and comparatively low frequency allow direct sampling by the 5 GSample/s Domino Ring Sampler (DRS) chip of the BPM electronics, without the need for an analog mixer scheme or a low-jitter clock distribution [1]. A schematic sketch of four resonant stripline electrodes (two per plane) is depicted in Fig. 1.

This BPM topology supports four independent TEM eigenmodes of operation $\underline{V}_0 = (V_1, V_2, V_3, V_4)$:

- sum mode, or monopole mode: $V_{0,M} = \frac{1}{2}(1, 1, 1, 1)$
- two delta modes, or dipole modes: $V_{0,D_x} = \frac{1}{\sqrt{2}}(1, 0, -1, 0)$ and $V_{0,D_y} = \frac{1}{\sqrt{2}}(0, 1, 0, -1)$
- quadrupole mode: $V_{0,Q} = \frac{1}{2}(1, -1, 1, -1)$

02 BPMs and Beam Stability

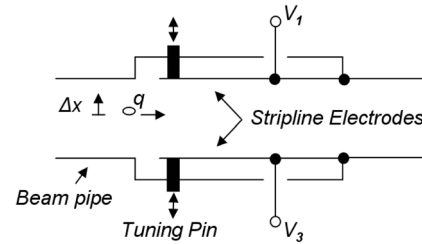


Figure 1: Resonant stripline pickup, one plane only.

The ratio of the signal voltages from opposing electrodes depends on the transversal beam position:

$$x \sim \frac{\Delta}{\Sigma} \text{ with } \Delta = (V_3 - V_1) \text{ and } \Sigma = (V_3 + V_1)$$

Each mode has a characteristic impedance and frequency spectrum that influences the BPM performance, representing the criteria for the pickup selection [4]. The pickup sensitivity, defined as the ratio of opposite voltages per beam offset in [dB/mm], is determined by the normalized shunt impedances and the loaded Q s:

$$S_x [\text{dB/mm}] \sim 20 \log(1 + 2s_x \cdot 1\text{mm}), \quad (1)$$

$$s_x [1/\text{mm}] \sim \sqrt{2 \frac{(R/Q)_{D_x} Q_{l,D_x}}{(R/Q)_M Q_{l,M}} \Big|_{x=1\text{mm}}} \quad (2)$$

The detection method employed is signal stretching by ringing filter, followed by direct sampling and digital envelope detection. To maintain high sensitivity of signal envelope voltage to beam position for the complete duration of the signal, the following conditions must be satisfied: at the appearance of the output signal $Q_{l,D}/Q_{l,M} \geq 1$, and the dipole and monopole frequencies must coincide, i.e. $f_D = f_M \pm 1 \text{ MHz}$. The frequency of the resonant stripline pickup was chosen equal to 500 MHz, which is well in the bandwidth range of the DRS4 sampler chip. The frequency choice also enabled easy adaptation of the design already used at the SLS linac and transfer lines [2], allowing electronics development and tests with existing SLS linac pickups while the new spectrally and mechanically improved pickup was being developed.

CONCEPTUAL DESIGN AND RESULTS

Prototype Design

Figure 2 shows geometry and mechanical solutions adopted for the prototype pickup.

IMPLEMENTATION OF AN FPGA-BASED LOCAL FAST ORBIT FEEDBACK AT THE DELTA STORAGE RING

P. Towalski*, P. Hartmann, G. Schuenemann, D. Schirmer, T. Weis, G. Schmidt, S. Khan
Zentrum fuer Synchrotronstrahlung DELTA, TU Dortmund, D-44221 Dortmund, Germany

Abstract

The beam orbit of the 1.5 GeV electron storage ring DELTA showed a variety of beam distortions with a pronounced frequency spectrum mostly caused by girder movements and ripples of the magnet power supplies. In order to enhance the orbit stability to at least 300 Hz bandwidth a global fast orbit feedback (FOFB) is under consideration. As a prototype an FPGA based local fast orbit feedback at a 10 kHz data acquisition rate has been developed. The digitized orbit data are distributed from I-Tech Libera and Bergoz MX-BPMs [1] to an FPGA board via a fibre interconnected network based on the Diamond Communication Controller [2]. The correction algorithm is written in VHDL and the corrections are applied with digital power supplies connected to the FPGA board through RS485 links. The first operational tests of the system achieved an effective damping of orbit distortions up to 350 Hz. The paper will give an overview on the layout of the FPGA-based local orbit feedback system, will report on the results of the measured uncorrected orbit distortions at DELTA and the stability enhancements that could be achieved by the local feedback system.

INTRODUCTION

The beam stability at the storage ring Delta is affected by low frequency distortions during the ramp of our booster BoDo and beam oscillations caused by mains power supplies generating distortions with the frequency of 50 Hz and its harmonics up to approx. 350 Hz. Furthermore girder movements at their resonance frequencies, excited by ground vibrations, lead to displacements of magnetic elements of the accelerator, particularly the quadrupoles and therefore deteriorate the photon beam stability at the beam lines. In order to supply higher brilliance synchrotron radiation a global fast orbit feedback is under consideration in connection with the existing slow orbit feedback working at frequencies at about 0.1 Hz. For this reason a local fast orbit feedback in the vertical plane (see Fig. 1) has been developed to prove the feasibility of the planned feedback and to test designated methods and components.

LOCAL ORBIT BUMPS

The dependency between the corrector strength θ_j at the corrector j and the orbit z_i at position i can be described

*patryk.towalski@udo.edu

02 BPMs and Beam Stability

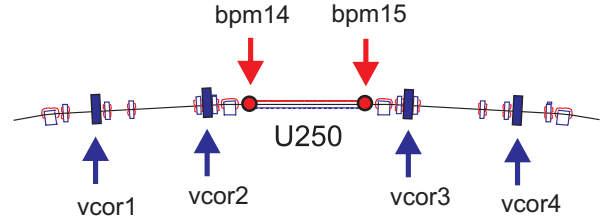


Figure 1: Setup of the vertical fast local orbit feedback at DELTA consisting of an undulator (U250), two beam position monitors (BPMs) and four vertical correctors (vcor).

using the orbit response matrix \mathbf{R} :

$$R_{ij} = \frac{\partial z_i}{\partial \theta_j} \quad (1)$$

The calculation of the expected orbit \vec{z} can be achieved by superposing the effects of all corrector θ_j :

$$\vec{z} = \mathbf{R} \vec{\theta}. \quad (2)$$

Using the technique of singular value decomposition (SVD) the calculation of a pseudoinverse is possible even if \mathbf{R} is a singular matrix. The corrector strength θ_j for given orbit \vec{z} is then directly derived from the pseudoinverse \mathbf{R}^+ of the response matrix \mathbf{R} via:

$$\vec{\theta} = \mathbf{R}^+ \vec{z}. \quad (3)$$

The vector \vec{z} represents the required orbit, the vector $\vec{\theta}$ represents the best approximation of the appropriate corrector strength to apply. Appropriate in the sense of being the best solution is achieved by the method of a least square fit. The superposition of two orbit bumps using four correctors allows for the adjustment of the orbit at bpm14 and 15. The bumps are created with the correctors vcor1 to vcor4 (see Fig. 1) mounted at appropriate positions [3].

A response matrix \mathbf{R} for all of the 54 BPMs and four correctors was measured with beam. In a next step the pseudoinverse of \mathbf{R} was used to calculate the corrector coefficients for the two orbit bumps using four correctors. Orbit bump induced crosstalk between bpm14 and bpm15, as well as the influence on the orbit outside the feedback section was less than 10 %, verified at 7 control BPMs.

ORBIT DISTORTIONS

To identify the typical orbit distortions, a frequency spectrum was created from decimated turn-by-turn data

A RESONANT FIRST TURN BPM FOR THE POSITRON INTENSITY ACCUMULATOR (PIA) AT DESY

M. Hüning[#], R. Jonas, J. Lund-Nielsen, F. Schmidt-Föhre, DESY, Hamburg, Germany

Abstract

The Positron Intensity Accumulator PIA at DESY is used to accumulate the intensity and damp down the emittance of the positrons produced in the Linac II before they are injected into DESY II. Up to 13 shots are collected and damped. During the damping process the (base band) peak current is increased by about a factor 4. Therefore the signal from the circulating beam can be up to 50 times bigger than the injected beam and hence overload any first turn detectors. The injected beam however is bunched by the 3 GHz RF of the linac. By filtering the 3 GHz component of the antenna signal and subsequent demodulation it is possible to set up a BPM system detecting exclusively the injected beam.

INTRODUCTION

The Linac II at DESY is an electron-positron linac delivering beams of 450 MeV. In order to reduce the transversal and longitudinal emittances of the beam it is injected into the accumulator and damping ring PIA [1]. PIA is a small ring with approximately 28 m of circumference. The revolution frequency therefore is 10.4 MHz. It is an octagon with 2 stretched and 2 shortened straights. Injection takes place in one of the short straights. The eight dipoles are combined function magnets and in addition there are 4 horizontally focusing and 4 horizontally defocusing quadrupoles. Each of the dipole chambers contains a button BPM. These BPMs and their readout however are optimized for measuring the closed orbit with 10.4 MHz bunches. Sufficient accumulations and damping are required in order to obtain a usable signal.

For monitoring the energy at the end of the Linac it is desirable to measure the beam position of the injected beam at a position with large dispersion. A suitable position for this is the first long straight, approximately 7 m from the injection septum. Here the dispersion is the largest and there is sufficient space to install a new BPM. It was decided to use a BPM of the PETRA III type [2]. This is a button type BPM with a large bandwidth.

SETUP

In order to separate the signal of interest from noise and the low frequency signal of the circulating beam, the pickup signal is first band-pass filtered (Figure 1). With a cavity-type BPM this could have been achieved directly at the source. But this would have required a completely new design while the PETRA III type BPM could be used with only minor modifications. The BPM has a diameter of approximately 98 mm.

The buttons are arranged with an angle of 45° to the usual coordinates of x and y. In this way the electrodes are less likely to be hit by stray particles from the low energy tail of the injected beam. The beam position then has to be calculated from a linear combination of the rotated coordinates.

By mixing with a 3.375 GHz reference the signal is converted to 375 MHz. The exact frequency and phase of the reference is not important as long as it is the same for all buttons. The signal is further improved by low-pass filtering and subsequent amplification. Finally it is fed into the actual BPM electronics.

The beam position is processed by readout electronics of the AM/PM type [3]. It was originally designed for the FLASH linac. In the AM/PM electronics a difference in voltage is translated into a phase difference of two normalized signals. In this way the BPM signal becomes independent of the beam current over a large dynamic range.

Given the high operating frequency of 3 GHz a phase shift between the individual buttons is likely. With a simplified model of the BPM it was calculated that a phase shift between corresponding buttons causes a reduction of the linear range of the BPM. The tolerable phase shift however was found to be up to 60° which can be achieved with a careful setup. With this phase shift the deviation of the measured from the real beam position increases from 1 mm to 2 mm at a beam position of 10 mm.

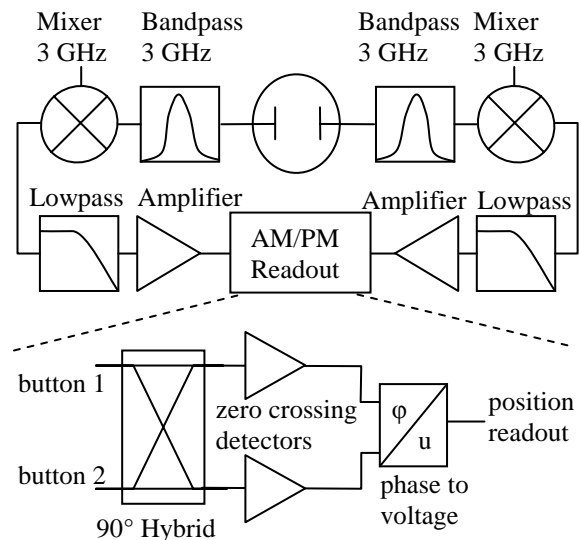


Figure 1: Block diagram of the BPM readout.

[#]markus.huening@desy.de

COMPARATIVE STUDIES OF RF BEAM POSITION MONITOR TECHNOLOGIES FOR NSLS II*

O. Singh[#], I. Pinayev, NSLS-II Project, BNL, Upton, NY 11973, U.S.A.
G. Decker, B.X. Yang, APS, ANL, Argonne, IL 60439, U.S.A.

Abstract

Sub-micron beam stability is a necessary performance requirement for the NSLS II light source, a substantial challenge testing the limits for currently available RF beam position monitoring methods. Direct performance comparisons between commercially available BPMs and Advanced Photon Source in-house developed BPM were made at the APS storage ring. Noise floor, fill pattern dependence, and intensity dependence were investigated and correlated with photon diagnostics at the beam diagnostic beamline at APS sector 35. Key results are presented.

INTRODUCTION

The comparative tests of different BPM receivers were performed at APS. The key features of the experimental arrangement are shown in Figure 1. The Libera Brilliance receiver [1] was connected to the S36A:P0 BPM station in the diagnostics straight. An in-house built APS FPGA-based BPM receiver [2] was connected to the S35B:P0 BPM station. Both stations use 4-mm diameter pick-up electrodes mounted on an 8-mm high vacuum chamber of a diagnostics undulator. Horizontal separation of the buttons is 9.6 mm center-to-center. Separation between 35B:P0 and 36A:P0 is about 4 meters. Bergoz electronics [3] was used for S35B:P1 and S36A:P1 equipped with 10-mm buttons mounted on the approximately 4x8 cm elliptical vacuum chamber.

At a distance of 30.045 meters from the center of the ID straight is a vertically moveable horizontal slit, and at 29.5 meters is a horizontally moveable vertical slit. Both the slit size and center are adjustable with high accuracy using stepper motors. The beamline uses an hourglass-shaped beryllium window to separate the ring vacuum from the beamline vacuum. By using this shape, heat is more efficiently removed, albeit at the expense of transmogrifying the transverse profile of any transmitted photon beam.

The slit assemblies are accessible and their motion can easily be calibrated against a reference dial indicator to quantify mechanical motion. Preliminary measurements indicate backlash at the level of 20 microns, although there are indications that repeatability is significantly better than this, below 5 microns.

Both horizontal and vertical calibrations were performed at 35-ID. The main idea was to independently determine the absolute calibration of S35B:P1 and S36A:P1 from the slit/flux monitor combination, and

compare the results with the lattice model.

Because S35B:P0 and S36A:P0 used experimental electronics, they have not been calibrated against the ring model. Instead, the local bump scans provide absolute calibration data for these electronics, in addition to supplying absolute calibration data for the front-end photon BPMs.

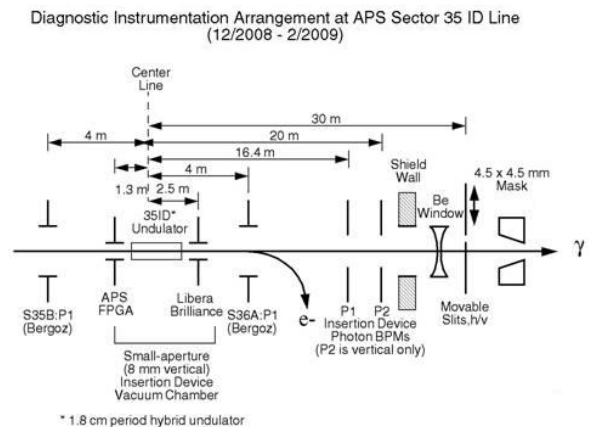


Figure 1: Diagnostics arrangement for 35-ID source point. Distances are approximate.

OBSERVING NOISE SPECTRUM OF CIRCULATING BEAM

During studies the Libera Brilliance signal level was manually set and direct measurement (no switching) was selected. The APS FPGA-based BPM receivers were in routine configuration. 262144 data points at a revolution frequency of 271.6 kHz were collected for both devices and the observed horizontal beam motion spectra are shown in Fig. 2.

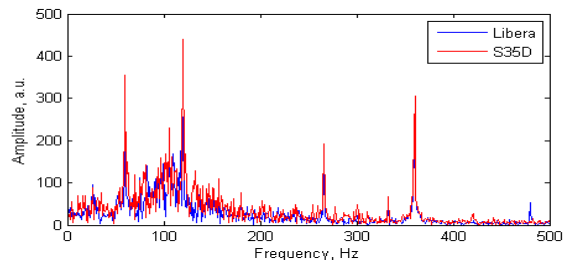


Figure 2: Overlaid spectra of beam motion in the horizontal plane. The data are from both Libera Brilliance and FPGA based receiver.

Excellent agreement of the two sets of data was found. The finest details are a perfect fit (see Fig. 2-4).

* Work supported by U.S. Department of Energy, Office of Science, Office of Basic Energy Sciences, under Contracts DE-AC02-98CH10886 and DE-AC02-06CH11357.

[#]singh@bnl.gov

PERFORMANCE OF EXPONENTIAL COUPLER IN THE SPS WITH LHC TYPE BEAM FOR TRANSVERSE BROADBAND INSTABILITY ANALYSIS*

R. de Maria, BNL, Upton, New York, J.D. Fox, SLAC, Menlo Park, California, USA
 W. Höfle, G. Kotzian, G. Rumolo, B. Salvant, U. Wehrle, CERN, Geneva, Switzerland

Abstract

We present the performance and limitations of the SPS exponential coupler [1] for transverse instability measurements with LHC type beam. Data were acquired in 2008 in the SPS in the time domain with a bandwidth of up to 2.5 GHz. The data were filtered to extract the time evolution of transverse oscillations within the less than 5 ns long LHC type bunches. We describe the data filtering techniques and show the limitations of the pick-up due to propagating modes.

INTRODUCTION

Two types of transverse instabilities limit the single bunch intensity of proton beams in the SPS. On the one hand with multi-bunch beams such as the LHC nominal beam with 25 ns bunch spacing the electron-cloud instability limits the maximum intensity per bunch [2]. On the other hand for very high bunch intensities the single bunch transverse mode coupling instability (TMCI) is a limitation as well [3]. Common to both instabilities is the appearance of high frequency signals caused by oscillations within the bunch. Diagnostics to probe the nature of the instabilities, their spectral components and time evolution must be able to resolve oscillations within the bunch.

Due to the relevance of the electron cloud driven instability and its adverse effect on the transverse emittance (blow-up) and because some of the LHC upgrade scenarios beyond ultimate luminosity call for bunch intensities higher than the LHC ultimate bunch intensity of 1.7×10^{11} protons per bunch where the TMCI may limit performance, an R&D program was launched to optimally diagnose and possibly cure these transverse single bunch instabilities by a wide band transverse feedback system [4].

The quest to adequately diagnose the instabilities motivated the analysis of existing pickup/kicker structures in the SPS and to evaluate their performance.

Exponential couplers were built and installed in the SPS [1] and are readily available. A fast digital oscilloscope was used to acquire the data from the pick-up with offline post processing to correct for imperfections, in order to evaluate the pick-up performance and provide the means to accurately diagnose the instabilities.

In the following we present the results of these activities, explain the elements of the acquisition chain, show some sample measurements and discuss the post processing methods. Conclusions are drawn and future plans outlined.

EXPONENTIAL PICKUP AND ACQUISITION CHAIN

The main component of the acquisition chain is a stripline pickup where the stripline has s -dependent (s being the coordinate in beam direction) width that translates in an s -dependent coupling constant. The distance of the stripline from the vacuum chamber diminishes as the width decreases such as to preserve a constant line impedance of 50Ω . If the coupling, i.e. the electrode shape, is exponential the resulting transfer function is almost flat in amplitude instead of having the typical notches of a constant width stripline pick-up. The absolute value of the transfer function in frequency domain is [1]

$$|F(\omega)| = \frac{K\omega l/c}{\sqrt{a^2 + \frac{4\omega^2 l^2}{c^2}}} \sqrt{1 + e^{-2a} - 2e^{-a} \cos(2l\omega/c)} \quad (1)$$

and the phase is

$$\text{Arg}\{F(\omega)\} = \arctan \left[\frac{2\frac{\omega l}{c} \sin \frac{2\omega l}{c} + a(e^a - \cos \frac{2\omega l}{c})}{2\frac{\omega l}{c} (e^a - \cos \frac{2\omega l}{c}) - a \sin \frac{2\omega l}{c}} \right] \quad (2)$$

where l is the kicker length, K a coupling constant and a is describe the exponential tapering ([1]). We assumed ultra-relativistic beams, $v = c$. Normally the pick-up is installed with the beam passing the wide end of the strip first, we will call this *forward* installed. A backward installed coupler has the beam interacting the narrow end of the strip first. Note that the coupler is directional and signals are always extracted at the upstream ports.

A drawback of the exponential coupler is its nonlinear phase response, but it can either be corrected by numerically filtering the data or in the case of a pickup-kicker combination one can take advantage of the mirrored phase response for a backwards installed coupler. With one coupler (kicker or pick-up) installed backward and the other forward we expect to compensate for an overall linear phase response.

The pickup has four electrodes at ± 45 degrees to the horizontal plane which allow to measure both bunch intensity, as well as horizontal and vertical displacement. In the SPS there are a total of four such pickups installed, two usually cabled for horizontal operation and two for vertical operation. The tests concentrated on the vertical observations, plane in which the electron cloud effect causes a high frequency instability.

The pickup could not be tested on a bench, but we measured with a network analyzer the properties of the electrodes, cables and hybrids. The installation orientation of

* Work supported by DOE and CERN

DESIGN OF THE STRIPLINE AND KICKERS FOR ALBA

U. Iriso*, T.F. Günzel and F. Pérez
CELLS, Ctra. BP-1413 Km 3.3, 08290 Cerdanyola, Spain

Abstract

The design of stripline kickers shall be adapted to match the line impedance, maximize the effective beam kick, reduce the heat load and minimize the transverse coupling impedance. These kickers are used for either tune measurements or transverse feedback. We describe the ALBA design of these kickers for the Storage Ring.

INTRODUCTION

The term “striplines” refers to a configuration of longitudinal electrodes that may be used either as beam pickup (to extract information about the beam motion), or beam kickers (to change its motion). Their design should be taken with due care. The electrodes must be adapted to match the line impedance, reduce heat load, and minimize the transverse coupling impedance. Moreover, when used as active devices, we shall maximize the beam kick efficiency.

ALBA has designed different stripline kickers. In the following we use the word “striplines” to the combination that allows the dual purpose of beam pickup and beam excitation, and “kicker” to the one used only to excite the beam. The two designs are:

- Storage Ring Stripline: only one unit is installed in the machine. Its purpose is to provide the beam excitation for tune measurements. In early phases of the commissioning, this unit will be also used for tune measurements. Thus, its length is $\lambda/4$, being λ the bucket length ($\lambda = 2$ ns in our case). See Fig. 1, left.
- Feedback Kickers: in order to cure the fast transverse instabilities, we will install two of these kickers (horizontal and vertical). See Fig. 1, right. Since their purpose is only beam excitation, their length is $\lambda/2$.

In this report we describe the steps followed for the design of these devices.

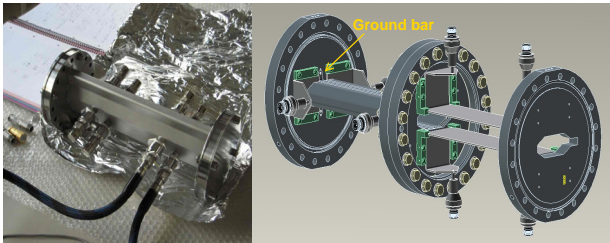


Figure 1: Stripline (left) and hor and ver kicker (right).

* ubaldo.iriso@cells.es

STORAGE RING STRIPLINE

In this case, we design a four-electrodes striplines for either beam measurement or beam excitation. We describe the line impedance matching, the effective kick produced by the stripline, and its coupling impedance.

Line Impedance Matching

First, the electrodes shall be matched to the line impedance. A four-electrode stripline supports 4 independent TEM eigenmodes: sum, dipole horizontal, dipole vertical, and quadrupole modes (see Fig. 2. left). Typically, when the purpose of a stripline is the beam position measurement, these devices are designed using the traditional sum-mode matching with wide electrodes to maximize the beam signals [1]. For the dual purpose case, we have adopted the compromise relation [1]:

$$Z_L = Z_{\text{dipole}} = \sqrt{Z_{\text{sum}} Z_{\text{quad}}} \quad (1)$$

where $Z_L = 50\Omega$, and we have assumed that the hor and ver dipole modes are identical (which, as seen “a posteriori”, is a good approximation).

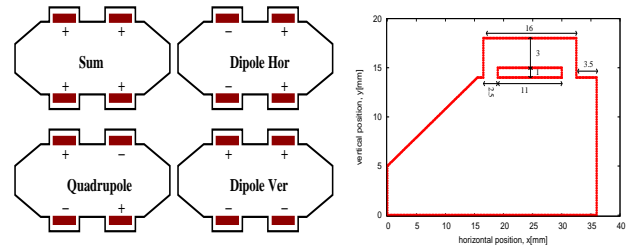


Figure 2: Independent modes in a four-electrode stripline (left), and geometry of one fourth of it (right).

For symmetry reasons and because of the low coupling between the strips, the differences between the 4 aforementioned modes can be neglected and it is common to focus the study on one fourth of the vacuum chamber [2]. As the results will show (see Table 1), this is not a bad approximation. Each of these eigenmodes has a characteristic impedance that can be easily computed with simple transverse 2-d electrostatic codes (in this case, we use SUPERFISH). The final geometry for one fourth of the vacuum chamber is shown in Fig. 2, right.

The results for the 4 modes are shown in Table 1. Note that $\sqrt{Z_{\text{sum}} Z_{\text{quad}}} = 51.16\Omega$, and so the last condition in Eq. 1 is fulfilled with $\sim 2\%$ of discrepancy.

HIGH RESOLUTION BPMS WITH INTEGRATED GAIN CORRECTION SYSTEM*

M. Wendt[#], C. Briegel, N. Eddy, B. Fellenz, E. Gianfelice, P. Prieto, R. Rechenmacher, D. Voy,
Fermilab, Batavia, IL 60510, U.S.A.

N. Terunuma, J. Urakawa, KEK, Tsukuba, Japan

Abstract

High resolution *beam position monitors* (BPM) are an essential tool to achieve and reproduce a low vertical beam emittance at the KEK *Accelerator Test Facility* (ATF) damping ring. The ATF *damping ring* (DR) BPMs are currently upgraded with new high resolution read-out electronics. Based on analog and digital down-conversion techniques, the upgrade includes an automatic gain calibration system to correct for slow drift effects and ensure high reproducible beam position readings. The concept and its technical realization, as well as preliminary results of beam studies are presented.

INTRODUCTION

The generation and preservation of low emittance beams is mandatory to achieve a high luminosity in the next generation linear acceleration-based lepton collider for *high energy physics* (HEP). Therefore, the damping and extraction of electron beams with ultra-low vertical emittance of < 2 pm is a mission critical goal [1], and has to be demonstrated at the damping ring of the KEK Accelerator Test Facility (ATF) [2]. This requires various optimization methods to steer the beam along an optimum (“golden”) orbit with minimum disturbance of non-linear field effects. A high resolution BPM system is one of the important tools; it needs to meet as initial specifications

- A resolution of ~ 100 - 200 nm in a “narrowband” mode.
- A high resolution (some μm) turn-by-turn measurement option.
- An automatic gain correction system, to compensate slow drift effects in the analog part of the read-out electronics – e.g. due to temperature variations, aging effects of components, etc.

The BPM concept was initiated as KEK/SLAC/Fermilab collaboration [3] in frame of the Global Design Initiative (GDI) of the International Linear Collider (ILC) activities. Today this ATF DR BPM upgrade collaboration is backed by Japan-US funds, with Fermilab as core partner.

As proof of principle prototypes and beam studies are performed on 20-of-96 BPM stations with new read-out hardware:

- 714MHz-to-15MHz downmix / calibration module (located in the ATF accelerator tunnel)

- VME-based digital signal processing and timing electronics, currently based on the commercial *Echotek* digital receiver (will be replaced by in-house digitizers).
- Various FPGA-firmware, control and diagnostics drivers and software (C++, VxWorks, Linux) and an EPICS interface to the ATF controls (V-system).

THE ATF DAMPING RING

The 1.2 GeV ATF damping ring is equipped with 96 button-style BPM pickups, and part of the Accelerator Test Facility (ATF) complex, which includes an S-Band electron linac, and an extraction beam-line (ATF2).

Table 1: ATD DR Machine and Beam Parameters

beam energy E	=	1.28 GeV
beam intensity, single bunch	\approx	~ 1.6 nC $\equiv 10^{10}$ e^- ($\equiv I_{\text{bunch}} \approx 3.46$ mA)
beam intensity, multibunch (20)	\approx	~ 22.4 nC $\equiv 20 \times 0.7 \cdot 10^{10}$ e^- ($\equiv I_{\text{beam}} \approx 48.5$ mA)
f_{RF}	=	714 MHz ($\equiv t_{\text{RF}} \approx 1.4$ ns)
f_{rev}	=	$f_{\text{RF}}/330 \approx 2.16$ MHz ($\equiv t_{\text{rev}} \approx 462$ ns)
bunch spacing t_{bunch}	=	$2/f_{\text{RF}} \approx 2.8$ ns
batch spacing	=	$t_{\text{rev}}/3 = 154$ ns
repetition freq. f_{rep}	=	1.56 Hz ($\equiv t_{\text{rep}} = 640$ ms)
beam time t_{beam}	=	460.41 ms ($\equiv 996170$ turns)
vert. damping time τ	\approx	30 ms
hor. betatron tune (typ.)	\approx	15.204 ($\equiv f_h \approx 441$ kHz)
vert. betatron tune (typ.)	\approx	8.462 ($\equiv f_v \approx 1$ MHz)
synchrotron tune	\approx	0.0045 ($\equiv f_s = 9.7$ kHz)

Table 1 lists some relevant machine and beam parameters of the ATF damping ring. In standard operation a single bunch is injected on axes from the S-Band linac. After ~ 200 ms all injection oscillations are fully damped, and the beam stays for another ~ 400 ms in the ring, before being extracted. Optional multi-batch / multi-bunch operation can be set up on a cycle-by-cycle basis (no extraction), with up to three equally spaced batches, each containing 1...20 bunches, spaced by 2.8 ns.

* This work supported by a high energy physics research program of Japan-USA cooperation, and by the Fermi National Accelerator laboratory, operated by Fermi Research Alliance LLC, under contract No. DE-AC02-07CH11359 with the US Department of Energy.

[#]manfred@fnal.gov

BPM SYSTEM UPGRADES IN THE PETRA III PRE-ACCELERATOR CHAIN DURING THE 2008 SHUTDOWN

F. Schmidt-Föhre, A. Brenger, G. Kube, R. Neumann, K. Wittenburg
Deutsches Elektronen-Synchrotron DESY, Hamburg, Germany.

Abstract

The new synchrotron light source PETRA III is powered by a chain of pre-accelerators including Linac II, PIA, transfer lines, and DESY II. The whole chain is equipped with upgraded versions of diagnostic systems that were installed during the 2008 shutdown. This paper presents the upgrade of the beam position monitor (BPM) systems at PIA together with the transfer lines and DESY II. All systems rely on the 'Delay Multiplex Single Path Technology' (DMSPT). It is demonstrated that the self-triggered design of the BPM electronics is specifically suited to the different needs of such a heterogeneous pre-accelerator chain. Structures and dependencies of the BPM systems will be described in detail.

INTRODUCTION

With the decision at DESY in 2004, to upgrade the injector storage ring PETRA II to a new high-brilliance 3rd generation synchrotron light source PETRA III, it was also decided to refurbish and upgrade the whole existing pre-accelerator chain during the 2008 shutdown [1]. This upgrade process also included the diagnostics systems in the pre-accelerators. Using different bunch patterns at a design beam current of 100mA, PETRA III will deliver brilliant synchrotron light for up to 14 user undulator beamlines. Minimum bunch spacings of 8ns (optional 4ns) are foreseen with 40ps long bunches in the multi bunch mode consisting of 960 equally spaced bunches ($f_{RF} = 499.6645$ MHz, $f_{revolution} = 130.1$ kHz).

To ensure stable top-up operation for PETRA III, the chain of pre-accelerators has to maintain stable conditions for bunch injection including controlled high timing accuracy and reasonably low emittance in the transfer line (E-Weg). This was accomplished by the refurbished and partly renewed pre-accelerator diagnostic systems, in particular using upgraded versions of DMSPT-type button-type BPM systems in most of the sections. This article gives an overview over these upgrades in the individual pre-accelerator sections, which were upgraded specifically taking into account their specific demands.

PREACCELERATOR BPM SYSTEMS

The PETRA injector chain is illustrated in Fig. 1. It consists of five different sections: (i) the injector Linac II (450MeV, 2,998GHz) which is used for positron and electron acceleration, (ii) the Positron Intensity Accumulator ring PIA (10,4 MHz/125 MHz, 450 MeV) which serves for intensity accumulation and re-formation of the linac time structure to match the subsequent synchrotron DESY II, (iii) the intermediate transfer line (L-Weg), (iv) the booster synchrotron Desy II which is

used to accelerate single bunches up to a particle energy of 6 GeV, and (v) the transfer line (E-Weg) towards Petra III.

BPM UPGRADE DESIGN GOALS

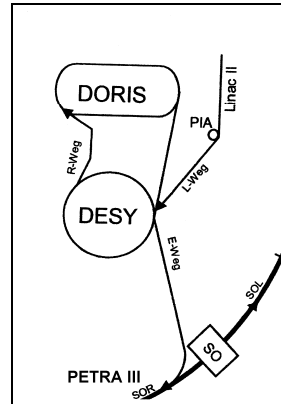


Figure 1: Petra III preaccelerator chain at DESY (Linac II, PIA, L-Weg, DESY II, E-Weg).

Prior to the upgrade in 2008, the DESY II booster synchrotron already used 24 BPM systems, while all other preaccelerator sections were not equipped with BPMs for regular operation before. Therefore an implementation of electrostatic button BPMs at certain accelerator and transport in positions defined by the accelerator optics was desired. The schedule for the upgrade of DESY II contained the refurbishment of the 24 existing button-type BPM chambers, buttons, cabling, and discrete signal conditioning front-end electronics.

In addition, the accumulation in PIA and the energy ramping in DESY II put high demands on the dynamic measuring range of the associated BPM systems. Before the upgrade, the existing BPM system of DESY II was designed to measure the maximum BPM signal level in the upper ADC count range with fixed input signal attenuation. Therefore low level input signals could not be measured. The upgraded BPM electronic system is intended to be able to cope with the high dynamic BPM signal ranges, enabling measurements in the full dynamic range of the BPM input signal.

For control of the injection process, the accumulation and energy ramping procedures in the circular accelerators, other types of measurements called '1st-turn' and 'turn-by-turn' were desired. Those kind of measurements store the BPM button signal information at each of the BPMs for a certain number of individual turns, delivering a turn-by-turn beam position history when reading the turn buffers of the BPM electronics. This operation mode can also be used for tune measurements.

SNS BEAM DIAGNOSTICS: PRESENT STATUS AND FUTURE PLANS

A. Aleksandrov, Oak Ridge National Laboratory, Oak Ridge, TN 37830, USA

Abstract

The Spallation Neutron Source accelerator systems will deliver a 1.0 GeV, 1.4 MW proton beam to a liquid mercury target for neutron scattering research. The accelerator complex consists of an H- injector, capable of producing one-ms-long pulses at 60 Hz repetition rate with 38 mA peak current, a 1 GeV linear accelerator, an accumulator ring and associated transport lines. The accelerator systems are equipped with variety of beam diagnostics. The beam diagnostics played important role during beam commissioning, they are used for accelerator tuning and monitoring beam status during production runs. The requirements to the various diagnostics systems are changing in the process of beam power ramp up. This talk will give an overview of the evolution of the major SNS beam diagnostics systems: commissioning, operation, power ramp up, and power upgrade.

INTRODUCTION

The SNS accelerator complex consist of an H⁻ injector, capable of producing one-ms-long pulses with 38 mA peak current, chopped with a 68% beam-on duty factor and a repetition rate of 60 Hz to produce 1.6 mA average current, an 87 MeV Drift Tube Linac (DTL), a 186 MeV Coupled Cavity Linac (CCL), a 1 GeV Super Conducting Linac (SCL), a 1 GeV Accumulator Ring (AR), and associated transport lines. After completion of the initial beam commissioning at a power level lower than the nominal, the SNS accelerator complex is gradually increasing the operating power with the goal of achieving the design parameters in 2009. Results of the initial commissioning and operation experience can be found in [1]. The SNS Power Upgrade Project (PUP) [2] aims at doubling the beam power by increasing SCL and AR beam energy to 1.3 GeV and peak current in the linac to 59 mA. The SNS baseline design included diverse suite of beam diagnostics [3], which, in main part, were brought on line simultaneously with other accelerator systems and played crucial role in fast and successful SNS commissioning and power ramp up. As the SNS operation is shifting more and more toward neutron production for users the roles and requirements for the beam diagnostics are changing as well. This paper describes the status and development plans for the major beam instrumentation systems.

BEAM INSTRUMENTATION ROLES

The beam time in the SNS operational schedule is divided in free parts: neutron production, machine tune up for production, and machine study periods.

Neutron Production Period

The neutron production period currently takes 80% of the scheduled beam time and this fraction is increasing steadily. The most important performance metric during this period is beam availability. Therefore only systems directly involved in beam delivery are of high importance. Beam instrumentation systems triggering the Machine Protection System (MPS) fall in this category. These include the Beam Loss Monitors (BLMs), distributed along the accelerator, the beam-in-gap detector (CHUMPS) in the Medium Energy Beam Transport (MEBT) line responsible for detection of the MEBT chopper failure, the Differential Beam Current Monitor (DBCM) protecting the MEBT chopper target, the beam dump current detectors (NCDs) protecting beam dumps from excessive power, and the beam current on target monitor (BCM25) monitoring beam power delivered to the neutron target. These systems have to operate at the beam rate up to 60 Hz and if any one fails the beam in the machine is inhibited.

Machine Tune Up Period

The machine tune up period is required after each maintenances period and currently takes about 10% of the scheduled beam time. If any one or even several systems fail operation is still possible. The most important performance metric during this period is accuracy of data, easy of use (user friendliness), and speed. Operators should be able to perform tune up as quickly as possible with as little support from diagnostics experts as possible. The main systems for machine tune up are the Beam Position and Phase Monitors (BPMs) and the Wire Scanners (WSs). These systems have to operate at a reduced pulse rate of 1-2 Hz. The BLMs are also used for the fine tuning of the losses.

Machine Study Period

About 10% of the scheduled beam time is dedicated for the machine study. All available diagnostics could be used during this period. If any one or even several systems fail operation is still possible. The most important performance metric during this period is accuracy of data. Physicists usually do measurements often with help from diagnostics experts. Some of the diagnostics systems for machine study can be of experimental nature or in prototype stage of development. Beam halo and transverse profile measurements in the ring are examples of such systems. These systems are required to operate at a reduced pulse rate of 1-2 Hz.

EMITTANCE MEASUREMENT DEVICES IN THE MUON IONIZATION COOLING EXPERIMENT

P. Kyberd, School of Engineering and Design, Brunel University, UK (for the MICE Collaboration)

Abstract

The Muon Ionisation Cooling Experiment (MICE) at the ISIS[1] accelerator located at the Rutherford Appleton Laboratory will be the first experiment to study muon cooling with high precision. The proposed operation of the experiment is described, and performance measurements on the crucial detector components are presented.

THE MICE EXPERIMENT

Introduction

The MICE experiment is designed to measure the performance of a cooling channel based on the design from Study II for a Neutrino Factory[2].

In this design the muon beam is passed through a series of absorbers of low atomic number to reduce the muon energy, each absorber followed by a set of RF cavities working at 201.25 MHz which accelerate the beam to the original energy. In MICE a small part of this cooling channel will be tested by measuring precisely the momentum and position of each muon as it enters and leaves the channel. From these measurements an input beam of given emittance can be synthesised[3] and the emittance of the resulting output beam measured. The results will allow a reliable prediction of the performance of the full channel. A set of plates of varying thickness (diffuser) placed just before the first emittance measurement is used to vary the incoming beam characteristics and allow a wider range of input beams to be synthesised.

The experiment runs parasitically in ISIS, by dipping a titanium target into the beam. The structure of the ISIS beam imposes constraints on the operation of the MICE target and beamline. ISIS runs at 50Hz and during each cycle a few $\times 10^{13}$ protons are injected into the ring and accelerated over the following 10ms to 800 MeV. If the titanium target enters the beam too early very few pions are produced and the beam is severely disrupted by energy loss and multiple scattering; thus the target can only intersect the beam during the last one to two milliseconds. The target is only dipped once per second, to minimise the disruption to other ISIS users. The required event rate of 600 muons per second then requires a readout and detector system capable of operating at MHz. We must be able to determine the phase of the RF in the cavities as the muons pass through the cavities, which requires sub nanosecond timing.

01 Overview and Commissioning

Overview

A schematic of the MICE beam and cooling channel is shown in Figure 1. The interactions of the protons with the target produce a spray of pions. The pions at 25° are focussed by a triplet and then bent to enter a superconducting solenoid which projects through the wall of the machine hall. Muons produced by pion decay in the solenoid are captured by the field and enter the MICE hall, where they are bent, focussed by two additional triplets and then enter the MICE cooling channel. Two Cerenkov counters, used for particle identification, are placed before the channel; a scintillator based timing system is placed before and after the channel and used as part of the particle identification system and for the timing with respect to the RF phase. Finally a ranger is used to confirm the identity of particles which traverse the full channel.

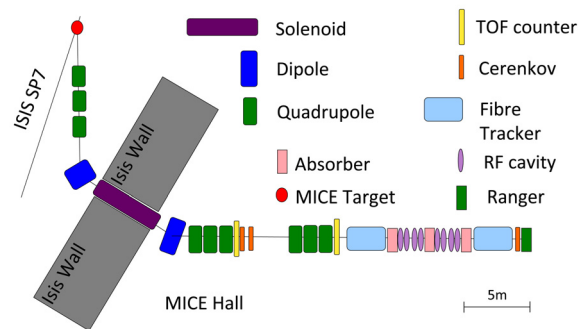


Figure 1: Schematic of MICE beam and cooling channel.

Muon Production

Once per second the MICE target is dipped into the beam. It was a titanium blade of length 35 mm which presents a target 1 mm wide and 10 mm deep. Simulations[4] show that 1.4×10^{12} protons must intercept the target in order to generate a flux of 600 good muons per target dip. (Good muons refer to those which are captured by the MICE beam line and traverse the whole cooling channel). Studies in 2006 allowed us to measure the external diameter of the beam and show that the target was capable of intercepting the beam during the last two milliseconds of the cycle and still clear the beam envelope before the next pulse. The number of muons produced can be varied by adjusting either the timing of the start signal or the depth of travel.[5]

AN OVERVIEW OF THE PROPOSED BEAM DIAGNOSTIC FOR ASTRID2

J.S. Nielsen[#], N. Hertel, S.P. Møller

ISA, Aarhus University, Ny Munkegade 120, 8000 Aarhus C, Denmark.

Abstract

This paper presents an overview of the proposed beam diagnostics for ASTRID2, the new 580 MeV 3rd generation low-emittance synchrotron light source to be built in Aarhus, Denmark. ASTRID2 will use the present ASTRID1 as booster, permitting full energy injection and thereby top-up-operation. The diagnostics will include viewing screens, beam current monitors, electronic beam position monitors, striplines, etc. The description includes both the storage ring and the transfer beam line.

INTRODUCTION

There has been a tremendous development of synchrotron radiation sources over the last two decades since ASTRID1 [1-3] was built. The biggest quantum leap possible came with the introduction of undulators, whereby the photon rate on a target increased by many orders of magnitude. ASTRID1 was not original equipped with insertion devices, although one undulator has been retrofitted. Therefore we have wanted to build a modern machine in Aarhus for several years. This has now become possible through a grant from the Danish government.

Table 1: Main parameters of the ASTRID2 storage ring compared to ASTRID1

	ASTRID2	ASTRID1
Energy [MeV]	580	580
Circumference [m]	45.704	40.00
Current [mA]	200	200
Revolution time [ns]	152.45	133.40
Length of straight sections [m]	2.7	
Number of straight sections	4	1
Horizontal tune	5.23	2.22
Vertical tune	2.23	2.63
Natural emittance [nm]	13	140

The main parameters of the ASTRID2 storage ring are shown in Table 1, together with the corresponding parameters for ASTRID1 as comparison. The major differences are the emittance, which is about ten times smaller for ASTRID2, and the number and length of straight sections. ASTRID2 will allow for 4 insertion devices, as opposed to ASTRID1's single.

The other marked difference is that ASTRID2 will have

full-energy injection, and hence top-up operation will be employed. This will in many ways make the machine much more stable. The current will be stable, which means that the Synchrotron Radiation (SR) intensity will be constant. And since the heat load will also be constant, it will be much easier to keep the beam parameters stable, such as the beam positions.

TRANSFER BEAM LINE

The primary purpose of the beam diagnostic in the transfer beam line is to facilitate easy steering of the beam through the beam line, with good transfer efficiency. Since ASTRID1 has not been designed as a rapid cycling booster, the injection rate will be slow (≤ 0.1 Hz). It is therefore even more essential to have the proper diagnostic and tools to help steering the beam from ASTRID1 to ASTRID2.

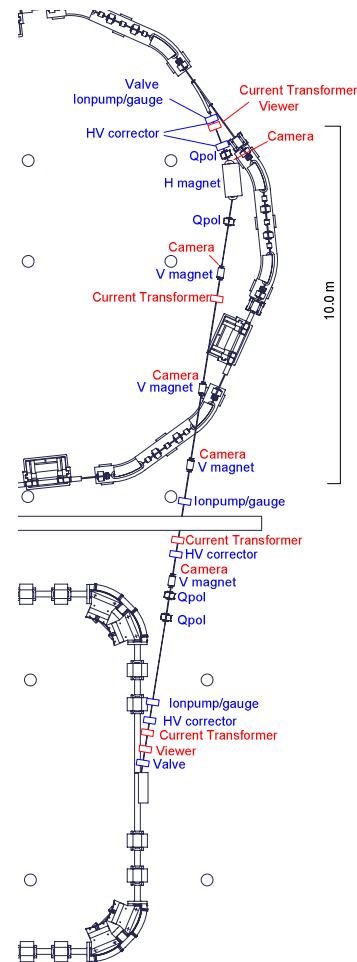


Figure 1: Layout of the transfer beam line from ASTRID1 to ASTRID2.

[#]jsn@phys.au.dk

THE TRANSVERSE AND LONGITUDINAL BEAM CHARACTERISTICS OF THE PHIN PHOTO-INJECTOR AT CERN

O. Mete, CERN, Geneva and EPFL, Lausanne, Switzerland

E. Chevallay, A. Dabrowski, S. Doebert, K. Elsener, V. Fedosseev, T. Lefèvre, M. Petrarca, CERN, Geneva, Switzerland

D. Egger, EPFL, Lausanne, Switzerland; R. Roux, LAL, Orsay, France

Abstract

The laser driven RF photo-injectors are recent candidates for high-brightness, low-emittance electron sources. One of the main beam dynamics issues for a high brightness electron source is the optimization of beam envelope behavior in the presence of the space charge force in order to get low emittance. Within the framework of the second Joint Research Activity PHIN of the European CARE program, a new photo-injector for CTF3 has been designed and installed by collaboration between LAL, CCLRC and CERN. Beam based measurements have been made during the commissioning runs of the PHIN 2008 and 2009 including measurements of the emittance, using multi-slit technique. The demonstration of the high charge and the stability along the long pulse train are between the goals of this photo-injector study as also being important issues for CTF3 and the CLIC drive beam. In this work the photo-injector will be described and the first beam measurement results will be presented and compared with the PARMELA simulations.

INTRODUCTION

A photo-injector was proposed as a new electron source for CTF3 (CLIC Test Facility 3) and later for the CLIC (Compact Linear Collider) drive beam [1, 2]. After the installation of the PHIN photo-injector at CERN, the longitudinal and the transverse properties of the commissioning beam have been measured in a range of parameters. In laser-driven RF photo-injectors the transverse phase space dynamics are influenced by several issues like time dependency of the RF field, space charge effects and transverse focusing. The adjustment of the laser properties such as spot size, radial and temporal distribution can effectively be used to control the properties of the beam in both directions. During the high charge operation at low energies, the space charge force is the dominating effect for emittance growth. The space charge effect can be compensated with the field created by a focusing magnet. The laser spot size dependence of the transverse size and emittance of the beam has been investigated for the laser spot sizes of 2 mm, 3 mm and 4 mm. The transverse emittance was measured with the multi-slit method in a range of focusing magnet current to study the emittance compensation. This method is applicable to the low energy, space charge dominated beams [3, 4].

01 Overview and Commissioning

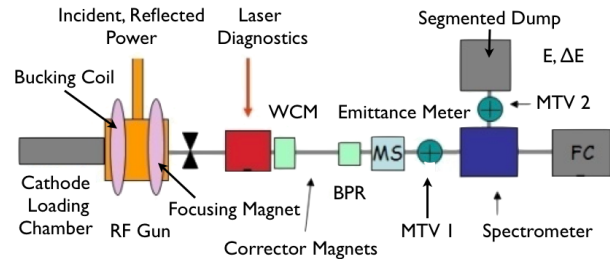


Figure 1: The PHIN photo-injector layout.

SET-UP

The beamline consists of three sections, cathode transfer chamber, RF gun and the beam measurements section (see Fig. 1). A semiconductor Cs₂Te cathode was introduced on one end of a 2+1/2 cell RF gun in order to extract the electrons. The cathode has been studied at the CERN photo-emission laboratory and demonstrated a lifetime to allow >100h run at a 3% quantum efficiency for a 262 nm laser wavelength. The so called “bucking coil” was installed in parallel to the cathode surface to maintain zero magnetic field in this location. This is to prevent the back-bombardment of the electrons onto the cathode surface that decreases the cathode lifetime and the achievable amount of extracted charge. Another magnet follows in the exit of the gun as a transverse focusing element and ensures the emittance compensation. A Nd:YFL oscillator produces the laser pulses at a repetition rate of 1.5 GHz with an average power of ~300 mW. The oscillator has the fundamental wavelength of $\lambda \sim 1047$ nm and a pulse width of $\tau \sim 8$ ps [5]. The laser diagnostics was placed close to the gun as shown in Fig. 1 providing the alignment of the laser and the cathode after the laser table. The third section of the beamline consists of several diagnostics tools: a wall current monitor (WCM) and a beam position RF monitor (BPR) have been included. A set of corrector magnets have been also installed for horizontal and vertical corrections in addition to the focusing magnet. For the emittance measurement a 2 mm thick tungsten multi-slit mask was utilized. The mask has 25 slits each having a width of 100 μm . FLUKA [6] simulations showed that the mask is able to totally stop a 5.5 MeV electron beam allowing the electron transmission only through the windows while 20% of the incoming electrons are backscattered. An OTR (Optical Transition Radiation) screen was used in the system to image the

PHYSICS AND TECHNICAL DESIGN FOR THE SECOND HIGH ENERGY DISPERSIVE SECTION AT PITZ*

S. Rimjaem[†], J. Bähr, Y. Ivanisenko, M. Krasilnikov, J. Rönsch, F. Stephan,
 DESY, 15738 Zeuthen, Germany
 M. Joré, A. Variola, LAL, 91898 Orsay, France

Abstract

Research activities at the Photo Injector Test facility at DESY, Zeuthen site, (PITZ) aim to develop and optimize high brightness electron sources for Free Electron Lasers (FELs) like FLASH and the European XFEL. To demonstrate the XFEL operation, an electron bunch train containing 3250 pulses of 1 nC charge at 10 Hz repetition rate is required. The spectrometers and related equipments for studying the longitudinal phase space for such long pulse trains do not yet exist at PITZ. Design and construction of a new high energy dispersive arm (HEDA2) is currently in progress. Besides the requirement to handle long electron bunch trains, the HEDA2 setup is designed to allow high resolution measurements of momentum distribution up to 40 MeV/c, a longitudinal phase space measurement with slice momentum spread down to 1 keV/c and transverse slice emittance measurements at off-crest booster phases. The status of the physics design and technical considerations of this dispersive section will be presented.

INTRODUCTION

The test facility PITZ was built and is developing as a pilot photo injector source for the FELs like FLASH and the European XFEL. The research goal is to produce, optimize and characterize the small transverse emittance electron beam of ≤ 1 mm-mrad with a bunch charge of 1 nC and an energy spread of smaller than 1%. In order to fulfill the characterization of high brightness electron beam, the PITZ beam line is continuously upgraded towards the final design (PITZ2) in parallel to the beam operation. The future PITZ2 set up (see Fig.1) will consist of a photocathode RF-gun, a booster cavity, and several diagnostics systems including 3 emittance measurement systems, 3 dispersive arms, an RF deflector, a phase space tomography module, and bunch length diagnostics. One of the key components which will be installed in the PITZ2 beamline is a new cut disk structure (CDS) booster cavity for emittance conservation corresponding to the peak field at the cathode of 60 MV/m [1]. The CDS booster can accelerate electron beams to reach higher energy than the current PITZ setup. This leads to the upgrade of the diagnostics components downstream the booster cavity for supporting the measurements with higher energy electron beams.

To fulfill the beam characterization, besides the intensive measurement program for the transverse phase space optimization the longitudinal phase space is studied using the low energy dispersive arm (LEDA) to measure beam momentum downstream the RF-gun, the first high energy dispersive arm (HEDA1) and the second high energy dispersive arm (HEDA2) to measure the beam momentum behind the booster. The upgraded LEDA and the new HEDA1 have been installed in the current PITZ setup [1]. The old high energy dispersive arm from the previous set up, which is able to measure the beam momentum up to about 16 MeV/c [2], was moved to the end of the beam line. Design and construction of the new HEDA2 is ongoing under the collaboration between DESY and LAL and it is planned to be installed at PITZ in the middle of year 2010.

SETUP

The HEDA2 setup is designed for high resolution measurements of momentum distribution up to 40 MeV/c, a longitudinal phase space measurement with slice momentum spread down to 1 keV/c, and a transverse slice emittance measurements. The contradictory between the measurements of the longitudinal phase space and the transverse slice emittance is the operation at different booster phases. The on-crest or nearly on-crest booster operation is required in the longitudinal phase space measurement for a small momentum spread, while in the transverse slice emittance measurement, the off-crest booster phases conduct the large momentum spread. Since the resolution of the transverse slice emittance measurement at the existing HEDA1 setup is expected to be very good [3], the good resolution of the longitudinal phase space measurement has higher priority in HEDA2 design.

To demonstrate an operation of electron bunches of 1 nC charge for the long bunch train up to 7200 pulses for the FEL at FLASH (720 μ s pulse, 10 Hz) and 3250 pulses for the European XFEL (650 μ s pulse, 5 Hz), the large beam dump with the size of about $2 \times 2 \times 2$ m³ is required and the existing beam dump in the PITZ straight section is planned to be upgraded to fulfill this requirement. The same size of the beam dump is also needed at the end of the HEDA2 section, but the space in the PITZ tunnel is limited. Thus, the transportation of the beam back to the beam dump in the straight section is foreseen. Three dipole magnets are used for this purpose. The HEDA2 setup (see Fig.2) will consist of 3 dipole magnets, 2 screen stations, a quadrupole magnet, 3 beam position monitors (BPMs) and 2 integrated

*This work has partly been supported by the European Community, contract RII3-CT-2004-506008 and 011935.

[†] sakhorn.rimjaem@desy.de

SPIRAL 2 INJECTOR DIAGNOSTICS

P. Ausset, IPN, Orsay, France

T.A. Andre, C. Doutressoulles, B. Ducoudret, C. Jamet, W. Le Coz, F. Lepoittevin, E. Swartvagher,
J.L. Vignet, GANIL, Caen, France

C. Maazouzi, C. Olivetto, C. Ruescas, IPHC, Strasbourg, France

Abstract

The future SPIRAL2 facility will be composed of a multi-beam driver accelerator (5 mA/40 MeV deuterons, 5 mA /14.5 MeV/u heavy ions) and a dedicated building for the production of radioactive ion beams (RIBs). RIBs will be accelerated by the existing cyclotron CIME for the post acceleration and sent to GANIL's experimental areas. The injector constituted by an ion source a deuteron/proton source a L.E.B.T. and a M.E.B.T. lines and a room temperature R.F.Q. will produces, transports and accelerates beams up to an energy of 0.75 MeV/u. An Intermediate Test Bench (B.T.I.) is being built to commission the SPIRAL2 injector through the first rebuncher of the M.E.B.T. line in a first step and the last rebuncher in a second step. The B.T.I. is designed to perform a wide variety of measurements and functions and to go more deeply in the understanding of the behaviour of diagnostics under high average intensity beam operations. A superconducting LINAC equipped with two types of cavity will allow reaching 20 MeV/u for deuterons beam. This paper describes injector diagnostic developments and gives information about the current status.

INTRODUCTION AND GENERAL DESCRIPTION OF THE FACILITY

The SPIRAL2 project aims at producing Radioactive Ion Beam (R.I.B.) by ISOL as well as low-energy in-flight methods. A collaboration of several French laboratories is now constructing the SPIRAL2 facility [1] composed of an injector including two E.C.R. sources, a R.F.Q. operating at 88.05 MHz, a LINAC based on 88.05 MHz superconducting independently phase quarter wave superconducting cavities able to accelerate high intensity (5 mA) deuteron beam up to 20 MeV/u and light heavy ion ($Q/A=1/3$) beam (1 mA) up to 14.5 MeV. Finally the H.E.B.T. lines will distribute those beams to a beam dump or to the experimental stable ion beam experimental areas or transported to the 200 kW target ion source system. The expected rate of fission is $10^{14}/s$

THE SPIRAL2 INJECTOR DIAGNOSTICS

The general layout of the L.E.B.Ts and M.E.B.T. is shown in Fig. 2. The first E.C.R. source produces 20 keV/u light heavy ions ($Q/A=1/3$). The second E.C.R. source produces deuterons beam (40 keV) and now according to a new experiment needs proton beam (20 keV) with characteristics very similar to those of the deuteron beam. The two lines merge in the shared L.E.B.T. which goal is to correctly match the beam to the entrance of the R.F.Q. [2].

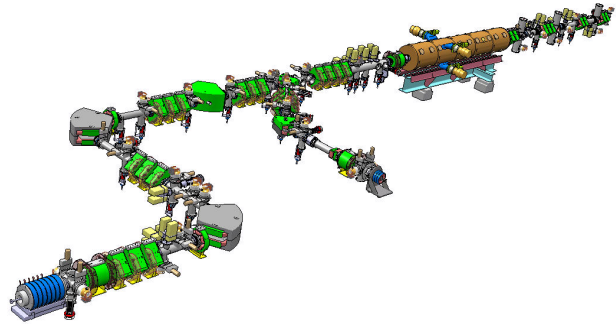


Figure 1: General layout of the SPIRAL2 injector.

Beam Characteristics

The maximum power of the beam under the nominal C.W. mode operation reaches 7.5 kW at the exit of the M.E.B.T. In order to lower the beam average power, Low Duty Factor Pulsed mode operation is also planned for commissioning periods. For this purpose, the operation of the source may be pulsed. A slow chopper located in the shared LEBT may pulse the beam in order to obtain duty cycle as low as 0.1 %. This mode of operation allows also the interceptive diagnostics to withstand the beam during the tuning of the injector. At last, a fast chopper located in the MEBT line removes selected bunches from the beam according to special experiment needs.

Destructive Beam Intensity Measurements

They are carried out by copper made water cooled Faraday Cup in the L.E.B.T and in the M.E.B.T. (end of the line). The first one following the E.C.R. ion source is specially devoted to the tuning of the source. The Faraday cups are designed for a 100 mm aperture in the LEBT and 60 mm in the M.E.B.T. The maximum beam power



Figure 2: Photograph of the Faraday Cup of the L.E.B.T.

FIRST BEAM TESTS OF THE CLIC POWER EXTRACTION STRUCTURE IN THE TWO-BEAM TEST STAND*

E. Adli[†], University of Oslo, Norway and CERN, Geneva, Switzerland
 R.J.M.Y. Ruber, V. Ziemann, Uppsala University, Sweden
 R. Corsini, S. Doebert, A. Dubrovskiy, G. Riddone, D. Schulte,
 I. Syratchev, CERN, Geneva, Switzerland
 S. Vilalte, IN2P3-LAPP, Annecy-le-Vieux, France

Abstract

The two-beam acceleration scheme foreseen for CLIC and the associated radio-frequency (RF) components will be tested in the Two-beam Test Stand (TBTS) at CTF3, CERN. Of special interest is the performance of the power extraction structures (PETS) and the acceleration structures as well as the stability of the beams in the respective structures. After the recent completion of the TBTS, the first 12 GHz PETS has been tested with beam, using so-called recirculation of the RF power inside the PETS. The TBTS allows precise measurement of beam parameters before and after the PETS as well as RF power and phase. Measurements of transverse kick, energy loss and RF power with recirculation are discussed and compared with estimations, including first measurements of pulse shortening probably due to RF breakdown.

INTRODUCTION

The Two-beam Test Stand (TBTS) is a unique and versatile facility devised to test key components of the two-beam acceleration concept that is the basis of the CLIC project [1]. Worldwide it is the only facility where CLIC type power production (PETS) and accelerating structures can be tested with beam. The TBTS is part of the CTF3 complex at CERN [2] that creates a high power drive beam which is then decelerated in order to generate the RF power needed to accelerate a second, probe, beam which is provided by another linac. The drive beam has a time structure suitable for power generation at all harmonics of 1.5 GHz but is optimised for the nominal CLIC frequency of 12 GHz. It can reach beam intensities up to 30 A, pulse lengths up to 1500 ns and beam energies up to 150 MeV. The probe beam can reach beam intensities up to 0.9 A, pulse lengths up to 150 ns and beam energies up to 170 MeV.

Commissioning of the TBTS drive beam line started last year. As the available drive beam current will be some four times lower than in the CLIC design, the installed PETS has a modified design. It has increased length to 1 m from 0.215 m and is equipped with external RF recirculation [3]:

the PETS operates as an amplifier feedback ring driven by the drive beam power. Up to 30 MW of 12 GHz RF power has been produced from a 5 A beam.

THE TWO-BEAM TEST STAND

The TBTS consists of two parallel beam lines for the drive and probe beam and a two meter long test area in each. The layout of the two beam lines is almost identical [4]. The experiments described in this report are performed on the drive beam line. The layout of the line with PETS installation is shown in Figure 1.

Two quadrupole triplets are used to vary and optimise the beam size inside the PETS and on an OTR screen following a spectrometer dipole in order to maximise the energy resolution. Moreover, four steering magnets are available to adjust the orbit inside the PETS with a closed bump. Five inductive BPMs [5] are installed for intensity and position measurements. Their bandwidth allows to observe the position within a bunch train and this is used to determine kicks and energy loss of the beam during normal operation and when a RF breakdown occurs inside the PETS. The achievable resolution to determine the kicks is in the order of a few micro radians and 4×10^{-4} for the energy [6].

The PETS RF recirculation loop contains a variable splitter to control the amount of power in the loop and a phase shifter to tune the loop's length. The RF power and phase are measured through directional couplers connected to 12 GHz diodes and I&Q demodulators.

RECIRCULATION

In the recirculator a fraction of the field g (product of the splitter ratio κ and the round-trip ohmic losses) is coupled

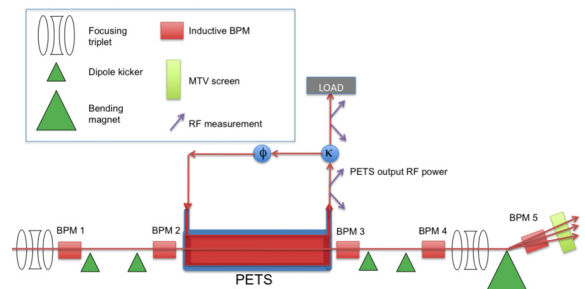


Figure 1: Sketch of the Two-beam Test Stand's drive beam line (not to scale).

* Work supported by the Swedish Research Council, the Knut and Alice Wallenberg Foundation, the Research Council of Norway and the Commission of the European Communities under the 6th Framework Programme Structuring the European Research Area, contract number RIDS-011899.

[†] Erik.Adli@cern.ch

BEAM DIAGNOSTICS FOR SPIRAL2 RNB FACILITY

P. Anger, T. Andre, A. Delannoy, E. Gueroult, B. Jacquot, C. Jamet, G. Ledu, A. Savalle, F. Varenne, J.-L. Vignet, GANIL, Caen, France, J.-M. Fontbonne, N. Orr, LPC, Caen, France

Abstract

The SPIRAL2 project is based on a multi-beam driver facility in order to allow both ISOL and low-energy in-flight techniques to produce intense radioactive ion beams (RIB) in a new Facility. A superconducting linac capable of accelerating 5-mA deuterons up to 40 MeV is used to bombard both thick and thin targets. These primary beams will be used for the RIB production by several reaction mechanisms (fusion, fission, etc.) The production of high intensity RIB will be based on fission of uranium target induced by neutrons.

These exotic particles will be produced, ionized, selected in a dedicated production building and transported to the existing CIME cyclotron for post acceleration. After this, they will be used in the present experimental area of GANIL. The construction phase of SPIRAL2 was officially started in 2005.

The beam diagnostics for the production facility allow a pre-tuning with a stable beam followed by an extrapolation to the radioactive beam. Some diagnostic devices may also provide for equipment protections and for the safety systems.

An overview is presented of the diagnostics which will allow tuning and control of the RIB in this new production facility.

SPIRAL2 RNB FACILITY

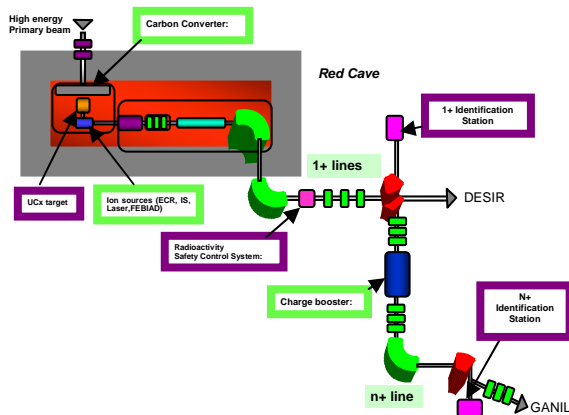


Figure 1: RNB general scheme.

The RNB facility will produce, from a high intensity primary beam, radioactive ion beam in a red radiological cave. The production of high intensity RIB will be based on fission of uranium target induced by neutrons. The mono-charged secondary beams will be selected in the 1+ beam line, used for low energy experiment or multi ionized to be post accelerated in the existing Ganil.

TUNING AND CONTROL METHODS

The tuning principle of the SPIRAL2 beams consists of pre-tuning with a stable beam followed by an extrapolation to the radioactive beam.

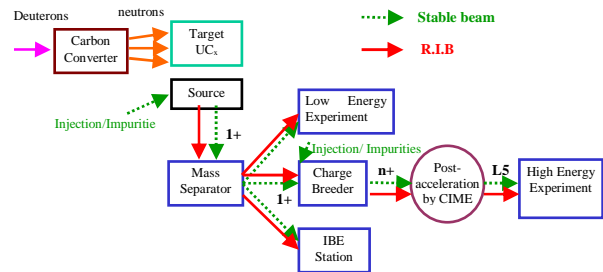


Figure 2: Stable beam tuning and R.I.B. tuning.

PRELIMINARY TUNING IN STABLE BEAM

Beam Intensity Measurement

Measurement of the beam intensity in the lines is based on the use of Faraday cups (Fig. 3) and a linear current to voltage converter. Their measurement dynamics extends from 10^9 pps up to I_{\max} ($P < 50W$) with an absolute accuracy of a few percent.



Figure 3: Faraday cup.

Beam Profile and Position Measurement

The measurement of the beam transverse profile in the lines is carried out by secondary emission multiwire profilers (Fig. 4). The principle is based on electron emission under the impact of the beam on wires. The range measurement is 10^9 pps – 10^{13} pps for energy from some keV to 25 MeV/A and the absolute positional accuracy is better than 1 mm.

It gives transverse profile dimensions and the gravity centre of the beam along a horizontal and vertical axis. This information will be distributed via electronic processing according to Ethernet or MODBUS protocol with the Spiral2 Command-Control.

BEAM DIAGNOSTICS IN THE CNAO INJECTION LINES COMMISSIONING

G. Balbinot, C. Biscari, J. Bosser, E. Bressi, M. Caldara, L. Lanzavecchia, M. Pullia, A. Parravicini, M. Spairani, CNAO, Milan, Italy

Abstract

The CNAO, the first Italian synchrotron for deep hadrontherapy [1-2], is presently in its final step of installation. It will deliver beam of both, Protons and Carbon ions, in three treatment rooms in order to treat solid tumours with active scanning technique.

CNAO beams are generated by two ECR sources [3], able to produce both particle species, and transferred to a RFQ and a LINAC through a Low Energy Beam Transfer line (LEBT) at 8 keV/u and then accelerated up to 7 MeV/u before being injected in the synchrotron ring [4].

A compact and versatile tank containing a complete set of beam diagnostic tools has been intensively used for the LEBT line commissioning successfully concluded in January 2009. In a length of 390mm, the tank houses two wire scanners, aimed to measure vertical and horizontal beam position and transverse profile, a Faraday Cup, for beam current measurement, and two vertical and horizontal metallic plates for beam halo suppression, emittance measurements, beam collimation and particles selection.

Using one tank only, phase space distribution reconstruction can be quickly performed as well as synchronous profiles and intensity measurements.

Five identical tanks are installed in the LEBT line [5], as consequence of a standardization strategy to improve diagnostic monitor knowledge and make maintenance easier.

LEBT LINES GENERAL DESCRIPTION

LEBT lines Beam Diagnostic (BD) elements are schematized in figure 1: the two sectors, called O1 and O2, are dedicated to the respective source and are both equipped with two diagnostic tanks and one 90° dipole spectrometer in order to make the tuning of each source independent from the use of the second one. When one of the Faraday cups upstream the first quadrupole triplet is inserted, the source can be monitored without interfering with the operation of the other one. Beam parameters can be measured also before the spectrometer dipole. The two sectors called L1 and L2, common for both the lines, include the beam injection chopper and a special Faraday cup (CFC) for beam current intensity monitoring.

BD INSTRUMENTATION

Slits

Four Copper plates compose the slits: working two by two the plates create vertical and horizontal slits

01 Overview and Commissioning

dedicated to beam scanning, phase space distribution measurements and particle specie selection (downstream the spectrometer).

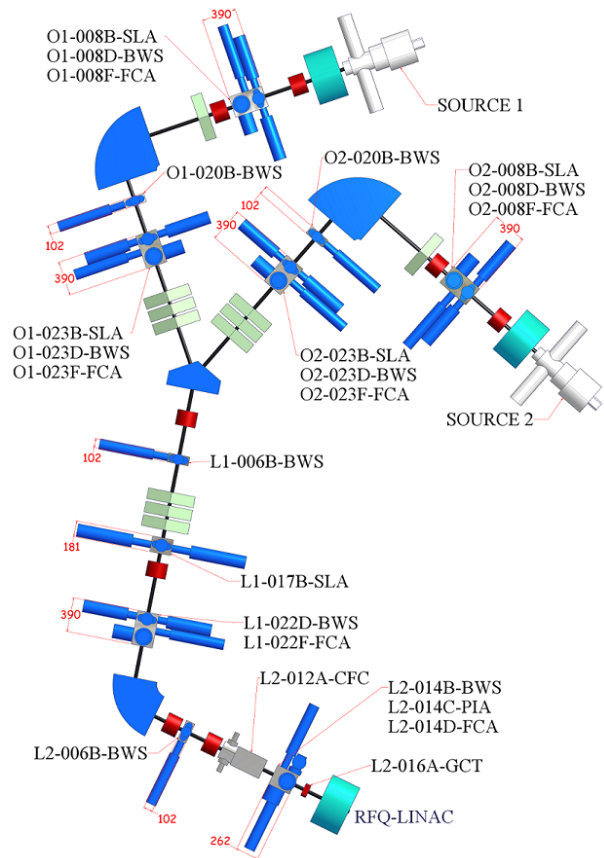


Figure 1: LEBT BD Instrumentation Layout with elements names. SLA are Slits, BWS are Wire Scanner in both planes, FCA is Faraday Cup, CFC is the Chopper Faraday Cup, PIA is Profile Grid and GCT is a current transformer.

Moreover, the plates positioning around the beam allows the beam halo suppression. Slits plates are 1mm shifted longitudinally in order to allow their overlapping; they are also water cooled to dissipate the large beam power (360W). Each plate is driven by a brushless motor at the maximum velocity of 250 mm/s with a position accuracy of about 20 μm: absolute position is read through a linear potentiometer. Secondary electrons emitted as a result of interaction between the beam and the plates can be suppressed by polarizing the plates up to 1kV.

BEAM DIAGNOSTICS AT THE ALBA LINAC

U. Iriso*, A. Olmos, and F. Pérez
CELLS, Ctra. BP-1413 Km 3.3, 08290 Cerdanyola, Spain

Abstract

The commissioning of the ALBA Linac (Autumn 2008) required a careful measurement of the beam parameters. This paper describes the diagnostics devices installed at the ALBA Linac and our experience with them.

INTRODUCTION

The ALBA Linac was supplied by Thales Communications and installed in Spring 2008 at the CELLS site. The installation of the first part of the transfer line Linac to Booster (LTB) and the Diagnostics Line (Lidia) was done simultaneously under the CELLS responsibility. The Linac beam commissioning was performed in Autumn 2008. More details about the Linac installation and commissioning are found at Refs. [1, 2].

The Linac is designed to work in two operational modes: Single and Multi Bunch Mode (SBM and MBM, respectively). In SBM, the Linac delivers up to 8 pulses with a bunch spacing that can range between 6 and 50 ns, and a maximum charge of 2 nC total. In MBM, it provides a train between 112 and 1024 ns length with a maximum charge of 4 nC and a fixed bunch spacing of 2 ns. The Linac specifications are listed in Table 1.

Table 1: Linac Parameters. The acronym “ptp” refers to “pulse-to-pulse” variation (rms).

Parameter	SBM	MBM
# of bchs	1 ... 8	56 ... 512
pulse length, ns	≤ 1	112 - 1024
bch spacing, ns	6 - 50	2
charge, nC	≥ 1.5	≥ 3
Bunch purity	$\leq 1\%$...
pos. stability* ptp	≤ 0.2 mm	≤ 0.2 mm
energy, MeV	≥ 100	≥ 100
energy spread	$\leq 0.5\%$	$\leq 0.5\%$
energy var. ptp	$\leq 0.25\%$	$\leq 0.25\%$
norm. emit, μrad	$\leq 30\pi$	$\leq 30\pi$

Figure 1 shows a sketch of the Linac, LTB and Lidia with the diagnostics systems. Thales responsibility ends after the diagnostics elements installed downstream the second accelerating structure. All components installed after that are CELLS responsibility and their goal is to check whether the Linac fulfills the required specifications.

This paper shows the diagnostics components installed at the LTB and Lidia to check the main beam parameters, that is: beam charge, position, and size. Description of

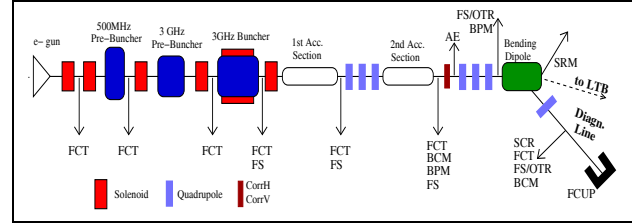


Figure 1: Sketch of Linac and LTB, with the diagnostics location.

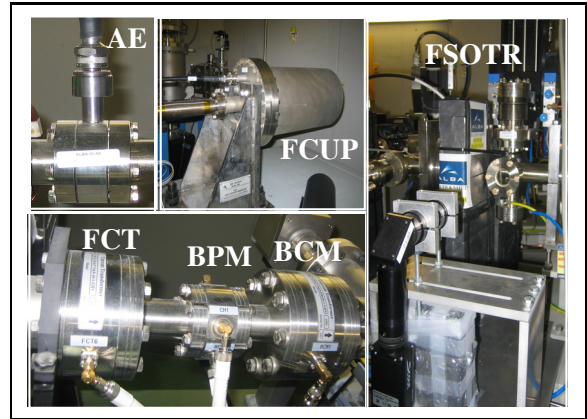


Figure 2: Diagnostics components at the Linac and LTB.

the emittance, energy and energy spread measurements is shown in Refs. [2, 3]. Figure 2 shows a picture with the diagnostics devices in the Linac and LTB, which will be seen throughout the text.

BEAM CHARGE MEASUREMENTS

Beam charge measurements are done using the commercially available Fast Current Transformer (FCT) and Beam Charge Monitors (BCM) [4], and with in-house designs manufactured by Cinel: Annular Electrode (AE) and Faraday Cup (FCUP).

Fast Current Transformers

Fast Current Transformers (FCT) are installed after each active element in the Linac and LTB (see Fig. 1). In total, we have 8 FCTs to monitor the transfer efficiency along the line, and they all have been very useful throughout the Linac commissioning.

Our model is the FCT-CF4”1/2-34.9-40-10:1, with a frequency range 5 kHz - 1.4 GHz. This limited frequency range implies that: 1) precise beam charge measurements

* ubaldo.iriso@cells.es

DIAGNOSTICS OVERVIEW FOR THE TAIWAN PHOTON SOURCE

K.T. Hsu, C. H. Kuo, K. H. Hu, C.Y. Wang, NSRRC, Hsinchu 30076, Taiwan

Abstract

A new high brilliant 3 GeV storage-ring-based light source - Taiwan Photon Source (TPS), is planned to be built at National Synchrotron Radiation Research Center. Various diagnostics will be deployed to satisfy stringent requirements for commissioning, operation, and top-off injection of the TPS. Specifications and overview of the planned beam instrumentation system for the TPS are summarized in this report. The efforts including diagnostic devices and subsystems will be addressed also.

INTRODUCTION

The TPS project will be a state-of-the-art synchrotron radiation facility featuring ultra-high photon brightness with extremely low emittance. It consists of a 150 MeV S-band linac, linac to booster transfer line (LTB), 0.15–3 GeV booster synchrotron, booster to storage ring transfer line (BTS), and 3 GeV storage ring. Latest generation diagnostic systems will equip TPS to fulfill its design goals. The storage ring has of 24 DBA lattices cells. It is a 6-fold symmetry configuration. The main beam diagnostics related parameters for the storage ring are shown below in Table 1.

Table 1: Major Parameters of the TPS Booster Synchrotron and the Storage Ring

	Booster Synchrotron	Storage Ring
Circumference (m)	496.8	518.4
Energy (GeV)	150 MeV – 3 GeV	3.0
Natural emittance (nm-rad)	10.32 @ 3 GeV	1.6
Revolution period (ns)	1656	1729.2
Revolution frequency (kHz)	603.865	578.30
Radiofrequency (MHz)	499.654	499.654
Harmonic number	828	864
SR loss/turn, dipole (MeV)	0.586 @ 3 GeV	0.85269
Betatron tune ν_x/ν_y	14.369/9.405	26.18 /13.28
Momentum compaction (α_1, α_2)	-	$2.4 \times 10^{-4}, 2.1 \times 10^{-3}$
Natural energy spread	9.553×10^{-4}	8.86×10^{-4}
Damping partition $J_x/J_y/J_s$	1.82/1.00/1.18	0.9977/1.0/ 2.0023
Damping time $\tau_x/\tau_y/\tau_s$ (ms)	9.34/ 16.96 / 14.32	12.20/ 12.17 / 6.08
Natural chromaticity ξ_x/ξ_y	-16.86/-13.29	-75 / -26
Dipole bending radius ρ (m)	-	8.40338
Repetition rate (Hz)	3	-

To realize the benefits of the high brightness and small sizes of TPS sources, photon beams must be exceedingly stable both in position and angle to the level of better than 10% of beam sizes and divergence. Table 2 provides the electron beam sizes and angular divergences for selected TPS sources. The most stringent beam measurement and stability requirement will be for the

01 Overview and Commissioning

vertical position at the 7 m straight for ID source ($\sigma_y = 5.11 \mu\text{m}$); this will require special consideration for measuring both electron and photon beams.

Table 2: The Electron Beam Sizes and Divergence

Source point	σ_x (μm)	$\sigma_{x'}$ (μrad)	σ_y (μm)	$\sigma_{y'}$ (μrad)
12 m straight center	165.10	12.49	9.85	1.63
7 m straight center	120.81	17.26	5.11	3.14
Dipole (1° source point)	39.73	76.11	15.81	1.11

LINAC DIAGNOSTICS

The TPS 150 MeV linac system was contracted to the RI Research Instruments GmbH (former ACCEL Instruments GmbH) in December 2008 [1]. The delivery schedule is around the border of 2010/2011. Beam instrumentation comprises five YAG:Ce screen monitors for beam position and profile observation, two fast current transformers (FCT) to monitor the distribution of charge and one integrating current transformer (ICT) for monitoring total bunch train charge. Wall current monitors (WCM) formed by equally spaced broadband ceramic resistors mounted on a flexible circuit board, wrapped around a short ceramic break, will also give information on beam charge as well as longitudinal profiles of electron bunches. Linac diagnostics are summarized in Fig.1 and Table 3. All of these mentioned diagnostics will be provided by the vendor. Acceptance test of the linac system will be performed at a temporary site near the TPS main building before its completion and move to the TPS building later. It is also planned that beam position monitors (BPM) might be added between accelerator sections are also planned. These BPMs will be useful for RF phasing monitoring, feedback control and on-line beam position jitter observation.

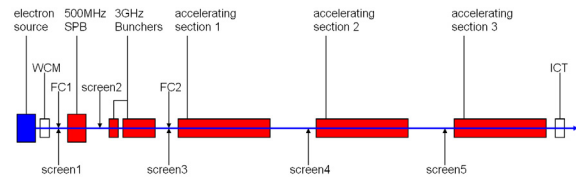


Figure 1: Functional block diagram of the linac diagnostic devices.

Table 3: Linac Diagnostics

Monitor	Quantity	Beam parameters
YAG:Ce screen	5	Position, profile
WCM	1	Intensity distribution
FCT	2	Intensity distribution
ICT	1	Charge at exit of the linac

“BUNCHVIEW”

A FAST AND ACCURATE BUNCH-BY-BUNCH CURRENT MONITOR

F. Falkenstern, F. Hoffmann, P. Kuske, J. Kuszynski,
Helmholtz Zentrum Berlin, Germany

Abstract

BunchView is a system for the direct measurement of the current from each bunch circulating in a storage ring based on the analysis of the RF-signals delivered by a set of striplines. This paper describes the development, achievements, operation, and results of this fast and accurate bunch current monitor built for the BESSY and MLS storage rings.

Using a combination of a 14/16Bit analog to digital converter (ADC), a high-speed FIFO, ECL technique, and FPGAs, a real-time measurement of the fill-pattern with high accuracy and bunch-by-bunch resolution was achieved. The results are identical to the fill-pattern determined by time correlated single photon counting based on synchrotron radiation detected with an avalanche photo diode.

BunchView is fully integrated into the EPICS control system. The data provided by the BunchView monitor give accurate bucket position in the ring and bunch current over a wide dynamic range. The smallest measured single bunch current is less than 100nA. In the future the system will be used in the top-up mode of operation in order to inject beam into the emptiest buckets and thus keep the fill-pattern stable over longer periods of time.

INTRODUCTION

The BESSY machine is a third-generation light source operating at energy of 1.7 GeV with a stored current up to 300 mA. In the storage ring, electrons might be stored in any pattern consisting of up to 400 bunches. Knowledge of the fill-pattern of the buckets in a ring is very important, especially as more sophisticated time-resolved experiments are considered. At the time, BESSY has three modes of operation with special fill pattern: 1st the multi bunch (MB) mode with 350 consecutive filled buckets and a gap of 100 ns for ion-clearing, 2nd the single bunch mode (SB) with up to 20 mA, and 3rd the hybrid mode where a single bunch of 10 mA is injected in the middle of the gap. The operation in top-up mode [1] requires a real-time, high resolution determination of the current stored in each individual bucket.

DIAGNOSTIC TASK

We looked for a detection system, which monitors the current in each bucket with more than 12 bit accuracy and updates the whole fill-pattern of 400 bunches in less than 100 ms. Moreover, the system must be synchronized to the timing control at BESSY and thus gets the bunch

number and its corresponding current value as shown in Figure 1.

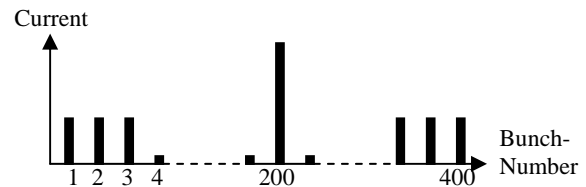


Figure 1: Fill-pattern in the storage ring.

Unfortunately, all commercial oscilloscopes have less than 8 bit amplitude resolution at the 500 MHz analog bandwidth. The best ADC-cards reach at best 10 bit resolution. The main reason is the track-and-hold (T/H) amplifier in the front-end of the ADC where the analog value is stored during the digitalisation process [2]. The hold time is essential for the amplitude resolution of the ADC. At present, many ADCs with a 14/16 bit amplitude resolution and an analog bandwidth of more than 500 MHz are on the market. But they all have a sampling rate below 130 MHz. Operating many ADCs in parallel would overcome this limit, however, would also lead to a more complicated design and a larger size. An alternative method for the data acquisition based on only one ADC and undersampling is used in our monitor and will be described in detail below.

PRINCIPLE OF MEASUREMENTS

In the storage ring the bunches circulate with a well defined revolution time which is 800 ns in case of the BESSY storage ring. Thus every revolution time the same bunch passes by the monitor. It is not necessary to detect all the bunch currents during just one revolution because the distribution of electrons distributed over the buckets does not change that fast. In addition we wanted to average the bunch current values over longer times in order to get a better resolution. Therefore, we decided to use signal undersampling [3].

For a better understanding, first consider a model of the storage ring with only 16 bunches as shown in Figure 2. If only every fifth bunch is sampled we catch all bunches in 5 revolution times and we get the following array of digitized bunch intensities:

“1,6,11,16, 5,10,15, 4,9,14, 3,8,13, 2,7,12”.

IMPACT OF ENVIRONMENTAL VARIABILITY ON VIBRATING WIRE MONITOR OPERATION

S.G. Arutunian, M.A. Davtyan, I.E. Vasiniuk, Yerevan Physics Institute, Yerevan, Armenia
 J. Bergoz, Bergoz Instrumentation, Saint Genis Pouilly, France
 G. Decker, Argonne National Laboratory, Argonne, IL, USA
 G.S. Harutyunyan, Yerevan State University, Yerevan, Armenia

Abstract

The Vibrating Wire Monitor (VWM) was developed for precise transversal profiling/monitoring of charged particle/photon beams. The extremely high sensitivity of VWM is achieved by sensitivity of wire natural oscillation frequency to wire temperature. Due to the rigidity of the wire support structure, the VWM is also sensitive to the environmental parameters. In this paper, it is shown that the main parameter of influence is the ambient temperature. The magnitude and character of this influence is investigated along with the effect of electromagnetic interference on the VWM electronics in an accelerator environment.

INTRODUCTION

VWMs for accelerator beam instrumentation are based on the change in the natural oscillations frequency of a vibrating wire depending on the temperature of the wire and environment in which oscillations take place [1]. During operation these conditions (VWM sensor and electronics temperatures, electromagnetic interference from high power accelerator elements, hyper-radiation, presence of high electric and magnetic fields etc) can change, leading to shifts in measurements.

In vacuum the dominant effect is the sensor temperature since the resonant frequency in first approximation depends exceptionally on the mechanical properties of resonator and weakly depends on electronics.

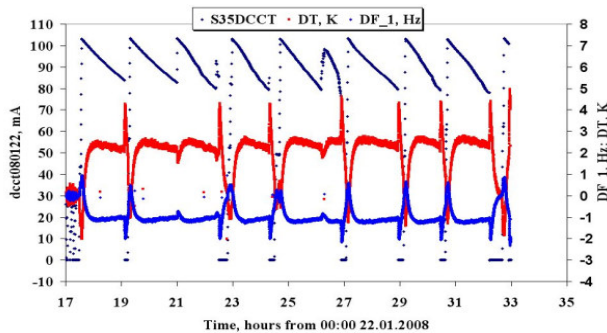


Figure 1: VWM005 reacts to the current change in APS.

Experiments at the APS ANL [2], [3] showed that a five-wire VWM005 reacts to electron beam current even in the case when beam synchrotron radiation does not touch the vibrating wire. In this experiment, a VWM was

mounted at terminating flange of APS storage ring. We explained this behaviour by shifts of copper flange temperature. In Fig. 1 we present the time dependence of the VWM005 first wire frequency shift (right axis) that correlates with beam current (left axis). At right axis we also present the calculated wire temperature with shifts of about 2 K and 30 min relaxation time.

EXPERIMENTS

VWM Dependence on Ambient Temperature

To decrease VWM dependence on ambient temperature normally we choose wire material and housing material with the same thermal expansion coefficients. But to accent the question we analyze a sensor with wires and housing made by different materials (housing – bronze, first wire – Kanthal, second wire – stainless steel). As a reference thermometer we used Platinum resistive temperature detector Pt100 (RTD) with 0.03 °C accuracy. Measurements were done by Eurotherm model 2416 PID controller. Calibration of VWM is presented in Fig. 2.

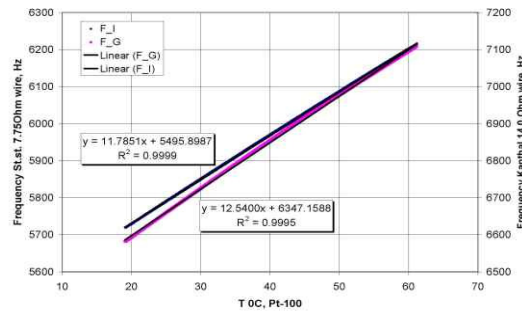


Figure 2: Calibration of two-wire VWM: magenta – Kanthal, blue –stainless steel.

The mean dependences on ambient T are 12.540 Hz/K (in range 6600-7100 Hz) for Kanthal wire and 11.785 Hz/K for stainless steel wire. The frequency measurement accuracy was about 0.01 Hz corresponding to 0.8 mK temperature drift. This value is extremely small so the long-term temperature measurements require detailed investigations to determine the stability of the VWM measuring system. Measurements with VWM and with Pt100 have some essential differences:

- The sensitive element of VWM has a mass of about 2 mg that is less massive than Pt100 (about 50 mg) although VWM contains housing of about 100 g surrounding the wire.

PROFILEVIEW - A DATA ACQUISITION SYSTEM FOR BEAM INDUCED FLUORESCENCE MONITORS*

R. Haseitl, C. Andre, F. Becker, P. Forck, GSI, Darmstadt, Germany

Abstract

Along the GSI linear accelerator, several Beam Induced Fluorescence (BIF) monitors are installed. Due to the non beam-intercepting measurement principle, multiple BIF monitors can be active simultaneously to observe the beam at different locations. For this novel possibility, the software called ProfileView has been developed, allowing users to view beam profiles coming from several BIF monitors. This contribution describes the different hardware devices of the GSI BIF monitor installation and the according software to control these devices.

MOTIVATION

Beam Induced Fluorescence monitors determine the transversal beam profiles without beam disturbance [1]. Therefore, they are well suited to observe the beam at several positions in the accelerator at the same time. Presently, two BIF monitors are installed in the GSI linear accelerator. In the next two years, a final number of seven BIF monitors will be installed to observe the beam throughout the linear accelerator and in the transfer line to the synchrotron. The readout of the two image intensified cameras of a BIF monitor has formerly been realised with outdated LabView programs. Just one camera could be monitored at a time, so horizontal and vertical profiles had to be measured successively. The new software called ProfileView overcomes these limitations and allows machine operators to view multiple BIF monitors at the same time through an easy-to-use graphical user interface (GUI) which can be seen in Fig. 1. Up to three different BIF monitors can be observed and compared at once. By default, the pressure is the only parameter to tweak the signal strength. For advanced users, every parameter of the system can be finetuned in a password protected 'Expert mode'.

HARDWARE

The hardware of the BIF system is in wide parts similar to the hardware of the BeamView system for scintillator screens [2]. Each BIF monitor consists out of the following hardware components depicted in Fig. 2:

- two FireWire cameras (for the horizontal and the vertical profile) with multi-channel plates (MCPs) for image intensification and remote-controllable irises
- a National Instruments Compact Vision System (CVS) [3] or standard PC for camera readout and digital image processing

* Work supported by EU, project FP6-CARE-HIPPI

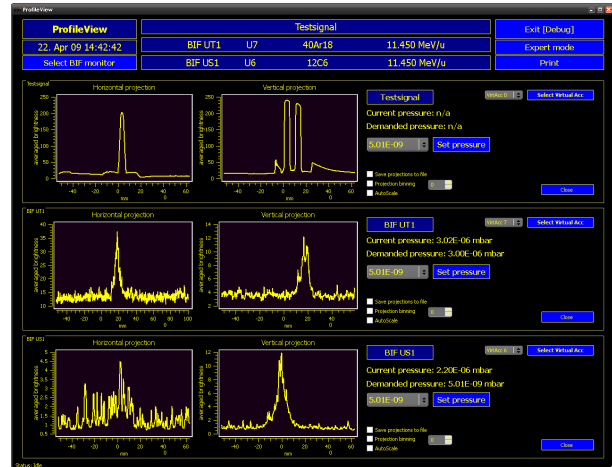


Figure 1: ProfileView graphical user interface.

- Ethernet connected DAC electronics for iris and MCP amplification control
- pressure control unit to inject defined gas pressures into the beam pipe
- timing decoder to trigger the cameras and the image intensifiers
- remote controllable power plugs to reset system components
- a computer running ProfileView to display images and projections and control all hardware devices

Image Acquisition System

To acquire images, standard FireWire cameras (Basler A311f) have been equipped with custom made image intensifiers (Proxitronic) for single photon detection. The cameras are connected to dedicated image processing hardware, acting as middle layer between the camera and the computer running the GUI. For this purpose, an embedded system (National Instruments Compact Vision System 1456 [3]) can be used. This embedded computer is equipped with FireWire interfaces, an FPGA with digital I/Os, network connectivity, a 733 MHz CPU, 128MB RAM and 256MB non-volatile storage. The CVS is capable to control up to 16 cameras connected via FireWire hubs, with four of them running simultaneously. It is programmed via LabView Realtime, FPGA and Vision packages. It is also possible to use a standard Windows PC with FireWire ports and an FPGA card instead of the CVS to achieve higher system performance. Besides some minor adaptations, the software for the CVS and the PC is the same.

IMPLEMENTATION OF THE ELECTRONICS CHAIN FOR THE BUNCH BY BUNCH INTENSITY MEASUREMENT DEVICES FOR THE LHC

D. Belohrad*, O. R. Jones, M. Ludwig, J. J. Savioz, S. Thoulet, CERN, Geneva, Switzerland

Abstract

The fast beam intensity measurements for the LHC are provided by eight Fast Beam Current Transformers (FBCT). Four FBCTs installed in the LHC rings are capable of providing both bunch-by-bunch and total turn-by-turn beam intensity information. A further four FBCTs, two in each of the LHC dump lines, are used to measure the total extracted beam intensity. In addition to providing intensity information the ring FBCTs also send signals to the machine protection system. This increases the complexity of both the RF front-end and the digital acquisition parts of the signal processing chain. The aim of this paper is to discuss the implemented hardware solution for the FBCT system, in particular with respect to the signal distribution, FPGA signal processing, calibration, and interaction of the FBCTs with the machine protection chain.

INTRODUCTION

The fast BCT measurement system consists of a Bergoz type transformer with a bandwidth from 400Hz to 1.2GHz. This is followed by an RF front-end consisting of an RF distributor, analogue integrator and beam circulating flag (BCF) detector, before entry into a 14bit digital acquisition system.

A simplified block schematic of the fast intensity measurement system is depicted in Fig. 2. In order to maintain the compatibility of the CERN-SPS and the LHC FBCT systems it was decided to use a digital processing chain based on the CERN-SPS system. This uses a DAB64x acquisition card developed by TRIUMF (Canada) on which are mounted two Individual Bunch Measurement System (IBMS) mezzanine cards [1]. The mezzanine cards are used to integrate the incoming signal using a 40MHz integrator ASICs developed for the LHCb experiment. The integrated signal is then digitized and processed on the DAB64x card to produce bunch-by-bunch intensity values.

Four channels (2 DAB64x boards) are used to provide measurements in two dynamic ranges: high gain with full scale= 2×10^{10} and low gain with full scale= 2×10^{11} particles. For each dynamic range the measurements can be acquired with a high bandwidth (HIBW, 200MHz) for bunch to bunch measurements and a low bandwidth (LOBW, 2.5MHz for low gain and 1.5MHz for high gain) for a timing insensitive total intensity measurement.

SIGNAL DISTRIBUTION

The purpose of the RF distributor is to split the beam signal appearing at the output of the transformer [2] into a total of six outputs. Four of these outputs are used for the measurement, and are connected via appropriate protection circuitry to the IBMS mezzanines. The remaining outputs are used for the BCF detector and an oscilloscope.

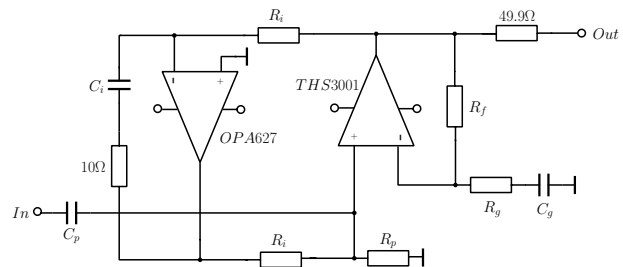


Figure 1: High gain amplifier with offset suppressor.

The signal coming from the transformer is divided by a resistive splitter, is separately amplified and then filtered. The signal amplification for the measurement outputs is dependent on the dynamic range and the bandwidth. Regardless of the bandwidth, the low gain range does not require any amplification as even the LOBW signal creates almost a full scale response at the output of the integrator. An amplification of 30dB and 40dB is required for the HIBW and the LOBW channels respectively for the high gain range.

Maintaining the required bandwidth with high gains is difficult to achieve using voltage feedback operational amplifiers (VFOA). Current feedback operational amplifiers (CFOA) were therefore used. These exhibit higher offset voltages, hence an active feedback to suppress the input offsets was developed (Fig. 1). The implemented method is based on the fact that the measured signal has no DC value. An AC coupled amplifier was designed, and its output actively low-pass filtered, inverted, and injected back to the input of the amplifier. The time constant of the filter is much longer than the one corresponding to the low-frequency cut-off of the measurement transformer.

All filters implemented in the RF distributor are of Gaussian type to ensure that no overshoot occurs in the response to the input signal. The HIBW filters are passive 2nd order LC circuits, and their goal is to reduce the peak amplitude of the incoming beam signal. Fourth order filters consisting of two Sallen-Key blocks were used to implement the LOBW channels.

The entire RF distributor was designed as a VME card. In order to control the impedance of the tracks

* david.belohrad@cern.ch

CHARGE AND LASER BEAM ENERGY MONITOR FOR SPARC LINAC*

L. Cultrera[#], F. Anelli, M. Bellaveglia, G. Di Pirro, D. Filippetto, E. Pace, C. Vicario, INFN National Laboratories of Frascati, Via E. Fermi 40, Frascati, Italy

Abstract

The experimental setup implemented in the SPARC linac control system used to monitor the laser beam energy and to measure the beam charge by means of a Faraday Cup will be illustrated and discussed. The experimental setup makes use of National Instruments 2 GS/s 8-Bit digitizer board. This tool has been shown to be useful in order to monitor the laser beam energy stability and to evaluate the quantum efficiency of the cathode.

INTRODUCTION

Within the goals of the SPARC high brightness photoinjector [1] the stability of the electron beam plays a crucial role. For this reason a new instrument of measure has been included in SPARC control system: the SPARC beam diagnostic system allows now monitoring continuously the laser energy delivered to the cathode and thus the quantum efficiency of the cathode itself. This new tool allowed us to keep under control the cathode performances in terms of its emission properties (QE mean value and uniformity of emission). The tool, now completely integrated inside the SPARC control system allows also to reconstruct the quantum efficiency map of the cathode surface.

EXPERIMENTAL SETUP

In the following paragraph the experimental setup for monitoring the laser energy and the beam charge and its implementation inside the SPARC control system [2] will be illustrated.

Laser Energy Monitor

The SPARC laser beam energy is measured by means of a fast photodiode (Thorlabs mod. DET210). The signal generated by the photodiode consists in a sharp current pulse with duration of approximately ten ns. The area of the photodiode signal results to be linearly dependent from the energy of the laser pulse. In order to deduce the energy carried out by laser beam, an accurate calibration is carried out by relating the area of the photodiode signal with respect to the laser energy measured by a commercial joulemeter (Molelectron mod. J3-05).

A typical calibration curve is reported in Fig. 1. In this figure is evident that the photodiode response can be considered linear, and its slope represents the conversion factor that should be used to convert the area of the measured photodiode signal to the energy of the laser

beam pulse.

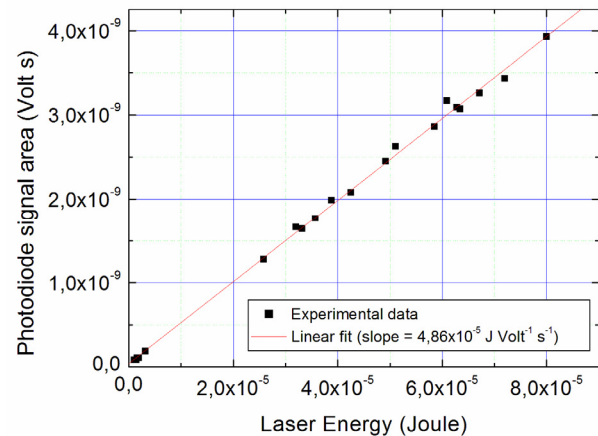


Figure 1: Typical calibration curve for the laser photodiode.

Due to the sensitivity of the photodiode with respect to the relative laser beam position with respect to the detector area the calibration factor is usually verified each time that the operators prepare the laser beam for the SPARC run. Moreover, a pointing procedure of the laser beam to the centre of the cathode is performed by means of a motorized mirror at the end of the optical transfer line. Thus the final path of the laser beam is frequently changed and this affects also the calibration constant. In order to avoid this problem we choose to sample the laser energy before the motorized mirror by means of a beam splitter as shown in Fig. 2 [3].

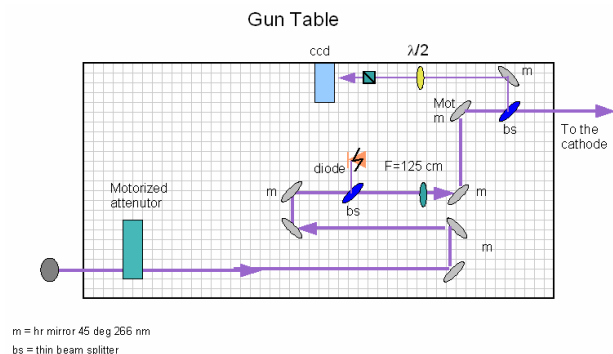


Figure 2: Layout of the final part of the laser beam transfer line. The position of the beam splitter and photodiode is also shown.

With this beam splitter and photodiode configuration, when the motors of the last mirror are used to move the laser spot over the cathode surface, the influence on the measurement of the laser energy pulse became negligible.

*Work supported by Italian National Institute of Nuclear Physics (INFN) and by Ministero Istruzione Università e Ricerca, Progetti Strategici, DD 1834, Dec. 4, 2002, within the SPARC project.

[#]luca.cultrera@lnf.infn.it

THE DCCT FOR THE LHC BEAM INTENSITY MEASUREMENT

P. Odier*, M. Ludwig, S. Thoulet, CERN, Geneva, Switzerland

Abstract

The LHC circulating beam current measurement is provided by eight current transformers, i.e. two DC current transformers (DCCT) and two fast beam current transformers (FBCT) per ring. This paper presents the DCCT, designed and built at CERN, including the sensor, the electronics and the front-end instrumentation software. The more challenging requirements are the needed resolution of $1\mu\text{A}$ rms for a 1s average, and the wide dynamic range of the circulating beam intensity from a single pilot bunch ($8\mu\text{A}$) to the total ultimate beam current of 860mA. Another demanding condition is the high level of reliability and availability requested for the operation and for the machine protection of this highly complex accelerator. The measurement of the first RF captured beam in ring 2 will be shown to demonstrate that the system is close to meeting these specifications both in terms of resolution and stability.

INTRODUCTION

The DCCTs, based on the fluxgate magnetometer principle [1], measure the mean current of the circulating beam. The DCCTs for LHC were designed according to tight engineering specifications [2] and built at CERN.

HARDWARE

General Layout

The DCCTs are installed in the long straight section in Point 4 of the LHC on a long girder which also supports the FBCT [3].

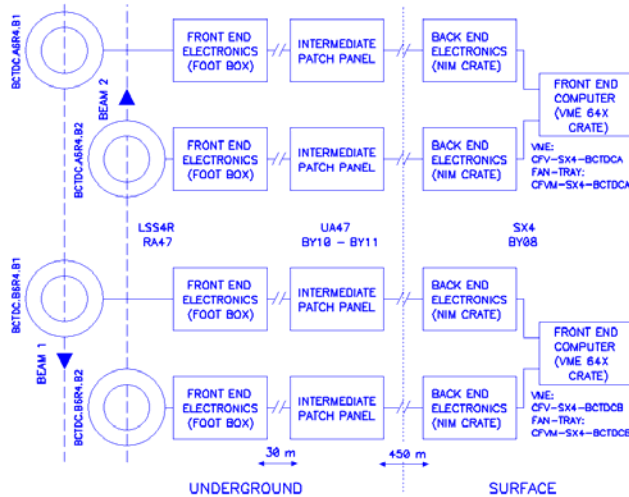


Figure 1: General Layout.

At this location the vacuum chamber is at room temperature and can be baked out to improve the quality

of the vacuum. The front end electronics (FEE) is located in a shielded shelter under the girder and thus protected to some degree from beam induced radiation. An intermediate patch panel located in a parallel gallery housing the FBCT electronics provides an underground monitoring facility. The back end electronics (BEE), as well as the Front End Computer (FEC), are located in a surface building in Point 4 (Fig.1). The two systems named A, normally in operation, and B, normally kept as a spare, each contain one 1 DCCT per ring and 1 FEC.

Sensor

Different elements are installed between the external diameter of the vacuum chamber (64mm) and the internal diameter of the DCCT (114mm) [3]. This includes an electrical heater for baking out the vacuum pipe at 200°C, combined with a thermal insulator and a water cooling circuit to ensure a temperature below 60°C at the level of the magnetic cores.

The magnetic shielding is made of three layers of Mu-metal plus one external layer of pure iron. The external diameter (265mm) is limited by the second ring vacuum chamber (at this location the 2 beam pipe axes are separated by 192mm).



Figure 2: The DCCT with the connexions for the beam intensity measurement.

The “heart” of the DCCT consists of three ring cores of nanocrystalline alloy (inner diameter 146mm, cross-section 190mm^2 , $\mu_i > 100000$) installed in a copper shielding. To avoid mechanical stresses and vibrations inducing noise, the cores are fixed loosely by flexible clips. Two cores, carefully matched to have an identical magnetization curve, are wound to form the fluxgate sensor. The third core is wound to form the AC part providing the bandwidth extension [4]. A magnetic shielding is placed between AC and DC cores to reduce the modulation ripple crosstalk. Two windings of 4 turns

*patrick.odier@cern.ch

SLICED BEAM PARAMETER MEASUREMENTS

D. Alesini, E. Chiadroni, M. Castellano, L. Cultrera, G. Di Pirro, M. Ferrario, D. Filippetto,
 G. Gatti, L. Ficcadenti, E. Pace, C. Vaccarezza, C. Vicario, INFN/LNF, Frascati, Italy
 B. Marchetti, A. Cianchi, University of Rome Tor Vergata and INFN-Roma Tor Vergata, Italy
 A. Mostacci, University La Sapienza, Roma, Italy
 C. Ronsivalle, ENEA C.R. Frascati, Italy

Abstract

One of the key diagnostics techniques for the full characterization of beam parameters for LINAC-based FELs is the use of RF deflectors. With these devices it is possible to completely characterize both the longitudinal and the transverse phase space. In the paper we illustrate the main design considerations for time resolved (sliced) beam parameter measurements using RF deflectors (RFDs). Measurement setups for longitudinal pulse shape as well as phase space and transverse beam slice emittance characterizations are described. The main sources of error are discussed and the design criteria of these devices are presented. In particular the SPARC RF deflector and the related diagnostic lines as well as recent measurement results are shown. Measurement results obtained at LCLS and FLASH are then shortly illustrated.

INTRODUCTION

The characterization of the longitudinal and transverse phase space of the beam at the end of an injector is a crucial point in order to verify and tune all photo-injector parameters. With the use of an RFD it is possible to measure the bunch longitudinal profile and, adding a dispersive system, the longitudinal beam phase space [1,2]. Similarly, since the longitudinal beam distribution can be projected along a transverse coordinate, the transverse emittance of each longitudinal bunch slice can be measured using the quadrupole scan technique [3]. In the first section of the paper we shortly review the basics principles of the longitudinal and transverse beam phase space characterization using an RFD. The main properties of both SW and TW deflecting structures in term of electromagnetic field configuration and performances are discussed in the second section. In the third section we illustrate the typical measurement setups and, in particular, those installed in the SPARC photo-injector [4]. The main measurement results obtained at SPARC are discussed in the fourth section. The last section shows some relevant results obtained at LCLS [5] and FLASH [6] and new proposed techniques.

BEAM DIAGNOSTICS USING RFD

The different types of measurements that can be done with RFDs are based on the property of the transverse voltage (V_{DEFL}) to introduce a correlation between the longitudinal coordinate of the bunch (t_B) and the transverse one (vertical, in general) at the screen

position (y_s). The phase of the deflecting voltage is chosen in order to have a zero crossing of the transverse voltage in the center of the bunch, giving a linear transverse deflection from the head and the tail of the bunch itself. After the deflector the transverse kick results into a transverse displacement of each longitudinal bunch slice, proportional to its position with respect to the bunch center. The mechanism is illustrated in Fig. 1.

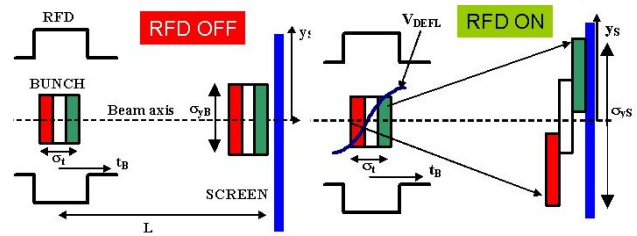


Figure 1: Longitudinal to transverse correlation induced by the RFD transverse voltage.

Since the beam has a finite transverse emittance, the distribution of the deflected bunch at the screen position is the superposition between the deflected beam profile and the transverse size of each bunch slice. In the plot we assumed that all longitudinal slices have the same transverse dimension on the screen (σ_{yB}) and that there is a simple drift (L) between the RFD and the screen. The total vertical rms distribution (σ_{yS}) at the screen is simply given by [2]:

$$\sigma_{yS}^2 \cong K_{cal}^2 \sigma_{tB}^2 + \sigma_{yB}^2 \quad (1)$$

where $K_{cal} = (V_{DEFL}/E)\omega_{RF}L$, ω_{RF} is the angular frequency of the deflecting voltage and E is the beam energy in eV units. From this formula one can define the resolution length (σ_{tB_RES}) as the bunch length that gives, on the screen, a distribution with rms vertical size equal to $\sqrt{2}\sigma_{yB}$. It is simply equal to:

$$\sigma_{tB_RES} = E \frac{\sigma_{yB}}{V_{DEFL} \omega_{RF} L} = \sqrt{E/E_0} \sqrt{\epsilon \beta_S} \frac{1}{V_{DEFL} \omega_{RF} L} \quad (2)$$

where ϵ is the transverse normalized emittance of the beam, β_S is the vertical β -function at the screen position and E_0 is the electron rest energy.

OPTICAL DIFFRACTION RADIATION INTERFEROMETRY AS ELECTRON TRANSVERSE DIAGNOSTICS*

E. Chiadroni[†], M. Castellano, INFN/LNF, Frascati, Italy
 A. Cianchi, University of Rome Tor Vergata and INFN Tor Vergata, Rome, Italy
 K. Honkavaara, G. Kube, DESY, 22607 Hamburg, Germany

Abstract

The characterization of the transverse phase space for high charge density and high energy electron beams is demanding for the successful development of the next generation light sources and linear colliders.

Due to its non-invasive and non-intercepting features, Optical Diffraction Radiation (ODR) is considered as one of the most promising candidates to measure the transverse beam size and angular divergence.

A thin stainless steel mask has been installed at 45° with respect to the DR target and normally to the beam propagation to reduce the contribution of synchrotron radiation (SR) background. In addition, interference between the ODR emitted on the shielding mask in the forward direction and the radiation from the DR target in the backward direction is observed. This is what we call Optical Diffraction Interferometry (ODRI) which, better than ODR, allows to separate the intrinsic ambiguity between the radiation produced by a single particle passing through a slit with an offset with respect to its center and a gaussian distributed particle beam with standard deviation of magnitude equal to such offset.

Results of an experiment, based on the detection of the ODRI angular distribution to measure the electron beam transverse parameters and set up at FLASH (DESY, Hamburg) are discussed in this paper.

INTRODUCTION

The development of high energy Linear Colliders (LC) [1] and short wavelength Free-Electron Lasers (FEL) [2, 3, 4] requires high quality electron beams, which means small transverse emittance (< 1 mm mrad) and high peak current (\approx kA). Due to the large power density of this kind of beams, a non-intercepting diagnostics needs to be developed and applied. In 1997 one of the authors suggested a new method for the non-intercepting measurement of transverse beam size [5]. The idea is based on the observation of diffraction radiation (DR) emitted by a charged particle beam going through a slit in a metallic foil due to the interaction of the charge electromagnetic (EM) field with the screen surface. The intensity of the radiation increases linearly with the number of charges and is proportional to $e^{-\frac{2\pi a}{\gamma \lambda}}$, where a is the vertical slit aperture, γ

the Lorentz factor and λ the emitted wavelength. The factor $\gamma \lambda / 2\pi$, called as DR impact parameter, is the natural size of the radial extension of the EM field, thus when $a \approx \gamma \lambda / 2\pi$ DR is emitted.

Since the beam goes through the slit, DR is a non-intercepting diagnostics and, therefore, excellent to be used parasitically without disturbing the electron beam.

The aim of our experiment is measuring the transverse beam size and divergence, in order to calculate the transverse emittance, by studying the angular distribution of Optical Diffraction Radiation (ODR). The DR angular distribution is produced by the interference of radiation from both edges of the slit. The visibility of the interference fringes is correlated to the beam size (see Fig. 1, left).

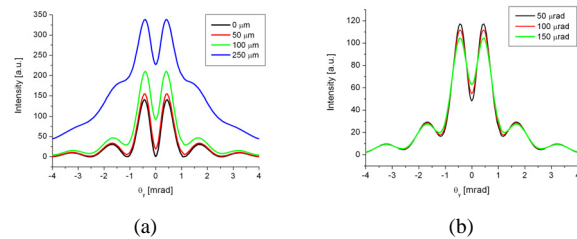


Figure 1: Theoretical calculation for the angular distribution of the vertical component of ODR for different transverse beam sizes and vertical angular divergences. The simulation has been performed assuming an electron beam energy of 680 MeV, with interference filter (800 nm) and 0.5 mm slit width.

The effect is also affected, in a slightly different way, by the angular divergence of the beam (Fig. 1, right): the ODR angular distribution becomes wider and the intensity of the minimum higher, when the beam divergence increases.

A dedicated analysis of the radiation angular distribution allows then to separate the two effects. If the beam waist is located in the plane of the DR screen, the transverse emittance can be derived with a single non-intercepting measurement.

EXPERIMENTAL APPARATUS

Our experiment is carried out at FLASH (DESY, Hamburg)[7]. FLASH is an excellent facility for this experiment, since it can drive long bunch trains, up to 800 bunches per macropulse allowing a high charge operation, and it has a good long term stability, a small transverse

* Work supported by the European Community Infra-structure Activity under the FP6 "Structuring the European Research Area" program (CARE, contract number RII3-CT-2003-506395)

[†] enrica.chiadroni@lnf.infn.it

ELECTRON SCANNER FOR SNS RING PROFILE MEASUREMENTS*

W. Blokland, S. Aleksandrov, S. Cousineau, ORNL, Oak Ridge, TN 37831, U.S.A.
 D. Malyutin, S. Starostenko, Budker Institute of Nuclear Physics, Novosibirsk, Russia

Abstract

An electron scanner has been commissioned to non-destructively measure the transverse profiles in the Spallation Neutron Source (SNS) Ring. The SNS Ring is designed to accumulate on the order of 1.6×10^{14} protons with a typical peak current of over 50 Amps. The electron scanner works by measuring the deflection of 50-75 keV electrons by the electric field of the proton beam. Two electron guns, one for each plane, with dipole correctors, quadrupole magnets and deflectors to shape the electron beam have been installed. This paper describes the system and the initial results.

INTRODUCTION

The electron scanner is the first instrument to measure the transverse beam profiles in the SNS accumulator ring. Alternative profile monitors such as wire-scanners were planned but not installed due to budget restrictions. The electron scanner projects electrons accelerated up to 75 keV through the proton beam as depicted in Fig.1.

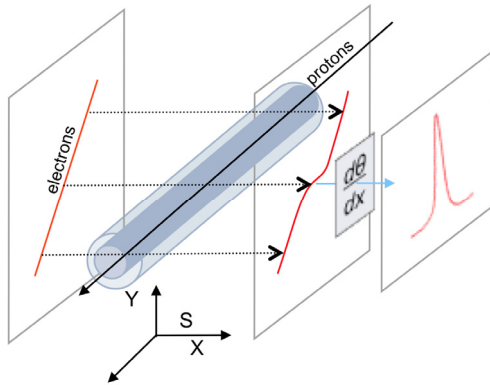


Figure 1: The deflection of the electrons.

The transverse profile is derived from the angle of deflection of the electron beam according to the following formula, see also [1,2,3]:

$$\frac{d\theta}{dx} = \int_L \frac{e}{mv^2} \cdot \frac{\delta(x,y)}{\epsilon_0} dy$$

where e , m are the electron charge and mass, respectively, v is the velocity, $\delta(x,y)$ is the proton beam density distribution, and θ is the electron beam deflection angle.

This assumes that the path of the electrons is approximately straight, the net energy change to the

* ORNL/SNS is managed by UT-Battelle, LLC, for the U.S. Department of Energy under contract DE-AC05-00OR22725

electrons by the proton beam is close to zero, and the effect of the proton magnetic field can be neglected.

ELECTRON SCANNER HARDWARE

The electron scanner layout is depicted in Fig. 2. The different parts are: (1) electron gun, (2) deflection scan system, (3) dipole correctors, (4) quadrupole magnets, (5) vacuum chamber for proton beam, and (6) the phosphor screen.

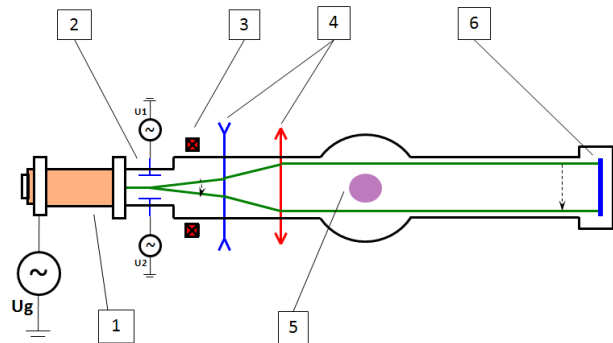


Figure 2: Diagram of electron scanner.

The electron gun produces a pulse of about 1 usec of up to 75 keV electrons with a maximum current of 5 mA. The scan system applies a 20 nsec long ramp to the deflectors to project the electrons on a diagonal line. The diagonal projection makes the deflection of the electrons by the proton beam visible as a deviation from a straight line. The first quadrupole extends the range of the deflection while the second quadrupole focuses the electron beam such that the electron beam is parallel. The electron gun is pulsed once a second but faster rep rates of up to 5 Hz are possible. The time line is shown in Fig. 3. To minimize the electron beam size, the cathode heating is turned off for a few milliseconds before the acceleration pulse.

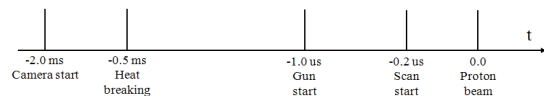


Figure 3: Time diagram.

One vertical and one horizontal scanner are installed in the tunnel, see Fig. 4. GigE Vision CMOS cameras acquire the images from the fluorescent screens. Because the scanners are located in a straight section of the ring, the radiation levels are low enough to not damage the cameras. A single PXI-based computer running LabVIEW controls the cameras, timing, pulse generators and power supplies of the electron scanner.

ELECTRON BEAM DIAGNOSTICS FOR THE EUROPEAN XFEL

D. Nölle, DESY, D-22607 Hamburg, Germany, on behalf of the XFEL Team

Abstract

The European XFEL is an X-ray free-electron-laser that is currently being built in Hamburg. It is organized as an international project and will be a large scale user facility [1,2]. Based on superconducting TESLA technology electron beams of high average power will be sent to several undulator lines simultaneously to produce hard X-rays with high average intensity and a peak brilliance by far superior to any 3rd generation light source. This paper will present the current status of the planning, the development and the prototyping process for the standard electron beam diagnostics of this facility. It will cover the main diagnostic systems, like the BPM system, beam size measurements, charge and beam loss measurements as well as the machine protection system.

INTRODUCTION

The European XFEL (E-XFEL) is a project to construct an international X-ray Free-Electron-Laser user facility close to DESY in Hamburg. The facility will be operated by a limited liability company with shareholders from the participating countries.

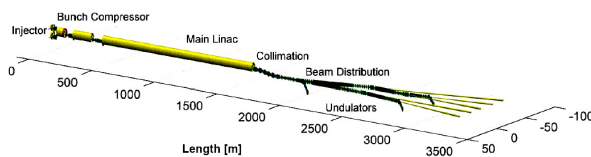


Figure 1: Sketch of the layout of the E-XFEL.

DESY will act as a host lab and leads the accelerator consortium, that is in charge for the construction of the accelerator. Like the FLASH facility [3] E-XFEL will also be based on superconducting TESLA RF technology. Therefore, this machine will provide much higher duty cycle as machines like SCCS and LCLS. An electron beam with a pulse length of 650 μ s and a bunch rep rate up to 5 MHz will be accelerated up to 17.5 GeV at a repetition rate of 10 Hz. The shortest XFEL wavelength will be 0.1 nm or about 10 keV. To make optimum use of the high duty cycle, the long bunch trains can be distributed into 2 SASE undulator lines, which will be ramified into additional lines for “secondary undulators” that make use of the spent beam producing either FEL or spontaneous radiation. The time structure of the beam can be adjusted independently for both main SASE undulators (SASE I and SASE II) by means of a kicker septum scheme in the beam distribution system.

While the contracts between the founder states of the XFEL Company are still in the phase of final negotiation, and the signature of the conventions can be expected for summer, the construction phase of the facility has already started. The contracts for civil construction are placed and

groundbreaking took place in winter 2008/2009. Also the procurement of main components will start this summer. The construction is scheduled to take about 5.5 years. According to this planning commissioning should start 2014. SASE is expected to follow about 1 year later.

STANDARD BEAM DIAGNOSTICS

This paper focuses on standard beam diagnostics like beam position, charge, beam size and beam loss. These systems are currently in the design phase. First prototypes are under construction or will be available soon. A description of the more specialized diagnostic systems can be found in Ref.[4].

BEAM POSITION MONITOR SYSTEM

Beam position monitors are the backbone of the diagnostic system. E-XFEL will distinguish between standard BPMs with moderate resolution and precision BPMs, where higher performance is required. For the standard BPMs mainly the button type will be used. About one third of the BPMs in the accelerator modules will be re-entrant cavity BPMs. About every third RF-Section of the LINAC, consisting of 4 accelerator modules, will be equipped with monitors of this type to provide a better resolution if required.

Cavity BPMs will be used mainly in and close to the undulator sections. One cavity BPM will be located in each undulator intersection. In addition before and behind the undulator sections there will be some of these cavity BPMs to allow for precise beam based alignment. Further high precision (cavity) monitors with a 40.5 mm beam pipe diameter will be used before the LINAC sections and in the collimation and distribution section. This type will also be used for the Intra Bunchtrain Feedback System (IBFB) developed by PSI [5].

Table 1: Numbers and types of the E-XFEL BPMs

BPM Type	Number	Diameter	Single Bunch Resolution
Standard Button BPM	228	40.5 mm	50 μ m
“cold” BPM (Button, Re-entrant Cavity)	101	78 mm	50 μ m
Precision BPM (Cavity)	117	10 mm	1 μ m
Precision BPM (Cavity)	12	40 mm	1 μ m

The BPM system for the E-XFEL will be provided by a collaboration of PSI, CEA and DESY. DESY will take

BEAM INDUCED FLUORESCENCE MONITOR & IMAGING SPECTROGRAPHY OF DIFFERENT WORKING GASES*

F. Becker[†], C. Andre, P. Forck, R. Haseitl, A. Hug, B. Walasek-Hoehne, GSI, Darmstadt, Germany, F. Bieniosek, P.A. Ni, LBNL, Berkeley, California, D.H.H. Hoffmann, TUD, Darmstadt, Germany

Abstract

Beam induced fluorescence spectra in the range of 300-800 nm were investigated with an imaging spectrograph. Wavelength-selective beam profiles were obtained for a 5.16 MeV/u sulphur beam in nitrogen, xenon, krypton, argon and helium at 10^{-3} mbar gas pressure. In this paper calibrated BIF spectra of specific gas transitions were identified and corresponding beam profiles presented. The measurement results are discussed for typical applications at the present setup and the future FAIR facility.

MOTIVATION

As conventional intercepting diagnostics will not withstand high intensity ion beams, **Beam Induced Fluorescence (BIF)** profile monitors constitute a pre-eminent alternative for online profile measurements [1]. At present, two BIF monitors are installed at the GSI UNILAC and several locations are planned for the FAIR high energy beam transport lines [2]. For further optimizations accuracy issues like gas dynamics have to be investigated systematically. Especially the determination of focused beams in front of targets with high line charge densities rely on a careful selection of proper working gas transitions to keep profile distortions as low as possible [3].

EXPERIMENTAL SETUP

Key issue of this experimental layout using an imaging spectrograph with an area scan intensified CCD (ICCD) camera (Fig. 1) was to have both, the spectral information of specific beam induced gas transitions along the diffraction axis and the spatial information about the beam profile width, transition wise along the imaging axis, see Fig. 2. For 150 mm object distance, a chromatically corrected UV-lens of $f=50\text{mm}$ and $f/2.8$ was chosen. A CCD height of 4.9 mm and a total reproduction scale $\beta_{tot}=0.42$ yield a 19.5 mm field of view.

Imaging Spectrograph & Gas Composition

The $\varnothing 70$ mm spherical mirror with 140 mm focal length is holographically etched and astigmatism corrected. 140 sinusoidal grooves per mm produce a spectral dispersion of 50 nm/mm and an image field of 8×12 mm on the vertical imaging axis and the horizontal dispersive axis, respec-

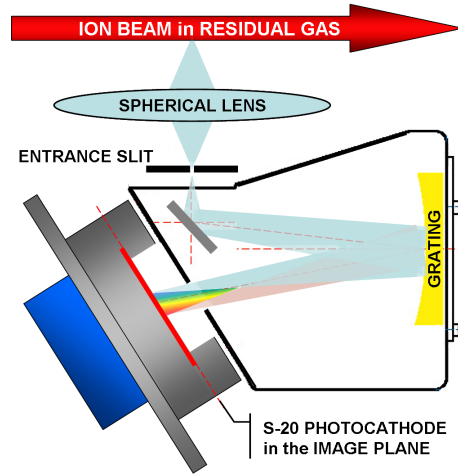


Figure 1: Top-view of the optical path in the diffractive plane. Length of spectrum in the image plane is 10 mm. 1:1 imaging from slit to image plane. All refractive optics adapted to UV-VIS [5]. ICCD performs single photon detection and has a $\varnothing 25$ mm UV-enhanced photocathode with a V-stack MCP [6] and digital VGA camera [7] (bluish).

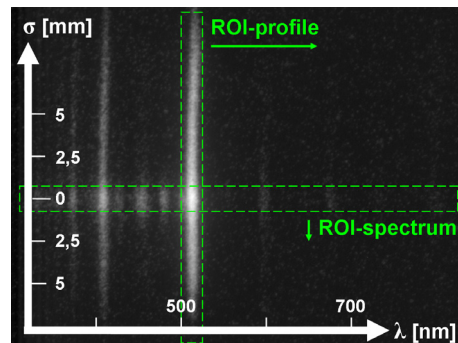


Figure 2: Spectrographic average image $n=2000$ of $3 \cdot 10^{11}$ S^{6+} ions @ MeV/u in 10^{-3} mbar helium gas, $\sigma_w=1.8\text{mm}$. Logarithmic gray-scale for better presentation.

tively. With an optical resolution of 33 lp/mm the ICCD limits the spectral resolution to 1.5 nm for an entrance slit $\leq 30 \mu\text{m}$. The total spectral system efficiency includes all single component efficiencies as a convolution, see Fig. 3 (upper plot). Most limiting factors in the wavelength range ≥ 600 nm are the tri-alkali (Na_2KSb)Cs photocathode and the decreasing grating efficiency. Investigation of optical gas spectra relies on a sufficient purity of the actual gas species. In order to measure and control impurities, a resid-

* Work supported by EU, project FP6-CARE-HIPPI

[†] Frank.Becker@gsi.de

THE LHC SYNCHROTRON-LIGHT MONITORS

A.S. Fisher*, SLAC National Accelerator Laboratory, Menlo Park, CA 94025, USA
A. Goldblatt and T. Lefevre, CERN, Geneva, Switzerland

Abstract

Synchrotron-light telescopes will measure the profiles of the two LHC beams of protons or lead ions, and verify that the abort gap is clear. At collision energy (7 TeV), each telescope will image visible light from a superconducting dipole used to widen beam separation at the RF cavities. At injection (0.45 TeV), this source must be supplemented by a 2-period superconducting undulator 1 m from the dipole. An optical “trombone” delay line will provide the large shift in focus. We discuss the optical design, diffraction, depth of field, and the expected signals over the energy ramp, for emission from the centre and edge of the dipole and from the undulator.

INTRODUCTION

The two LHC synchrotron-light telescopes (BRST [1]) will measure the transverse beam profiles. The abort-gap monitor (AGM or BRSA [2]) will verify that the 3- μ s gap contains an acceptably small number of particles, since a partial kick during the rise of the abort kicker may drive them into a magnet and cause a quench.

Protons will be injected at 450 GeV and ramped to collisions at 7-TeV, where they emit enough synchrotron light in superconducting dipoles for imaging. However, arc dipoles are interconnected in a long series of cryostats, with no access to this light. In the IR-4 straight, a chicane of four 9.45-m dipoles widens the beam separation from 194 to 420 mm for RF cavities. As the beam exits the cavities, dipole D3 bends it by 1.57 mrad. In the 62-m drift to the fourth dipole, light from the first 3 m of D3 diverges from the protons, reflects from an extraction mirror at 26 m, and passes through a fused-silica vacuum viewport to optics below the beamline. The dipoles ramp to 3.88 T at 7 TeV, bringing the critical wavelength λ_c from 0.23 mm to 61 nm in an orbit with radius $\rho=6$ km.

At injection, since the dipole’s visible emission is negligible, a short superconducting undulator [3] with $N_u=2$ periods of $\lambda_u=28$ cm was added to the cryostat 937 mm before D3. With $B_u=5$ T (not ramped), its spectrum for 450-GeV protons peaks in the visible, at 610 nm.

The ALICE detector will study lead-ion rather than proton collisions. With fewer particles and a red-shifted spectrum, this experiment requires separate evaluation.

Since ρ must be the same for proton and ion orbits, at a given dipole field the energy must scale with charge. Lead ions will collide at $Z=82$ times the 7-TeV proton energy (92 μ J/ion!). The relativistic factor γ scales by Z/A .

EMITTED ENERGY PER PARTICLE

For central dipole radiation, the energy per particle emitted (in both polarizations) into solid angle and fre-

quency $d\xi d\psi d\omega$ (where the horizontal and vertical angles ξ/γ and ψ/γ are conveniently expressed in normalized form) is expressed using modified Bessel functions K [4]:

$$W_d = Z^2 \frac{3}{4\pi^2} W_0 \left(\frac{\omega}{\omega_c} \right)^2 (1 + \psi^2)^2 \left[K_{2/3}^2(\zeta) + \frac{\psi^2}{1 + \psi^2} K_{1/3}^2(\zeta) \right] \quad (1)$$

$$W_0 = \frac{e^2}{4\pi\epsilon_0 c} = 7.6956 \cdot 10^{-37} \text{ J} \cdot \text{s} \quad (2)$$

$$\zeta = \frac{\omega}{2\omega_c} (1 + \psi^2)^{3/2} \quad (3)$$

$$\omega_c = \frac{2\pi c}{\lambda_c} = \frac{3}{2} \gamma^3 \frac{c}{\rho} \quad (4)$$

We model the dipole’s edge field as:

$$B(z) = \frac{B_d}{2} \left(1 + \frac{2}{\pi} \arctan \frac{z}{L_e} \right) \quad (5)$$

The edge radiation is then given by [5]:

$$W_e = Z^2 \frac{8}{9\pi^2} W_0 \left(\frac{\omega_c}{\omega} \right)^2 \frac{(1 - \xi^2 + \psi^2)^2 + (2\xi\psi)^2}{(1 + \xi^2 + \psi^2)^6} \cdot \exp \left[-\frac{\omega L_e}{\gamma^2 c} (1 + \xi^2 + \psi^2) \right] \quad (6)$$

Note that this expression diverges for $\omega \ll \omega_c$; these low frequencies are emitted as the particle moves from the edge to the uniform field, and so edge and central radiation are not really distinct in this range.

The energy from undulator radiation is given by [4]:

$$W_u = \frac{Z^4}{A^2} N_u^2 K_u^2 W_0 \frac{(1 - \xi^2 + \psi^2)^2 + (2\xi\psi)^2}{(1 + \xi^2 + \psi^2)^4} \quad (7)$$

$$\cdot \left(\frac{2\omega}{\omega + \omega_1} \right)^2 \text{sinc}^2 \left(\pi N_u \frac{\omega - \omega_1}{\omega_1} \right)$$

with undulator parameter K_u and first-harmonic ω_1 :

$$K_u = \frac{eB_u \lambda_u}{2\pi m_p c} \quad (8)$$

$$\omega_1 = \frac{4\pi\gamma^2 c}{\lambda_u (1 + \xi^2 + \psi^2)} \quad (9)$$

OPTICAL CONSIDERATIONS

Depth of Field in the Dipole

Due to the small bend angle, dipole light will be collected over a long path. In the horizontal plane, rays are emitted tangent to the orbit (Fig. 1). They focus in the optical system as if originating at their intersection R with the focal plane. We see which ray angles from a point M

*afisher@slac.stanford.edu

HIGH CURRENT ION BEAM INVESTIGATIONS ON INORGANIC SCINTILLATION SCREENS

E. Gütlich*, P. Forck, B. Walasek-Höhne, GSI, Darmstadt, Germany
 W. Ensinger, Technical University of Darmstadt, Germany

Abstract

At the GSI heavy ion LINAC, the properties of scintillating screens irradiated by the ion beam were studied. Different ion beams from H^+ to U^{28+} in the energy range from 4.8 to 11.4 MeV/u were used with currents up to some mA. The investigations were focused on ceramic materials. Their properties (light yield, beam width and higher statistical moments) were compared with different quartz glasses. The image of each ion beam pulse was recorded by a digital CCD camera and individually evaluated. The recorded beam width shows dependence on the used scintillator material. Additionally, the light yield and beam width depend significantly on the screen temperature. For ZrO_2 the influence of the screen temperature on the statistical moments was investigated. Furthermore, the spectra of the scintillation screens were studied in the UV-VIS region with different ion species.

INTRODUCTION

Since decades, scintillation screens are widely used for beam profile measurement in nearly all accelerator facilities. Moreover, these screens are an essential part of a pepper-pot emittance system. The realization at GSI, as used for the high current operation of the LINAC, is described in [1]. However, there had been doubts concerning the accuracy of the pepper-pot method [2], which might be related to a possible image deformation by the scintillating screen as reported in [3, 4, 5]. The properties of the luminescent materials (see Table 1) were investigated with ion beams of H^+ , C^{2+} , Ar^{10+} , Ni^{9+} , Ta^{24+} and U^{28+} at energies between 4.8 and 11.4 MeV/u and different beam currents as delivered by the LINAC. The typical size of the ion beam was $\sigma = 2$ mm. Sensitive scintillation screens, like the single crystal $YAG:Ce$ or $ZnS:Ag$, were irradiated with lower currents [4]. The ceramic materials with less light yield, like BN , ZrO_2 , $ZrO_2:Mg$, pure Al_2O_3 and $Al_2O_3:Cr$ (Chromox), were investigated and compared to Quartz-glass (Herasil 102) and Quartz-glass doped with Ce (M382). The realised experimental setup and the data acquisition system are described in [4, 6]. The original image of the beam spot was projected to the horizontal and vertical plane of the beam. In this work the results for the horizontal projection are presented, but comparable results were also obtained for the vertical one. For the characterization of the distribution $p_i(x_i)$ not only the centre μ (1st moment) and standard deviation σ (2nd mo-

Table 1: Compilation of Investigated Materials

Type	Material	Supplier
Ceramic	ZrO_2 (Z700-20A), $ZrO_2:Mg$ (Z507), BN , Al_2O_3 , $Al_2O_3:Cr$,	BCE Special Ceramics
	Quartz glass	

ment) were used, but also the skewness γ (3rd moment, parameter of the asymmetry) and the kurtosis κ (4th moment, the peakedness) [7].

SCREEN INVESTIGATION

The interest of pepper-pot emittance measurements arises from the UNILAC high current operation with several mA. As reported in [3, 4, 5], the imaged beam width depends significantly on the temperature of the scintillating screen. An example for high current measurement is shown in Fig.1 where the screens were irradiated by Ar^{10+} with a current of $310 \mu A$ within $100 \mu s$ delivery time corresponding to $2 \cdot 10^{10}$ ppp. The peak power was 14 kW while the average power was 3.8 W. As expected the light yield of the various materials differs by several orders of magnitude. For the four materials $Quartz:Ce$, $ZrO_2:Mg$, BN and $Herasil$ the yields drop significantly during the irradiation. The determined beam width varies within a factor of two. The light yield decreases coincidentally with the imaged beam width, but with a slightly different time constant. Since it is known that the light yield reduction is correlated with the screen temperature [3, 4, 5], a break in the beam delivery of 3 minutes was scheduled to let the screens cool down. For *Herasil*, Al_2O_3 , $Al_2O_3:Cr$ and $ZrO_2:Mg$ the light yield and the beam width show reproducible time behaviour and reach a constant value. For Al_2O_3 the light yield is constant whereas for $Al_2O_3:Cr$ the yield even increase. In both cases, a broadening of the image width occurs in a reproducible manner. Using a PT100 temperature sensor at the backside of $ZrO_2:Mg$ screen the average temperature of $240^\circ C$ was determined for comparable beam parameters with an average power of 2.3 W (respectively to 3.8 W for the measurements shown in Fig.1). The interpretation of the temperature behaviour is challenging. As reviewed in [8] and [9] the light yield of crystal scintillators like $NaI:Tl$, BGO and $CdWO_4$

* E-Mail: e.guetlich@gsi.de

FAST WIRE SCANNER CALIBRATION

J. Koopman, A.G Ollacarizqueta, CERN, Geneva, Switzerland
A. Likhovitskiy¹, JINR, Dubna, Russia, CERN

Abstract

The fast rotating wire scanners installed in the PS and the PS booster are used for the precise transversal profile measurements in horizontal and vertical planes. The scanners may show large position measurement errors if no special treatment is applied to the acquired data. The aim of the calibration is to obtain a correction algorithm for the systematic position measurement error due to mechanical and electronic offsets.

A new calibration system has been developed and introduced in CERN for the scanners implementing position feedback control. The calibration method is based on a substitution of a particle beam by a laser one where the laser beam position is well known. According to the previous experience the following crucial requirements to the system have been taken into consideration: heavy and mechanically stable design of the calibration bench to reduce mechanical oscillations of scanner parts; automation of the calibration procedure to exclude human errors in data taking, storing and analysis; high precision of the laser positioning; minimization of the total amount of scans and calibration time for each scanner.

SYSTEM OVERVIEW

The setup consists of a massive vacuum tank that can receive either a horizontal or a vertical scanner with 2 viewports at the position where normally the vacuum chamber is situated. A laser beam, split into two parallel beams of nearly equal intensity distant by 2.7 mm by means of special optics, through which the wire travels at high speed, is mounted in front of one viewport. Behind the second viewport a large fixed mirror is positioned.

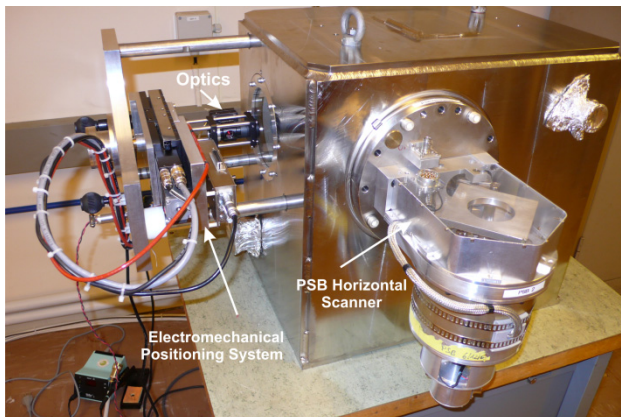


Figure 1: Calibration bench with a horizontal PS booster scanner

The carbon wire scanning through the beams creates thus twice a shadow detected by one single photo-detector, resulting in 2 negative peaks and otherwise con-

stant signal. Correlating the measured peak positions with the real laser beam position allows the creation of a correction algorithm. For the automation purposes the laser and photo-detector are mounted together on a translation table and moved by a stepping motor (Parker MX80S, stepping motor driven linear stage.).

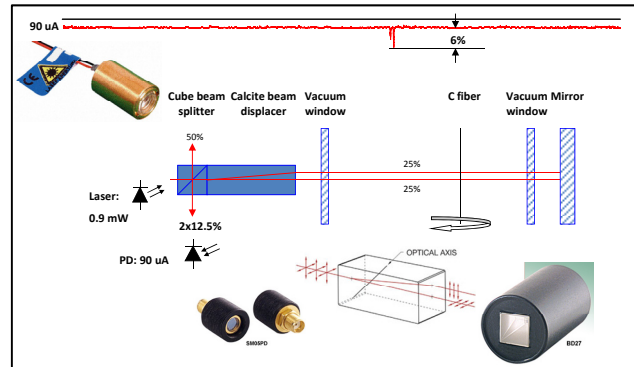


Figure 2: Measurement principal.

An expected and observed signal from the 30 μm C-fiber travelling with a speed of 10 to 20 m/s through a 200 μm (σ) laser beam (1mm diameter) only has a modulation depth $\sim 6\%$. A precise adjustment of the optical subsystem is required to provide conditions at which a peak detection algorithm works stable. One should note it impacts on the total number of scans which is needed to be done during the calibration of a scanner. A minimal number of bad scans, when peaks cannot be detected precisely, is allowed to make less repeated scans and to extend the life-time of bellows and wires.

Motion Control and Acquisition Electronics

The electronics for the acquisition and control of the wire-scanner movement and laser positioning are hosted in a standard VME64x crate. The motion control card [5] is in charge of the scanner positioning and the laser beam acquisition. The laser movement and position acquisition are controlled through a TVME200/IP-OCTAL-422 card connected to a MIDI crate [6]. Two FESA [3] classes running on a RIO3-8064 CPU card control the system. When a scan is launched, the position of the scanner is measured by means of a precision rotary potentiometer. A 16-bit ADC performs the read-out of each position measurement which is then stored in a 256k memory block. The standard wire-scanner installation acquires the signal coming from a photomultiplier using a logarithmic amplifier. The calibration installation has to use the laser detector signal instead. The signal is read with a 12-bit ADC configured to acquire an external input signal. The measurement in both cases is stored in another 256k memory block of the motion control card. The rate of acquisition is

¹ Arkady.Likhovitskiy@cern.ch

TRANSVERSE PROFILE MONITORS BASED ON FLUORESCENCE FOR IFMIF-EVEDA ACCELERATOR

J.M. Carmona*, B. Brañas, A. Ibarra, I. Podadera, CIEMAT, Madrid, Spain

Abstract

IFMIF-EVEDA prototype accelerator will be a 9 MeV, 125 mA continuous wave (CW) deuteron accelerator, focused on validating the technology that will be used in the future IFMIF facility [1]. In such a high current low energy deuteron accelerator, any interceptive diagnostic could be destroyed. In the quest of non interceptive beam transverse profilers required for IFMIF-EVEDA, two different options are considered: A monitor based on the fluorescence of residual gas developed by CIEMAT and another based on ionization developed by CEA [2]. In this contribution, a description of the beam transverse profile monitor prototype based on fluorescence, together with a brief analysis of the reliability of the profiles captured with this monitor will be presented.

INTRODUCTION

The International Fusion Materials Irradiation Facility (IFMIF) aim is to provide a materials irradiation database for the design, construction, licensing and safe operation of the future Fusion Demonstration Reactor (DEMO) [2]. In such a reactor, high neutron fluxes may generate up to 30 dpa/fpy (displacements per atom/full power year). IFMIF facility will be a dual 40 MeV deuteron accelerator (2 x 125 mA operating in continuous wave), colliding with a liquid lithium target with the aim to produce high neutron fluxes to test new materials.

In the framework of the “Broader Approach”, the IFMIF-EVEDA (Engineering Validation and Engineering Design Activities) project includes the construction of an 9 MeV and 125 mA (CW) deuteron accelerator prototype. Most of the components of the accelerator are being developed by France, Italy and Spain [3].

In such high current accelerator, non-interceptive diagnostics are required. Hence, in the following sections, a brief description of the first prototype for the EVEDA fluorescence profile monitor will be provided. Such monitor is actually in design and prototyping phases.

PROTOTYPE PROFILE MONITORS

As part of the diagnostics package, non interceptive profile monitors will be installed along the line of the EVEDA accelerator with the aim to measure and characterize the beam. A fluorescence profile monitor is based on the interaction between the beam particles and the residual (or injected) gas inside the vacuum chamber of the accelerator. Photons are produced due to the excitation and de-excitation of the gas molecules or atoms (in the case of injected atomic gas). This technique has been tested already at different accelerator e.g. CERN-

PSB [4] and GSI-UNILAC [5].

The light emitted, can be collected and used for the determination of the beam profiles. The low cross sections between the beam and the gas at those energies (9 MeV), can be counteract by increasing the integration time (taking advantage of CW operation) and optics optimization.

A set of collection optics will be installed to obtain horizontal and vertical projections of the beam at the same position. Briefly it consists of a special optical window and a set of optics plus a detector. Depending on the results of the first prototype, the detector could be finally located in front of the viewport or installed in a safety place inside of a shielded box, using a coherent fibre bundle to transport the image from the viewport to the camera. A movable calibration system and a gas valve will be installed in order to provide spatial calibration and to increase the pressure locally, respectively. Finally, a filter wheel could be installed to select different line transitions.

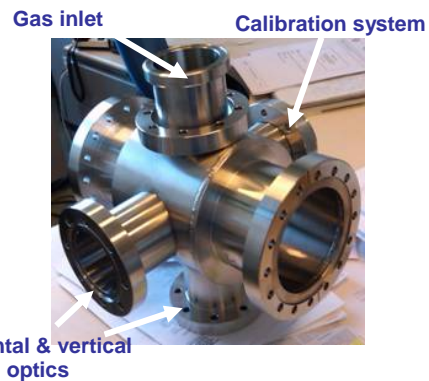


Figure 1: Illustration of the prototype vacuum chamber for the fluorescence profile monitor, showing the vertical and horizontal viewports, as well as those for gas injection and calibration.

Challenges for IFMIF-EVEDA Profile Monitors

The high neutron and gamma fluxes can lead into a permanent damage for electronic devices like detectors or standard fibres. Detectors usually loose dynamic range and contrast with radiation and can become inoperative even at low dose rates [6]. The detector which suits better our requirements must be chosen carefully, taking into account quantum efficiencies, readout times, spatial resolution, dynamic range and rad-hard operation. CCD's and CID cameras from several companies have been considered. To date, the most promising candidate for EVEDA are CID rad-hard cameras because of its dynamic range and rad-hard resistance operation of some models (up to 3 Mrad). Other detectors like PMT's or

*jm.carmona@ciemat.es

THE BEAM PROFILE MONITORS FOR SPIRAL 2

J.L. Vignet, A. Delannoy, E. Guérault, P. Gangant, J.C. Foy, S. Cuzon, C. Houarner, M. Blaizot, GANIL, BP 55027, 14076 Caen Cedex 5, France

Abstract

In order to visualize the SPIRAL 2 beam dynamics, several beam profile monitors are under development. Multiwires beam profile monitors (SEM) will be used on the driver and RIB lines. Non interceptive beam profile monitor (RGM) should be mounted on the LINAC diagnostics box before experiments room, and low intensity beam profile monitor (EFM) on the RIB lines. For the signals acquisition of all this kind of monitor, a new associated electronics will be used. These electronics digitize 94 channels in a parallel system. Each channel integrates the current of the associated wire or strip and performs a current-voltage conversion. The dedicated GANIL data display software has been adapted for these different new monitors.

SPIRAL2 DESCRIPTION

The SPIRAL2 facility is based on a high-power superconducting driver LINAC which delivers a high-intensity, 40-MeV deuteron beam, as well as a variety of heavy-ion beams with mass-to-charge ratio equal to 3 and energy up to 14.5 MeV/u (Table 1). The driver accelerator will send stable beams to a new experimental area and to a cave for the production of Radioactive Ion Beams (RIB). The Accelerator building construction (phase 1) will start in 2010 and the RIB production building (phase 2) in 2012 (Fig. 1). The commissioning of the driver should start in 2011 at GANIL.

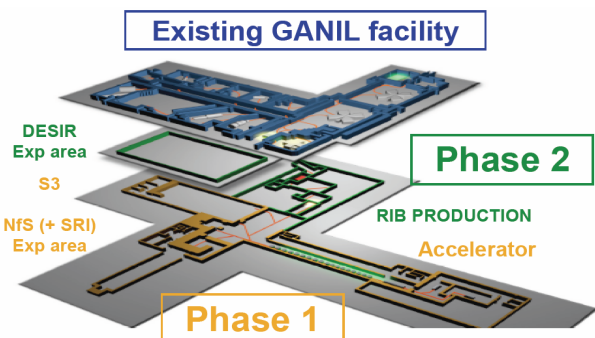


Figure 1 : SPIRAL 2 and GANIL facilities.

DRIVER ACCELERATOR

The Injector, dedicated to protons, deuterons and ions of $Q/A=1/3$, is mainly composed of two ECR ion sources with their associated LEBT (Low Energy), a warm RFQ and the MEBT (Medium Energy) line connected to the LINAC. The LINAC accelerator is based on superconducting independently-phased resonators. It is composed of 2 families of quarter-wave resonators (QWR) at 88 MHz, 12 resonators with $\beta=0.07$

(1 cavity/cryomodule), and 14 resonators at $\beta=0.12$ (2 cavities/cryomodule).

STABLE BEAM CHARACTERISTICS

Table 1: SPIRAL 2 Stable Beam Characteristics

	Q/A	Intensity range (mA)	Energy range (MeV/u)	CW beam Power (kWatt)
Protons	1	0-5	2-33	165
Deuterons	1/2	0-5	2-20	200
Ions	$\geq 1/3$	0-1	2-14.5	43.5
Ions	$\geq 1/6$	0-1	2-8.5	51

RIB PRODUCTION

The 40 MeV, 5 mA deuteron beam impinging on the converter produces an intense neutron flux with a energy centered at 14 MeV. Neutrons induce fission in the UC target located downstream of the target converter. The converter has to withstand up to 200kW beam power. The converter is a high speed rotating target which limits the peak surface temperature of converter materials far below 2000°C. The thermal power deposit in the converter material is dissipated only by thermal radiation.

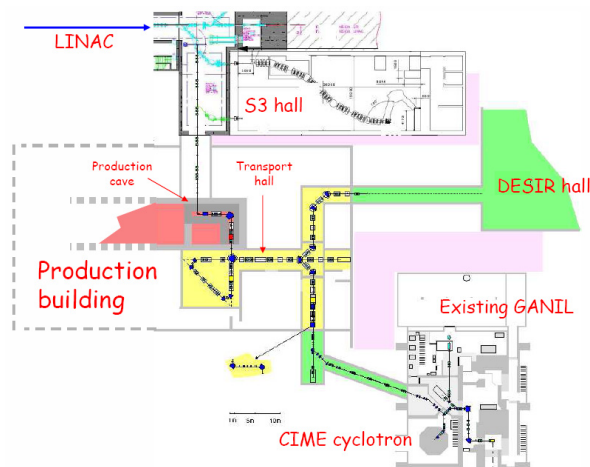


Figure 2 : Radioactive beam facilities.

Table 2: Radioactive Beam Characteristics

	Line 1+	Line n+	Existing ganil
Ion mass range	6 to 240	6 to 160	6 to 160
Intensity range (pps)	10^3 to 10^{11}	10^3 to 10^{10}	10^3 to 10^9
Beam energy	10 to 60 keV	10 to 45 keV	1.2 to 20 MeV/u
Example of RIB	132 Sn^{1+}	132 Sn^{20+}	132 Sn^{20+}
	20 keV	400 keV	792 MeV

DESIGN OF A NOZZLE-SKIMMER SYSTEM FOR A LOW PERTURBATION IONIZATION BEAM PROFILE MONITOR*

M. Putignano[†], C. P. Welsch, Cockcroft Institute and University of Liverpool, UK
K.-U. Kuehnel, Max Planck Institute for Nuclear Physics, Heidelberg, Germany

Abstract

Growing interest in the development of low energy projectiles, in particular heavy ions and antiprotons, calls for new beam instrumentation to be developed to match the strict requirements on ultra-high vacuum and low beam perturbation. When it comes to transverse profile monitoring, a convenient solution for simultaneous determination of both transverse profiles is found in a neutral supersonic gas-jet target shaped into a thin curtain and the two-dimensional imaging of the gas ions created by impacting projectiles. The resolution and vacuum efficiency of this monitor is directly linked to the characteristics of the gas-jet curtain.

In this contribution we describe the design of a nozzle-skimmer system to be used for the creation of the jet curtain in the first prototype of such monitor, together with the geometry and extraction field shape of the experimental chamber which will house the experiment. Using numerical fluid dynamics simulations, we present the effects resulting directly from changes in the geometry of the nozzle-skimmer system on the characteristics of the jet curtain.

INTRODUCTION

Low-energy physics and storage rings are recently attracting growing interest in the scientific community, as remarkable characteristics of quantum systems are most conveniently studied at low projectile energies in the keV range [1,2].

Development of low-energy storage rings causes widespread beam diagnostic technologies to become obsolete. In particular preservation of the beam lifetime causes perturbing profile monitoring, like e.g. interceptive foils, to be ruled out [3]. Furthermore, existing non-perturbing techniques such as residual gas monitors can take up to about 100 ms [4] to make meaningful measurements, due to the low residual gas pressure, at the expected operating pressure of around 10^{-11} mbar.

A possible solution around these limitations is constituted by a neutral supersonic gas jet target shaped into a thin curtain and bi-dimensional imaging of the gas ions created by impact with the projectiles. Such monitor, as compared to those based on residual gas, allows injection of additional gas, in order to increase the ionization rate, together with efficient evacuation to keep the required vacuum level elsewhere in the storage ring, due to the high directionality of the supersonic jet [5];

furthermore, it allows simultaneous determination of both transversal profiles and even beam imaging.

Crucial to such monitor is the control of the gas-jet in terms of achieved density and directionality. In the following section we present the results of numerical simulations which show that the geometry of the nozzle-skimmer system has a dramatic impact on the final result, and hence plays a central role in the optimization process. We then describe the nozzle skimmer system, the chamber which has been designed to house the experimental validation, the extraction field for the curtain probing experiment, and finally draw our conclusions.

NUMERICAL SIMULATIONS

The most common technique for the creation of a supersonic curtain-shaped gas jet involves the creation of an axis-symmetric jet of great intensity and the subsequent reshaping via collimators, after supersonic speed is attained [6]. Nevertheless, this approach results in several difficulties, amongst which the need of a large setup, which is needed for the gas jet to expand to the desired dimension; the use of large focusing magnetic fields to be coupled to the magnetic moment of the gas molecules, generally O_2 ; and the use of large quantities of gas, since most gas is collimated out, which results in large stagnation pressure needed at the source. We performed preliminary simulations, showing that it is possible to achieve a curtain-shaped jet by means of a suitable nozzle-skimmer system already at the gas source, if a rectangular slit nozzle and a skimmer shaped as a hollow trapezoidal prism is used in a suitable geometry, instead of the circular nozzle used in common applications.

To show the importance of the geometry of the nozzle-skimmer system for the curtain characteristics, we run several set of simulations, varying 5 geometric parameters, which we will refer from now on as variables, while monitoring 3 relevant observables, as described below.

The variables are: the skimmer aperture angles in the direction parallel (α), and perpendicular (β) to the curtain expansion, the width of the skimmer slit (SW), the depth of the skimmer structure (SD) and the nozzle-skimmer distance (Dist). We observed the Mach Number downstream the skimmer (M), which gives an indication of the efficiency of the expansion and hence of the directionality of the jet, as well as the geometrical dimensions of the gas curtain: width and depth (W and D respectively), which directly affect the resolution of the monitor [5].

* Work supported by the EU under contract PITN-GA-2008-215080, by the Helmholtz Association of National Research Centers (HGF) under contract number VH-NG-328 and GSI Helmholtzzentrum für Schwerionenforschung GmbH.

[†]corresponding author: massimiliano.putignano@quasar-group.org

EMITTANCE MEASUREMENT USING UNDULATOR RADIATION

F. Ewald, ESRF, Grenoble, France

Abstract

An additional electron beam emittance measurement that uses X-ray radiation from an undulator at the ESRF storage ring is now installed. The method consists in detecting the monochromatic spatial profile of the fifth harmonic of the undulator spectrum at 29.3 keV. The X-rays are converted to visible light using a scintillating screen which is then imaged to a CCD camera. The emittance value is deduced from the image size, the photon beam divergence, the source distance, and the lattice functions at the source point. The direct use of undulator radiation is advantageous in terms of the precise knowledge of the source position and lattice parameters in the straight section. For this reason this device will find its main application as a horizontal emittance monitor with improved absolute precision compared to that of the pinhole cameras which are making use of bending magnet radiation.

MOTIVATION

The electron beam emittance at the ESRF is currently monitored through two different families of devices: Two pinhole cameras [1] and eight so-called In-Air-X-Ray (IAX) detectors [4]. Both kinds of devices use X-rays emitted from dipoles. While the pinhole cameras deliver both, horizontal and vertical emittance values, the IAX detectors allow for precise measurement of the vertical emittance only. Due to the strong gradient of the beta-function along a dipole and difficulties in the precise determination of the X-ray source point position, the beta-value involved in the emittance calculation from the pinhole cameras is prone to errors. In order to cross-check the results with a different method, an emittance measurement using undulator radiation has recently been set up. The advantage of this method, which will be described in detail in the next section, is the very precise knowledge of the lattice parameters in the center of the straight sections in a storage ring.

BACKGROUND

Assuming that the β -function is well known, we can determine the emittance ε from the electron beam size σ and β at a given point in the storage ring. In our case, the point in which we measure ε , is the center of a straight section, where we can ideally suppose β' and η' to be zero. In reality, however, this may not be true, even if, after all, the values will be small, and β' can be neglected without worries. The electron beam size σ and its divergence σ' are then given by

$$\sigma^2 = \varepsilon \cdot \beta + (\eta\delta)^2 \quad , \quad \sigma'^2 = \varepsilon/\beta + (\eta'\delta)^2 \quad (1)$$

In an ideal storage ring, the dispersion in the vertical plane would be zero, especially in the straight sections. Since, in reality, this may not be the case, we keep the above relations for both, the horizontal and the vertical plane.

Since the parameters β , η , η' and the energy spread δ are a priori known, measuring the emittance is now reduced to the measurement of the electron beam size. This will be done non-intrusively using the X-ray radiation emitted by the electrons traveling through the magnetic field of an undulator. The X-rays emitted by the electrons are freely propagating towards the detector conserving the divergence σ' of the electron beam at the source point. The X-ray beam size on a screen positioned at a distance D downstream the undulator is then given by the convolution of the electron beam size and the angular distribution of electron trajectories, the finite natural divergence of undulator radiation (σ'_u), and an image broadening (σ_{opt}) of the optical system. We assume that we have to deal only with Gauß-distributions, such that the rms X-ray spot size measured on the screen can be expressed by:

$$\Sigma^2 = \sigma^2 + (\sigma'D)^2 + (\sigma'_u D)^2 + \sigma_{opt}^2 \quad . \quad (2)$$

Substituting σ and σ' , as given above, allows to calculate ε from the measured beam size Σ :

$$\varepsilon = \frac{\Sigma^2 - (\eta\delta)^2 - (\eta'\delta)^2 \cdot D^2 - \sigma_u'^2 \cdot D^2 - \sigma_{opt}^2}{\beta + \frac{D^2}{\beta}} \quad . \quad (3)$$

Under the condition that the working point is located at the peak of an odd undulator harmonic, the natural photon beam divergence and the natural source size can be approximated by [3]:

$$\sigma'_u = \sqrt{\frac{\lambda_X}{2L}} \quad , \quad \sigma_u = \frac{\sqrt{2\lambda_X L}}{4\pi} \quad , \quad (4)$$

with λ_X being the X-ray wavelength of the respective harmonic, and L the undulator length. The natural source size is of the order of 1 μm at about 30 keV, and therefore negligible in our measurements. The above approximation indicates that, in order to keep the photon divergence small, a high X-ray energy is favourable. In general it is desirable not to work at the peak of the harmonics, but at slightly higher energies, in order to minimise the photon divergence. Therefore, σ'_u was calculated using the exact expression for the spatial distribution of undulator radiation rather than using the above equation.

EXPERIMENT

On the basis of a previous experiment [2] the setup is implemented in the beamline ID30, the latter being shared

BEAM PROFILE MONITORING AT COSY VIA LIGHT EMITTED BY RESIDUAL GAS*

C. Böhme[†], T. Weis, Technical University of Dortmund, Germany
 J. Dietrich, V. Kamerdzhev, Forschungszentrum Jülich, Germany
 J.L. Conradie, iThemba LABS, South Africa

Abstract

Scintillation is one of the outcomes of beam interaction with residual gas. This process is utilized for non-destructive beam profile monitoring. Test bench measurements at various gas compositions and pressures have been performed, as well as measurements at the 3.14 MeV cyclotron beam line at iThemba LABS as well as ones with the circulating proton beam at COSY-Juelich. The test bench measurements have been mainly done using a single large photocathode photomultiplier to estimate the photon yield. A multichannel photomultiplier was used along with a lens system to monitor the ion beam profile at iThemba LABS. Experimental results are presented and the challenges of the approach are discussed.

INTRODUCTION

The knowledge of the beam position and profile is essential for the successful operation of an accelerator facility. At hadron accelerators the high beam current limits the use of traditional intersecting methods like wire scanners or secondary electron emission (SEM) grids, because the used materials are heated or melted through the beam energy. At synchrotrons non destructive methods are preferred to monitor the circulating beam. Several kinds of diagnostic devices, using the products of the interaction between the ion beam and the residual gas, are under development or in

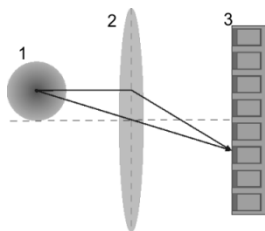


Figure 1: Measurement principle (not to scale): The light from the beam (1) is focused with a glass lens (2) onto the multichannel photomultiplier (3).

use. Usually the devices register the ions and/or electrons produced in collisions of the beam particles with the residual gas. Some attempts have already been made which use the emitted light of the excited residual gas atoms in order to monitor the beam [1]. This method of registering

photons has the advantage of being insensitive to electric or magnetic fields. Also the spatial and time resolution is considerably higher, allowing a single pulse measurement. The limitation of this method is the cross section of light emission, which is about three orders of magnitude lower compared to ionization. Nevertheless, a wide range of applications can still be covered with this method.

MEASUREMENT TECHNIQUE

The light emitted by the residual gas is focused by a glass lens onto a position sensitive multichannel photo-multiplier (PMT) array, as shown in Figure 1. A Hamamatsu PMT (7260-type, 32 channels, 0.7·10 mm photocathode size, 1mm pitch size) was used for the position sensitive measurements. Along with that, a Philips XP2020 single channel PMT (44mm round photocathode) was used for basic research, mainly without an optical lens system in order to

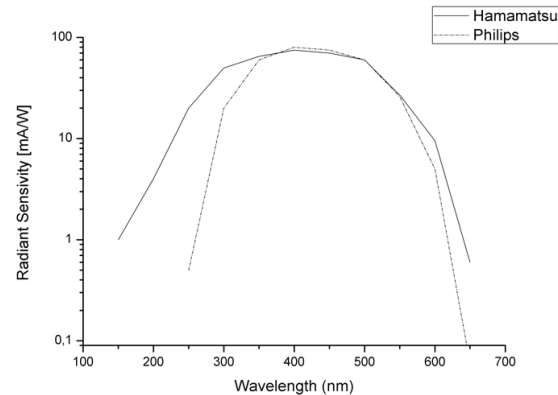


Figure 2: Luminous characteristics of the Photomultipliers used.

have a large aperture angle for the registration of photons. Depending on the amount of photons registered the readout of the PMT was adapted. For low intensities a discriminator was used together with a counter, in order to count the number of events. For high intensities a direct current measurement was performed using a 48 multichannel current digitizer, developed at iThemba LABS.

PHOTON YIELD

While measuring the beam profile using photons emitted by the residual gas the only controllable parameters of

* Work supported by BMBF and NRF, Project code SUA 06/003

[†] c.boehme@fz-juelich.de

FAST AND HIGH ACCURACY WIRE SCANNER

M. Koujili, CERN, Geneva, Switzerland and SeT-UTBM, Belfort, France

B. Dehning, J. Koopman, D. Ramos, M. Sapinski, J. De Freitas, CERN, Geneva, Switzerland

Y. Ait Amira, FemtoST-UFC, Besançon, France

A. Djerdir, SeT-UTBM, Belfort, France

Abstract

Scanning of a high intensity particle beam imposes challenging requirements on a Wire Scanner system. It is expected to reach a scanning speed of 20 m.s^{-1} with a position accuracy of the order of $1 \mu\text{m}$. In addition a timing accuracy better than 1 ms is needed. The adopted solution consists of a fork holding a wire rotating by a maximum of 200° . Fork, rotor and angular position sensor are mounted on the same axis and located in a chamber connected to the beam vacuum. The requirements imply the design of a system with extremely low vibration, vacuum compatibility, radiation and temperature tolerance. The adopted solution consists of a rotary brushless synchronous motor with the permanent magnet rotor installed inside of the vacuum chamber and the stator installed outside. The accurate position sensor will be mounted on the rotary shaft inside of the vacuum chamber, has to resist a bake-out temperature of 200°C and ionizing radiation up to a dozen of kGy/year . A digital feedback controller allows maximum flexibility for the loop parameters and feeds the 3 phases input for the linear power driver. The paper presents a detailed discussion of the selected concept and selected components.

INTRODUCTION

Wire scanners are installed and operated on a daily basis on all circular accelerators of CERN. However, they present some drawbacks:

- For high intensity beams the energy deposited by the incident particles on the wire may be sufficient to break the wire [1].
- The wire can also be destroyed due to the energy transferred by the beam to the wire through its accompanying electromagnetic field [2].
- Inaccuracy of position measurement primarily due to vibrations of the mechanics and the wire.
- Vacuum leakage in the bellows due to wear.

To improve the optimization of the luminosity in the Large Hadron Collider (LHC), much higher measurement accuracies than those currently achievable are required. The new performance demands include a wire travelling speed of up to 20 m.s^{-1} and a position measurement accuracy of the order of $1 \mu\text{m}$, in addition to a timing accuracy better than 1 ms . This implies the design of a system

05 Beam Profile and Optical Monitors

with extremely little vibration and electro-magnetic interference. Other requirements related to interface and environment issues such as radiation, temperature, vacuum and interactions with the beam must also be accounted for.

The baseline solution (Fig. 1) consists of a small diameter rotary brushless synchronous motor with the rotor's magnetic field provided by permanent magnets, installed inside the vacuum chamber. This rotor is supported on a shaft by roller bearings with materials and solid lubricants to be selected for low outgassing and friction characteristics in vacuum environment. Attached to the same shaft is a fork on which the wire is stretched. In order to minimise the outgassing from the motor, the stator windings which excite the rotor are placed outside the vacuum chamber. The air-vacuum interface is made in the magnetic gap through a low magnetic permeability stainless steel wall. A position transducer to be mounted on the rotating shaft shall provide its absolute angular position for the feedback control loop of the motor and also a highly repeatable relative position during the scan.

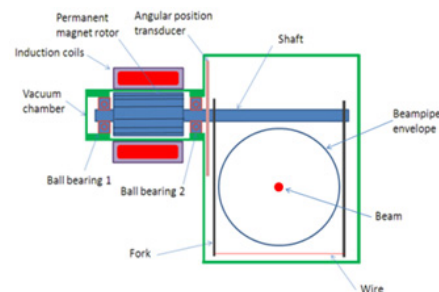


Figure 1: Simplified drawing of the future wire scanner. The green lines enclose the vacuum area.

In this paper, the motor requirements are defined first starting from the wire scanner specifications. Thus, the motor and its power supply are chosen with regard to the constraints obtained in terms of the needed torque, speed, and acceleration. After a brief description of the motor model some simulations achieved on the base of the physical parameters given by the manufacturer are included and commented based on the specifications.

WIRE SCANNER SPECIFICATIONS AND MOTOR CHOICE

In this section, the different requirements to be met by the wire scanner device are listed and used to choose the

BEAM TEST OF THE FAIR IPM PROTOTYPE IN COSY

C. Böhme, Technical University Dortmund, Germany
 J. Dietrich, V. Kamerdzhev[#], FZJ, Jülich, Germany
 P. Forck, T. Giacomini, GSI, Darmstadt, Germany
 D. Liakin, ITEP, Moscow, Russia

Abstract

The advanced ionization beam profile monitor is being developed at GSI for the future FAIR facility in collaboration with ITEP and FZ-Jülich. In January 2009 the IPM prototype was installed in COSY-Jülich. After successful hardware test the beam tests followed. The prototype was operated without magnetic field, thus only residual gas ions were detected. An arrangement consisting of an MCP stack, a phosphor screen, and a CCD camera was used to detect ions. We report the first profile measurements of the proton beam up to 2.8 GeV at COSY.

INTRODUCTION

The Ionization Profile Monitor (IPM), currently under development at GSI, is intended to provide fast and reliable non destructive beam profile measurements at the future FAIR machines as well as the existing accelerators at GSI [1]. The ionisation products are guided to a position sensitive detector by transverse electric field. Two modes of operation are foreseen. Ion detection is used to obtain the profiles with high spatial resolution by means of a phosphor screen (PS) and a CCD camera [2]. Detection of electrons is required to allow for turn-by-turn profile measurements. This will be done by using a multichannel photomultiplier [3]. Collection of electrons makes the presence of a guiding magnetic field necessary in order to prevent the electrons from spreading out. The magnetic system is being designed in collaboration with iThemba LABS, South Africa.

THE IPM SETUP AT COSY

The IPM prototype was installed in COSY to study its performance and gain operational experience. It is not equipped with a magnet; hence only ion detection technique can be applied. An arrangement consisting of an MCP stack (100x48 mm²), a P47 phosphor screen, and a 656x494 pixel CCD camera is used to detect ions. High voltage electrodes provide the electric field for ion extraction. The IPM prototype actually contains two identical units to provide simultaneous measurements in both, horizontal and vertical, planes. Figure 1 shows the design of the IPM prototype installed in the arc downstream of the cooler telescope.

The cameras are read out by a LabView server application running on a PXI based front end. The user interacts with the front end from the accelerator control room by means of a client program running on a PC. Both

the server and client applications were developed by a private company according to the GSI specifications.

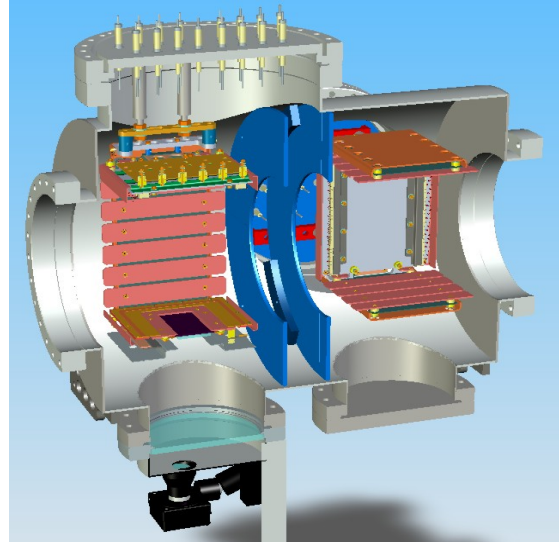


Figure 1: Mechanical design of the FAIR IPM prototype.

In order to be able to monitor and control the aging of the MCPs the monitor is equipped with UV lamps that are capable of homogeneously irradiating the whole MCP surface. This feature is used to correct the detector sensitivity inhomogeneity. Profiles of the polarized and unpolarized proton beams circulating in COSY were measured covering the full energy range of the machine.

BEAM PROFILE MEASUREMENTS

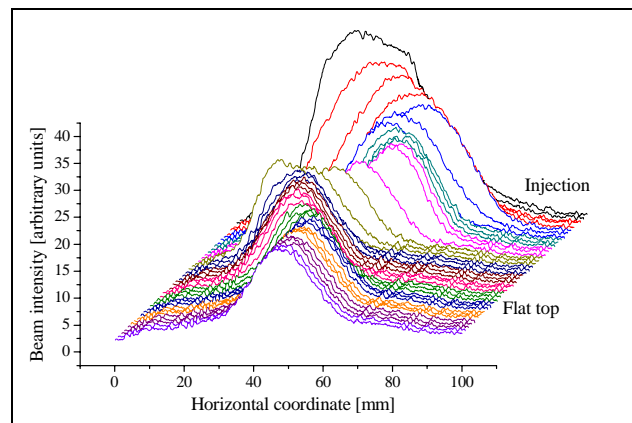


Figure 2: Evolution of the horizontal proton beam profile during injection and acceleration to 1.343 GeV/c. About $3 \cdot 10^9$ polarized protons reached flat top. Time span is 2 s. Corrected for spatial detector sensitivity distribution via UV calibration. 5 pts moving average smoothing was applied.

[#]v.kamerdzhev@fz-juelich.de

IR PHOTON ARRAY DETECTOR FOR BUNCH BY BUNCH TRANSVERSE BEAM DIAGNOSTICS

A. Bocci, M. Cestelli Guidi, A. Clozza, A. Drago, A. Grilli, A. Marcelli, A. Raco, R. Sorchetti,
INFN – Laboratori Nazionali di Frascati, Via Enrico Fermi 40, I-00044 Frascati RM, Italy

L. Gambicorti,

Istituto Nazionale di Ottica Applicata – CNR, Largo Fermi 6, 50125 Firenze, Italy

A. De Sio, E. Pace,

Università degli Studi di Firenze, Largo Fermi 2, 50125 Firenze, Italy

J. Piotrowski,

VIGO System SA, 3 Swietlikow Str. 01-389 Warsaw, Poland

Abstract

Beam diagnostics based on synchrotron radiation (SR) may use real time imaging methods that monitor the beam transverse dimensions. In particular the bunch-by-bunch transverse beam diagnostics is a powerful method that allows investigations of transient phenomena in which bunch motion and instabilities are correlated to the position in the bunch train. Such diagnostic methods need photon array detectors with response time from ns to ps range and dedicated fast electronics. At DAΦNE, the e^+/e^- collider of the Frascati National Laboratory (LNF) of the National Institute of Nuclear Physics (INFN), tests with an IR array prototype made of 32×2 pixels and its electronics are in progress. The size of the pixels is $\sim 50 \times 50 \mu\text{m}^2$ and their response time ~ 1 ns. In this contribution we describe an experimental set-up to obtain IR imaging of the SR source and a turn-by-turn and a bunch-by-bunch transverse diagnostics of the stored bunches with a sub-ns time resolution. Preliminary measurements obtained using the IR emission of the SINBAD beamline will be presented. Tests of the array detector with its 64 channels electronics are in progress at the *Time Resolved e+ Light (3+L)* experiment, a dedicated diagnostics of the DAΦNE positron ring which monitors the longitudinal and transverse dimensions of the positron beam.

INTRODUCTION

Beam diagnostics tools based on synchrotron radiation (SR) are fundamental features of any collider dedicated to high-energy physics experiments and to storage rings optimized as synchrotron radiation sources. Moreover the SR, used for beam diagnostics, gives, as main advantage, a direct and non-destructive system of probing. Typical diagnostics by SR are usually based on expensive imaging techniques that allow measurements of the beam transverse dimensions as well as the longitudinal structure and the bunch length of stored particles (e.g., using a streak camera device). In particular, the real time measurements of the transverse beam dimensions and emittances are growing in interest for next generation of lepton colliders, synchrotron radiation sources and FELs.

In order to measure the beam emittance, the real time analysis of the beam transverse profile is a fundamental requirement of any particle accelerator.

Besides, bunch-by-bunch beam diagnostics is a powerful method for experiments of accelerator physics, such as studies of transient phenomena in which motion and instabilities of bunches depend on the position in the bunch train [1].

Turn by turn and bunch by bunch diagnostics can be implemented using very fast IR, visible, UV or X array detectors (from the sub-ns to the ps range) with dedicated electronics in order to collect and store a large amount of data. Recently at DAΦNE, the Frascati e^+/e^- collider, measurements of the time structure of synchrotron radiation emitted by the bunches have been performed using uncooled IR photon detectors, achieving a time resolution of a few hundred picoseconds [2]. Future foreseen applications of this technology are based on faster photo-voltaic devices with < 100 ps response time and IR uncooled array detectors, to achieve bunch by bunch imaging of the photon source and to investigate transverse instabilities on the DAΦNE rings. In particular, the *Time Resolved e+ Light (3+L)* experiment, dedicated to beam diagnostics, has been installed in the DAΦNE hall to collect the SR extracted by a bending magnet of the positron ring [3]. The SR is focalized by a set of mirrors in air in front of a fast IR photo-detectors in order to measure longitudinal lengths and transverse sizes of the bunches and to investigate bunch instabilities [4].

This novel device and its electronics have been assembled to test the first transverse diagnostics of the e^+ beam at DAΦNE at IR wavelengths. The device consisting of a fast array detector with 2×32 pixels exhibits a response time of ~ 1 ns. Preliminary data from single elements of the array and of the electronics have been acquired in order to characterize the assembled device. After completion of the device and its dedicated electronics we could monitor the beam both in the bunch-by-bunch and turn-by-turn transverse modes, two fundamental tools to improve accelerator performances, e.g., at DAΦNE to increase the positron current and the luminosity, and to monitor transverse beam instabilities.

In the following we describe the experimental set-up and present preliminary tests performed with several pixels of the array illuminated by the IR SR emission at the SINBAD beamline of DAΦNE.

DIAGNOSTICS FOR HIGH POWER ION BEAMS WITH COHERENT OPTIC FIBER FOR IFMIF-EVEDA INJECTOR

F. Senée*, G. Adroit, R. Gobin, B. Pottin, O. Tuske, CEA Saclay, IRFU, F-91191 Gif-sur-Yvette, France.

Abstract

Optical diagnostics based on the excitation of residual gas molecules are routinely used for high intensity beam characterization. Beam intensity, beam position and profile are measured by means of a digital camera. In addition species fraction and profile of each beam are measured using a Doppler shift method. As part of IFMIF-EVEDA project, CEA is in charge of the design and realization of the 140 mA-100 keV cw deuteron source and low energy beam transport line. In the beam line, (D,d) reaction will occur and high neutron flux will be emitted when deuteron beam interacts with surfaces. Moreover gamma ray and activation will also occur. In order to protect diagnostics, coherent optic fibers could be used to transport the beam image outside the irradiated zone. A comparative study of two coherent fibers will be presented (FUJIKURA & SCHOTT), along with the characterization in magnification and transmission of a 610 mm long fiber and its associated optics. To estimate the capability of such fibers to transport beam image, a dedicated experiment has been performed with proton beam produced by the SILHI source. The beam profile has been compared with and without the optic fiber.

INTRODUCTION

The International Fusion Materials Irradiation facility (IFMIF) aims at producing an intense flux of 14 MeV neutrons, in order to characterize materials envisaged for future fusion reactors. Such a machine facility is based on two high power continuous wave accelerator drivers, each delivering a 125 mA D^+ beam at 40 MeV to a liquid lithium target. In the first phase of the "Broader Approach", the IFMIF-EVEDA (Engineering Validation and Engineering Design Activities) project includes the construction of an accelerator prototype with the same characteristics as IFMIF, except a lower energy of 10 MeV instead of 40 MeV for the incident deuteron energy. CEA-Saclay is in charge of the design and realization of both deuteron source and the associated low energy beam transport (LEBT) line. This part, named the IFMIF injector, will be built and tested at Saclay and then moved to Japan. The deuteron beam will be extracted from a 2.45 GHz ECR source based on the SILHI design [1], the Saclay source. It has been developed to produce cw 100 mA proton beams with 95 keV energy. In the framework of preliminary IFMIF studies, SILHI has been tuned to analyze deuteron beam characteristics [2]. That enabled to demonstrate that the emission spectrum in the visible region of deuterium differs slightly from that of proton due to the influence of hyperfine interactions

among others. Therefore, all optical diagnostics realized on SILHI and presented in section 2 will be transposable on IFMIF injector. But high neutron flux and gamma rays, emitted when deuteron beam interacts with surfaces, push to use coherent optic fiber to transport the beam image outside the irradiated zone or radiations hardened camera (CID camera). Recent tests of such devices performed on SILHI beam are presented in section 3 and 4.

OPTICAL BEAM DIAGNOSTICS

The interaction between the proton beam and the residual gas produces excited and ionized gas atoms and molecules. An analysis of the emitted light with different devices allows getting ion beam characteristics.

With Digital Cameras (CCD Camera or CID Cameras)

Direct fluorescence beam profile measurement with digital camera perpendicular to the beam direction allows the following parameter measurement:

- Beam current proportional to fluorescence intensity
- Beam size
- Beam center position
- Beam profile

With Monochromator and CCD Camera

With a digital camera installed in the focal plane of a monochromator with 20° angle. Doppler shift observation of the H_α hydrogen Balmer series allows isolating the fluorescence only resulting from proton beam interaction with the residual gas. As a result, other parameters are achievable:

- Species fraction
- Species fraction beam profile
- Source impurities

With Coherent Optic Fiber, Monochromator and CCD Camera

Adding a coherent optic fiber to transport the beam image outside the irradiated zone and until the device (digital camera or monochromator) seems to be a good solution to prevent these devices from the high neutron flux and gamma ray produced on IFMIF-EVEDA (Fig. 1). All optical diagnostics above should be able to run with this fiber type. That is what we tried to prove with a comparative study made with of two coherent fibers of two manufacturers (FUJIKURA & SCHOTT). Radioprotection simulations show that the radiation level produced by 165 mA deuterons beam at 100 keV should be in the range of 100 mSv/hr around the diagnostic box.

*franck.senee@cea.fr

EXPERIENCE WITH YAG AND OTR SCREENS AT ALBA

U. Iriso*, G. Benedetti, and F. Pérez
CELLS, Ctra. BP-1413 Km 3.3, 08290 Cerdanyola, Spain

Abstract

One of the key diagnostics instruments during the ALBA Linac commissioning was the screen monitors that allowed the control of beam size and position. These screen monitors are equipped with a YAG and an OTR screen. This paper describes our screen monitor setup and the experience with both types of screens.

INTRODUCTION

During the ALBA Linac commissioning [1], beam transverse position and profiles are obtained using the setup named “FSOTR” (Fluorescent Screen and Optical Transition Radiation monitor). It includes a Fluorescent Screen (Cerium activated Yttrium Aluminum Garnet, named hereafter “YAG”, with chemical formula $Y_3Al_2O_{12}$), and a second screen that produces Optical Transition Radiation (named hereafter “OTR”).

After collision with the electron beam, both screens emits light, but their nature differs: YAG screen emits light by scintillation, the OTR screen emits light by Transition Radiation. In both cases, a lens system brings the light to the CCD screen, where the image is collected.

We adopted the solution of YAG and OTR screens in the same setup to obtain a proper beam image for the cases of low and high beam charges. As shown in next Sections, the YAG usage is appropriate for low beam charges because these screens produce lots of light. Its drawback is the saturation at high charges. In these circumstances, the usage of the OTR is convenient, albeit its low photon flux production and so, dynamic range.

In the following, we describe our mechanical setup and experience during the Linac Commissioning, and compare beam images produced with both OTR and YAG screens. We would like to stress that our experience is based with low energy electron beams (up to 100 MeV), which is a relevant factor for both YAG and OTR imaging.

EXPERIMENTAL SETUP

Figure 1 (left) shows a picture of the experimental setup. Using a pneumatic system, the FSOTR monitor allows to introduce either screen into the beam’s path. Once the beam collides with either screen, an optical system directs the light to the CCD camera, where the beam image is analyzed.

The optical system is bought off-the-shelf from *EHD-Imaging* with a manually controlled zoom. The working

distance of this system is about 300 mm. The CCD camera is *Basler Scout* model, Ethernet controlled, 12-bit resolution, 1034x779 pixels and a square pixel size of 4.65 μm . To minimize the luminic noise, we set the CCD shutter to the minimum time aperture: 100 μs . Since the slowest light emission is the one produced by the YAG screen, and this is only 70 ns [2], this shutter is enough to collect the light produced by either screen.



Figure 1: Picture of the FSOTR (right) installed at the Diagnostics line and screen holder with the YAG (bottom yellowish) and OTR screens (top).

Figure 1 (right) shows a picture of the screen holder with the YAG (yellowish and translucent screen) and the OTR (“mirror-like” screen). The YAG screen manufactured by Crytur [2] has a 0.5 mm thickness and 30 mm diameter. The second is a Silicon substrate of 0.3 mm with a thin layer (100 nm) of Aluminum to enhance the transition radiation. The reference marks on the holder edges are used for calibration purposes and image focusing. The calibration in the FSOTR monitors varies from one to another, but it is generally 1 pixel = 20 μm .

BEAM IMAGING WITH YAG SCREENS

The number of photons arriving at the CCD camera produced after a single electron hits the YAG screen is

$$N_{\text{ph}} = Y \times \Omega, \quad (1)$$

where $Y = 35 \times 10^3$ ph/e-/MeV is the YAG photon yield [2], and $\Omega = 4 \times 10^{-4}$ sr is the solid angle covered by the optical system. This means that a single electron at 100 MeV

* ubaldo.iriso@cells.es

A COMPACT ELECTRON PHOTON DIAGNOSTIC UNIT FOR A SEEDED FEL*

J. Bödewadt[†], J. Roßbach, University of Hamburg, Germany
 B. Polzin, H. Schlarb, A. de Zubiare Wagner, DESY, Hamburg, Germany
 R. Ischebeck, PSI, Villigen, Switzerland

Abstract

A seeded free-electron laser (FEL) operating in the soft X-ray (XUV) spectral range will be added to the SASE FEL facility FLASH. The seed beam will be generated by higher harmonics of a near infrared laser system. A dedicated transport system will guide the radiation into the electron accelerator environment. Within the seed undulator section compact diagnostic units have to be designed to control the transverse overlap of the photon and the electron beam. These units contain a BPM a wire scanner and an OTR screen for the electron diagnostic. A Ce:YAG screen and a MCP readout for the wire scanner are foreseen to measure the photon beam position.

INTRODUCTION

The free-electron laser in Hamburg (FLASH) offers high brightness photon beam with sub-10 fs pulse length in the vacuum ultra-violet (VUV) and soft x-ray (XUV) regime to various experiments [1]. It operates using the principle of self-amplified spontaneous emission (SASE) where radiation is emitted by a 1 GeV high peak current (~kA) electron beam in a planar undulator. Due to the start up from shot noise this results in a statistical behavior of the emitted spectrum [2]. Beside that the arrival-time jitter of the FEL pulses is in the order of a few 100 fs which limits the temporal resolution for pump-probe experiments [3] where an external laser system has to be synchronized with the accelerator. One way to reduce this time jitter is to seed the FEL process with an external laser and combine the amplified radiation pulse with near infra-red pulses from the same laser system. Since the two radiation pulses originate from the same source they are intrinsically synchronized. A directly seeded FEL configuration is going to be installed at FLASH in winter 2009 [4]. A 40 m long section upstream the existing SASE undulator will be rebuilt for that purpose. Figure 1 shows a general layout of that section. The XUV seed radiation is created by higher-harmonic generation (HHG) from NIR femtosecond laser pulses focused in a rare gas jet and guided through a 15 m long differentially pumped transfer line from a laser laboratory into the adjacent accelerator tunnel and into the electron beam pipe.

This transfer line includes two motorized mirror chambers to steer the beam and thus to control the spatial overlap between the electron and the photon beam. In order to obtain the overlap, diagnostic units will be installed at either end of each undulator module. Each unit accommodate an electron beam position monitor (BPM), vertically and horizontally installed wire scanners (WS), an aluminum coated silicon screen for optical transition radiation (OTR) measurements and a Ce:YAG crystal.

SPATIAL OVERLAP

One of the key challenges of the seeding experiment is to achieve the spectral, temporal and spatial overlap. The latter will be obtained by either steering the electron beam onto the photon beam or vice versa. Therefore two pairs of dipole corrector magnets (horizontal and vertical) preceding the sFLASH undulator and two motorized mirrors inside the XUV-seed transfer line will be installed. Each of the mirrors can be steered in two dimensions thus the

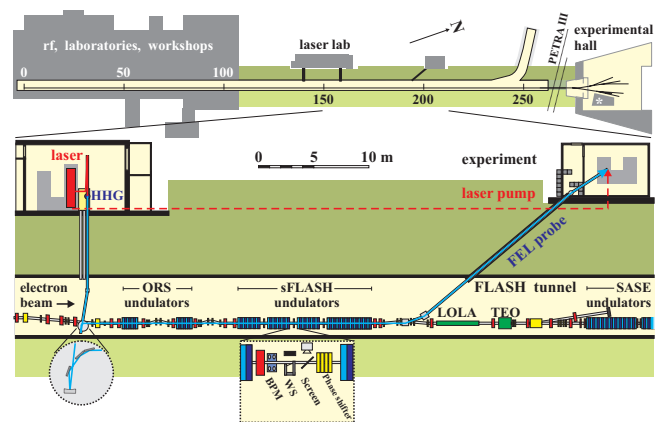


Figure 1: The FLASH facility (top) comprises a 260 m long tunnel housing the linac and undulators of a SASE FEL, followed by an experimental hall. A 40 m long section (bottom) will be rebuilt to accommodate four additional undulators for sFLASH. Seed pulses from an HHG-source in a building adjacent to the FLASH tunnel will be aligned to the electron beam. At the undulator exit, the FEL radiation is sent by mirrors to an experimental hutch. Delayed laser pulses will be sent directly to the hutch for pump-probe applications (dashed line).

* Funded by the Federal Ministry of Education and Research of Germany under contract 05 ES7GU1

[†] contact: joern.boedewadt@desy.de

VIMOS, BEAM MONITORING FOR SINQ

K. Thomsen, PSI, Villigen, Switzerland

Abstract

For the neutron spallation source SINQ at PSI a novel visual monitor (VIMOS) has been devised to guarantee correct beam conditions, triggered at the occasion of irradiating the delicate liquid metal target during the MEGAPIE project. VIMOS is looking directly for the most relevant parameter: it checks whether any point on the target is hotter than allowed. For this purpose the incandescence of a glowing mesh right in front of the beam entrance window is observed by means of dedicated radiation hard optics and suitable cameras. Starting from the initial goal of reliably detecting beam anomalies in a timely manner the scope of the system has been extended to serve as a standard device for beam monitoring and fine tuning of the settings of the proton beam transport lines. Over the course of the five years of continuous reliable operation of this unique system valuable experience has accumulated, which is employed for steady improvements of the device with respect to endurance in the radiation environment, calibration, maintenance, and price.

INTRODUCTION

Five years of operation of VIMOS clearly produced a wealth of operational experience and also resulted in some data, which were not expected from the beginning. In the following, a few selected highlights are presented as well as their impact on the course of the further development of the system.

VIMOS in its original configuration derived its sensitivity in part from the spectral response of the imaging tube in the used radiation resistant camera [1]. With a steep cut-off towards the infra-red, the detected signal rises steeply in case mesh-temperatures get higher and more emitted intensity is shifted to shorter wavelengths correspondingly.

INITIAL SENSITIVITY EVOLUTION

One observation at the start of the system five years ago was a significant decrease of the observed signal for identical beam conditions during the first year of operation. This had been attributed to blackening, i.e. an increase of effective emissivity, of the tungsten mesh under proton irradiation [2]. Starting with an effective emissivity of 0.3 and increasing it to 1, results in a reduction of signal in the sensitive wave band of the first VIMOS camera of 100.

Employing the same special tool as during the initial set-up, further evidence for this change in emissivity has been obtained in the meantime. A light emitting diode close to the mesh can be used for fine alignment of the camera. Whereas the image taken in 2005 (Fig. 1, top) clearly shows some reflections these are absent in the corresponding image of 2009 (Fig. 1, bottom).

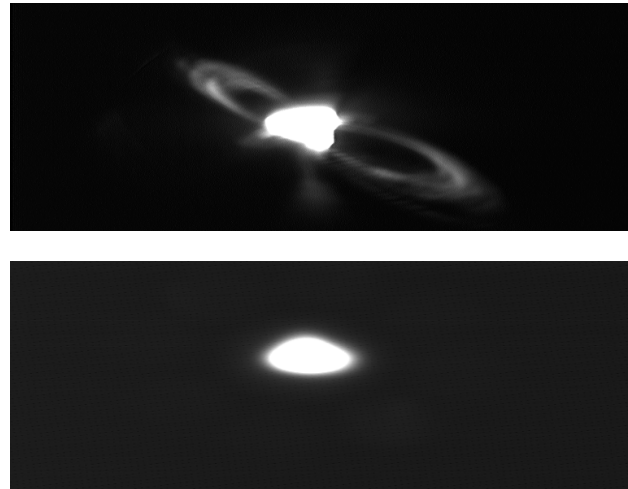


Figure 1: Set-up of the VIMOS camera by means of a special tool with a light emitting diode five years apart. Whereas the top image from the very start of operation features some reflections, nothing of this kind is visible after “seasoning” of the mesh. The absence of reflected light is consistent with the observed decrease in overall signal during the first year of irradiation.

CAMERA LIFE TIME

Initially, the tube based cameras showed very reliable and constant performance over the course of the operation periods at SINQ. During the irradiation of MEGAPIE severe degradation occurred within weeks [3]. The current amplification of some transistors inside the camera was reduced by a factor of five, which, most importantly, lead to a reduction of the usable sensitive area on the entrance window of the camera and to a shift of the image. Whereas there was no immediate loss of sensitivity with respect to the required safety function, because of easy software compensation, the expensive cameras had to be replaced at short intervals to guarantee their full functionality. An increase in the amount of fast neutrons scattered downwards from the target by a factor of two was found responsible for the damage to the cameras, most probably due to these neutrons after thermalisation [4].

A new design of the standard target in SINQ will result in similar neutron fluxes also for a solid target [5]. In order to cut down on camera wear (and maintenance cost) a radiation resistant light guide has been introduced with the aim of placing the camera four meters away at a location with much reduced radiation exposure.

During the irradiation period of 2008 no dramatic deterioration in the transmission of the light guide has been observed. The tube based camera employed during this time exhibited unchanged performance.

FIRST EXPERIENCE AT SARAF WITH PROTON BEAMS USING THE RUTHERFORD SCATTERING MONITOR

L. Weissman, D. Berkovits, Y. Eisen, S. Halfon, I. Mardor, A. Perry, J. Rodnizki,
Soreq NRC, Yavne 81800, Israel
K. Dunkel, C. Piel, D. Trompetter, P. vom Stein,
Research Instruments GmbH, 51429 Bergisch Gladbach, Germany

Abstract

The first phase of the SARAF high current proton/deuteron accelerator is currently under commissioning. The first experience with 3 mA, pulsed proton beam included the measurement of the energy spectra of the protons of energies up to 2.2 MeV scattered at 45° from a 0.3 mg/cm² thick gold foil. The beam was accelerated by the RFQ and by several superconducting resonators. The energy spectra of the scattered particles were taken for different accelerator settings. The results were compared with time-of-flight and with Monte-Carlo calculations. Monitoring the energy of the scattered particles proved to be a useful tool for beam tune and calibration of the accelerator components such as the RFQ and the superconducting resonators.

INTRODUCTION

SARAF accelerator, a medium energy high current RF superconducting linac of protons and deuterons (2 mA, 40 MeV), is currently under construction at Soreq center [1]. Phase I of the accelerator includes the Electron Cyclotron Resonance (ECR) ion source, Low Energy Beam Transport (LEBT), Radiofrequency Quadrupole (RFQ) accelerator-buncher, Medium Energy Beam Transport (MEBT), Prototype Superconducting Module (PSM), Diagnostic plate (D-plate) and beam dumps (Fig. 1). A detailed description of the accelerator is out of scope of this paper and can be found in [1,2] and references therein. At the moment Phase I is fully installed and being commissioned by ACCEL-Research Instruments GmbH, in collaboration with Soreq personnel.

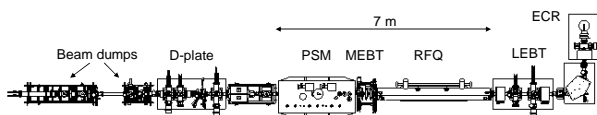


Figure 1: Overview of Phase I of SARAF accelerator.

Most of the beam diagnostics of the SARAF linac are situated on the D-plate. The main diagnostic components are: a slow Faraday cup (FC), set of vertical and horizontal slits and wires for profile and emittance measurements, two phase probes for time-of-flight measurements (TOF), two beam position monitors, a parametric current transformer (from Bergoz) and two fast FCs. Earlier report on the use of the D-plate for proton beam commissioning through the RFQ is given in [3].

07 Hadron Accelerator Instrumentation

Along with traditional beam diagnostics instruments, a Beam Halo Monitor (BHM) station is implemented into the SARAF D-plate [4]. The beam halo is planned to be characterized using a mini FC, on-line and off-line measurements of radiation from LiF target crystals and by monitoring energy spectra of Rutherford Scattered (RS) particles from a thin target gold foil.

The extensive use of the BHM is planned only after full commissioning of Phase I. However, a specific part of the BHM, the RS monitor, was used in the recent commissioning efforts for transport and acceleration of the pulsed proton beam through the RFQ and PSM. In this paper we present results of these measurements.

USE OF THE RS MONITOR FOR TUNING OF THE ACCELERATOR

The Conditions of the Commissioning Tests

Main commissioning tests were done in a mode where both the ECR ion source and the RFQ were pulsed. The timing overlap between these pulses defines the length of the proton pulse. Typically short pulses of 100 μsec duration at a frequency of a few Hz were used. Such low duty cycle (10⁻⁴) is necessary for use of interceptive beam diagnostics. The 20 keV pulsed beam from the ECR was transported via the LEBT, bunched and accelerated to 1.5 MeV by the RFQ and further transported and accelerated for the first time by the PSM module. The module contains six Half Wave Resonators (HWR) made of bulk Nb and three 6 T superconducting solenoids inserted among them [5]. The optical elements of the LEBT, MEBT, PSM solenoids and a quadrupole doublet after the PSM were set to optimize the beam transmission. However, the beam current measured at the D-plate was 3 mA, corresponding to a 60% transmission from the LEBT, where 5 mA was measured. Most of the beam loss occurred at the low-energy part of the RFQ. This issue will be the subject for further investigations.

Description of the RS Monitor

The energy of the beam as a function of various parameters of the accelerator components was measured at the D-plate by comparing timing signals from the two phase probes (TOF) and the RS monitor measurements (Fig. 2).

DETECTORS FOR SLOWLY EXTRACTED IONS IN HIRFL-CSR*

R.S. Mao[#], J.W. Xia, T.C. Zhao, Z.G. Xu, B. Tang, Z.G. Hu, J.X. Wu, H.S. Xu, G.Q. Xiao, Y.J. Yuan, J.H. Zheng, IMP, Lanzhou, China

Abstract

This paper gives the detectors used for slowly extracted heavy ions from CSR. The beam profiles are measured with viewing screens and anode-stripped ion-chambers. The currents are determined with scintillators and ion-chambers. The signal processing system and the measurement results are also presented.

INTRODUCTION

HIRFL-CSR [1] is a double cooling-storage-ring system with a main ring (CSRm) and an experimental ring (CSRe). The beam is accumulated, cooled and accelerated in CSRm, and will be extracted in slow extraction [2] mode for many external-target experiments. The ions can be accelerated to 200~1100MeV/u and the number of stored ions ranges between 10^6 and 10^9 . The spill length will be several seconds (actually during the CSR commissioning it was always set to three seconds), so the beam current is about 106 ~ 109pps. In this range, the typical detectors such as the ionization chamber (IC), the scintillator, the diamond monitor or secondary electron monitor (SEM) can be used for beam intensity measurements [3], the gas filled grids and viewing screens for beam profile measurements. These devices are commonly used for many years in GSI, CERN, etc [4][5]. In HIRFL-CSR, the anode-stripped ion-chamber is installed to measure the beam profile, and the scintillation screen with CCD to measure beam profile directly for high intensity beam. For beam intensity measurement (lower than 10^9 pps), the use of the IC together with scintillator filled the measurement requirements. For the convenience of the commissioning, we installed the scintillator detectors as beam loss monitors on the upside, downside, left side and right side of the beam tube to monitor the beam transmission status and help to judge the beam direction. In Jan. 2008, the beam extracted by RF-knock out method was measured for the first time. The detectors and some results are given below.

IONIZATION CHAMBER AND SCINTILATOR

In the beam line, the IC and scintillator are installed together(similar to the detector of GSI [4]) into the pockets [6] with 60mm×60mm entrance window (50 μ m stainless-steel), shown in Fig.1. To prevent the detector from radiation damage, it will be pulled in only if it is necessary. The anode-stripped ion-chamber is chosen so that the beam intensity and profile could be measured simultaneously. The plate of the anode and the cathode are made of ultra-thin printed circuit board with the thickness of 0.1mm. The schematic of detector is shown in Fig. 2.

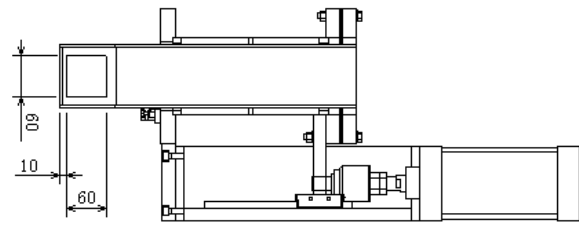


Figure 1: Detector pockets driven by pneumatics (CF150).

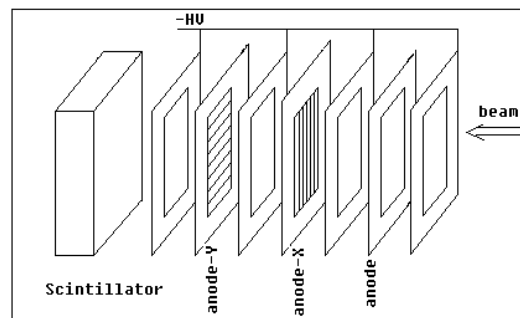


Figure 2: Structure of detector in pocket.

Taking one detector in the beam line as an example, the width of the anode strip is 2.7mm and the interval is 0.3mm, the space between the two plates is 3mm. The sensitive area is 45mm*45mm. At present, the detector gas is air (except one detector filled with nitrogen), but in the future it will be nitrogen for all. The voltage is about -10V~400V and can be adjusted during measurement process. The current produced by the strip or whole anode of IC is converted to voltage signal using I/V converter and then sampled directly with NI-PXI-6133 A/D card [7]. The real time beam profiles or intensity can be given using the LabVIEW. One of the results is shown in Fig.3 (one strip signal is lost because of the broken cable).

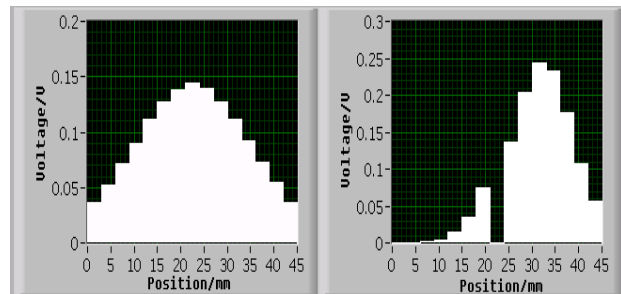


Figure 3: Beam profile left: profile x, right: profile y.

The detector at the experiment terminal is installed in air without pocket, the structure is similar to which installed in beam line, except the sensitive area, the width and the number of the anode strip.

*Work supported by the center government of China and NSFC
[#]maorsh@impcas.ac.cn

DESIGN REPORT OF A NON-DESTRUCTIVE EMITTANCE INSTRUMENT FOR RUTHERFORD APPLETON LABORATORY'S FRONT END TEST STAND FETS

C. Gabor*, STFC, ASTeC, Rutherford Appleton Laboratory (RAL), OX11 0QX, UK
 A.P. Letchford, STFC, ISIS, RAL, OX11 0QX, UK
 J.K. Pozimski, STFC, ISIS, RAL, OX11 0QX, UK and
 Imperial College London, High Energy Physics Department, SW7 2AZ, UK

Abstract

The RAL front end FETS is currently under construction to demonstrate a fast chopped, high power H^- ion beam at 3 MeV of up to 18 kW. Therefore emittance instruments should use photo detachment because mechanical parts could be affected by heat loading. This emittance instrument uses a dipole to separate negative ions from produced neutrals and a scintillator to measure particle distribution and deflection. This means a careful design of the diagnostic instrument according to other beam parameters and existing focusing elements because reasonable results require high enough phase space advance. A conceptual design layout will be presented considering the current status of the MEBT simulations along with a discussion

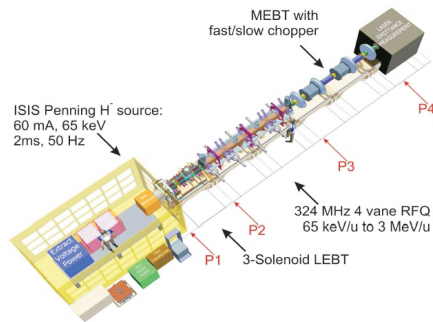


Figure 1: Overview of the FETS set up. The main elements are a Penning type ion source, 3 solenoid LEPT, RFQ and the MEBT consisting of quadrupoles, four buncher cavities and the chopper. The emittance diagnostic and beam dump are located at the end of the beamline.

INTRODUCTION

In order to contribute to the development of high power proton accelerators in the MW range, to prepare the way for an ISIS upgrade and to contribute to the UK design effort on neutrino factories [1, 2] a Front End Test Stand FETS (see Fig. 1) is being constructed at the Rutherford Appleton Laboratory RAL in the UK [3]. The aim of FETS is to demonstrate the production of a 50 to 60 mA, 2 ms, 50 pps chopped beam at 3 MeV with sufficient beam quality. This means in particular very high demands for the chopper unit which provides a fast unit for short rise time and a slow chopper for the long pulse duration. The chopper itself is integrated in a MEBT which firstly has to match

* christoph.gabor@stfc.ac.uk

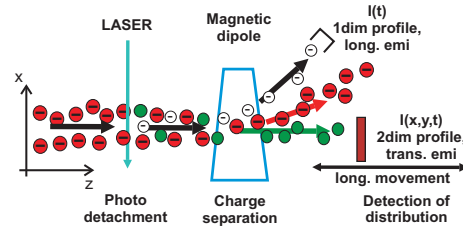


Figure 2: Basic principle of photo detachment ion beam diagnostics The H^- ions get neutralized by laser light. The diagnostics is in general a three stage process: detachment, charge separation and detector.

the RFQ output to the chopper and secondly to a DTL further downstream both in longitudinal and transverse phase space. The MEBT design is still under discussion [4] and all design schemes are confined by constraints given by a future LINAC but the actual end of the FETS beamline will consist of an emittance instrument and two beam dumps ("diagnostic beam line").

Thus, first studies to investigate changes to adapt the beam parameters to the demands of the test facility FETS are presented. A brief introduction of the applied diagnostics and main parameters of the bending dipole are also provided.

LASER BASED ION BEAM DIAGNOSTICS

The basic principle of the implemented Photo Detachment Emittance Instrument (PD-EMI) is illustrated in Fig. 2. Compared to more common devices like a slit-grid (harp) and pepperpot scanner the laser acts like a slit whereas the particle detector takes the place of a pepperpot device, therefore the transfer function of PD-EMI is a so called slit-point mapping. In Fig.2 the laser is parallel to the x -axis therefore the yy' emittance can be measured in a direct way by gathering angle profiles for each y -position of the laser [5, 6].

According to this idea the laser has to rotate to access information of the xx' plane. Previous studies have shown that this would be possible but means a very complicated magnetic design: since the gap of the dipole has to provide enough clearance for a second set of mirror the fringe field can be significant and, even without considering the poor field homogeneity, could cause avoidable beam perturbations. Therefore, in [7] another possibility is presented where a longitudinally movable detector in combination with an image reconstruction method (Maximum Entropy,

MEASUREMENT OF ELECTRON CLOUD DENSITY WITH MICROWAVES IN THE FERMILAB MAIN INJECTOR*

J. Crisp#, N. Eddy, I. Kourbanis, K. Seiya, B. Zwaska, FNAL, Batavia, IL 60510, U.S.A.
S. De Santis, LBNL, Berkeley, CA 94720, U.S.A.

Abstract

Electron cloud density in the Fermilab Main Injector was measured by observing microwave transmission along the vacuum tube. Presence of the electron cloud reduces the velocity of the microwave signal. Both frequency and time domain methods reveal relative cloud density and time evolution. The effect of beam time structure is clearly evident. The accelerator magnetic field effects the distribution of electrons making it difficult to estimate density.

INTRODUCTION

The Main Injector is a synchrotron which accelerates 53 MHz proton bunches from 8 GeV to either 120 GeV or 150 GeV. It has a revolution frequency of 90 kHz. While the Main Injector currently provides over 300 kW of beam power, Project X [1] requires up to 2.1 MW. There is concern about electron cloud instabilities at these beam currents. It is necessary to rely on simulations or models to predict this effect. In this regard, it is prudent to compare measurements of electron cloud development with simulations before extrapolating to higher beam currents.

An electron cloud can be created and trapped in the electromagnetic fields originating from the positively charged proton beam. Depending on the emissivity of the surface and the energy of the electrons striking it, the charge density can increase until the beam fields are neutralized. With the increased beam intensities anticipated, the electron density could adversely affect operation.

Presence of the electron cloud can be measured by observing the propagation of microwaves along the beam pipe [2]. For a uniform distribution of electrons, the phase shift through length L can be estimated as shown below [3].

$$\phi \approx \frac{L}{c} \frac{\omega_p^2}{2\sqrt{\omega^2 - \omega_c^2}}, \quad \omega_p \approx 2\pi 9 \sqrt{\frac{N_e}{m^3}} \text{ plasma frequency} \quad (1)$$

$$\omega_c = \text{beam pipe cut-off frequency}$$

The time response of the electron cloud is observed to be faster than the batch structure (~100 nsec). Thus, the phase shift will be modulated with the electron cloud density which in turn follows changes in beam current each turn. The variation in beam current is provided by the gaps required to accommodate injection and extraction kicker rise times. The rotation frequency of

90 kHz results in the largest component in the beam current spectrum. For a phase modulation of $\pm\beta$ radians the sideband amplitude relative to the carrier will be $\beta/2$. The amplitude of these sidebands reveals the electron cloud density.

EXPERIMENTAL SETUP

The measurement makes use of existing Main Injector Beam Position Monitors (BPMs) which are 25 cm long shorted stripline pickups. The BPMs and the beam pipe have a 50x120 mm elliptical aperture. BPMs are located inside the downstream end of each quadrupole magnet. The BPMs are connected as shown in Fig. 1 to drive the TE₁₁ mode which has the lowest cut-off frequency (1.484 GHz). It is necessary to remove the BPMs from operation which limits acceptable locations.

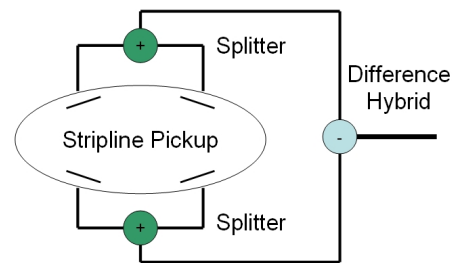


Figure 1: Connections at BPM pickups are configured to couple to the TE₁₁ mode and cancel the common beam signal. The coupling was measured at -30 dB through both pickups and 17 m of pipe.

The experimental setup is shown in Fig. 2. An Agilent E4428C signal generator provides the source which is amplified by a mini-circuits ZHL-10W-2G power amplifier. To first order, the mixer detects phase modulation and rejects amplitude modulation. Measurements have been performed at two locations in the Fermilab Main Injector.

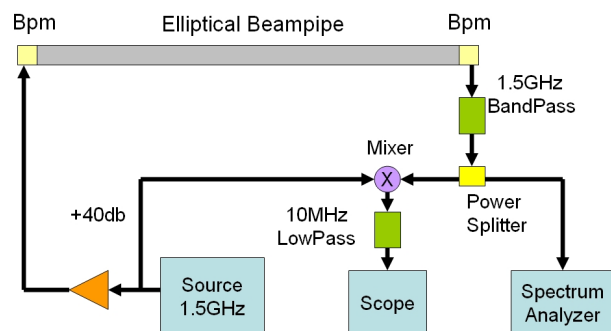


Figure 2: Basic experimental setup.

* Operated by Fermi Research Alliance, LLC under Contract No. DE-AC02-07CH11359 with the United States Department of Energy
#crisp@fnal.gov

BEAM HALO MONITOR USING DIAMOND DETECTOR FOR INTERLOCK SENSOR AT XFEL/SPring-8

H. Aoyagi[#], T. Bizen, K. Fukami, N. Nariyama, JASRI/SPring-8, Hyogo, Japan
Y. Asano, T. Itoga, H. Kitamura, T. Tanaka, RIKEN/SPring-8, Hyogo, Japan

Abstract

An electron beam halo monitor has been developed in order to protect undulator permanent magnets against radiation damage for the X-ray free electron laser facility at SPring-8 (XFEL/SPring-8). The halo monitor will be installed at the upstream of the undulator and detect the electron beam that might hit the undulator magnets. Diamond detector, which operates in photoconductive mode, is good candidate for electron beam sensor, because diamond has excellent physical properties, such as, high radiation hardness, high insulation resistance and sufficient heat resistance. Pulse-by-pulse measurement suppresses the background noise efficiently, especially in the facilities having extremely high intense beam with low repetition rate, such as XFELs. The feasibility study of this monitor was performed at the SPring-8 compact SASE source (SCSS) test accelerator for XFEL/SPring-8. We observed the unipolar pulse signal with the pulse length of 0.4 nsec FWHM. The beam profiles of the halo can be also measured by scanning the sensor of this monitor.

INTRODUCTION

The XFEL machine is composed of a low emittance electron beam injector, a high gradient C-band accelerator, and in-vacuum undulators. The charge of electron beam is designed to be 1 nC/pulse (60 Hz). Even if the undulator permanent magnets are irradiated continuously with the small part of the electron beam halo, whose energy is 8 GeV or less, the magnetic field is to be degraded [1]. The intensity of the halo part of the electron beam must be monitored during machine operation, and an electron injector must be halted immediately, when the electron intensity exceeds a threshold. The position of core part of the electron beam is controlled accurately, so usually the magnets are not to be irradiated with the core part directly. The halo part of the beam, however, may be broadened by the slight changes of the beam conditions, and may hit the magnets. Therefore, we are considering the machine protection interlock system, which detects overdose of electrons and send an alarm signal to stop the beam operation.

We have been developing a beam halo monitor for the interlock sensor, which is equipped with diamond detectors to measure directly electron intensity of the halo part of the electron beam. Diamond detector, which operates in photoconductive mode, is good candidate for electron beam sensor, because diamond has excellent physical properties, such as high radiation hardness, high insulation resistance and sufficient heat resistance. This

diamond detector is based on the technique of X-ray beam position monitors for the SPring-8 X-ray beamlines [2, 3]. We adopted a pulse-by-pulse measurement for the halo monitor, because it suppresses the background noise efficiently, especially in the facilities having extremely high intense beam with low repetition rate, such as XFEL machines.

The detector head of the beam halo monitor is made of CVD diamond [4]. The structure of the diamond detector, which was fabricated by Kobe Steel, Ltd., is shown in Fig. 1. One electrode is for signal reading and the other is for applying bias voltage. The active area is the bottom part of the plate between electrodes. The electron-hole pairs that are created in the active area can be extracted toward the electrodes. The cross section of this active area is designed to have the size of 5 mm by 1 mm. The depletion layer thickness is estimated to 0.3 mm. This detector has a self-sustaining structure, which is not mounted on a package. Therefore the active area of the diamond detector can be put closer to the beam center. The typical dark current is the order of 100 pA at the bias voltage of 100 V. In the case of pulse mode measurements, the dark current does not have effects on the output signal, because the charge from dark current in one pulse is negligibly small.

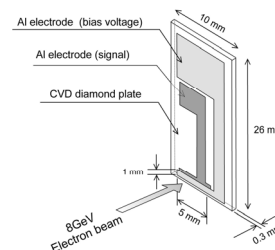


Figure 1: Structure of the diamond detector.

In order to evaluate the basic characteristics of the diamond detectors, such as detection sensitivity against electron beam and linearity, the beam tests have been undertaken at the beam dump of the 8 GeV SPring-8 booster synchrotron [4]. The oscilloscope having the sampling rate of 20 GS/sec and the analogue band width of 4 GHz was used. We prepared low attenuation cables, because the oscilloscope must be set out side of the machine tunnel and the cable length must be long, such as about 20 m. The coaxial cables of 50 Ω are used for impedance matching.

The typical pulse shape of the output signal is shown in Fig. 2 (a). This is one-shot measurement. The bias voltage is +100 V. The number of electron in one pulse is about 10^4 . The pulse length of 0.33 nsec FWHM was obtained.

[#]aoyagi@spring8.or.jp

THE DESIGN AND IMPLEMENTATION OF THE MACHINE PROTECTION SYSTEM FOR THE FERMILAB ELECTRON COOLING FACILITY *

A. Warner[#], L. Carmichael, K. Carlson, J. Crisp, R. Goodwin, L. Prost, G. Saewert, A. Shemyakin, FNAL, Batavia, IL 60543 U.S.A. *

Abstract

The Fermilab Recycler ring employs an electron cooler to store and cool 8.9-GeV antiprotons. The cooler is based on a 4.3-MV, 0.1-A, DC electrostatic accelerator for which current losses have to remain low ($\sim 10^{-5}$) in order to operate reliably. The Machine Protection System (MPS) has been designed to interrupt the beam in a matter of 1-2 μs when losses higher than a safe limit are detected, either in the accelerator itself or in the beam lines. This paper highlights the various diagnostics, electronics and logic that the MPS relies upon to successfully ensure that no damage be sustained to the cooler or the Recycler ring.

INTRODUCTION

Stable operations of a 4.3 MeV Pelletron (an electrostatic accelerator) with a 100 mA DC electron beam has lead to the successful demonstration of electron cooling of 8 GeV anti-protons in the Recycler ring [1][2]. The electron beam is transported to interact with the antiproton beam in a common 20-meter long straight section (i.e. cooling section) after which electrons are separated from the antiprotons and recaptured at the high voltage terminal of the machine; there the beam is dumped in the collector at the energy of 3 kV. Losses during this energy recovery process are kept below, $\sim 10 \mu\text{A}$. Increased beam loss during this process can lead to a reduction of the terminal voltage and, in turn, an interruption in recirculation. In severe cases the terminal voltage of the machine can be discharged to near zero in a microsecond, releasing $\sim 3 \text{ kJ}$ of stored energy. This so-called full discharge results in an increased vacuum pressure of the accelerating tubes, it can damaged electronics in the terminal and may degrade the electric strength of the tubes [3]. In addition a sustained current loss in a single location could melt and drill a hole in the vacuum chamber. At the R&D stage of the project encountering these types of scenarios indicated a need for an elaborate protection scheme. Twice the electron beam drilled a hole in the vacuum chamber. As a result we limited the current available to DC losses to $\sim 20 \mu\text{A}$ so that the timescale for melting the beam pipe is of the order of several seconds, in which case the loss monitor system mentioned below insures that the electron beam can be turned off in less than 1 second.

To mitigate these effects fast protection circuitry has been developed at the terminal level as part of a Machine Protection System (MPS) which closes the gun in 1 μs if the terminal voltage decreases because of higher losses. The MPS consists of two interconnected parts: a permit

system and a crash recovery system. The permit system monitors several critical machine- and subsystem-related alarms as well as the loss monitors for the entire beam-line. The crash recovery system is a slower, higher-level application which regulates the beam given the status of a range of machine parameters. Figure 1 shows a simplified flow diagram of the whole system.

PROTECTION SYSTEM OVERVIEW

The main hardware components of the protection system comprise: (1) the electron gun's modulator and fast circuitry in the terminal along with its fiber optically connected interface module located at ground level, (2) the beam permit box and (3) an Internet Rack Monitor (IRM) processor which is capable of interfacing up to 64 analog channels with digitization of all 64 channels done by the hardware at 1 kHz.

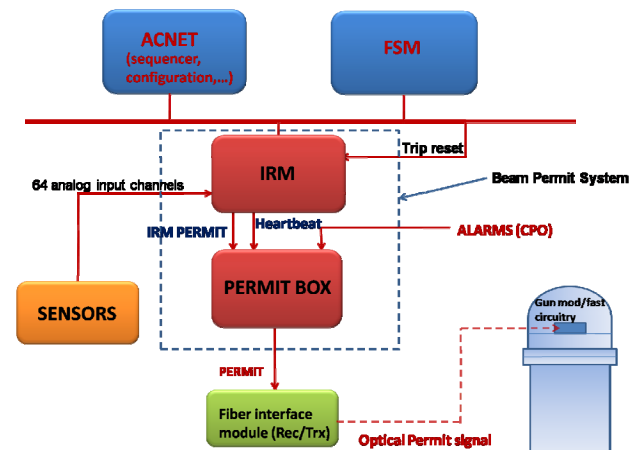


Figure 1: Protection system diagram.

Gun Modulator and Fast Circuitry

The Gun Modulator is located inside the deck enclosure which is inside of the Pelletron terminal. Its output drives the “control electrode” of the electron gun located in the terminal at the top of the accelerating column. The modulator is used to control the beam generated by the electron gun for either cooling antiprotons in the Recycler (DC beam) or for machine diagnostic purposes (Pulsed beam). In the same way the voltage on the grid of a triode tube defines the tube current, the voltage on the control electrode defines the gun current (i.e. electron beam current). Depending on the desired operating mode when producing the electron beam, the modulator either adds an AC voltage to the DC voltage of the control

* FNAL is operated by Fermi Research Alliance, LLC under Contract No. DE-AC02-07CH11359 with the United States Department of Energy.

[#]warnar@fnal.gov

A CONCEPT TO IMPROVE THE AVAILABILITY OF PETRA III BY CORRELATION OF ALARMS, TIMESTAMPS AND POST-MORTEM-ANALYSIS

M. Werner, DESY, Hamburg, Germany

Abstract

For current and future accelerators, in particular light sources, high availability is an important topic. Therefore the causes of beam losses must be diagnosed and eliminated as fast as possible. This paper presents a concept using the following signals and data from diagnostic instruments and other sources: i) software alarms transmitted by the control system, ii) hardware alarms received and timestamped by the machine protection system, and iii) Post-Mortem-Analysis. By analysing alarm dependencies and the chronological order of alarms, the cause of the problem can be tracked down. The help of diagnostic instruments is highlighted.

INTRODUCTION

A manual alarm analysis in the case of a beam loss can be a time consuming task. In some cases alarms cause an alarm avalanche, by this hiding the initial alarm. In other cases alarms are mutually dependent and the question arises which alarm occurred first. The following ideas could help to solve some of these problems, and it is intended to use some of them in the context of the Machine Protection System for the new PETRA III light source [1].

SOFTWARE ALARMS

Software alarms are transmitted from the hardware to the server for this hardware via a field bus or via Ethernet or the server generates the alarm by itself. The server sends the alarms to a dedicated alarm server and shows the alarms through the control system interface. The time of an alarm can be determined with a precision in the order of 1 second, and the reaction time is also in the order of 1 second. The alarm description can be very specific, e.g. the name of a magnet circuit (out of hundreds of circuits) can be displayed without big effort. Adding new alarms is just a matter of software.

Non-dangerous events which always cause a beam loss

Alarms from these events can be transmitted by software, and there is no need for a precise timestamp to localize the error, because these events do not depend on other events in a difficult way, so they must be the initial cause of a beam loss. Examples:

- Main dipole or quadrupole power supply breakdown
- RF system breakdown (not triggered by beam loss)
- Mains breakdown

04 Beam Loss Detection

HARDWARE ALARMS

Hardware alarms need dedicated cables, therefore they are limited to critical alarms which need a fast reaction time (order of 1ms) and/or a precise timestamp (order of 1us can be achieved).

Dangerous events which must trigger a fast beam dump

Alarms for these events must dump the beam by the use of the machine protection system (MPS) and they should be timestamped. Together with the timestamps of the other alarms, a statement about the initial alarm can be made in many cases. Examples:

- Cavity sparking
- Vacuum shutter closed
- Temperature too high
- Personal interlock broken (e.g. door opened, emergency button pressed)
- Beam Orbit out of limits or critical BPM not working correctly

Non-dangerous events which need a precise timestamp

These events sometimes cause a beam loss. They should not initiate a beam dump. For alarms from these events the cause of the beam loss cannot be clearly assigned, but if the event occurs shortly before a beam loss, there is a high probability that it is the cause of the beam loss. Examples:

- Main dipole or quadrupole power supply spike
- RF spike
- Mains brownout or spike
- Corrector power supply breakdown

There is an overlap to the software alarms (see above), because, for example, the alarm line for a main dipole power spike will also trigger in the case of a main dipole power failure.

COMBINATION OF SOFTWARE AND HARDWARE ALARMS

A combination of software and hardware alarms can be useful for a group of devices such as corrector magnet supplies: the individual names of the faulty channels can be transmitted by software, while an "OR"-combination of all channels add up to a single hardware alarm to provide a precise timestamp of the first alarm in this group.

FEASIBILITY STUDY OF AN OPTICAL FIBRE SENSOR FOR BEAM LOSS DETECTION BASED ON A SPAD ARRAY*

A. Intermite[†], Max Planck Institute for Nuclear Physics, Heidelberg, Germany
M. Putignano, C. P. Welsch, Cockcroft Institute and University of Liverpool, UK

Abstract

This contribution describes an optical fibre sensor based on the use of a silicon photomultiplier (SiPM) composed of an array of Single Photon Avalanche Detectors (SPADs). This sensor will be used for the detection and localization of particle losses in accelerators by exploiting the Cerenkov Effect in optical fibres. As compared to conventional vacuum photomultipliers, the SPAD array allows for maximizing the geometrical efficiency of Cerenkov photon detection. The array can be directly integrated into the fibre end while retaining the same quantum efficiency (20%) in the wavelength range of interest. The SiPM is intrinsically very fast due to its small depletion region and extremely short Geiger-type discharge, which is in the order of a few hundreds of picoseconds. Therefore, the combined use of optical fibres and SiPMs seems a promising option for a modern Cerenkov detector featuring subnanosecond timing, insensitive to magnetic fields, capable of single photon detection and allowing for the possibility of realization in the form of a smart structure. We present the layout and operating principle of the detector, its characteristics, and outline possible fields of application.

INTRODUCTION

Beam loss monitor systems are designed for measuring beam losses around an accelerator or a storage ring [1]. Particles showers penetrate the optical fibre and generate Cerenkov radiation. Using two parallel sensors along the most critical parts of the accelerator such as collimators, scrapers and aperture limitations the losses can be detected and localized. To couple the highest number of photons into the fibres, the geometrical features of the sensor have to be optimized. For this purpose a simulation code was developed, to achieve the best collection efficiency with the optical fibres available commercially in the range between 450-550 nm. The Numerical Aperture (NA) of these fibres is chosen considering the meridional and skew rays contribute to the coupling efficiency and the attenuation curves in the specific range of wavelengths where the SiPMs have their highest photosensitivity.

*Work supported by the Helmholtz Association of National Research Centers (HGF) under contract number VH-NG-328 and GSI Helmholtzzentrum für Schwerionenforschung GmbH

[†] Corresponding author: angela.intermite@quasar-group.org

CERENKOV RADIATION IN OPTICAL FIBRES

A charged particle passing through an optical fibre of large enough radius ($a \gg \lambda$) produces Cerenkov radiation inside the fibre if its velocity exceeds the phase velocity of light in the medium. Cerenkov photons are immediately generated and the number of photons N_{ph} per wavelength interval λ and distance L is given by [2]:

$$\frac{d^2 N_{ph}}{d\lambda dL} = 2\pi \alpha z^2 \frac{\sin^2 \theta}{\lambda^2} \quad (1)$$

where $\alpha = 1/137$ is the fine structure constant, θ is the Cerenkov cone semi-angle, λ the wavelength and L the path length of the particle with charge z in the fibre.

Cerenkov light is emitted on the surface of a cone with an angular opening semi-angle given by:

$$\cos \theta = \frac{1}{n\beta} \quad (2)$$

where $\beta = v/c$ and n the refractive index of the fiber.

From Eq. (1), the intensity of Cerenkov light increases inversely to the cube of the wavelength as it is plotted in Fig. 1, consequently the blue color dominates in the visible spectrum.

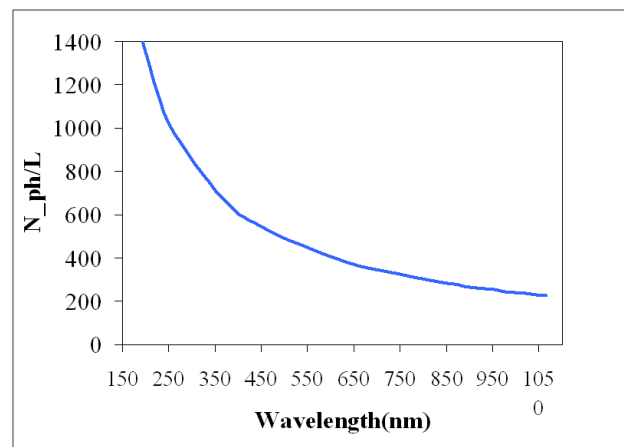


Figure 1: Number of photons produced per incident electron and per unit length L between 193 – 1064 nm.

When we consider the Cerenkov propagation inside a fibre we have to consider the probability of survival of the created photons (Collection Efficiency, CE) in the waveguide: this is determined by NA of the fibre and by the direction of the Cerenkov photons. In Fig. 2 we can see CE as a function of the incidence angle of the charged particle with respect to the fiber axis and the impact parameter, i.e. the shortest distance between the charged

LOSS MONITOR ON THE BASIS OF DIFFUSIVE RADIATION FROM ROUGH SURFACES

S.G. Arutunian*, Zh.S. Gevorkian, K.B. Oganessian,
 Yerevan Physics Institute, Alikhanian Brothers St. 2, Yerevan 375036, Armenia

Abstract

Diffusive Radiation is generated when a charged particle passes through a randomly inhomogeneous medium. Such a situation can be realized when a charged particle slides over a rough metallic surface. One of the important properties of DR is that the emission maximum lies at large angles from particle velocity direction. Therefore it can be used for detection of beam touch to the accelerators vacuum chamber wall in case when generated photons will be observed on the opposite side of the vacuum chamber. Such a diagnostics can be especially useful for monitoring of beam particle losses.

There is substantial interest in the development of different tools for beam diagnostics. Particularly, optical transition radiation is widely used for this goal [1, 2, 3]. With modern powerful optical detectors OTR based devices are very convenient. However there is also a problem with use of OTR. For relativistic particles, TR photons are emitted at very small angles $\theta \sim \gamma^{-1} \ll 1$. DR that we are going to discuss is free from such a shortage. In the present paper we consider the possibility of using of DR from rough surfaces for beam diagnostics.

A charged particle passing through a stack of plates placed in a homogeneous medium is known to be radiating electromagnetic waves. Radiation originates because of the scattering of electromagnetic field on the plates. Considering this problem theoretically it was shown [6, 7] that the spectral angular radiation intensity can be represented as a sum of single scattering I_0 and multiple scattering I_D contributions of pseudophotons

$$I = I_0 + I_D \quad (1)$$

where

$$I_0(\theta, \omega) = \frac{e^2 B(|k_0 - k \cos \theta|) \sin^2 \theta \omega^2}{2c [\gamma^{-2} + \sin^2 \theta k^2/k_0^2]^2 k_0^4 c^2} \quad (2)$$

and diffusive contribution is determined as

$$I_D(\theta, \omega) = \frac{5e^2 \gamma^2 L_z l_{in}(\omega) \sin^2 \theta}{2\epsilon c l^2(\omega) |\cos \theta|} \quad (3)$$

Here L_z is the path of the particle in the medium, θ is the observation angle, $k_0 = \omega/v$, v is the particle velocity, $k = \omega\sqrt{\epsilon}/c$, B is the correlation function of random dielectric constant field created by randomly located plates.

Assuming that parallel plates with equal probability can occupy any point of z axis one finds correlation function as follows

$$B(q_z) = \frac{4(b - \epsilon)^2 n \sin^2 q_z a/2 \omega^4}{q_z^2 c^4} \quad (4)$$

where $n = N/L_z$ is concentration of plates in the system, a is their thickness, b is their dielectric constant and ϵ is the average dielectric constant of the system. In Eq. (3), l and l_{in} are average elastic and inelastic mean free paths of photon in the medium. Inelastic mean free path is mainly associated with the absorption of electromagnetic field in the medium. Elastic mean free path is associated with the photon refraction on plates. It depends on the falling angle on plates. In the case when photon falls normally elastic mean free path is determined as follows

$$l = \frac{4k^2}{B(0) + B(2k)} \quad (5)$$

Note that just this quantity enters into spectral angular intensity Eq. (3). Eqs. (3, 5) are correct in the weak scattering limit $\lambda/l \ll 1$ and for observation angles $\theta = \pi/2 - \delta$, $\delta \gg (1/kl)^{1/3}$. Last restriction over angles appears because when $\theta = \pi/2$ pseudophotons are moving parallel to plates and no any refraction happens and the condition of weak scattering is failed. When the conditions of multiple scattering of electromagnetic field are fulfilled the diffusive contribution to the radiation intensity Eq. (3) is the main one because $I_D/I_0 \sim l_{in}/l \gg 1$. As it is seen from Eq. (3) the radiation intensity is determined by elastic and inelastic mean free paths of photon in the medium. It follows from Eq. (4) that when $ka \gg 1$, $B(2k)/B(0) \sim 1/(ka)^2 \ll 1$. Therefore in both cases $ka \gg 1$ and $ka \ll 1$ the photon mean free path has the form

$$l \sim \frac{k^2}{B(0)} \quad (6)$$

where $B(0) = k^4(b - \epsilon)^2 na^2/\epsilon^2$. Substituting this expression into Eq. (6) and taking into account that $k = \omega\sqrt{\epsilon}/c$, we have

$$l \sim \frac{\epsilon}{\frac{\omega^2}{c^2} (b - \epsilon)^2 na^2} \quad (7)$$

Remind that ϵ is the average dielectric constant of the system which for a layered stack has the form:

$$\epsilon(\omega) = nab(\omega) + (1 - na)\epsilon_0(\omega) \quad (8)$$

Here ϵ_0 is the dielectric constant of a homogeneous medium into which plates with dielectric constant $b(\omega)$ and

* femto@yerphi.am

BEAM BASED DEVELOPMENT OF A FIBER BEAM LOSS MONITOR FOR THE SPring-8/XFEL

X.-M. Maréchal[#], JASRI SPring-8 and XFEL Project RIKEN, Sayo-gun, Hyogo, 679-5198 Japan
Y. Asano, T. Itoga, XFEL Project, RIKEN, Sayo-gun, Hyogo, 679-5148 Japan.

Abstract

To select the best candidate for a fiber based beam loss monitor, glass fibers of different diameter (100~600 μm), index profile (graded/stepped) and from different makers were characterized (signal strength, attenuation, dispersion) at the SPring-8 Compact SASE Source (SCSS). Beam tests showed that at 250 MeV the detection limit corresponding to a 10 mV signal is below 1 pC/bunch over 60 m and 3 pC/bunch over 120 m, with a position accuracy better than 30 cm. The fiber lifetime has been estimated to be over 13000 hours from dose measurements at the SCSS.

INTRODUCTION

Optical fibers have been used as radiation detectors for more than 20 years in a wide range of experiments. Recently several facilities have worked on the development of fiber-based local beam loss detection systems [1]. Fiber-based beam loss monitors offer the possibility to detect beam losses over long distances in real time, with good position accuracy and sensitivity at a reasonable cost. For the undulator section of the 8 GeV SPring-8/XFEL [2], radiation safety considerations set the desirable detection limit at 1 pC (corresponding to a 0.1% beam loss) over more than a hundred meter. While the intensity of the Cerenkov radiation generated in and transmitted down a multimode fiber has been predicted theoretically [3,4], the selection of the optimum fiber is not straightforward. A beam-based approach was therefore chosen to characterize different glass fibers (signal strength, attenuation, dispersion).

EXPERIMENTAL SET-UP

The experiments were carried out at the SCSS, a 1/16th model of the future SPring-8/XFEL. The SCSS has a maximum electron energy and repetition rate of 250 MeV and 60 Hz respectively. The optical fiber was set along (for beam loss measurements) or across (for attenuation/dispersion measurement) the accelerator vacuum chamber (Fig. 1). The signals from the photomultiplier tubes (PMTs) set at both end of the fiber are read out with an oscilloscope. A trigger signal from the accelerator master oscillator is used as time reference. The beam current was measured with current transformer (CT) monitors placed along the beam accelerator. Inserting the screen of an optical transition radiation (OTR) monitor into the beam path generates an electromagnetic shower: This artifice is used to simulate a beam loss (stray electrons hitting the vacuum chamber). To measure the attenuation/dispersion of the light signal,

the fiber is set across behind an OTR screen. The signal is then measured for different distances (A, B in Fig. 1b).

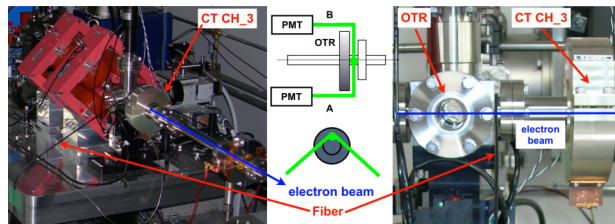


Figure 1: Experimental set-up used for the measurement of the attenuation of the beam loss monitor.

Several kinds of fibers (different diameters, numerical aperture and index profile) were tested (Table 1). All fibers were coated to limit the noise from ambient light. The choice of the photomultiplier (Hamamatsu H6780-02) resulted from a compromise between the fiber attenuation and the characteristics of Cerenkov spectrum. An additional criterion was the possibility to add a connector: The fibers were equipped with FC connectors at both ends to insure easy (“plug and play”) and clean connections (low insertion loss) as well as a good reproducibility. With this experimental set-up, it is possible to test the response (signal strength, attenuation, dispersion) of these fibers in realistic (The continuous spectrum of a Cerenkov signal from stray charged particles) and standardized conditions.

Table 1: Main characteristics of the fibers. The numerical aperture of the Fujikura and Corning fibers are respectively 0.2 and 0.39.

Maker	Reference	Index	Length [m]
Mitsubishi	ST100	Step	10.1
Fujikura	GC200/250	Graded	10.2
	GC400/500	Graded	61.4
	GC600/750	Graded	10.1
	SC200/220	Step	10.1
	SC400/440	Step	32.4 & 121.4
Corning	COR200VIS39	Step	25.4

SIGNAL STRENGTH AND ATTENUATION

Figure 2 shows the strength of the Cerenkov signal as a function of the fiber length. The signal from the PMT has been normalized by the average beam charge impacting the screen of the OTR monitor. The error bars reflect the standard deviation from the PMT signal (typically taken over a few hundreds samples) as well as the standard deviation of the CT signal (typically less than one

[#]marechal@spring8.or.jp

FLEXIBLE CORE MASKING TECHNIQUE FOR BEAM HALO MEASUREMENTS WITH HIGH DYNAMIC RANGE

J. Egberts, S. Artikova, MPI-K, Heidelberg, Germany

C.P. Welsch, Cockcroft Institute, Warrington, Cheshire, UK, University of Liverpool, Liverpool, UK

Abstract

The majority of particles in a beam are located close to the beam axis, called the beam core. However, particles in the tail distribution of the transverse beam profile can never be completely avoided and are commonly referred to as beam halo.

The light originating from or generated by the particle beam is often used for non- or least destructive beam profile measurements. Synchrotron radiation, optical transition, or diffraction radiation are examples of such measurements. The huge difference in particle density between the beam core and its halo, and therefore the huge intensity ratio of the emitted light is a major challenge in beam halo monitoring.

In this contribution, results from test measurements using a flexible core masking technique are presented indicating way to overcome present limitations. This technique is well-known in e.g. astronomy, but since particle beams are not of constant shape in contrast to astronomical objects, a quickly adjustable mask generation process is required. The flexible core masking technique presented in this paper uses a micro mirror array to generate a mask based on an automated algorithm.

INTRODUCTION

The detection and possible control of the beam halo is of utmost importance for high energy accelerators, where unwanted particle losses lead to an activation or even damage of the surrounding vacuum chamber. But also in low-energy machines like the USR [1] one is interested in minimizing the number of particles in the tail region of the beam distribution. Since most part of the beam is normally concentrated in the central region, observation techniques with a high dynamic range are required to ensure that halo particles can be monitored with sufficient accuracy. One option to monitor the beam halo is to use light generated by the beam, either through synchrotron radiation (SR), optical transition radiation (OTR), or luminescent screens. In this case, a special detection technique is required to allow for high dynamic range measurements.

The flexible core masking technique is based on the core masking technique which is well established in astronomy to observe the corona of the sun [2]. For an accurate image acquisition of the corona, an exposure time is required at which a normal camera overexposes due to the bright central region of the sun. The resulting blooming effects will superimpose the corona light and make an accurate image acquisition impossible. Therefore, the central bright region

region of the sun is masked out to allow for a corona measurement without any negative blooming effects. The same principle can be applied for beam halo measurements, as already shown in [3, 4]. Test measurements of this kind have been performed at CERN by T. Lefèvre et al [5].

Unlike astronomical objects, an accelerator beam's profile is typically variable in shape. A technique using a fixed mask does not suffice any more and a flexible core masking technique is required. Taking advantage of the unique features of *Micro Mirror Arrays (MMA)*, flexible masks required for this technique become feasible.

MICRO MIRROR ARRAY

The *Micro Mirror Array* used for the measurements consists of an array of 1024×768 micro mirrors of $13.68 \mu\text{m} \times 13.68 \mu\text{m}$ size. Each of them can individually be set to $\pm 12^\circ$ [6]. Light will then be reflected in different directions depending on the micro mirror state. It is thereby possible to use the MMA as a reflective display which can be utilised as an adjustable mask.

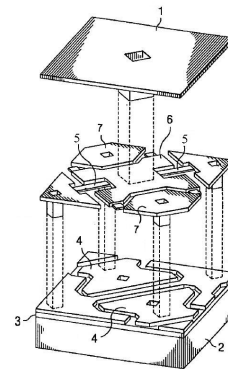


Figure 1: *MMA* Pixel Scheme [7].

Each single pixel of the *MMA* can be separated in a substructure and superstructure. The mirror itself is attached to the superstructure. The substructure of the pixels consists of a silicon substrate (fig.1-2) with an insulating layer (fig.1-3) on top, which isolates the superstructure from the substructure. Upon the insulating layer, there is a thin metallic layer, which forms the lower address electrodes (fig.1-4) and also supports the hinge. The hinge consists of the flexible torsion beam (fig.1-5), the large hinge yokes (fig.1-6), and upper address electrodes (fig.1-7).

If there is an appropriate potential applied to the upper and the lower electrodes (fig.1-4; 1-7), the electrostatic

CONFIGURATION AND VALIDATION OF THE LHC BEAM LOSS MONITORING SYSTEM

C. Zamantzas, B. Dehning, J. Emery, J. Fitzek, F. Follin, S. Jackson, V. Kain, G. Kruk,
M. Misiowiec, C. Roderick, M. Sapinski, CERN, Geneva, Switzerland

Abstract

The LHC Beam Loss Monitoring (BLM) system is one of the most complex instrumentation systems deployed in the LHC. As well as protecting the machine, the system is also used as a means of diagnosing machine faults, and providing feedback of losses to the control room and several systems such as the Collimation, the Beam Dump and the Post-Mortem. The system has to transmit and process signals from over 4'000 monitors, and has approaching 3 million configurable parameters.

This paper describes the types of configuration data needed, the means used to store and deploy all the parameters in such a distributed system and how operators are able to alter the operating parameters of the system, particularly with regard to the loss threshold values. The various security mechanisms put in place, both at the hardware and software level, to avoid accidental or malicious modification of these BLM parameters are also shown for each case.

INTRODUCTION

The Large Hadron Collider (LHC) is the next circular accelerator being constructed at the European Organisation for Nuclear Research (CERN). It will provide head-on collisions of protons at a centre of mass energy of 14 TeV for high energy particle physics research. In order to reach the required magnetic field strengths, superconducting magnets cooled with superfluid helium will be used. The energy stored in the LHC can potentially damage many elements of the accelerator or could make its operation very inefficient.

The strategy for machine protection and quench prevention of the LHC is mainly based on the Beam Loss Monitoring (BLM) system. At each turn, there will be several thousands of data to record and process in order to decide if the beams should be permitted to continue circulating or their safe extraction is necessary to be triggered. The decision involves a proper analysis of the loss pattern in time and a comparison with predefined threshold levels that need to be chosen dynamically depending on the energy of the circulating beam. This complexity needs to be minimized by all means to maximize the reliability of the BLM system and allow a feasible implementation. The processing of the acquired data and the comparison with predefined threshold levels is needed to be performed in real-time and thus requires dedicated hardware to meet the demanding time and performance requirements.

To overcome such limitations, a great effort has been committed to provide a highly efficient, reliable and feasible implementation of the BLM system by

employing various state of the art techniques in analogue and digital electronics, databases and computing, which include redundancies and optimizations across all of its levels of abstraction.

SYSTEM CONFIGURATION

The BLM system is making use of modern field programmable gate arrays (FPGAs), which include the resources needed to design complex processing and can be reprogrammed making them ideal for future upgrades or system specification changes. There is a common FPGA firmware that is deployed to all crates at the Front-End Computer's (FEC) boot procedure or if required could be read from the flash memory on power on.

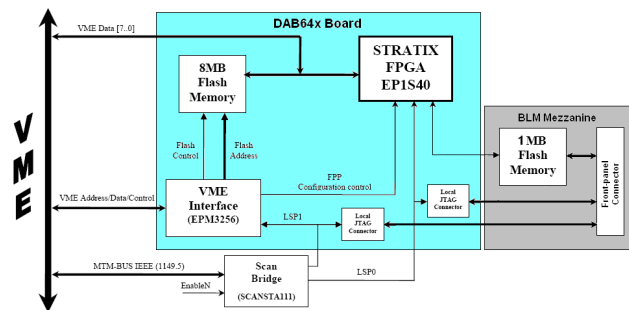


Figure 1: Block diagram of the FPGA firmware deployment and initialisation options.

More specifically, the FPGA configuration can be forced to be loaded either remotely via the FEC and the VME bus, locally via the JTAG connection that is provided in the front panel, or set to auto-configurable by utilising the on-board memory. Figure 1 shows a block diagram of the interconnections in the Threshold Comparator (BLETC) module.

The dataset of thresholds and settings for the complete BLM system during the deployment procedure is split to the relevant parameters for each module. In that way, they include only information which is unique for each monitor, crate or sector that the module will need to protect. Among those it includes the monitor names, their threshold values, the serial numbers for the BLETC and the two acquisition modules [1] which are connected to it, as well as the Connection and Masking matrices. Table 1 shows the complete list of the parameters stored on each processing module.

These channel and board specific parameters are stored in the normally unused space of the configuration memory

DESIGN SPECIFICATIONS FOR A RADIATION TOLERANT BEAM LOSS MEASUREMENT ASIC

G.G. Venturini, B. Dehning, E. Effinger, C. Zamantzas, CERN, Geneva, Switzerland

Abstract

A novel radiation-hardened current digitizer ASIC is in planning stage, aimed at the acquisition of the current signals from the ionization chambers employed in the Beam Loss Monitoring system at CERN. The purpose is to match and exceed the performance of the existing discrete component design, currently in operation in the Large Hadron Collider (LHC). The specifications include: a dynamic range of nine decades, defaulting to the 1 pA-1 mA range but adjustable by the user, ability to withstand a total integrated dose of 10 kGy at least in 20 years of operation and user selectable integrating windows, as low as 500 ns. Moreover, the integrated circuit should be able to digitize currents of both polarity with a minimum number of external components and without needing any configuration. The target technology is the IBM 130 nm CMOS process. The specifications, the architecture choices and the reasons on which they are based upon are discussed in this paper.

INTRODUCTION

It is expected that with the increase in LHC beam intensity an increase in beam losses will be observed as well. Accordingly, the BLM electronics installed in the facility will be exposed to a higher radiation level. The current discrete component front-end electronics will be replaced by an Application Specific Integrated Circuit (ASIC) chip, designed to operate in the radioactive environment and, at the same time, to deliver higher performance. The employment of the new integrated circuit will allow the placement of the acquisition boards closer to the detectors in the most radioactive locations.

DESIGN SPECIFICATIONS

The charge digitizer provides a digital output proportional to the integral of the input current over a time window. Figure 1 shows a functional diagram of the device.

The main objectives of the design are summarized as follows (Table 1):

- *Dynamic range*: nine decades (or 180 dB).
- *Minimum input current*: the ASIC design will be compatible with the different detectors and setups employed in the BLM system, in line with the specifications. Considering a current digitizer based on a current-to-frequency converter, the input-output relationship is given by $f_{OUT} = I_{in}/Q_{REF}$, where Q_{REF} is here referred to as the reference charge. Enabling the user to select different values of the reference charge

provides an effective method to scale the maximum and minimum signals, while internally the range of frequencies of operation and the value of the DR are kept constant. As other design-dependent constraints affect the value of the maximum and minimum input currents, care should be taken in the implementation of different input ranges. Additionally, independently of the chosen design, the inverse saturation current of the protection diodes and its variation due to temperature, radiation effects and aging set a limit on the minimum detectable current that can be measured. To overcome this drawback, the protection circuit on the analog input pins will be opportunely designed, to decrease the lower limit under 1 pA. The trade-off between the overload tolerance of the custom-protected inputs and the input leakage will be analyzed to provide a satisfactory solution, to provide a leakage below 100 fA.

- *Bipolar input currents*: the converter should work with currents of either polarity, without requiring any pre-configuration. It is currently under consideration whether or not the converter will provide the same range for each of them or a full and a reduced one. The measurement of dual polarity currents with a single supply device requires the input to be biased at approximately $V_{DD}/2$. The availability of this voltage on an output pin is useful when a circuit is connected to the input and it is thus provided to the user (REFOUT pin in Fig. 1).
- *Radiation tolerance*: the design aims for a Total Ionizing Dose (TID) equal or greater than 10 kGy over a 20 years period. The requirements regarding Transient Dose Effects, maximum Single Event Effects (SEE) rates are being investigated and will be split into maximum Single Event Upsets (SEU) and Single Event Latch-up (SEL) rates.

In addition to the main features listed above, *the acquisition time window* should be selected by the user from a set, by means of dedicated setup pins, the shortest interval being 500 ns. Additionally, care should be taken in the design to ensure a *minimum number of external components*. The components required to assemble an acquisition board are one or more ASICs, a crystal, power management ICs and a controller for data transmission – depending on the selected transmission medium – and a few minor elements, such as decoupling capacitors. A diagram of an acquisition board is shown in Fig. 2, displaying the substantially reduced component count with respect to previous designs.

SYSTEMATIC STUDY OF ACQUISITION ELECTRONICS WITH A HIGH DYNAMIC RANGE FOR A BEAM LOSS MEASUREMENT SYSTEM

G.G. Venturini, B. Dehning, E. Effinger, J. Emery, C. Zamantzas, CERN, Geneva, Switzerland

Abstract

A discrete components design for a current digitizer based on the current-to-frequency converter (CFC) principle is currently under development at CERN. The design targets at higher current inputs than similar designs, with a maximum equal to 100 mA and a minimum of 1 nA, as required by the ionization chamber that will be employed in the Proton Synchrotron and Booster accelerators as well as in the LINAC 4. It allows the acquisition of currents of both polarities without requiring any configuration and provides fractional counts through an ADC to increase resolution. Several architectural choices are considered for the front-end circuit, including charge balance integrators, dual-integrator input stages, integrators with switchable-capacitor. Design approach and measurements are discussed in this article.

INTRODUCTION

The Beam Loss Monitoring system employed in the CERN accelerator chain determines the energy density deposited in the individual accelerator elements as well as the residual radiation. For this reason, a wide dynamic range is required, equal to approximately seven decades. The ionization chambers employed are suitable sensors for this purpose, as they are able to provide a current signal with a dynamic range that exceeds the aforementioned requirements. The acquisition electronics must be designed accordingly, in order not to decrease the dynamic range below the system specifications. The dynamic range of the whole chain is limited by the very first stage: the acquisition of the signal has to be carried out with a circuit architecture other than a Miller integrator, since its dynamic range is limited to approximately 60dB.

GENERAL SCHEME OF RECYCLING INTEGRATORS

The general scheme of a recycling integrator is shown in Fig. 1. It contains a loop composed of an integrating system and a comparator block closed by the reset circuitry of the integrator.

The current signal at the input (I_{in}) is integrated and every time the result (V_o) exceeds a threshold (V_{TH}), the integrator is reset, lowering its output again under the threshold value. At the same time, the value stored by a counter is incremented by one unit, to keep track of the acquired charge. At the end of the measurement time window (T_M), the out-

04 Beam Loss Detection

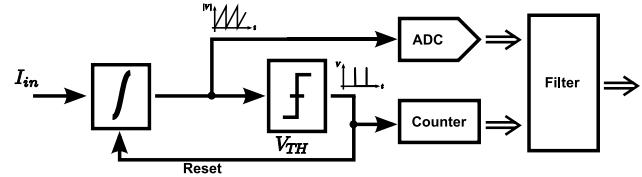


Figure 1: General scheme of a recycling integrator.

put of the integrator is sampled and its value is combined with the number of resets, according to the formula:

$$Q = C (V_O(T_M) - V_O(0)) + n Q_{REF} \quad (1)$$

Q is the charge acquired in the interval $(0, T_M)$,

n is the number of resets performed during the said time interval,

Q_{REF} is the charge that is lost by the integrator at every reset event,

C is the proportionality factor between the output voltage and the stored charge in the integrator.

Two successive commutations of the comparators are separated by a time interval given by the time required to accumulate a charge equal to the amount subtracted in the last reset. If the input is a constant current, the switching frequency of the comparator is ideally linked to the value of I_{IN} by the following relationship,

$$f_{SW} = \frac{I_{IN}}{Q_{REF}} \quad (2)$$

which can be generalized for an arbitrary input waveform as:

$$f_{SW} = \frac{1}{T_{SW}} = \frac{\overline{I_{IN}(t)}_0^{T_{SW}}}{Q_{REF}} \quad (3)$$

$\overline{I_{IN}(t)}_0^{T_{SW}}$ is the average value of the input current in the time interval $(0, T_{SW})$ between two consecutive commutations.

DESCRIPTION OF THE CIRCUITS

The charge-to-voltage conversion of the recycling integrator is determined by the reset circuit, as seen in Eq. 2 (Q_{REF} dependence). According to the specifications of the circuit, several implementations of the described scheme have been performed in this work.

VELOCITY OF SIGNAL DELAY CHANGES IN FIBRE OPTIC CABLES

M. Bousonville*, GSI, Darmstadt, Germany
J. Rausch, Technische Universität Darmstadt, Germany

Abstract

Most timing systems used for particle accelerators send their time or reference signals via optical single mode fibres embedded in cables. An important question for the design of such systems is how fast the delay changes in the fibre optic cable take place, subject to the variation of the ambient air temperature. If this information is known, an appropriate method for delay compensation can be chosen, to enable a phase stabilised transmission of the timing signals. This is of interest particularly with regard to RF synchronisation applications.

To characterise the velocity of the delay change, the delay behaviour after a sudden temperature change will be described.

When trying to determine the step response, two problems occur. On the one hand, the material parameter of the coating, necessary for the calculation, is typically unknown. On the other hand, the measurement of the step response under realistic conditions is very laborious.

Thus in this presentation it will be shown how the step response and, accordingly, the velocity of the delay change in a fibre optic cable can be calculated by means of theoretical considerations, utilizing the typical geometry of fibre optic cables.

INTRODUCTION

The following analysis was performed as part of the development of the timing system for the cavity synchronisation of the Facility for Antiproton and Ion Research (FAIR) [1-3]. Loose tube cables frequently used in telecommunications are considered. The coating of this cable type can be described as a tube in which the standard single mode fibres (SMF) are loosely inserted (Fig. 1). The fibres and the coating are thus mechanically decoupled. This and the fact that the fibres are about 2% longer than the cable coating means that the tension on the cable to a certain extent does not act on the fibres and thus does not cause any delay change (see Eq. (3)).

Accordingly, only temperature fluctuations are responsible for a delay change.

In the following, a way of calculating analytically not only the absolute delay change but also the speed at which such change takes place is presented for the first time.

ABSOLUTE DELAY CHANGE

Signals need the group delay τ to pass through a fibre of length L and group index N_g [4]

$$\tau = \frac{N_g \cdot L}{c}, \quad (1)$$

wherein c stands for the speed of light in a vacuum. With a transmission length of $L = 1$ km and a group index of $N_g \approx 1.5$, delays of approximately $5 \mu\text{s}$, for example, occur. According to [4], a change in the group delay can have two causes. First of all, fluctuations in the temperature T

$$\frac{d\tau}{L \cdot dT} = \frac{1}{c} \left(N_g \frac{dL}{L \cdot dT} + \frac{dN_g}{dT} \right) \quad (2)$$

and secondly, mechanical tension σ acting on the length of the fibre

$$\frac{d\tau}{L \cdot d\sigma} = \frac{1}{c} \left(N_g \frac{dL}{L \cdot d\sigma} + \frac{dN_g}{d\sigma} \right). \quad (3)$$

Both bring about both a change in the length of the fibre and a change in the group index. For a non-jacketed fibre this results, according to Eq. (2) with $N_g = 1.4682$ at a wavelength of 1550 nm [5], the length expansion coefficient $dL/(L \cdot dT) = 5.6 \cdot 10^{-7} \text{ K}^{-1}$ and the temperature coefficient of the group index of $dN_g/dT = 1.2 \cdot 10^{-5} \text{ K}^{-1}$ [6], in a value of

$$\left(\frac{d\tau}{L \cdot dT} \right)_{\text{fibre}} = 40 \frac{\text{ps}}{\text{km} \cdot \text{K}}. \quad (4)$$

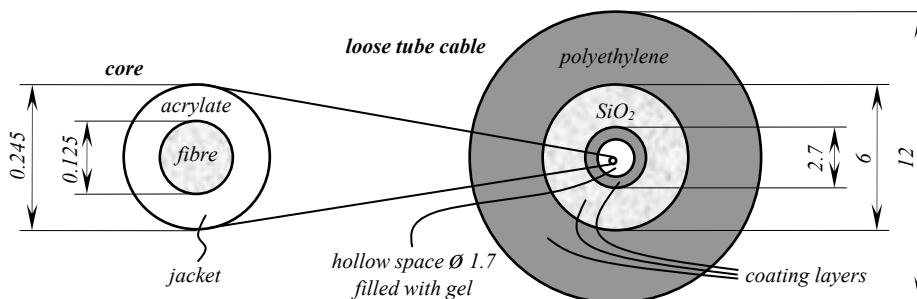


Figure 1: Cross-section of a loose tube fibre optic cable.

*M.Bousonville@gsi.de

COHERENT OPTICAL TRANSITION RADIATION AS A TOOL FOR ULTRASHORT ELECTRON BUNCH DIAGNOSTICS

Gianluca Geloni, Petr Ilinski, Evgeni Saldin, Evgeni Schneidmiller and Mikhail Yurkov,
DESY, Hamburg, Germany

Abstract

In this contribution we describe how Coherent Optical Transition Radiation can be used as a diagnostic tool for characterizing electron bunches in X-ray Free-electron lasers. The proposed method opens up new possibilities in the determination of ultrashort, ultrarelativistic electron bunch distributions. Our technique is described more extensively in [1], where the interested reader will also find relevant references.

INTRODUCTION

Operational success of XFELs will be related to the ability of monitoring the spatio-temporal structure of sub-100 fs electron bunches as they travel along the XFEL structure. However, the femtosecond time-scale is beyond the scale of standard electronic display instrumentation. Therefore, the development of methods for characterizing such short electron bunches both in the longitudinal and in the transverse directions is a high-priority task, which is very challenging.

A method for peak-current shape measurements of ultrashort electron bunches using the undulator-based Optical Replica Synthesizer (ORS), together with the ultrashort laser pulse shape measurement technique called Frequency-Resolved Optical Gating (FROG) was recently proposed (see references in [1]). It was demonstrated that the peak-current profile for a single, ultrashort electron bunch could be determined with a resolution of a few femtoseconds. The ORS method is currently being tested at the Free-electron laser in Hamburg (FLASH). Novel results will be reported at this conference.

In this paper we present a feasibility study for integrating the ORS setup with a high-resolution electron bunch imager based on coherent Optical Transition Radiation (OTR). Our ideas are discussed in detail in [1], where the interested reader will also find relevant references that are omitted here for reasons of space.

Electron bunch imagers based on incoherent OTR constitute the main device presently available for the characterization of an ultrashort electron bunch in the transverse direction. They work by measuring the transverse intensity distribution. Since no fast enough detector is presently available, the image is actually integrated over the duration of the electron bunch. Therefore, incoherent OTR imagers fail to measure the temporal dependence of the charge density distribution within the bunch. For these reasons, the use of standard incoherent OTR imagers is limited to transverse electron-beam diagnostics, to measure e.g. the projected transverse emittance of electrons. However, it is

primarily the emittance of electrons in short axial slices, which determines the performance of an XFEL. Therefore, there is a need for electron diagnostics capable of measuring three-dimensional (3D) ultrashort electron bunch structures with micron-level resolution.

The main advantages of coherent OTR imaging with respect to the usual incoherent OTR imaging is in the coherence of the radiation pulse, and in the high photon flux. Exploitation of these advantages leads to applications of coherent OTR imaging that are not confined to diagnostics of the transverse distribution of electrons. The novel diagnostics techniques described here can be used to determine the 3D distribution of electrons in a ultrashort single bunch. In combination with multi-shot measurements and quadrupole scans, they can also be used to determine the electron bunch slice emittance.

The possibility of single-shot, 3D imaging of electron bunches with microscale resolution makes coherent OTR imaging an ideal on-line tool for aligning the bunch formation system at XFELs. In order to ensure SASE lasing at X-ray wavelengths, a very high orbit accuracy of a few microns has to be ensured in the 200 m long undulator. The resolution of incoherent OTR imagers is not adequate to characterize the position of the center of gravity of an electron bunch with such accuracy. Our studies show that coherent OTR imaging can be utilized as an effective tool for measuring the absolute position of the electron bunch with the required micron accuracy. Finally, the improvement of bunch-imaging techniques up to the microscale level does not only yield a powerful diagnostics tool, but opens up new possibilities in XFEL technology as well.

OPTICAL REPLICA SETUP

We propose to create a coherent pulse of optical radiation by modulating the electron bunch at a given optical wavelength and by letting it pass through a metal foil target, thus producing coherent OTR at the modulation wavelength. The radiation pulse should be produced in such a way to constitute an exact replica of the electron bunch. Reference [1] includes a discussion about how to avoid the influence of self-interaction effects. The optical replica can be used for the determination of the 3D structure of electron bunches. Although other projects may benefit from our study too, throughout this paper we will mainly refer to parameters and design of the European XFEL.

In order to produce the optical replica we need to modulate the electron bunch at a fixed optical wavelength. One may take advantage of an Optical Replica Synthesizer

SPECTRAL RESPONSE OF A MARTIN-PUPLETT INTERFEROMETER FOR ELECTRON BUNCH LENGTH MEASUREMENTS

C. Kaya^{*}, U. Lehnert, Forschungszentrum Rossendorf, Dresden, Germany

Abstract

At the ELBE Free Electron Laser (FEL) at Forschungszentrum Dresden Rossendorf (FZD) electron bunches having lengths between 1 to 4 ps are generated. It is required to compress these electron bunches to lengths below 1 ps which necessitates diagnosis of the electron bunch parameters. We use a Martin-Puplett interferometer (MPI) which is a modification of the Michelson interferometer, where the beams are linearly polarized at specific orientations. It measures the autocorrelation function of the coherent transition radiation (CTR) from a view screen which is an optical replication of the electron bunch.

The interferometer setup consists of various optical components like polarizers, beam splitter, mirrors and Golay cell detectors. In our measurement a wire grid was used as a polarizer and also as a beam splitter. A thorough understanding of the response of the optical components, as a function of the CTR wavelength range of our interest, is required for correct analysis of the measured signal. We have therefore simulated the response of the entire interferometer setup including the diffraction losses and the window transmission and compared the results to experimental measurements.

INTRODUCTION

ELBE is based on a superconducting electron linac. The ELBE linac is designed to operate with an accelerating field gradient of 10 MV/m so that the maximum design electron beam energy at the exit of the second module is 40 MeV. ELBE delivers an electron beam with an average current of up to 1 mA. The electron source is a DC thermionic triode delivering beam with energy of 250 keV. The gun beam quality predefines the accelerated beam quality. In the ELBE the electron bunch is compressed to 10 ps after the electron beam injector. In the accelerator the electron bunch length is in the range of 1 to 10 ps. We use a Martin-Puplett interferometer (MPI) which is a modification of the Michelson interferometer, where the beams are linearly polarized at specific orientations. It measures the autocorrelation function of the coherent transition radiation (CTR) from a view screen which is an optical replication of the electron bunch.

In our work we want to determine the workable wavelength range for our Martin-Puplett interferometer setup. We have therefore simulated the response of the entire experimental setup. We also describe in this study

our measurements of the electron bunch length, which is in the picosecond range. The bunch length is estimated from a frequency domain fit of a specially constructed analytical function to the measured power spectrum of the bunch. The power spectrum is obtained as a Fourier transform of the measured autocorrelation function of the CTR. The CTR autocorrelation function is measured with the help of a Martin-Puplett interferometer.

EXPERIMENTAL SETUP

A polarizing Martin-Puplett interferometer (shown in Fig. 1) is used to analyze the spectrum of the far-infrared radiation. CTR passes through a quartz window and is reflected by a parabolic mirror. Then the CTR is polarized vertically by a wire-grid linear polarizer and made incident on a beam splitter. For our measurements the wire grids are wound from 20 μm gold plated tungsten wire with 100 μm spacing (from center to center), which are used as polarizers and beamsplitters. The reflected beam from the beamsplitter then goes to a roof mirror which is fixed, while the transmitted beam goes to a movable roof mirror. These two reflected beams then interfere and then split by a second beam splitter (analyser) the polarization directions are detected using two Golay cell infrared (IR) detectors.

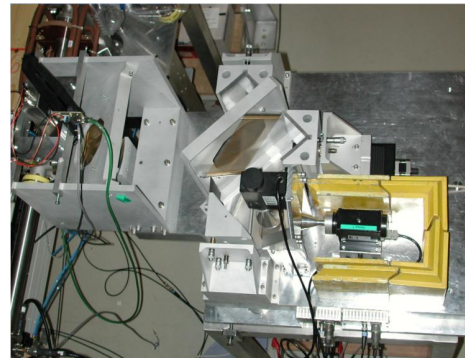


Figure 1: Martin-Puplett Interferometer.

GENERAL DESCRIPTION OF TRANSITION RADIATION

In our experiment the transition radiation is generated when the electron beam is impinging on an aluminum target rotated by 45° with respect to the incoming beam (shown in Fig. 2). The spectral energy flux of backward transition radiation is given for electrons by the Ginzburg-Frank formula [1]:

^{*}E-Mail : c.kaya@fzd.de

TIME RESOLVED SPECTROMETRY ON THE TEST BEAM LINE AT CTF3

M. Olvegård, A. Dabrowski, T. Lefèvre and S. Doebert, CERN, Geneva, Switzerland
 E. Adli, University of Oslo, Norway

Abstract

The CTF3 provides a high current (28 A) high frequency (12 GHz) electron beam, which is used to generate high power radiofrequency pulses at 12 GHz by decelerating the electrons in resonant structures. A Test Beam Line (TBL) is currently being built in order to prove the efficiency and the reliability of the RF power production with the lowest level of particle losses. As the beam propagates along the line, its energy spread grows up to 60%. For instrumentation, this unusual characteristic implies the development of new and innovative techniques. One of the most important tasks is to measure the beam energy spread with a fast time resolution. The detector must be able to detect the energy transient due to beam loading in the decelerating structures (nanosecond) but should also be capable to measure bunch-to-bunch fluctuations (12 GHz). This paper presents the design of the spectrometer line detectors.

CTF3 TEST BEAM LINE

CLIC Test Facility 3 (CTF3) [1] is an electron accelerator test facility at CERN, built by an international collaboration, in order to test CLIC technology [2]. The first part of the machine generates a high current beam (almost 30 A for 140 ns pulse length and bunched at 12GHz), which is transported to the CLIC EXperimental area (CLEX). One of the CLIC crucial issues is the reliability and efficiency of the RF power production. This is addressed in CLEX in the Test Beam Line (TBL) [3]. Built in stages, with a first Power Extraction and Transfer Structure (PETS) module installed in 2009, the TBL will experimentally characterize the stability of the drive beam during the deceleration.

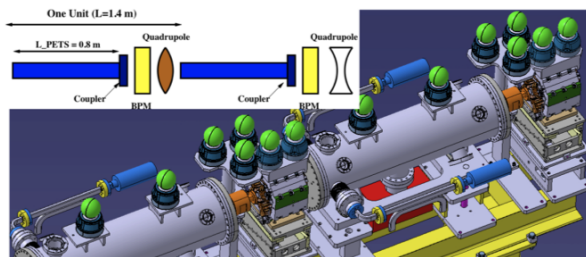


Figure 1: Schematic view of a typical TBL girder containing two PETS modules, 2 BPMs and 2 quadrupole magnets.

In its final form, the TBL will be composed of sixteen identical modules. Each module will consist of a 0.8 m PETS with a coupler, a beam position monitor (BPM) and a quadrupole on a precision movable support, see Fig. 1. The 28 A beam from CTF3 is decelerated by about 5 MeV

in each PETS, producing about 150 MW of 12 GHz power. Due to transient effects during the filling time of the PETS, the first 3 ns of the bunch train will have a huge energy spread from the initial energy down to the final energy of the decelerated beam, see Fig. 2. Time-resolved spectrometry is therefore an essential beam diagnostics tool in order to measure the beam energy spectrum after deceleration.

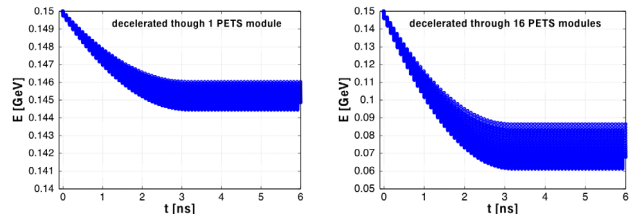


Figure 2: Time resolved energy distribution of decelerated beam after 1 PETS module (left) and 16 PETS modules (right), for the first 6 ns of the 140 ns pulse train.

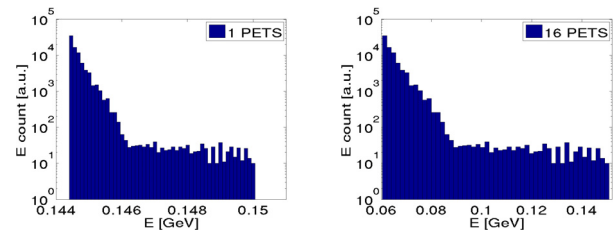


Figure 3: Histogram of the final energy distribution of a 140 ns pulse train after deceleration through 1 PETS module (left) and 16 PETS modules (right).

This paper presents the time resolved spectrometer design for the TBL.

TIME RESOLVED SPECTROMETRY

The spectrometer under design (see Fig. 4), will consist of a bending magnet, which provides an energy dependent horizontal deflection to the electrons, followed by an optical transition radiation (OTR) screen [4] observed by a CCD camera to provide a high spatial resolution profile measurement and then lastly a novel segmented beam dump for the time resolved energy measurement.

The segmented dump is a device composed of parallel metallic plates designed to stop the incident particles. By measuring the deposited charge in each segment, the beam profile can be reconstructed. The material and the dimension of the segments must be optimized depending on the beam parameters, in particular the energy and the expected energy spread. The segments need to be long enough to stop the primary particles. On the other hand the segment thickness must be chosen to optimize the

INVESTIGATION OF EXTREMELY SHORT BEAM LONGITUDINAL MEASUREMENT WITH A STREAK CAMERA

C.A. Thomas*, I. Martin, G. Rehm, Diamond Light Source, Oxfordshire, UK

Abstract

During normal operation of synchrotron third generation light sources like Diamond, the measurement of the electron bunch profile, of the order of 10 ps, is perfectly done with a streak camera. However, in 'low alpha' operation, the shorter bunch length becomes extremely close to the resolution of the camera. In such a case, performing a good measurement and extracting the real information requires a good knowledge of the impulse response of the streak camera. We present analysis and measurement of the contributions to the point spread function (PSF) of the streak camera. The first contribution is the static PSF and is obtained by measuring a focussed beam without any sweep. The second contribution is the dynamic PSF, which is due to a chirp introduced by refractive optics. For pulse with large spectral bandwidth the dynamic PSF can be larger than 5 ps.

INTRODUCTION

Third generation synchrotron light sources are characterised by low emittance, small beam size, but also short bunch lengths. At Diamond we have been carrying out tests in the so-called low alpha mode, reducing the momentum compaction factor by up to a factor of 250, which gives a smallest theoretical bunch length of 0.7 ps, 15 times smaller than our 10.8 ps nominal bunch duration [1]. Measuring the real profile of such a short pulse is challenging. At Diamond, to measure bunch longitudinal profiles and length, we measure synchrotron radiation (SR) pulses with a dual sweep streak camera (SC) with a synchroscan at 250 MHz from Optronis GmbH. The manufacturer's specification of the camera gives 2 ps for the resolution with Rayleigh criterion and monochromatic light. This provides a good resolution for the normal operation mode of the camera but leads to extremely challenging measurement in low alpha mode.

We present measurement of the instrumental response of the streak camera that is decomposed into a static and dynamic response. The static response is measured as the point spread function of the image of a focussed photon beam on the SC, with no sweep from the electrodes. The dynamic response, as observed by previous authors [2, 3, 4], is the additional pulse lengthening measured while sweeping the electrodes of the SC, due to the dispersion in material traversed by the pulse. The decomposition of the PSF is firstly evidenced by means of spectral filters, and then measured with introduction of a spectrograph in the focussing optics of the SC.

*cyrille.thomas@diamond.ac.uk

STREAK CAMERA RESOLUTION

The SC is composed of a photocathode, a streak tube in which the electrons undergo a longitudinal constant accelerating voltage, and then a transverse varying high voltage from two sweep electrode pairs. The images are obtained by a phosphor screen, coupled to a multi channel plate (MCP) and a CCD camera [5]. The best probe of the resolution is to measure known short pulses. Measurement of broadband synchrotron light pulses in low alpha mode allows to evidence not only the static PSF, but also the dynamic PSF induced by group velocity dispersion of optical materials.

Electron Bunch Length in Storage Rings

In storage rings, the r.m.s length of small charge bunches is proportional to the relative energy spread of the relativistic electrons, σ_ϵ , to the momentum compaction factor, α_c , and inversely proportional to the synchrotron frequency, f_s . The expression governing the bunch length at very low charge is given (in s) by:

$$\sigma_{bunch} = \frac{\alpha}{2\pi f_s} \sigma_\epsilon \quad (1)$$

For the Diamond storage ring in normal operation we have $\alpha = 1.7 \cdot 10^{-4}$, $f_s = 2.5$ kHz, and $\sigma_\epsilon = 10^{-3}$, which make the bunch length $\sigma_{bunch} \approx 10.8$ ps. In the low alpha mode reported here, we had $\alpha = 10^{-5}$, $f_s = 0.6$ kHz, and $\sigma_\epsilon = 10^{-3}$, which make the bunch length $\sigma_{bunch} \approx 2.6$ ps.

Setup and Measurements

Bunch length is measured with the SC using the visible part of the SR from a bending magnet. The spectrum from the diagnostics beamline is selected by the mirrors of the transport line and the vacuum-air sapphire window. It ranges from 200 nm to over 800 nm. Further filtering by UV absorption is introduced by the BK7 focussing lens.

In the low alpha mode operation the measurements of the electron bunch length were performed with white beam and with a series of spectral filters at the same current.

Preliminary, the static PSF has been measured for the white beam and also with 10 nm bandwidth filters at 490 nm and 560 nm, and with a 400-450 nm bandpass filter. As the static PSF is measured in pixels, it translates to a resolution in ps with the sweep unit scale calibration factor (0.1863, 0.3137 and 0.6374 ps/pixel for the 15, 25 and 50 ps/mm sweep speeds respectively). The results are reported in table 1. The smaller resolution, around 7.33 pixel, is for the narrow bandwidth filter at 560 nm. In all other cases, the PSF is larger at 10 pixels and even 11.66 pixels for the

A COMPACT SINGLE SHOT ELECTRO-OPTICAL BUNCH LENGTH MONITOR FOR THE SwissFEL

B. Steffen*, V. Schlott, PSI, Villigen, Switzerland
 F. Müller, PSI, Villigen and IAP Univ. Bern, Bern, Switzerland

Abstract

The knowledge and control of electron bunch lengths is one of the key diagnostics in XFEL accelerators to reach the desired peak current in the electron beam. A compact electro-optical monitor was designed and build for bunch length measurements at the SwissFEL. It is based on a mode locked ytterbium fiber laser probing the field-induced birefringence in an electro-optically active crystal (GaP) with a chirped laser pulse. The setup allows the direct time resolved single-shot measurement of the Coulomb field (THz-radiation) of the electron beam - and therefore the bunch length - with an accuracy as good as 200 fs. Simulations of the signals expected at the SwissFEL will be presented.

INTRODUCTION

Paul Scherrer Institut is planning a free electron laser for X-Ray wavelengths, the SwissFEL. The baseline design foresees to generate electron bunches with a charge between 200 and 10 pC and bunch lengths between 10 ps and a few fs. These bunches will be accelerated in a normalconducting linear accelerator (linac) to a particle energy of up to 6 GeV to radiate coherently at wavelengths between 0.1 and 7 nm in one of the two undulators. To test the feasibility of novel accelerator concepts and components needed for the generation of such high-brightness beams, their longitudinal compression and the preservation of the emittance, a 250 MeV Injector is currently being assembled at PSI (see Fig. 2).

Precise measurements of the temporal profile of extremely short electron bunches are indispensable for a detailed understanding of the bunch compression and lasing mechanisms in a FEL. Single-shot electro-optical (EO) detection techniques are ideally suited for this purpose since they are non-destructive and can be carried out during regular operation of the free-electron laser for user experiments [1, 2]. An important aspect is that they permit correlation studies between the measured time profile of electron bunches and other measured beam parameters as well as the properties of FEL pulses produced by the same bunch. A second technique for the single-shot direct visualization of longitudinal electron bunch profiles are transverse-deflecting structures (TDS) [3]. The TDS converts the temporal profile of the electron bunch charge density into a transverse streak on a view screen by a rapidly varying electromagnetic field. The measurement with the TDS of-

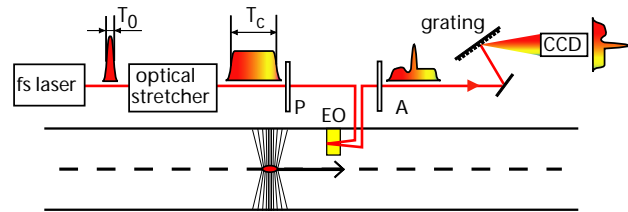


Figure 1: Schematic drawing of a spectrally encoded electro-optical detection setup. P: polarizer; EO: EO crystal; A: analyzer.

fers the highest resolution but is inherently destructive, so it cannot be used as an online monitor of the bunch length.

EO BUNCH LENGTH DETECTION

When a relativistic picosecond duration bunch passes within a few millimeters of an electro-optic crystal, its transient electric field is equivalent to a half-cycle THz pulse impinging on the crystal. The temporal profile of this equivalent half-cycle THz pulse provides a faithful image of the longitudinal charge distribution inside the electron bunch if the electrons are highly relativistic. The transient electric field induces birefringence in the electro-optic crystal. As the electric field propagates through the crystal, the birefringent properties of the crystal also propagate. This birefringence can be probed by a copropagating optical laser pulse [2].

Several variants of EO bunch diagnostics have been applied in electron bunch diagnostics [4, 5, 6], all sharing the underlying principle of utilizing the field-induced birefringence in an electro-optic crystal to convert the time profile of a bunch into a spectral, temporal, or spatial intensity modulation of a probe laser pulse.

THE COMPACT EO MONITOR

The presented compact EO bunch length monitor utilizes the spectral decoding technique, where the bunch shape information is encoded into a chirped laser pulse and then retrieved from its modulated spectrum using the known relationship between wavelength and longitudinal (temporal) position in laser pulse.

The chirped laser pulse passes through the polarizer and the EO crystal in the beam pipe, where the polarization becomes elliptical. The ellipticity of the polarization is proportional to the electric field of the electron bunch and has the same temporal structure. The analyzer, a combination

* email: bernd.steffen@psi.ch

TOWARDS AN ULTRA-STABLE REFERENCE DISTRIBUTION FOR THE NEW PSI 250 MeV INJECTOR

S. Hunziker[#], V. Schlott, Paul Scherrer Institut, CH-5232 Villigen, Switzerland

Abstract

The PSI 250 MeV Injector, a precursor to the SwissFEL, with its extreme jitter and stability demands poses new challenges for the synchronization system. Our concept is double-tracked: low risk electrical and best potential performance and flexibility optical. The electrical distribution system, being established first, relies on reliable technology. Optimized to achieve a benchmark jitter performance of around 10 fs and a long term drift stability of some 10 fs in the most critical parts of the machine it will also backup the optical system. Sub 10 fs jitter and drift figures are being aspired for the latter. In this contribution, both system designs are presented, expected and first measured electrical and optical reference signal jitter and long term cable and coupler drifts are presented. A cable temperature stabilization system is discussed, too. Finally, a first jitter measurement of the optical master oscillator (OMO) laser will be presented.

INTRODUCTION

The 250 MeV Injector will be ≈ 65 m long and basically consist of an electron gun (with photocathode), S-band structures, an X-band structure and a bunch compressor as depicted in Fig. 1. These structures are driven by RF signals, which are synchronized to the distributed reference signal. Other “customers” of the reference distribution system are e.g. photocathode laser, timing system, diagnostics in general. The building is ready, first installations are being done now (Spring 2009). The reference distribution is one of the key challenges. Extremely tight timing jitter requirements demand for solutions on the edge of technical feasibility. On the other hand cost and reliability issues have to be considered. Both distribution concepts, the electrical and the optical one, are sketched in Fig. 2.

ELECTRICAL REFERENCE DISTRIBUTION

Architecture

The coaxial cable based baseline system consists of:

- Low phase-noise 214.14 MHz RF master oscillator (RF MO), will be ready by June 2009.
- RF power amplifier ($P_{out} > 37$ dBm) providing required signal levels at the terminals (points where the reference signal is needed) reference inputs.
- Directional couplers, feeding and decoupling reference inputs of the various terminals, e.g. PLO (=phase locked oscillator for 1.5, 3.0 and 12 GHz) reference inputs, located along a trunk line.

Active subsystems are supplied with ultra-low noise linear power supplies.

Drift, Temperature Stabilization, RF MO

Multiple coaxial cables form the trunk line within the accelerator tunnel (depicted in red in Fig. 2). They are guided within a thermally isolated pipe, which is supplied with a temperature controlled heater cable (Fig. 3). The pipe is supported with hard foam plates on cable trays and periodically furnished with temperature sensors. Various cables (basically 3/8” and 7/8” coax, which are relatively inexpensive) are installed in parallel, offering the possibility to find the one with lowest drift after installation by optimizing the temperature within the pipe. It has been found that the temperature stability as well as the optimum operating temperature for minimum drift of low loss corrugated coaxial cables may strongly vary from production lot to production lot, which requires flexibility and redundancy during installation.

The measured temperature stability of various cables is listed in Table 1.

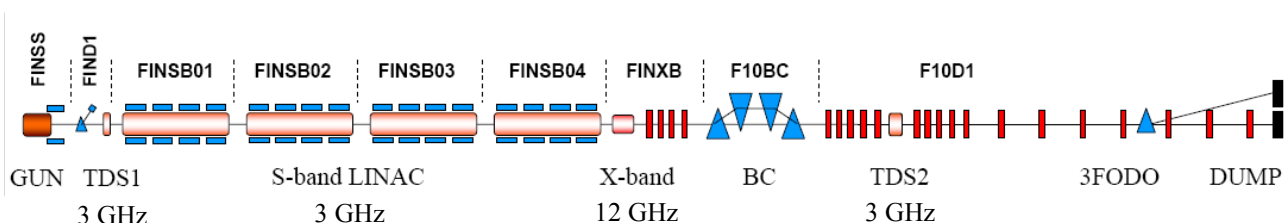


Figure 1: Simplified layout drawing of the PSI 250 MeV Injector [1].

[#]stephan.hunziker@psi.ch

ON THE LIMITATIONS OF LONGITUDINAL PHASE SPACE MEASUREMENTS USING A TRANSVERSE DEFLECTING STRUCTURE

C. Behrens* and C. Gerth,
Deutsches Elektronen-Synchrotron DESY, D-22603 Hamburg, Germany

Abstract

High-brightness electron bunches with low energy spread, small emittance and high peak currents are the basis for the operation of high-gain Free-Electron Lasers (FELs). As only part of the longitudinally compressed bunches contributes to the lasing process, time-resolved measurements of the bunch parameters are essential for the optimisation and operation of the FEL. Transverse deflecting structures (TDS) have been proven to be powerful tools for time-resolved measurements. Operated in combination with a magnetic energy spectrometer, the measurements of the longitudinal phase space can be accomplished. Especially in case of ultra-short electron bunches with high peak currents for which a time resolution on the order of 10 fs would be desirable, both the TDS and magnetic energy spectrometer have intrinsic limitations on the attainable resolution. In this paper, we discuss the fundamental limitations on both the time and energy resolution, and the relation between them.

INTRODUCTION

Recently developed Free-Electron Lasers for the generation of photons in the extreme ultraviolet and soft X-ray regime are based on an exponential gain of the radiation power in a single pass through a long undulator magnet system. These high-gain FELs put stringent demands on the electron bunch parameters. In order to initiate the lasing process and to reach power saturation in reasonable undulator lengths, a high charge density which is related to the peak current, a low energy spread, and a small emittance is mandatory.

Projected measurements of the electron bunch parameters are not sufficient to understand and to control the lasing process. For this reason, sliced electron bunch measurements are essential, which can be accomplished by Transverse Deflecting Structures (TDS). In combination with a magnetic energy spectrometer, the longitudinal phase space can be investigated.

In order to get the most information concerning the lasing process, the measurements may be carried out in front of the undulators. This is very challenging since the electron bunches are, in particular in front of the undulators, very short with bunch lengths in the femtosecond range and peak currents on the order of kiloampere.

GENERIC BEAMLINE LAYOUT

An experimental layout for sliced beam parameter measurements is presented schematically in Fig. 1. The entire beamline is equipped with quadrupole magnets to ensure the required optics for standard machine operation as well as for dedicated sliced beam parameter measurements. For operation without affecting the entire bunch train, e.g. bunch profile measurements, a fast kicker can be used to pick out individual bunches for off-axis screen operation. The magnetic energy spectrometer consists of at least one dipole magnet, followed by a drift section for building up dispersion.

Further requirements are imaging screens, e.g. OTR-screens or scintillators, and optical camera systems providing high spatial resolutions.

ACCELERATOR OPTICS

In order to obtain desired time¹ and energy resolutions, the accelerator optics has to be designed and adapted according to the following considerations.

In linear beam dynamics, the general transverse motion of charged particles can be described as combination of betatron motion and dispersion trajectory. The deflection plane of the energy spectrometer is assumed to be in the horizontal, e.g. the x-plane. The horizontal particle motion is then given by

$$x(s) = x_{\beta}(s) + D_x(s) \cdot \delta, \quad (1)$$

with the horizontal betatron motion $x_{\beta}(s)$, horizontal dispersion function $D_x(s)$, and relative momentum deviation δ . After passing the magnetic energy spectrometer, the horizontal rms beam size at screen location s_1 can be expressed by $\sigma_x = \sqrt{\sigma_{x_{\beta}}^2 + D_x^2 \cdot \sigma_{\delta}^2}$. In order to achieve energy resolutions on the order of σ_{δ} , the beam size due to dispersion and energy spread has to be larger than the natural rms beam size $\sigma_{x_{\beta}} = \sqrt{\epsilon_x \cdot \beta_x}$. This condition yields

$$D_x(s_1) \cdot \sigma_{\delta} > \sqrt{\epsilon_x \cdot \beta_x(s_1)}, \quad (2)$$

with the horizontal geometric emittance ϵ_x and beta function β_x . The reachable energy resolution is then given by

$$\sigma_{\delta} > \sqrt{\epsilon_x} \cdot \frac{\sqrt{\beta_x(s_1)}}{D_x(s_1)}. \quad (3)$$

¹The time resolution expresses the resolution of the longitudinal coordinate ζ within the bunch. The relation is given by $t = \zeta/c$.

* christopher.behrens@desy.de

TEMPORAL PROFILES OF THE COHERENT TRANSITION RADIATION MEASURED AT FLASH WITH ELECTRO-OPTIC SPECTRAL DECODING

V. Arsov^{1*}, M-K. Bock, M. Felber, P. Gessler, K. Hacker, F. Loehl², F. Ludwig, K.-H. Matthiesen, H. Schlarb, A. Winter³, DESY-Hamburg, Germany
S. Schulz, L. Wißmann, J. Zemella, Hamburg University, Germany

Abstract

We present absolute electric field time-profiles measured on the coherent transition radiation (CTR) beamline at FLASH using electro-optic spectral decoding (EOSD) in near crossed-polarizers scheme with a (20-200) μm thick GaP crystal in vacuum. The CTR spectrum is in the range 200 GHz - 100 THz and the pulse energy in the focus is over 10 μJ . The measured narrow CTR temporal profiles in the range 400 - 500 fs FWHM demonstrate that the short THz-pulses emitted by the compressed electron bunches are transported through the 19 m long beam line without significant temporal broadening.

INTRODUCTION

The reliable operation of the ultraviolet and x-ray free electron lasers require precise and non-destructive measurement of the electron bunch structure in the sub-100 fs scale. Recent numerical [1] and experimental [2], [3] works reveal the potential of the electro-optic detectors for such time-profile monitors. For even shorter, sub-10 fs structures, spectroscopy of coherent transition radiation (CTR) offers an alternative, although not allowing direct reconstruction of the longitudinal profile. For such diagnostic purposes 200 GHz - 100 THz broadband CTR beamline is constructed and characterized [4]. The ability of the CTR beamline at FLASH to preserve the narrow CTR pulses was first demonstrated using electro-optic balanced detection with 0.5 mm thick ZnTe crystal in air [5], followed by measurements with the same crystal in vacuum in near crossed-polarizers scheme [6]. To fully utilize the resolution of the electro-optic spectral decoding method, thinner crystals with better optical properties, such as GaP should be used. In this paper, we report electro-optic spectral decoding measurements at the CTR beamline of FLASH using a (20-200) μm wedge GaP crystal in vacuum.

EXPERIMENTAL SETUP

The setup for measurement of the CTR electric field temporal profiles is shown in Fig. 1.

The CTR beamline is installed in the straight section between the last accelerating module and the undulator at the 140 m of FLASH. The generation and transport of the ultrabroadband CTR radiation in the range of 200 GHz - 100 THz with energies more than 10 μJ is described

thoroughly in [4]. The CTR is produced by kicking of a single bunch from a pulse train on an off-axis screen, inclined at 45° with respect to the accelerator axis. The 18.7 m long beam line is designed specially to minimize diffraction and to avoid waveguide effects, by using focusing mirrors and corrugated bellows. The pressure in the beamline is below 0.1 mbar and is isolated from the accelerator vacuum by a wedge diamond window.

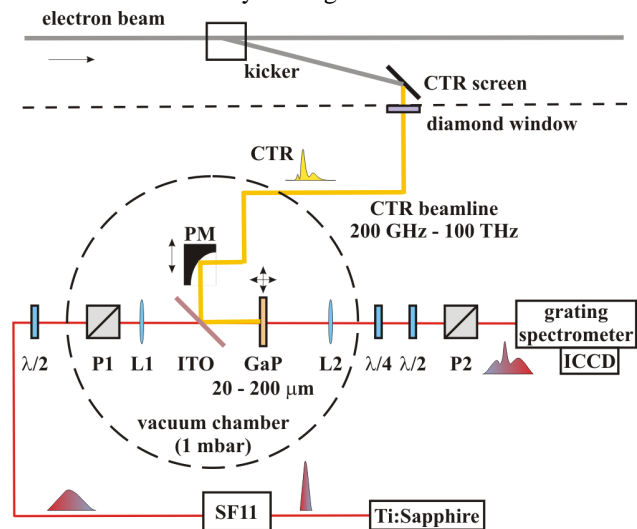


Figure 1: Schematic layout of the setup for EO detection of coherent transition radiation (CTR) transported from the linac to the laboratory through a 19 m beamline.

In a laboratory outside the linac tunnel, the beamline ends in a large vacuum vessel hosting several diagnostic experiments, taking full advantage of the broad band THz spectrum - interferometric, spectroscopic and electro-optic (EO).

The principles of single-shot electric field profile measurements using EO techniques is described in [3]. In this experiment, we apply the spectral decoding method. A $\tau_0 = 16$ fs (Fourier-limited) pulse from a commercial Ti:Sapphire oscillator (Micra-5 from Coherent) is linearly chirped in a 10 cm long glass block (SF11) to $\tau_c \approx 5$ ps. The EO signal broadening, imposed by the chirp is $\sqrt{\tau_0 \cdot \tau_c} \approx 280$ fs. The laser center wavelength is 800 nm, the bandwidth 60 nm and the repetition rate 81 MHz. The typical output power of the laser is 500 mW.

Except for the first polarizer P1 and the lenses for the crystal, all other elements are placed on the same optical table. Shortly before the entrance port of the vacuum chamber, there is a half-wave plate, which in combination with the first polarizer P1 serves as a power attenuator. The energy on the EO the crystal is 2.5 nJ. The EO crystal

¹ now at PSI, Villigen, Switzerland

² now at Cornell University, USA

³ now at ITER, Cadarache, France

*vladimir.arsov@psi.ch

BEAM POSITION MEASUREMENT WITH SUB-MICRON RESOLUTION

B. Keil, Paul Scherrer Institut, 5232 Villigen PSI, Switzerland

Abstract

This paper gives an overview of transverse sub-micron beam position measurement systems and techniques for 3rd and 4th generation light sources and collider projects. Topics discussed include mechanical, electrical, and digital design aspects, environmental influences, machine operation and design considerations, as well as system- and beam-based measurement and calibration techniques.

INTRODUCTION

Beam position measurement (BPM) systems belong to the most vital instrumentation systems of particle accelerators. The following sections discuss selected aspects of high-resolution BPMs, with a focus on the requirements of linac-based 4th generation (4G) FEL light sources in comparison to 3rd generation (3G) ring accelerators. However, due to the large technological overlap between light sources and colliders, most BPM-related topics are equally relevant for both accelerator types. The scope of the discussion in the following sections is limited to RF BPMs and does not cover the large variety of alternative beam position measurement techniques like mechanical or laser wires, screens, photon detectors, residual gas, beam loss or halo detectors.

REQUIREMENTS AND APPLICATIONS

Beam Stability

The main objective of submicron resolution BPMs in 3G light sources is the measurement of the electron beam position at the photon beam line source points. Typical photon beam stability requirements for experiments at the beam line end stations translate into $\sigma/10$ position and/or $\sigma'/10$ angular stability of the electron beam at the source point. Due to a typical emittance coupling in the order of 1% or less, the vertical beam stability is usually at least an order of magnitude more critical than the horizontal one. Vertical electron beam sizes of 2-5 μm in low-beta insertion devices of modern low-emittance storage rings result in position stability requirements of a few 100nm.

Electron beam movements significantly below $\sim 100\text{Hz}$ may be directly visible as an undesired modulation in the time structure of the recorded experimental data of photon beam line end stations. Movements at much higher frequencies are often averaged out by the experiment and are thus perceived as an effective increase of the electron beam emittance, with an accordingly reduced effective photon beam brilliance.

The required electron beam stability in 3G light sources is usually ensured by a fast orbit feedback (FOFB) system that measures and corrects the beam positions with sufficiently fast BPM electronics and corrector (dipole) magnets. Typical FOFB systems apply corrections at a rate of several kHz, with overall feedback loop latencies

in the order of some 100 μs to 1ms. This allows suppression of perturbations due to e.g. mechanical magnet vibrations, power supply noise, or changing insertion device gaps. Most FOFB systems suppress perturbations up to a cut-off frequency in the order of 100-200Hz [1].

BPM requirements for 3G storage rings are primarily driven by FOFB systems, since BPM electronics noise and drift as well as movements of BPM pickup mechanics are modulated back onto the beam or even amplified by the feedback loop if they exceed its cut-off frequency. Noise and drift of the BPM system within the FOFB bandwidth of some 100Hz should therefore be lower than the desired beam stability of typically some 100nm.

In contrast to 3G ring accelerators with continuously circulating bunches and typical bunch spacings of a few ns, 4G linac-based light sources often operate in single-bunch mode, at typical bunch repetition rates of 10-100Hz. This limits the cut-off frequency of beam-based transverse feedback systems to about 1-10Hz, thus not allowing to suppress perturbations induced e.g. by girder vibrations or power supply noise in the order of some 10Hz. Consequently, such 4G accelerators must be inherently stable and need a very careful design of mechanical and electrical subsystems in order to achieve sufficient beam stability. Therefore, the BPM requirements of 4G accelerators are not primarily driven by the requirements of fast feedbacks: Their BPMs only allow to observe fast perturbations and to identify their sources, but not their active suppression.

An exception are 4G linear or re-circulating energy recovery accelerators with bunch repetition rates above $\sim 1\text{kHz}$ that may operate in CW mode, or superconducting pulsed accelerators with long accelerating RF pulses like ILC or the European X-Ray FEL (E-XFEL) where trains of several 1000 bunches with 200ns bunch spacing and $\sim 10\text{Hz}$ repetition rate allow the implementation of intra bunch train feedback systems [2] with sub-microsecond latency that are able to suppress perturbations from DC up to a cut-off frequency in the order of 100kHz.

4G hard X-Ray FEL accelerators typically have round beams with $\sigma \sim 30\text{-}40\mu\text{m}$ in the undulators, while modern 3G accelerators with usual emittance couplings of 0.1-1% have flat beams with typically 2-5 μm vertical size and at least an order of magnitude larger horizontal size. Thus, the absolute transverse stability requirements of 4G accelerators in both planes are similar to the horizontal plane in 3G rings and relaxed compared to the vertical plane in 3G rings. However, future 4G SASE FELs might operate at very low emittance and bunch charge ($\sim 10\text{pC}$ or less) in order to lase in single-spike mode with beam sizes below 10 μm in the undulators [3], thus converging towards the vertical stability requirements of 3G rings.

CAVITY BPM DESIGNS, RELATED ELECTRONICS AND MEASURED PERFORMANCES

D. Lipka*, DESY, Hamburg, Germany

Abstract

Future accelerators like the International Linear Collider and Free-Electron Lasers require beam position measurements with submicron resolution in critical parts of the machines. This is achievable using the Cavity Beam Position Monitors (BPM). This paper presents the basic principles of this monitor type. Different institutes are working on the design of cavity BPM systems. An overview of recent developments with results and limitations is given.

INTRODUCTION

The international linear collider (ILC) will require high performance beam position monitors (BPM) to control the beam trajectory with high precision in order to maintain a stable collision of nanometer sized beams. The BPMs have to be located at specific positions along the linac up to the interaction point, where a few nanometer resolution is required. Additionally a spectrometer will be used in order to measure the beam energy. The spatial beam offset corresponds directly to the beam energy. To minimize the influence to the emittance the offset has to be small, therefore high precision BPMs are required for the ILC spectrometer with a resolution of 500 nm or better [1].

In case of Free-Electron Lasers (FEL) the overlap of the electron beam with the photon beam along the undulators less than 10% of the transverse size is required. Typical transverse sizes of beams are of the order of 30 μm . Therefore a resolution better than 1 μm is required.

In comparison to other types of BPMs, like e.g. the button [2] or stripline [3] BPM, only the cavity BPM has the potential to achieve such high resolutions on a bunch by bunch time-scale. In this paper the cavity BPM principle is discussed, followed by the description of the electronics, resolution limitations and measurement methods. A few examples of such BPMs are presented.

THEORY OF CYLINDRICAL CAVITY BPMs

Electric Fields

The electric field \mathbf{E} of a cavity can be derived from the d'Alembert equation

$$\Delta \mathbf{E} - \frac{1}{c^2} \frac{\delta^2 \mathbf{E}}{\delta t^2} = 0 \quad (1)$$

with c being the speed of light. For a cavity with radius R and length L only the z component is of interest. The

solution can be represented as

$$E_{z,mnp}(r, \phi, z, t) = C J_m \left(\frac{j_{mn} r}{R} \right) \cos(m\phi) e^{-i(\omega_{mnp} t \mp \frac{p\pi z}{L})}. \quad (2)$$

Here j_{mn} denotes the n -th zero of the Bessel function J_m of order m and

$$\omega_{mnp} = c \sqrt{\left(\frac{j_{mn}}{R} \right)^2 + \left(\frac{p\pi}{L} \right)^2} \quad (3)$$

is the angular resonant frequency of the mode mnp . The two first modes have $j_{01} = 2.405$ and $j_{11} = 3.832$ [4]. The first mode (monopole mode, TM_{010}) does not depend on the spatial component ϕ , therefore a cylinder symmetric mode is generated, as shown in Fig. 1. The Bessel func-

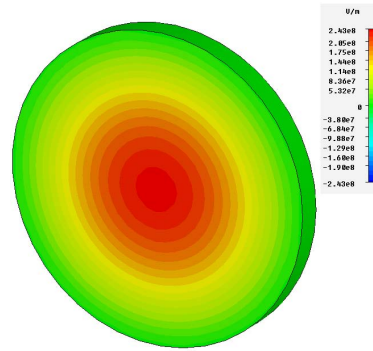


Figure 1: Field distribution of the first monopole mode in a cylindrical resonator. Simulation [5] is used.

tion of the order $m = 0$ does not depend of the radius r close to the cavity center. Therefore the field strength is proportional to the beam charge. The second mode (dipole mode, TM_{110}) depends on ϕ resulting in a field distribution as shown in Fig. 2. For a beam passing close to the cavity center the Bessel function of order $m = 1$ can be derived proportional to r . For that reason the field strength is proportional to the beam offset and charge.

Nowadays cylindrical cavities can be produced with very high accuracy. Therefore by measuring the field strength of the dipole mode a high resolution of the position information can be obtained.

Line Voltage

The normalized shunt impedance

$$\frac{R}{Q} = \frac{V^2}{\omega W} \quad (4)$$

* dirk.lipka@desy.de

LCLS CAVITY BEAM POSITION MONITORS*

S. Smith, S. Hoobler, R.G. Johnson, T. Straumann, A. Young,
 SLAC National Accelerator Laboratory, Menlo Park, CA 94025, U.S.A.
 R.M. Lill, L.H. Morrison, E. Norum, N. Sereno, G.J. Waldschmidt, D. Walters,
 Argonne National Laboratory, Argonne, IL 60439, U.S.A.

Abstract

The Linac Coherent Light Source (LCLS) is a free-electron laser (FEL) at SLAC producing coherent 1.5 Å x-rays. This requires precise, stable alignment of the electron and photon beams in the undulator. We describe the beam position monitor (BPM) system which allows the required alignment to be established and maintained. This X-band cavity BPM employs a TM_{010} monopole reference cavity and a single TM_{110} dipole cavity detecting both horizontal and vertical beam position. Processing electronics feature low-noise single-stage three-channel heterodyne receivers with selectable gain and a phase-locked local oscillator. Sub-micron position resolution is required for a single-bunch beam of 200 pC. We discuss the specifications, commissioning and performance of 36 installed BPMs. Single shot resolutions have been measured to be about 200 nm rms at a beam charge of 200 pC. Initial LCLS commissioning is described.

FEL COMMISSIONING

LCLS photocathode RF gun and injector systems were commissioned in 2007, followed by linac and bunch compressor systems in 2008. Beam was first taken through the undulator beamline (with no undulators installed) in December, 2008. After aligning each undulator segment individually, 21 undulator magnets were inserted in April 2009. We observed lasing at 1.5 Angstroms essentially immediately [1].

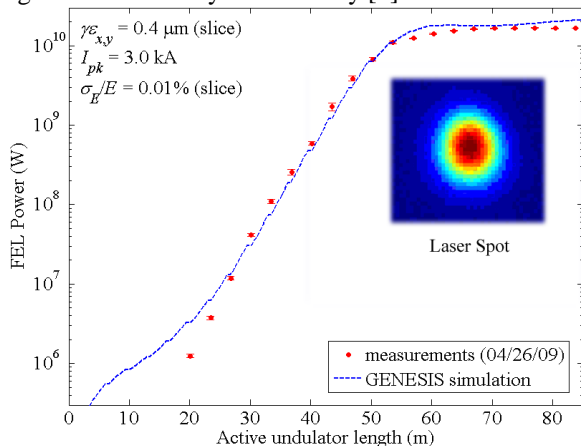


Figure 1: FEL power gain length measurement at 1.5 Å made by kicking the beam after each undulator sequentially (red points), a prediction (blue line) and the laser spot seen on a YAG screen.

*Work supported by U.S. Department of Energy under Contract Numbers DE-AC02-06CH11357 and DE-AC02-76SF00515.

02 BPMs and Beam Stability

BPM REQUIREMENTS

Laser saturation in the LCLS FEL requires the electron and photon beams be collinear in the 131 meter-long undulator to about 10% of the 37 μm rms transverse beam spot size over scales of the FEL amplitude gain length (~4m) [2,3]. BPM system requirements include centering accuracy, reproducibility, small physical size, radiation hardness, and sub-micron resolution at 200 pC.

SYSTEM DESIGN

The major subsystems for the LCLS undulator BPM system are the cavity BPM, receiver, and data acquisition components. The cavity BPM and downconverter reside in the tunnel while the analog-to-digital converters (ADC) and processing electronics are in surface buildings.

Thirty-four BPMs are installed on undulator girders while two are placed in the linac-to-undulator (LTU) transport line. The BPMs provide stable and repeatable beam position data for both planes on a pulse-to-pulse basis for up to a 120-Hz repetition rate.

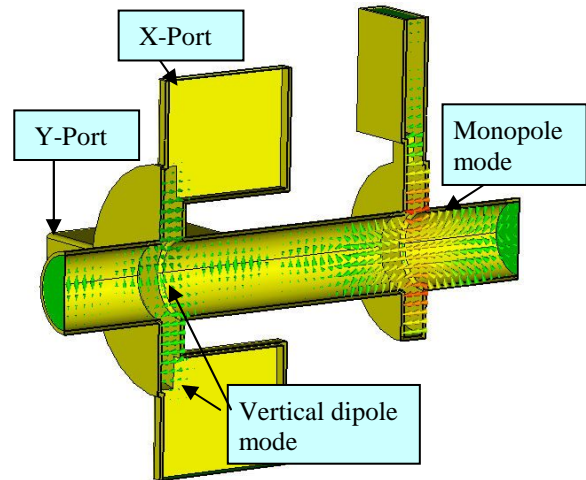


Figure 2: BPM Cavity schematic with electric fields of position (dipole) and reference (monopole) cavities.

X-Band Cavity

Figure 2 shows the electric field vectors in the cavity BPM simulated when the beam is offset[4,5]. Beam passes through the monopole reference cavity on the right, exciting the TM_{010} monopole mode signal resonant at 11.384 GHz. The TM_{110} dipole cavity is located 36 mm downstream through the 10-mm-diameter beam pipe. Monopole-dipole isolation is 130 dB, due to a below-

POSITION PICKUPS FOR THE CRYOGENIC STORAGE RING

F. Laux, M. Grieser, R. von Hahn, T. Sieber, A. Wolf, K. Blaum,
Max-Planck-Institut für Kernphysik, Heidelberg, Germany

Abstract

A cryogenic electrostatic storage ring (CSR) is under construction at the Max-Planck-Institut für Kernphysik in Heidelberg (MPI-K), which will be a unique facility for low velocity and in many cases also phase-space cooled ion beams. Amongst other experiments the cooling and storage of molecular ions in their rotational ground state is planned. To meet this demand the ring must provide a vacuum in the XHV range (10^{-13} mbar room temperature equivalent) which will be achieved by cooling the ion beam vacuum chambers to 2 - 10 K. This also provides a very low level of blackbody radiation. The projected beam current will be in the range of 1 nA - 1 μ A. The resulting low signal strengths together with the cold environment put strong demands on the amplifier electronics. We plan to make use of a resonant amplifying system. Using coils made from high purity copper, we expect quality factors of ~ 1000 . The mechanical design has to provide stability and reproducibility of the alignment despite thermal shrinking when switching from room temperature operation to cryogenic operation. A prototype pickup has been built in order to test resonant amplification and the mechanical design using the wire method. The resonant amplification principle was tested in the MPI-K's Test Storage Ring (TSR).

INTRODUCTION

The CSR will be a fully electrostatic storage ring used to store atomic and molecular ion beams [1]. The beam optics consist of quadrupoles, 6° deflectors to separate the ion beam from neutral reaction products and 39° deflectors. It will be possible to merge the ion beam with neutrals and a laser beam. The experimental straight sections contain an electron cooler and a reaction microscope for reaction dynamic investigations. One linear section is uniquely reserved for diagnostics which will contain quartz profile monitors, Schottky pickups, an ionization rest gas monitor, a sensitive squid based cryogenic current comparator and two beam position monitors [2].

For the cold supply a commercially available Linde 4.5 K helium liquefier is combined with an additional connection box assuring the adaption to the CSR's helium pipe system. To reduce blackbody radiation, a maximum temperature of 10 K of the inner vacuum chamber is required. Efficient pumping of hydrogen as the main rest gas component is necessary to reach a vacuum in the XHV range which will be achieved by cooling parts of the vacuum chamber down to 2 K. For commissioning of the ring the ability of room temperature operation is required and part of the cryogenics concept is the possibility of baking

02 BPMs and Beam Stability

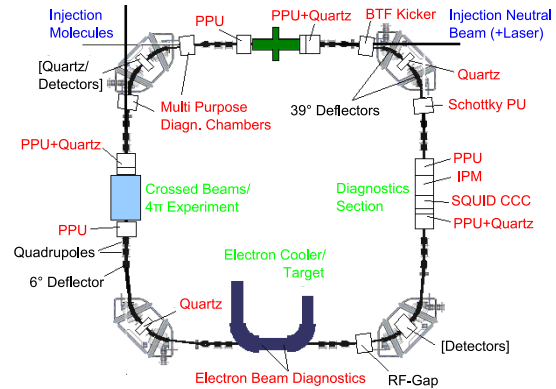


Figure 1: Overview over the CSR beam diagnostics system.

out the system to at least 300 °C. The cryogenic concept leading to the ability to reach vacua in the desired range was successfully tested with the Cryogenic Trap Facility (CTF) [3].

The extremely low temperatures, the large operational temperature range and the low pressures together with expected low signals are extremely challenging factors for the design of the storage ring components, particularly for the diagnostics equipment.

POSITION PICKUPS

Mechanical Design

In total six beam position monitors, each consisting of two pickups, are foreseen. One beam position monitor will be placed at each end of the diagnostics section as well as on both sides of the reaction microscope and of the third experimental section. The diagonal slit type linear pickups with a circular aperture will be used. The overall beam position monitor length will be ~ 35 cm and the diameter of the electrodes will be 10 cm.

The pickups themselves will be situated in a grounded shielding chamber which has two functions. Firstly, it shields the pickup plates from the cryo-pump, which is a panel made from metal and coated with charcoal to provide a large absorption area. This layer introduces extra electrical capacity and an implied unsymmetry into the system and it added up to the loss budget lowering the quality factor of the resonant circuit. Secondly, the shielding separates the actual signal from disturbing signals on the ground set up by the storage ring chambers. A provision of small holes in the chamber that shield against high frequency electric fields but improves pumping will be con-

EXPERIENCE WITH THE COMMISSIONING OF THE LIBERA BRILLIANCE BPM ELECTRONICS AT PETRA III

A. Brenger, I. Krouptchenkov, G. Kube, F. Schmidt-Föhre, K. Wittenburg, DESY, Hamburg, Germany

Abstract

PETRA III, a new 3rd generation synchrotron radiation source, is presently under commissioning at DESY. Its beam position measurement system is based on the Libera Brilliance electronics. The BPM system is used for the machine start up and development. Later on, the system will be used for the orbit monitoring and orbit feedback. This paper presents the infrastructure and features of the BPM system together with the commissioning experience of the BPM electronics.

INTRODUCTION

In 2004 DESY decided to reconstruct its storage ring PETRA II into a new 3rd generation synchrotron radiation source PETRA III [1]. After two-years upgrade, one eighth of the 2.3-kilometer long ring was completely rebuilt and equipped with 14 undulator beamlines. The remaining seven eighth were completely removed, modernized and reinstalled. The electron beam position monitor (BPM) system that was installed in PETRA II did not meet the resolution and stability requirements of PETRA III. A simple upgrade was not possible; therefore it was decided to equip PETRA III with a completely new BPM-system. The BPM pickup stations, cables, BPM read-out electronics and all related infrastructure were renewed. Installation of the BPM system began in summer 2008 and commissioning with beam started in the end of March 2009.

BEAM POSITON MONITORS AND READ-OUT ELECTRONICS

PETRA III is equipped with 227 BPMs for the orbit measurement. There are 8 different types of electrostatic button pickup stations because the vacuum system of PETRA III has various types of vacuum chamber cross sections. Commercial RF button feedthroughs from PMB and Meggitt are used as pickups for the BPM blocks. All feedthroughs were individually tested and grouped together per BPM by similar test pulse response.

The requirements for the readout electronics are quite tight for new light sources. The BPM system for PETRA III has to support the machine commissioning as well as orbit feedback and the beam position observation. All of the BPMs have to be equipped with single turn and single pass, i.e. Turn-by-Turn (TbT) capabilities with the resolution of 50...100 μm (rms) in this operation mode. For standard user operation the orbit of the stored beam has to be kept constant with high accuracy: the beam should be stabilized to 1/10th of the beam width σ . For the BPMs located near the undulators required vertical

resolution is 0.3 μm (rms), i.e. the BPM system must have very high accuracy. Additionally, position data with TbT frequency about 130 kHz and resolution not worse than 50 μm (rms) are needed for the Fast Orbit Feedback (FOFB) system. Other important requirements are the temperature drift ($\leq 0.2 \mu\text{m}/^\circ\text{C}$) and 8-hours stability (1 μm peak to peak).

Libera Brilliance BPM electronics from Instrumentation Technologies was chosen as BPM read-out electronics. This beam position processor meets all technical requirements of the BPM electronics. Additionally it is an all-in-one solution that allows simplifying the infrastructure, and therefore the reliability of the system. Liberas were successfully used at other light sources like Soleil, Diamond, Elettra and ESRF.

In the beginning, the Libera Electron version was comprehensively tested in the laboratory and during a beam test at the ESRF [2]. Later on it was estimated that the monitor signals from the buttons might be higher than allowable input signal level of the Libera Electron [3]. Libera Brilliance, the next version of the beam position processor, has different characteristics of the input RF chain and allows operating with higher input signal levels. In addition the Brilliance version has better TbT resolution, temperature drift, beam current and bunch pattern dependency. Finally it was decided to equip PETRA III with the Libera Brilliance. The functional block diagram of Libera Brilliance together with the input chain is shown in Fig. 1.

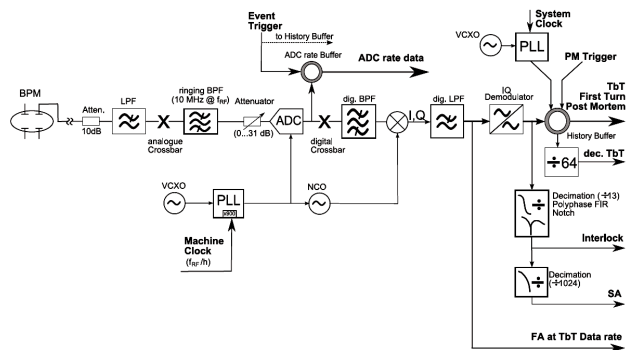


Figure 1: Functional block diagram of one channel of the Libera Brilliance BPM read-out electronics at PETRA III.

There are five data paths: ADC raw data, TbT data, decimated TbT data (factor 64), slow acquisition (SA) data for closed orbit measurement at approx. 10 Hz and fast acquisition (FA) data. External 10 dB attenuators are placed on each input in order to avoid damage of the

DUAL BEAM X-RAY BEAM POSITION MONITOR

C. Bloomer, J. Brandao-Neto, G. Rehm, C. Thomas, Diamond Light Source, Oxfordshire, UK

Abstract

Presented are the first results from the custom built I04 X-ray Beam Position Monitors at Diamond Light Source, using a single device to measure two adjacent beams in one front end. Synchrotron Light Sources are increasingly in demand by both academic and commercial users, and the number of 3rd generation light sources is growing rapidly. In order to make best use of the facilities a number of synchrotrons have adopted a scheme whereby two canted Insertion Devices occupy a single straight. Two beams are produced, separated by an angular divergence in the order of 1mRad, and both beams proceed down the same front end before being separated into two experimental hutches. This paper describes the techniques used at Diamond to accurately measure the position of both beams simultaneously with micron precision.

INTRODUCTION

A relatively new development in Synchrotron Sources is the concept of utilizing a single Insertion Device (ID) straight to produce two independent X-ray beams into two experimental stations. Such beamlines have been constructed and operated at both the APS [1], and at the ESRF [2]. At Diamond such a system has been designed and developed for the I04 Macromolecular Crystallography (MX) beamline. I04 has been operating now since January 2007 as an in-vacuum 23mm period undulator beamline, tunable over the wavelength range 0.5 - 2.5Å, to enable Multiwavelength Anomalous Diffraction (MAD) experiments to be carried out. J04 is a complimentary out of vacuum monochromatic undulator for MX fixed at 0.916Å that was installed in November 2008.

The IDs are located in the same straight, spatially separated by 1.9m and canted to produce beams separated by 0.98mRad (Fig. 1).

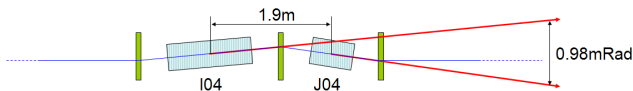


Figure 1: Schematic of I04 ID straight.

Both beams pass down the same front end and enter the first optics hutch where a beam splitter separates the beams further into two separate experimental cabins. This technique saves space within the synchrotron and allows more experiments to be performed for lower additional cost.

02 BPMs and Beam Stability

Each beam is capable of being independently tuned by altering each ID gap without the neighboring beam being affected. We verify this by observing the behavior of the electron orbit as the gap changes.

BEAM POSITION MEASUREMENTS

Traditional tungsten blade X-ray Beam Position Monitors (XBPMs) are capable of making sub-micron precision measurements of the position of a single beam. Four negatively biased blades intercept the edges of the X-ray beam (Fig. 2, left) and photons striking the surface of the blades liberate electrons. A low current monitor detects this loss of electrons as a current, and using the difference-over-sum method [3] one can deduce the position of the centre of the beam.

The four blade device is an elegant solution to the problem of accurately resolving beam positions, but unfortunately the system only works when dealing with a simple near-Gaussian beam distribution. Trying to resolve the centre of none-Gaussian distributions, such as that from a Helical Undulator, is much harder [4], and trying to resolve the distribution formed by two beams (Fig. 2, right) is impossible. Other Light Sources do not even attempt to measure the beam position in the front end in these circumstances.

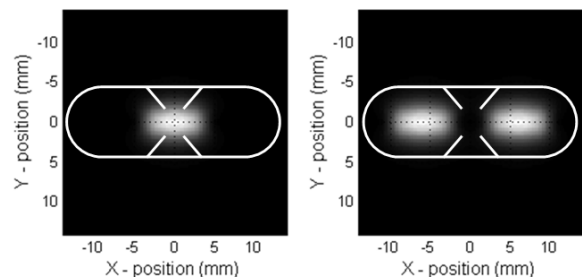


Figure 2: A standard four blade XBPM with the light from a normal ID (left) and light from two canted IDs (right). In this example the light from the two canted IDs has been normalised so they are of equal intensity.

EIGHT BLADED XBPM

However, a new XBPM designed and built as part of a collaboration between Diamond Light Source and FMB is capable of making sub-micron precision position measurements of both beams independently. Two sets of four blades are arranged within a single device using two blade holders (Fig. 3, Fig. 4). The two sets of four are treated

IMPROVEMENT OF THE FAST ORBIT CORRECTION ON THE ESRF STORAGE RING

E. Plouviez, L. Farvacque, J.M. Koch, J.L. Pons, F. Uberto, ESRF, Grenoble, France

Abstract

Until the end of 2008, the suppression of the closed orbit distortion on the storage ring of the ESRF was obtained using two separate systems: A slow system using 224 BPM and 96 correctors performing a correction every 30 seconds with a bandwidth of $1.5 \cdot 10^{-2}$ Hz, and a fast system, using only 32 BPMs and 32 correctors but working at 4.4 KHz, damping the orbit distortion from $5 \cdot 10^{-2}$ Hz up to 150 Hz; the $1.5 \cdot 10^{-2}$ Hz to $5 \cdot 10^{-2}$ Hz frequency span was left uncorrected [1].

This separation of the frequency range of the two systems by a dead frequency span avoided cross talks between them, but prevented the efficient cancellation of the very low frequency orbit distortions caused by the frequent modification of the insertion device (IDs) settings required by the beamlines operation. We found a way to coordinate the operation of the slow and fast systems in order to suppress this dead frequency span. This paper describes the principle and the beneficial effect of this new scheme, and its limitations. To overcome these limitations, we are now developing a single new orbit correction system that will damp the orbit distortion from DC to 150 Hz; this system will use the Libera Brilliance BPM electronics recently implemented at ESRF, and new fast correctors. This new scheme is also briefly presented in this paper.

INITIAL SLOW AND FAST CORRECTION SCHEMES

Both slow and fast correction systems derive the orbit correction from the BPM data using a correction matrix obtained from the inversion of the response matrix of the BPMs to each corrector. These response matrixes are inverted using the SVD method; for the slow correction 96 Eigen vectors are used; for the fast correction 16 vectors are used. As mentioned in the abstract, the slow and fast orbit correction systems used at ESRF were able to operate independently by leaving the $1.5 \cdot 10^{-2}$ Hz to $5 \cdot 10^{-2}$ Hz frequency span uncorrected; the cancellation of the DC response of the fast system was obtained by the following algorithm: the vector I_{av} , average value of the currents in the fast system correctors magnets is continuously computed; using the response matrix of the BPMs of the fast system to the fast correctors, it computes the position offset at the location of the fast BPMs produced by this currents set I_{av} . If we subtract this offset to the reading of the fast BPMs, it will result in the cancellation of the fast correctors currents at low frequency; the proper choice averaging time used for the calculation of I_{av} and for the frequency of the fast BPMs offset subtraction allows us to set the cut off frequency of the cancellation of the DC response of the fast system to

$5 \cdot 10^{-2}$ Hz. At the startup of the fast system, the initial offset of the BPMs is set at the values read before the loop closing, so the initial value of the currents set in the fast correctors magnets should be null. When the IDs settings are fixed, there are very few orbit perturbations in this $1.5 \cdot 10^{-2}$ Hz to $5 \cdot 10^{-2}$ Hz frequency span, so the choice of this dead span looked good. But over the last years of operation of the ESRF storage ring we found that the most detrimental cause of orbit distortion had become the frequent changes of the settings of the insertion devices (gap and phase) which perturb the orbit precisely in this $1.5 \cdot 10^{-2}$ Hz to $5 \cdot 10^{-2}$ Hz frequency span. Each of the most troublesome IDs have then been equipped with a feedforward correction system which sets the field of two dedicated correctors magnets located at both ends of the ID as a function of the insertion device settings, using a look up table; however the maintenance and periodic calibration of a large number of these feedforward systems is very inconvenient. To overcome this problem, we have implemented a control of the slow and fast orbit correction system allowing them to coordinate their correction over the DC to $5 \cdot 10^{-2}$ Hz frequency span allowing the fast correction system to cancel without delay the orbit distortion caused during a change of the settings of an ID occurring during the 30 s time interval between two slow orbit corrections.

PRINCIPLE OF THE COUPLING METHOD

We are using the following scheme to operate both systems down to DC; the slow system computes and applies an orbit correction every T_s period of 30 s; it is able to offset the closed orbit over a range of several mm; in this new scheme, the fast system should also works from DC to 150 Hz between two slow corrections, without the scheme described above for the cancellation of I_{av} ; the correctors of the fast system are only able to offset the closed orbit by a fraction of mm; so, before the computation of a slow correction, the slow system reads the vector I_{av} , average value of the currents in the fast system correctors ; using the response matrix of the BPMs of the slow system to the fast correctors, it computes the orbit offset at the location of the slow BPMs which was caused by the current set I_{av} ; then by adding this offset to the real orbit read by the its BPMs, the slow system will compute a correction which will be the sum of the correction that he would apply plus the static correction already applied by the fast system; when the slow system applies this total correction, the fast system automatically removes from the fast correctors the set of currents I_{av} ; in this way the slow system downloads the DC part of the correction from the fast system every 30 seconds avoiding

OPTIMISATION STUDIES OF A RESONANT CAPACITIVE PICK-UP FOR BEAM POSITION MONITORING OF LOW INTENSITY, LOW VELOCITY ANTIPROTON BEAMS AT FLAIR*

J. Harasimowicz[†], C.P. Welsch, Cockcroft Institute and the University of Liverpool, UK

Abstract

The Ultra-low energy Storage Ring (USR) at the future Facility for Low-energy Antiproton and Ion Research (FLAIR) at GSI, Germany will decelerate antiproton beams of very low intensities from 300 keV down to 20 keV. Such beams can be easily disturbed by standard monitoring devices and the development of new sensitive diagnostic techniques is required. To overcome the limitations related to a very low number of particles, a low signal-to-noise ratio and ultra-low kinetic energies, a resonant capacitive pick-up has been proposed as a beam position monitor. In the planned solution, the signal gain will be realised by the use of a specially designed resonant circuit optimized to meet the requirements of the USR. The current overall design studies of the resonant capacitive pick-up, including simulations of the beam displacement sensitivity and linearity for different pick-up geometries and the equivalent resonant circuit characterisation, will be discussed.

INTRODUCTION

The novel Ultra-low energy Storage Ring (USR) is currently being developed for the future Facility for Low-energy Antiproton and Ion Research (FLAIR) [1]. It will be able to accept, store and decelerate a 300 keV beam of $\leq 2 \cdot 10^7$ antiprotons down to 20 keV.

For the standard operation of the USR, ~ 100 -ns-long bunches might be of the main interest. With the ring circumference of 42.6 m, the revolution time t_{rev} of the 300 keV antiproton beam will be equal to $5.6 \mu\text{s}$. In this case, a harmonic mode $h = 10$, corresponding to the RF frequency $f_{RF} = 1.78 \text{ MHz}$ and RF buckets of about 560 ns, might be chosen. The RF field will typically be applied after the beam has reached a quasi-DC state which will lead to the generation of 10 bunches not longer than $\approx 150 \text{ ns}$. After the deceleration stage, the main RF frequency will have to be decreased to 459 kHz to follow the longer revolution time $t_{rev} = 21.8 \mu\text{s}$ of 20 keV antiprotons resulting in bunches being not more than $\approx 550 \text{ ns}$ long. Therefore, the standard operation of the USR will include $\approx 1.1 \text{ m}$ long bunches of ultra-slow particles ($\beta = 0.006\text{--}0.025$) carrying a very low charge (300 fC) with the repetition rates in the range of $\sim 0.4\text{--}2 \text{ MHz}$.

In addition, a production of ultra-short (1–2 ns) bunches for in-ring experiments is also foreseen for the USR [2]. Initially, a 20 keV coasting beam is planned to be adiabatically captured into 50 ns stationary buckets formed by a 20 MHz cavity operating at a high harmonic mode. With $h = 436$ one gets only $\leq 5 \cdot 10^4$ particles (8 fC) per bunch. The final bunch length will depend on the initial RF voltage applied to capture the circulating beam. The desired ultra-short bunches of 1–2 ns duration, corresponding to $\approx 2 \text{ mm}$ only, will then be formed by an additional double drift buncher with a voltage of $\approx 300 \text{ V}$.

Accurate beam position measurements, necessary for the successful operation of the USR, will require devices suitable for the proposed beam distributions. For the standard mode ($h = 10$) with the bunch repetition frequencies of the order of 1 MHz and the bunches much longer than the space available for a beam monitor, a capacitive diagonal-cut pick-up (PU) is a favourable solution. It offers a high linearity which is a huge advantage when the beam diameter can reach up to 2 cm in some parts of the USR before electron cooling. However, this relatively simple device will not be suitable for the ultra-short, very slow bunches intended for the in-ring experiments. In this case, other monitors extracting information from electromagnetic fields of moving charged particles might also fail to measure the beam displacement. Figure 1 shows the transverse electric field calculated at a distance of 125 mm from the beam for 20 keV antiproton \cos^2 -like bunches formed with h equal to 10, 75, 200 and 436. For the highest h , the modulation of the signal is practically lost, thus none of the beam position pick-ups will work.

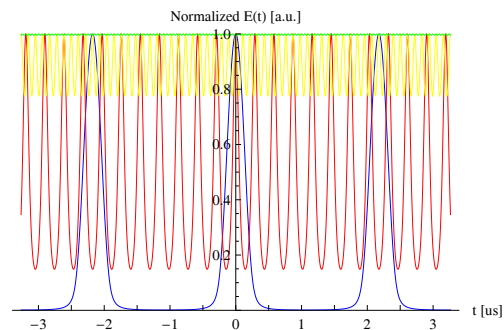


Figure 1: Normalized transverse electric field at a distance of 125 mm from the 20 keV \cos^2 -like bunches formed with $h = 10$ (460 kHz, blue curve), 75 (3.5 MHz, red curve), 200 (9.2 MHz, yellow curve), and 436 (20 MHz, green curve).

* Work supported by the EU under contract PITN-GA-2008-215080, by the Helmholtz Association of National Research Centers (HGF) under contract number VH-NG-328, and GSI Helmholtz Centre for Heavy Ion Research.

[†] Janusz.Harasimowicz@quasar-group.org

AN FPGA BASED DATA ACQUISITION SYSTEM FOR A FAST ORBIT FEEDBACK AT DELTA

G. Schuenemann, P. Hartmann, D. Schirmer, P. Towalski, T. Weis, K. Wille,
 DELTA, Technical University of Dortmund, Germany
 P. Marwedel, Technical University of Dortmund, Germany

Abstract

The demand for beam orbit stability for frequencies up to 1kHz resulted in the need for a fast orbit position data acquisition system at DELTA. The measurement frequency was decided to be 10kHz which results in a good margin for 1kHz corrections. It is based on a Xilinx University Program Virtex-II Pro Development System in conjunction with an inhouse developed Analog-Digital Converter board, featuring two Analog Devices AD974 chips. An in-house developed software written in VHDL manages measurement and data pre-processing. A communication controller has been adopted from the Diamond Light Source [1] and is used as communication instance. The communication controller is versatile in its application. The data distribution between two or more of the developed measuring systems is possible. This includes data distribution with other systems utilizing the communication controller, e.g. the Libera beam diagnostic system¹.

To enhance its measuring capabilities one of the two on-board PowerPC cores is running a Linux kernel. A kernel module, capable of receiving the measurement data from the Field Programmable Gateway Array (FPGA) measurement core, was implemented [2], allowing for advanced data processing and distribution options. The paper presents the design of the system, the used methods and successful results of the first beam measurements.

INRODUCTION

Since DELTA faces the demand for improved beam orbit stability for supplying a higher brilliance synchrotron radiation, a suitable data acquisition system for fast orbit feedback had to be found. Measurements regarding the electron beam disturbances have shown a variety of sources [5]. Slow orbit shifts have been observed, caused by thermal drifts on a day to week scale. In addition ground motion and girder movement in the low frequency range of up to 10Hz (DELTA girder resonance) have also been observed. On the other hand much faster excitation is caused by the mains power frequency of 50Hz and its harmonics up to 300Hz. The existing analog position measurement system used for the slow orbit feedback at 0.1Hz may be operated at a maximum orbit position data rate of 10kHz. To exploit this capability a most versatile adoption to this data had to be found and a data acquisition system had to be designed and implemented without any interference with the existing global slow orbit feedback system, which is supplied with

orbit data from the same orbit calculating devices. This approach includes cost effectiveness (by using existing orbit electronics) as well as modularity (modular system) and versatility (broad range of communication options).

GENERAL LAYOUT

DELTA's orbit feedback is a classic control loop. The data is acquired, corrections are calculated and applied to the beam by means of magnetic fields. Modern fast orbit feedback systems [1, 3] are based on turn-by-turn (TBT) beam position data reduced to kHz bandwidth. Only a minor number of Deltas BPMs are TBT measurement capable. Therefore the idea to use the existing analog Bergoz MX-BPMs in combination with TBT capable devices for a fast orbit data acquisition system came up. To achieve the systems desired versatility and modular design a decentralized solution was chosen. Initial design ideas were adopted from the concept of the Libera Electron fast orbit feedback at Diamond Light Source, England, including data interchange with any device running the underlying communication structure, the Diamond Communication Controller (DiamondCC) [1].

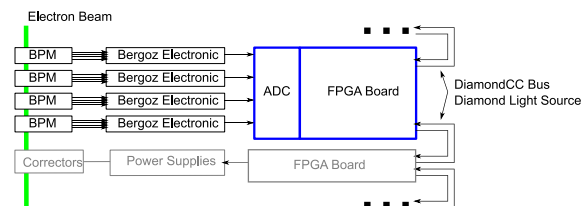


Figure 1: Data acquisition system (DAQ) layout. Additional bus participants can be connected if desired.

The system follows the idea of a classic control loop (see figure 1). The electron beam induces a voltage on the four beam pickup buttons. The position of the electron beam is calculated by the Bergoz MX-BPMs. The analog position value is then digitized by an ADC-board and transferred to the FPGA being part of the Xilinx University Program development board [6]. The FPGA takes over the task of pre-processing and then distributing the data amongst the feedback participants. These are typically either data pickup stations, correction calculation instances or data logging devices. The DiamondCC is the communication instance used for this data distribution. It features a synchronized, global position data exchange on a fast time basis, thereby avoiding the common bottleneck for orbit feedback applications. Adjustment to the possible maxi-

¹Instrumentation Technologies d.o.o., Solkan, Slovenia

BEAM TESTS WITH LIBERA IN SINGLE PASS MODE

A. Stella, M. Serio, INFN-LNF, Frascati, Italy

S. Bassanese, R. De Monte, M. Ferianis, ELETTRA, Trieste, Italy

Abstract

The single pass functionality available in the recent release of the Libera Brilliance software, takes particular interest when compared with the requirements of FEL machines, that need stable and precise control of the beam trajectory throughout Linacs and transfer lines in order to meet the stringent beam quality and transverse position constraints inside undulators.

Results from tests performed on Libera with beam from ELETTRA, SPARC and DAFNE operating in Sincrotrone Trieste and LNF Frascati are reported to characterize the resolution of single shot transverse beam position measurements.

INTRODUCTION

The Libera Brilliance detection electronics, developed by Instrumentation Technologies, implements the digital receiver technology to measure the beam position.

When used on a machine with stored beams, the narrow band signals from the pickups are downconverted to baseband with an undersampling technique for amplitude measurement.

Nevertheless one can perform accurate measurement of short single bunches signals, typical of transfer lines or Linacs, by working directly on the ADCs samples provided by the same boards used for the storage rings [1].

In the following chapter we report results of single pass tests obtained with beams from different accelerators, acquired as reported in Table 1.

Table 1: Beams parameters during measurements

	Bunch Charge	Acquisition Rate	FWHM Pulse Length
SPARC	0.08 nC	10 Hz	.5 ns
ELETTRA	.01+1 nC	10 Hz	.2 ns
DAFNE	1 nC	2 Hz	.8 ns

SINGLE PASS DATA

Signals from beam position monitor (BPM) have been connected, through low attenuation coaxial cables, to Libera Brilliance.

Before sampling, the short single pulses are fed to the Libera RF front-end which includes passband filters of bandwidth larger than the accelerator revolution frequency and placed around a center frequency given by the RF frequency.

02 BPMs and Beam Stability

Raw data are collected from the four 16 bit ADCs buffer at a sampling frequency of ~116.8 MHz, which is customizable for each accelerator. To allow measurement on the stored beam it is usually chosen as a multiple of the revolution frequency. The buffer is 1024 samples long and acquisition can be started by an external trigger.

Beam Position Reconstruction

Stripline BPM have been used. The beam position is reconstructed from the amplitude difference of voltage signals from opposite pickups times the k sensitivity, according to:

$$x = k \cdot \frac{\Delta V}{\Sigma V}$$

Different BPM sensitivities k , dependent solely on the vacuum chamber geometry, must be taken into account when comparing results (Table 2).

Table 2: Pickup parameter

	BPM type	chamber	k [mm]
DAFNE	Short circuited stripline	Circular	18.3 mm
ELETTRA	50 Ω matched stripline	Diamond shape	19.8 mm
SPARC	50 Ω matched stripline	Circular	10 mm

Libera release 2.00 provides a dedicate algorithm working over the raw buffer data and implemented directly onboard, to reconstruct the beam position

The amplitude from each electrode is assumed as the square root of the sum of the squared samples. Data used for this calculation are selected by setting an amplitude threshold on the waveform and taking into account only N points specified with the *pre-trigger* and *post-trigger* Libera parameters [2].

A further algorithm based on the Hilbert transform [3] has been applied offline to the sampled data. In this case the Hilbert transform has been used as amplitude envelope detector on the narrowband ADC samples.

The signal amplitude from each electrode has been extracted from the integral of the envelope amplitude.

RESOLUTION MEASUREMENTS

SPARC, the 150 MeV S-band photoinjector operating in Frascati (Italy) to produce high brightness electron beams for SASE-FEL experiments, has been equipped with stripline BPMs for trajectory measurement. Figure 1 shows a typical signal from a single stripline at the end of the coaxial cable and the sampled waveform available in the Libera ADC buffer.

THE BPM MEASUREMENT SYSTEM IN HIRFL-CSR *

J.X. Wu[#], J.W. Xia, G.Q. Xiao, R.S. Mao, T.C. Zhao, Y.J. Yuan, J.H. Zheng, IMP, Lanzhou, China

Abstract

HIRFL-CSR [1], a new heavy ion cooler-storage ring in China IMP, had been installed and started commission from 2005. We report here the BPM system on the main ring (CSRm) and the experimental ring (CSRe). The BPM structure, the signal processing system and on-line measurement experiments are presented. The measurement results such as turn-by-turn bunch observation, closed-orbit measurement, Schottky noise measurement are also presented in this paper.

INTRODUCTION

HIRFL-CSR is a new heavy ion cooler-storage ring synchrotron system in Lanzhou. It consists of a main ring (CSRm) and an experimental ring (CSRe) with multi-usages and multi-functions, shown in Fig. 1. The two existing cyclotrons SFC (K=69) and SSC (K=450) of the Heavy Ion Research Facility in Lanzhou (HIRFL) are used as its injector system. The heavy ion beams from HIRFL with the energy of 7-25MeV/u will be first injected into CSRm, accompanying with the accumulation, e-cooling and acceleration, and finally extracted slowly with the energy of 500-1100MeV/u for many external-target experiments, or extracted fast with the energy of 200-700MeV/u to produce radioactive ion beams (RIBs) or high Z beams at the primary target of the beam line. The secondary beams will be accepted and stored in CSRe for many internal-target experiments. From 2006 to 2008 all the commissioning activities of HIRFL-CSR were made, including stripping injection, multi-turn injection, cooling accumulation with hollow electron beams, ramping in a wide range with different RF harmonics, isochronous mode commission of CSRe, mass measurement of RIBs in CSRe with ToF and slow extraction from CSRm.

As the eyes of an accelerator, the diagnostic system is built together with the construction of the CSR. The whole CSR commission was proceeded and succeeded with the support and help of it. Of course the BPM system is the key part of the diagnostic system. The shoe-box type BPMs are used in CSR because of its good linear dependence with respect to the beam displacement [2]. There are 16 BPMs distributed around the CSRm and 11 around the CSRe. The structure is shown in Fig. 2. The length of the BPM is 300 mm and the cross section is 170*110 mm² for the CSRm and 250*130 mm² for the CSRe. To avoid the influence of the beam injection and extraction of the CSRm, the dimension of the BPM at these two positions is larger than others and its cross section is 240*170 mm².

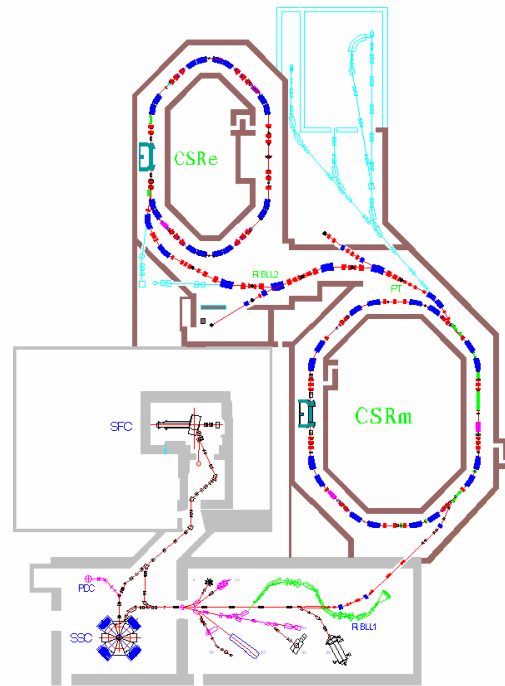


Figure 1: Overall layout of HIRFL-CSR.

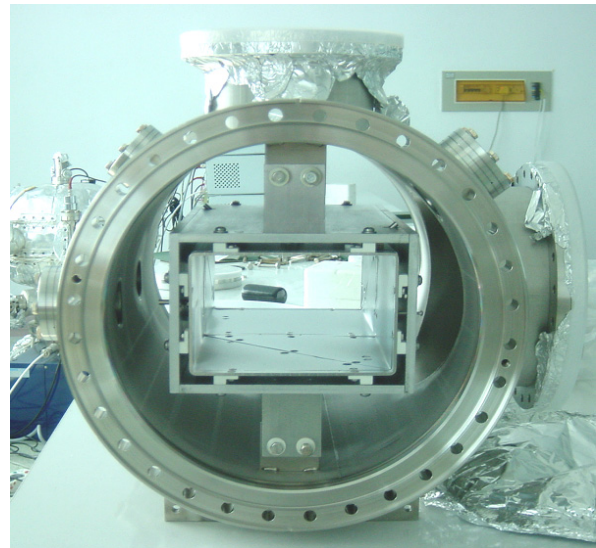


Figure2: The BPM structure of HIRFL-CSR.

BPM PROCESSING SYSTEM

As the beam frequency is low in CSR and the range of the frequency is 0.25~1.7MHz in CSRm and 0.5~2.0MHz in CSRe. So the broadband processing is used in the CSR BPM system, as in Fig.3. After pre-amplification, the BPM signal is directly digitized by a fast ADC. The low-noise amplifier has the bandwidth of DC-1GHz, the gain of 52dB and the noise figure of $1.7 \mu V / \sqrt{Hz}$. It has a

*Work supported by the center government of China and NSFC

[#]wujx@impcas.ac.cn

BPM SYSTEM AND FAST ORBIT FEEDBACK UPGRADE FOR THE TAIWAN LIGHT SOURCE

C.H. Kuo, P.C. Chiu, K. H. Hu, Jenny Chen, C.Y. Wu, Demi Lee, K.T. Hsu
NSRRC, Hsinchu 30076, Taiwan

Abstract

The BPM electronics of the Taiwan Light Source (TLS) have been upgraded to the Libera Brilliance in August 2008 to improve performance and functionality. Orbit feedback system is also migrated into fast orbit feedback system to enhance orbit stability. Infrastructure of the orbit acquisition system and orbit feedback system has been reconstructed to accommodate the new BPM electronics and to satisfy requirements of fast orbit feedback loops. Gigabit Ethernet grouping was adopted for the data transfer of 10 KHz rate orbit data to the orbit feedback system. The efforts and performance of this upgrade will be summarized in this report.

INTRODUCTION

Orbit stability is an extremely important for a modern synchrotron light source. Generally, beam motion should be less than 10 % of its beamsize or even smaller. There are many efforts make to improve orbit stability of Taiwan Light Source (TLS) such as control of the ambient environment, removing various mechanical vibration passively, feed-forward compensation of insertion devices, locating faulty power supply and etc. Nevertheless, the limited loop bandwidth led incapability to suppress fast orbit excursion above 6 Hz. The fast orbit feedback system was thus proposed. The commissioning of the new fast orbit feedback system will come to an end soon. In the report, the upgrade progress and performance of the BPM system will be presented. Measurement of the system response and latency are discussed next. Finally, the infrastructure and performance of fast orbit feedback are summarized.

BPM SYSTEM UPGRADE AND ACQUIRED DATA MEASUREMENT

The Libera Brilliance [1] is employed to replace the existed BPM electronics for the TLS. Its integration started from 2007 until finish in August 2008. It was gradually deployed and performed without interfere routine operation. There are 59 Libera Brilliances online operation for more than 8 months. The adequate long-term reliability has been achieved. The typical Libera acquired slow and fast data which are extreme critical for FOFB performance will be shown in the latter.

Libera Grouping

The Libera provided a Gigabit Ethernet interface to transfer data with 10KHz update rate. The data sending in

the same time, there is network packet collision and interrupt queue over buffer problem in the receiving node. That will take fatal jitter effect and data lost. To eliminate this phenomenon, Libera Brilliance units are grouped together by a redundant multi-gigabit links via the LC optical links and copper "Molex" cables. This link can exchange the data among all Libera Brilliance units to be a single and large packet size by FPGA and send the gathered data via Gigabit Ethernet. It is effective to reduce the packet numbers in network, banish jitter and data lost in the communication with processor [3,4].

Fast Data

Resolution is an important issue for fast orbit feedback system. The resolution of the Liberas FA data at 10 kHz is around 0.2~0.3 μm when the simulated beam current intensity is operated at 300 mA. Each unit slightly differs while the whole of 59 Liberas should be within 0.35 μm .

Slow Data

Vertical orbit data is shown as Fig. 1. The standard deviation is around 0.1~0.8 with real beam corresponding to respective location.

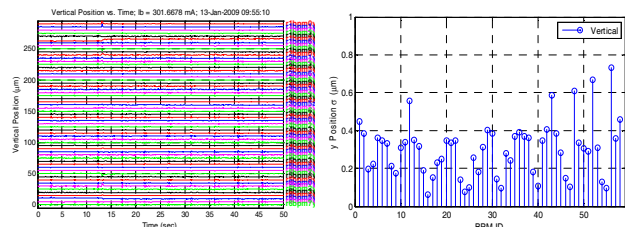


Figure 1: Slow data of vertical position and its RMS value.

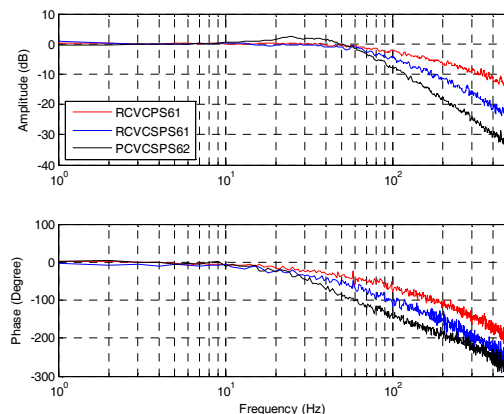


Figure 2: Three vertical correctors' (RCVCPS61, RCVCS61, RCVCS62) response functions.

PHOTODIODE-BASED X-RAY BEAM-POSITION MONITOR WITH HIGH SPATIAL-RESOLUTION FOR THE NSLS-II BEAMLINES*

P.S. Yoon[†], NSLS-II, Brookhaven National Laboratory, Upton, NY 11973 USA
D. P. Siddons, NSLS, Brookhaven National Laboratory, Upton, NY 11973 USA

Abstract

We developed a photodiode-based monochromatic X -ray beam-position monitor (X-BPM) with high spatial resolution for the project beamlines of the NSLS-II. A ring array of 32 Si PIN-junction photodiodes were designed for use as a position sensor, and a low-noise HERMES4 ASIC chip was integrated into the electronic readout system. A series of precision measurements to characterize electrically the Si -photodiode sensor and the ASIC chip demonstrated that the inherent noise is sufficiently below tolerance levels. Following up modeling of detector's performance, including geometrical optimization using a Gaussian beam, we fabricated and assembled a first prototype. In this paper, we describe the development of this new state-of-the-art X -ray BPM along the beamline, in particular, downstream from the monochromator.

MOTIVATION

The end stations for user's experiments at NSLS-II are located far from the X -ray sources. Hence, a small number of displacement- and angular-errors in a radiation source can degrade the end experiments. Accordingly, there is a pragmatic demand for a novel X -ray beam-position monitor (X-BPM) with high spatial resolution. A suite of six project beamlines under design are to be commissioned in the NSLS-II infrastructure[1]. A new X-BPM system developed specifically for these beamlines will serve as a diagnostic device for aligning beamline components and for real-time monitoring of a series of the beamline optics elements. The beam shape changes during its transportation through various optical elements. Therefore, it is anticipated that the performance of the new X-BPM will be less dependent upon the beam optics. Moreover, the mode of operation should affect the beam as little as possible to meet the stringent requirements for beam stability.

PHOTODIODE-SENSOR DESIGN

Figure 1 depicts the ring array of 32 photodiode pads that were designed and fabricated at in-house facilities¹. Boron ions are implanted on the front side of the wafer through 1

kA oxide, forming a $p-n$ junction[2]. Phosphorous ions are implanted on the back side to make an ohmic contact with the front side. All 32 pads, configured as a polar array, are positioned between an inner ring radius of $5,050 \mu\text{m}$ and an outer ring radius of $6,763 \mu\text{m}$. The active surface area of each pad is about $2.0 (mm^2)$, and each photodiode is $470\text{-}\mu\text{m}$ thick. In the photoconductive mode, the photodiodes are operated with reverse bias voltage of about 100. Upon impinging on a scatterer as a source of fluorescence radiation, the incident X -ray beam scatters and isotropically illuminates the backside of the ring photodiode. The photon sensor was devised for both back-side and front-side illumination. Our first prototype adopts a scheme of forward scattering using a silicon-nitride (Si_3N_4) substrate metalized with different species such as Cr , Ni , Ti , and Au . As Fig. 2 illustrates, the next version will utilize a backward-scattering scheme, employing bi -HERMES4 configuration that will be implemented later in the electronic readout.

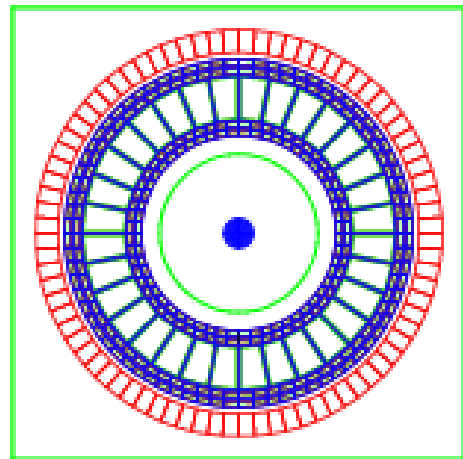


Figure 1: The ring array of segmented Si photodiodes. – drawing courtesy of the Instrumentation Division of BNL.

ELECTRICAL CHARACTERIZATION OF PHOTODIODE SENSOR

Achieving the desired level of detector performance requires a detailed electrical characterization of the optical sensor of the position-monitoring system. Hence, we undertook a comprehensive evaluation of each individual segment on the photodiode ring prior to completing the assem-

* This work was supported by the Department of Energy under contract number DE-AC02-98CH10886.

[†] yoon@bnl.gov

¹ There is a one-on-one correspondence between 32 pads and 32 ASIC channels.

CHARACTERIZATION TESTS OF THE BEAM POSITION MONITOR SERIES PRODUCTION FOR THE TBL LINE OF THE CTF3 AT CERN*

C. Blanch-Gutierrez, J.V. Civera-Navarrete, A. Faus-Golfe, J.J. García-Garrigós
IFIC (CSIC-UV), Valencia, Spain

Abstract

A set of two Inductive Pick-Up (IPU) prototypes with its associated electronics for Beam Position Monitoring (BPM) in the Test Beam Line (TBL) of the 3rd Compact Linear Collider (CLIC) Test Facility (CTF3) at CERN were designed, constructed, and tested by the IFIC team. One prototype and two units of the series production are already installed in the TBL line. In the first part of the paper we describe the characterization tests of these two prototypes carried out at CERN, and the first beam tests performed to one of them. The second part of this paper is dedicated to the description of the issues addressed by the start of the series production and the characterization tests of the first series units performed with a custom-made low-frequency wire setup. This setup which emulates the beam position variation allows to carry out the series tests in an automated manner and with higher accuracy.

INTRODUCTION

The CLIC Test Facility will demonstrate the essential parts of the CLIC drive beam generation scheme consisting of a fully loaded linac, a delay loop and a combiner ring. The final CTF3 drive beam is delivered to the CLIC Experimental Area (CLEX) comprising the TBL and a two beam test stand. The TBL is designed to study and validate the drive beam stability during deceleration. The TBL consists of a series of FODO lattice cells and a diagnostic section at the beginning and end of the line to determine the relevant beam parameters. Each cell is comprised of a quadrupole, a BPM (labeled as BPS) and a Power Extraction and Transfer Structure (PETS) [1]. A 3D view of a TBL cell is shown in Fig. 1. The available space in CLEX allows the construction of up to 16 cells with a length of 1.4 m per cell. The BPS's are IPU type and the expected performances for a TBL beam type (current range 1-32 A, energy 150 MeV, emittance 150 μm , bunch train duration 20-140 ns, microbunch spacing 83ps (12GHz), microbunch duration 4-20 ps, microbunch charge 0.6-2.7 nC) are summarized in Tab. 1.

BPS PROTOTYPES

A set of two prototypes of the BPS's labeled as BPS1 and BPS2 with its associated electronics has been designed, constructed and characterized by the IFIC team with the collaboration of the CTF3 team at CERN. The BPS has

* Work supported by FPA2007-31124-E

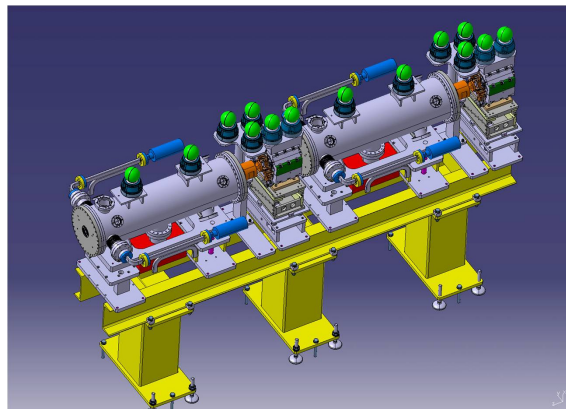


Figure 1: 3D view of a TBL cell with the PETS tanks, the BPSs and the quadrupoles.

Table 1: Expected BPS Characteristics

Analog bandwidth	10 kHz-100 MHz
Beam position range	± 5 mm (H/V)
Beam aperture diameter	24 mm
Overall mechanical length	126 mm
Number of BPS's	16
Resolution at maximum current	≤ 5 μm
Overall precision $\sigma_{H/V}$	≤ 50 μm

four electrodes setting up the vertical and horizontal coordinate planes. The current intensity induced by the beam is distributed through these electrodes depending on the beam proximity. The electrodes current is then sensed by their respective transformers in a conditioning circuit placed in an internal PCB. This gives the four output voltage signals (V_+ , H_+ , V_- , H_-) that will drive an external amplifier to yield three signals for determining the beam position: sum signal ($\Sigma = V_+ + H_+ + V_- + H_-$), to get the beam current intensity; and two difference signals ($\Delta V = V_+ - V_-$ and $\Delta H = H_+ - H_-$) which are proportional to the horizontal and vertical coordinates of the beam position. There is also two input calibration signals, Cal+ and Cal-, to check the correct function of the sensing PCB halves. A detailed description of the mechanics, electrical model and the electronics of this two prototypes can be found in [2].

Prototypes Characterization Tests

The BPS characterization parameters for each coordinate plane: sensitivity, overall precision (accuracy), electrical offset and cut-off frequencies with its associated time constants; has been determined with the wire method test in the BI-PI labs at CERN. This test is based on a test bench

PARTICLE IDENTIFICATION DEVICES IN MICE

V. Verguillov,* University of Geneva - DPNC, Geneva, Switzerland

V. Palladino, INFN-Napoli, Napoli, Italy

Abstract

The international Muon Ionization Cooling Experiment (MICE) is being built at the Rutherford Appleton Laboratory (RAL). It will carry out a systematic investigation of ionization cooling of a muon beam. This is one of the major technological steps needed in the development of a muon collider and a neutrino factory based on muon decays in a storage ring. MICE will use particle detectors to measure the cooling effect with high precision, achieving an absolute accuracy on the measurement of emittance of 0.1% or better. A PID system based on three Time-of-Flight stations, two Aerogel Cherenkov detectors, a KLOE-like calorimeter in combination with Electron-Muon Ranger calorimeter has been constructed in order to keep beam contamination (e, π) well below 1%. The MICE time-of-flight system will measure timing with a resolution better than 70 ps per plane, in a harsh environment due to high particle rates, fringe magnetic fields and electron backgrounds from RF dark current. The aim of this paper is to give a quick overview of the particle identification system in MICE.

OVERVIEW

The physics program at a neutrino factory is very rich and includes long-baseline ν oscillations, short-baseline ν physics and slow muon physics [1]. The performance of a Neutrino Factory depends not only on its clean beam composition (50% $\nu_e, 50\%\bar{\nu}_\mu$ for the $\mu^+ \mapsto \bar{\nu}_\mu \nu_e e^+$ case), but also on the available beam intensity. The cooling of muons (accounting for $\sim 20\%$ of the final costs of the factory) is thus compulsory, increasing the performance up to a factor 10 [2], [3], [4], [5].

The process of ionization cooling of the transverse phase-space coordinates of a muon beam was proposed more than 20 years ago by A.N. Skrinsky [6]. Essentially it can be accomplished by passing it through an energy-absorbing material and an accelerating structure, both embedded within a focusing magnetic lattice. Both longitudinal and transverse momentum are lost in the absorber while the RF-cavities restore only the longitudinal component. The Muon Ionization Cooling Experiment (MICE) [7], [8], [9] at Rutherford-Appleton Lab is the first test of the ionization cooling concept for muon beams in the approximate momentum range 140 to 240 MeV/c. A minimum ionizing muon beam will be transversely cooled by stages of $-dE/dx$ in LH₂ absorbers and longitudinal energy restoration in a series of 201 MHz RF cavities; (Figure 1) The 6D emittance reduction is measured before and after the cooling stage by tracking individual muons through the system. To establish muon cooling the in-flight muon beam is positively identified by three time-of-flight (TOF) stations

* for the Mice Collaboration

[10], by two threshold Cherenkovs (CKOVs), and by a low energy ranging electron-muon calorimeter (KL/EMR) near the beam exit.

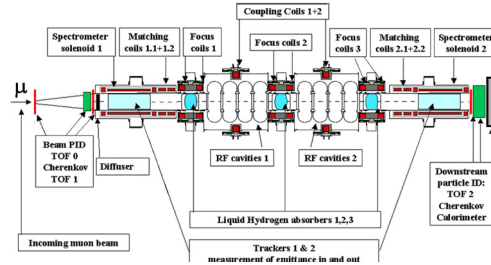


Figure 1: MICE Spectrometer Layout.

TIME OF FLIGHT DETECTORS

Three time-of-flight (TOF) stations are positioned in the MICE channel at the beginning (TOF0), midway (TOF1), and near the rear (TOF2). Each station is approximately 50cm \times 50cm in active cross section and spaced apart by a ≈ 10 m flight path. The TOF stations are used in establishing a precision particle trigger which can be synchronized to within ≤ 70 ps of the RF cavity phase of the experiment. The TOF 0/1/2 stations consist of 10/7/10 X-counter and 10/7/10 Y-counter arrays constructed of BC404/420 scintillator bar with dual R4998 PMT (TOF0) readout (Fig. 2). The HV dividers have been modified for high rate performance (≈ 2 MHz). The dual photomultiplier (PMT) readout gives typically $\sigma_t = 50-60$ ps intrinsic timing resolution for each bar assembly. The bars are 2.5 cm thick, optimizing between light collection and energy loss. The transit time and associated dispersion, σ_{tt} , of the signal through the PMT, cable delay, and the discriminating electronics is not known and are measured for each channel by a calibration procedure which can use particle beam and/or cosmics. Leading edge discriminators have been

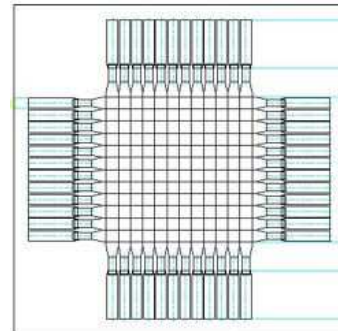


Figure 2: X/Y planes for TOF0 station. Each bar assembly is 4 cm wide.

adopted for the timing measurements. This introduces a dependence of the discrimination crossing time, "time-walk", with its associated dispersion σ_{tw} . To calculate the time-walk correction the difference of the time measured by the

BASEBAND TUNE MEASUREMENTS AT GSI SIS-18 USING DIRECT DIGITIZED BPM SIGNALS*

U. Rauch[†], P. Hülsmann, GSI, Darmstadt, Germany and Goethe University, Frankfurt, Germany
P. Forck, P. Kowina, P. Moritz, GSI, Darmstadt, Germany

Abstract

A precise tune determination is crucial for stable operation of GSI SIS 18 synchrotron especially for intense beam conditions. In order to avoid nearby resonances in the tune diagram the fractional part of coherent betatron motion needs to be measured with a resolution of 10^{-3} also during ramping mode. This is achieved using a fast digital readout system for Beam Position Monitors (BPM) which delivers a bunch-by-bunch position. The tune is then determined in baseband directly by Fourier-transformation of the positions of a certain bunch typically over 2048 turns. This algorithm does not require any additional input parameter. Since particle losses due to emittance blow-up have to be avoided, excitation power has to be kept as low as possible. In order to find a working range where tune measurement can be implemented in normal machine operation without disturbing the beam several series of measurement have been performed using a digital random noise generator for beam excitation and an Ionization Profile Monitor for displaying alterations of beam profile.

SYSTEM OVERVIEW

The new data acquisition system for BPMs based on fast and direct signal digitization followed by digital signal processing offers a sensitive method for tune measurement [1, 2, 3]. By using the integrated bunch-by-bunch position information the coherent betatron motion can be extracted in baseband without external parameters. Such frequency spectrum is expressed in units of q and ranges from $0 < q < 0.5$. The GSI heavy ion synchrotron has some particular machine parameters, namely the comparatively long bunches, the injection at non-relativistic velocity $\beta = 15,5\%$ and the acceleration frequency ramping from 0.8 to 5 MHz. The new method acts as a low pass filter with dynamically adapted filter bandwidth. Therefore it offers a high flexibility for the varying beam parameters at SIS 18, which cannot be realized by the sensitive analog baseband- q detection system BBQ [4].

As schematically shown in Fig. 1, the analog single plate BPM signals from all four plates of a shoebox type BPM [5] are fed to a high impedance amplifier and digitized. The digitization of the broadband BPM signal is performed using a sampling rate of 125 MSa/s which corresponds to a range of 18 to 140 Sa per bunch for SIS 18 typical beam parameters, depending on the revolution frequency. The signal is integrated bunch-by-bunch which minimizes thermal and digitization noise and the beam position is calculated.

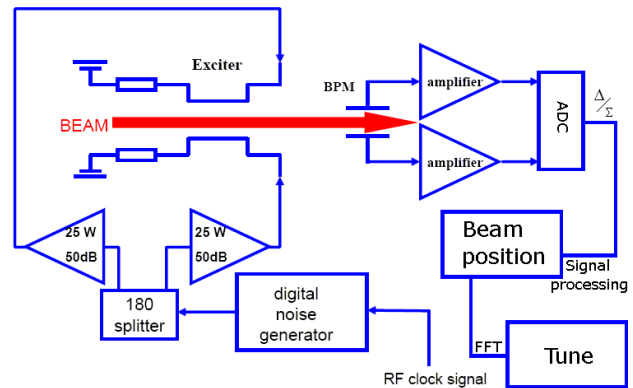


Figure 1: System schematics. The Beam Position Monitor is read out using a fast ADC. A white noise generator with limited bandwidth is connected to an exciter.

The position processing algorithm delivers a single value for vertical and horizontal position for each bunch and thus a certain bunch can be traced digitally. Signal shape and treatment as well as algorithm details for position evaluation have been described earlier [1, 2].

The coherent betatron motion cannot be observed for a stable and well adjusted beam, therefore the beam has to be slightly excited. This excitation is applied using a digital random noise generator connected to an exciter installed at SIS 18 (Fig. 1). It produces white noise with adjustable bandwidth on side bands of a carrier frequency f_c [6]. f_c is set by a frequency tracker connected to the SIS 18 rf signal. The noise bandwidth is set broad enough to cover the range of expected maximum tune deviation, which usually was chosen as $\Delta q = 0.05$. The noise generator signal is split and each branch is amplified up to a maximal power of 25 W. Both signals are fed to a stripline exciter of 750 mm length and 200x70 mm horizontal/vertical aperture. Two independent exciters are installed at SIS 18 for horizontal and vertical plane respectively.

Excessive excitation of the beam must be avoided to prevent emittance blow-up. The search for a standard working range for tune measurement is subject of the studies presented in this contribution.

TUNE AND BEAM POSITION RESULTS

Detailed measurements have been performed with this system for various beam parameters. In the following we discuss the properties for a typical beam with the following parameters: $6.5 \cdot 10^9 A_r^{18+}$ ions accelerated from 11.4 to 300 MeV/u within 400ms, which corresponds to 220.000 turns. The vertical plane is discussed if not otherwise men-

* Work supported by EU, DIRAC secondary beams, 515873

[†] u.rauch@gsi.de

PHASE AND AMPLITUDE MEASUREMENT FOR THE SPIRAL2 ACCELERATOR

C. Jamet, W. Le Coz, C. Doutressoulles, T. Andre, E. Swartvagher, GANIL, Caen, France

Abstract

The SPIRAL2 project is composed of an accelerator and a radioactive beam section. Radioactive ions beams (RIBs) will be accelerated by the current cyclotron CIME and sent at GANIL experimental areas. The accelerator, with a RFQ and a superconducting Linac, will accelerate 5 mA deuterons up to 40MeV and 1 mA heavy ions up to 14.5 MeV/u. A new electronic device has been evaluated at GANIL to measure phase and amplitude of pick-up signals. The principle consists of directly digitizing pulses by under-sampling. Phase and amplitude of different harmonics are then calculated with a FPGA by an I/Q method. Tests and first results of a prototype are shown and presented as well as future evolutions.

SPIRAL2 ACCELERATOR DESCRIPTION

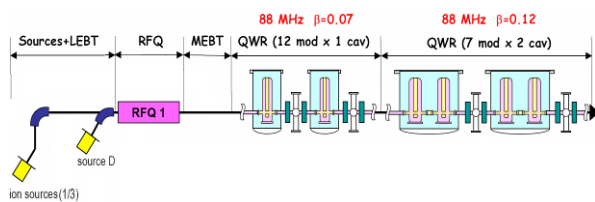


Figure 1: Accelerator Layout.

The accelerator is divided in 3 main parts, an injector, a superconducting linac and a high energy line. The injector part is composed of a deuteron/proton line, an ion line (LEBT), a RFQ and a MEFT line. Two kinds of superconductivity cavity are used for the Linac ($\beta=0.07$, $\beta=0.12$).

Table 1: Beam Intensity and Power

	Intensity	Energy	Power
LEBT1 (ions)	1 mA	20 keV/A	60 W
LEBT2 (deut.)	5 mA	40 keV	200 W
MEBT	5 mA	750 keV/A	7.5 kW
HEBT	5 mA	20 MeV/A	200 kW

BEAM ENERGY MEASUREMENT

During the RFQ and the MEFT commissioning, an Injector Test Bench (BTI) will be used to qualify beam characteristics. Beam energy will be measured at the exit of the RFQ by the “time of flight” method. Another beam energy measurement by TOF is foreseen in the HEBT at the exit of the superconducting LINAC.

07 Hadron Accelerator Instrumentation

Table 2: Phase Measurement Accuracy

	Energy Accuracy	Distance (mm)	Phase Accuracy
BTI	10^{-3}	1500 ± 0.2	$\pm 0.5^\circ$
HEBT	$5 \cdot 10^{-3}$	5000 ± 2	$\pm 2^\circ$

Intensity dynamic ($50 \mu A < I_{beam} < 5 mA$)
 Beam ratio (CW to $100 \mu s / 100 ms$) 10^{-3}
 Phase measurement gives the possibility to subtract the offset, an advantage compared to the time measurement.

INJECTOR TEST BENCH PICK-UP

3 pick-ups will be used to measure beam energy. The third pick-up allows determining the bunch number between two first pick-ups.

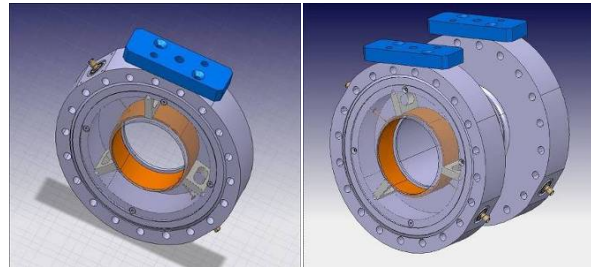


Figure 2: Pick-up Design. Diameter: 80 mm, Length: 30 mm.

PICK-UP SIGNAL SIMULATIONS

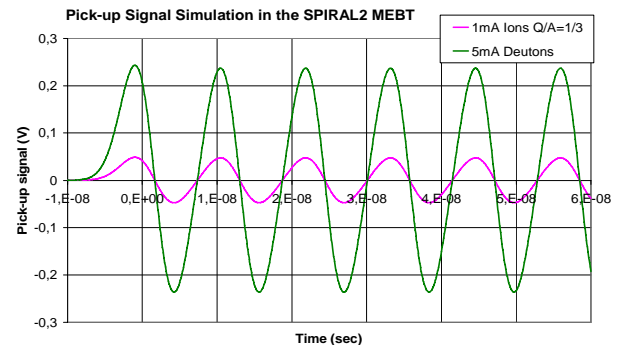


Figure 3: MEBT Pick-up Signal Simulation.

Signal amplitudes
 - 1mA ions $Q/A=1/3$: $V_{h1} = 50 mV$
 - 5mA deuterons : $V_{h1} = 230 mV$
 Ratio $h1/h2 = 13$

LONGITUDINAL EMITTANCE MEASUREMENT USING PARTICLE DETECTORS

T. Milosic, P. Forck, GSI, Darmstadt, Germany

D. Liakin, ITEP, Moscow, Russia

Abstract

A device for accessing the longitudinal phase space at low energy sections (1.4 MeV/u) of the GSI heavy ion LINAC is presented. The interceptive measurement is based on the coincident detection of single particles by means of two detectors: The first detector provides measurement of secondary electrons emitted from a thin Al-foil by the impinging ion beam. Secondly, after a drift beam particles are registered directly by a fast diamond detector. This contribution describes the measurement setup in detail including the principle of particle number attenuation by Rutherford scattering in the Ta foil. The achievements concerning the required timing resolution are presented and the investigations are accompanied by recently recorded data. Finally an outlook towards post-processing is given.

MOTIVATION

The existing facility at GSI will be used as injector for the future project FAIR which requires optimizations of the existing accelerator facility. Depending on the kind of a certain optimization crucial information may be obtained from beam diagnostics. The device presented is located at the linear acceleration UNILAC and is aimed at providing information about the longitudinal phase space in order to improve injection into the Alvarez section (Fig. 1). Due to the location in front of the Alvarez tank spatial constraints led to a novel approach that is based on the time-of-flight (TOF) between two particle detectors [1].

WORKING PRINCIPLE

The measurement setup can basically be divided into three crucial parts. At first a mechanism has to provide feasible particle number attenuation to satisfy single particle coincidence measurements. Secondly, two timestamps are needed to account for the energy of the particle. Lastly,

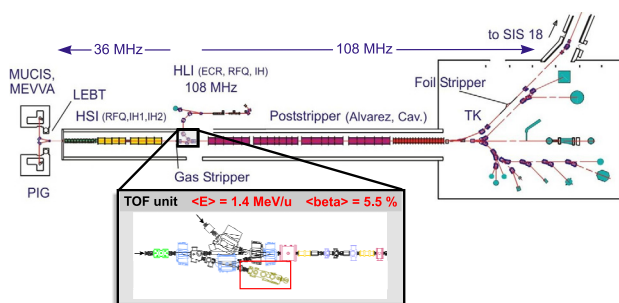


Figure 1: Setup located at GSI UNILAC after IH structures, accessible by the high current injector.

07 Hadron Accelerator Instrumentation

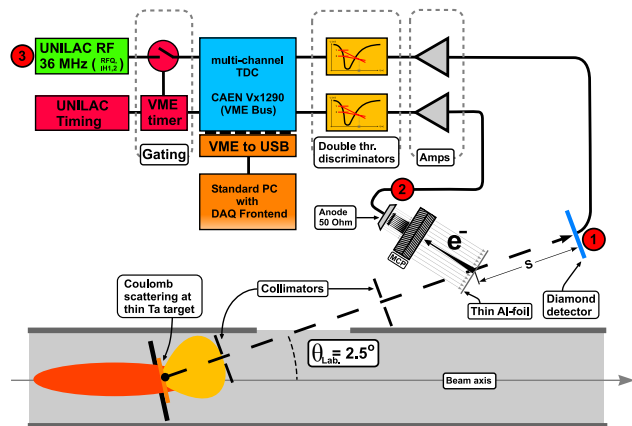


Figure 2: Device schematics. Single particles are detected indirectly at MCP module (2) and directly at diamond detector (1). UNILAC rf (3) is used as timing reference.

a method to determine the relative phase information is required to complete the longitudinal degrees of freedom within the phase space. The schematic of the measurement setup is depicted in Fig. 2.

Particle number attenuation is accomplished in two stages. Once the beam enters the device attenuation is carried out by coulomb scattering using a thin Ta foil of $210 \mu\text{g}/\text{cm}^2$ and selecting scattered particles under an laboratory angle of 2.5° with respect to the beam axis. Two plates with $\varnothing 0.5 \text{ mm}$ and 1 mm at a distance of 155 mm act as a collimator to achieve a small solid angle of $\Omega \approx 10^{-4}$. This assumes incoming beam intensities that have already been lowered to several μA in order to prevent damages of the Ta foil. This allows for a single particle coincidence per bunch at maximum in conjunction with coulomb scattering utilising the aforementioned selection of particles under a certain solid angle. Primary beam attenuation needs different approaches for low current and high current measurements. The attenuation of the primary beam from a maximal current of $\approx 10 \text{ mA}$ to about $10 \mu\text{A}$ is done using transverse defocusing at different locations along the UNILAC. By this space charge effects along the Linac structures are influenced. Variation of the gas pressure inside the stripper section provides an additional parameter to adjust the primary beam attenuation which is used in particular at high current measurements.

The detector setup consists of a Microchannel Plate (MCP, Hamamatsu F4655-13) and a diamond detector separated at 80 cm , the drift length relevant for the TOF.

BEAM PROFILING AND MEASUREMENT AT MIBL

O. F. Toader and F.U. Naab,

Michigan Ion Beam Laboratory, University of Michigan, Ann Arbor MI, U.S.A.

Abstract

Michigan Ion Beam Laboratory (MIBL) is equipped with a 1.7 MV tandem particle accelerator and a 400 kV ion implanter. Ion beams can be produced from a variety of ion sources and delivered to different beamlines. Precise beam profiling and current measurements are critical aspects of everyday activity in the laboratory and influence the success of each experiment. The paper will present the devices used at MIBL to precisely determine the parameters of the ion beams in order to produce successful proton irradiations and ion implantations.

INTRODUCTION

The Michigan Ion Beam Laboratory (MIBL) is located in Ann Arbor and is a part of the Department of Nuclear Engineering and Radiological Sciences at the University of Michigan. The laboratory is equipped with a 1.7 MV Tandetron accelerator, a 400 kV ion implanter and an ion beam assisted deposition system (IBAD). The accelerator is a solid-state gas insulated, high frequency device, capable of operation between 0.4 and 1.7 MV (Fig. 1).



Figure 1: 1.7 MV Tandetron accelerator.

Various beams can be produced, starting with protons (up to 300 μA) and continuing with D^+ , He^+ , C^+ , O^+ , N^+ , heavier ions like Fe^+ and Ni^+ and many others. The Tandetron can operate with three types of sources: a Torvis by (NEC) [1] that reliably delivers proton and deuterium beams, a duoplasmatron 358 source (HVEE) [2] used mainly for Alfa particles for surface analysis and a sputtering source PS120 (Peabody Scientific) [3] used to produce heavy ions. The Tandetron has two beamlines; a 15° beamline for ion beam modification (implantation, and ion mixing) and radiation damage, and a 30° beamline for ion beam analysis, each terminated with a target chamber. Both beamlines contain a quadrupole triplet for focusing, an analyzing magnet, a raster-scanner and a steerer. The 15° beamline and the chamber are equipped with cryopumps that can routinely achieve pressures in the 10^{-9} Torr range.

Beyond the main chamber on the 15° beamline there is an electrically isolated irradiation sub-chamber. A temperature controlled sample stage can be attached next for radiation damage experiments (between 50 and 600 $^\circ\text{C}$). The 30° beamline contains an aperture system, a Faraday cup for charge collection, a beam viewer, a translation two-axis goniometer and detectors for backscattering and glancing angle measurements. It is turbo-pumped and equipped for rapid sample turn-around. Rutherford backscattering spectroscopy (RBS), nuclear reaction analysis (NRA), elastic recoil detection (ERD), and ion channelling are conducted in this chamber. All the control and monitor software programs for the proton irradiation and the Torvis source are written in Labview from National Instruments (NI) and were developed at MIBL

The 400 kV NEC is an air-insulated ion implanter (Fig. 2). The ion source Model 921 made by Danfysik [4] is designed for production of high current and high brightness ion beams. It is capable of ionizing materials that have low vapor pressure, and can produce ions by sputtering solid targets or by ionizing gases.



Figure 2: 2 NEC's 400 kV ion implanter.

The implanter can provide beams from most elements in the periodic table, with energies between 10 and 400 kV and with beam currents ranging from several microamperes to more than a milliampere (in some cases). Beam fluencies of up to 10^{20} atoms/cm² could be achieved in an area of a square inch in a few hours. Double ionization states for some elements (Ar^{2+} , O^{2+} , etc) allow for implants at energies of up to 800 kV. The target chamber and beam line operating pressure is in the 10^{-8} Torr range. A rotating carousel permits simultaneous loading of twelve 2-inch wafers, five 4-inch wafers or four 6-inch wafers for sequential implantation. The target chamber (3) is equipped with a 4-point Faraday cup system that allows for precise beam monitoring and dose measurements.

DESIGN AND OPERATION OF A CURRENT MONITOR UNDER HEAVY HEAT LOAD

P. A. Duperrex, P. Baumann, S. Joray, D. Kiselev, Y. Lee, U. Müller,
Paul Scherrer Institut, 5232 Villigen PSI, Switzerland

Abstract

For high intensity beam operation (3 mA, 1.8 MW) in the PSI 590 MeV 50 MHz cyclotron, a new current monitor for proton beams has been built. This monitor uses a re-entrant cavity tuned at the 2nd RF harmonic. Compared to the current monitors already in operation, the design has improved cooling. The circuit resonance has been optimized in the laboratory to minimize the gain drift due to temperature changes. Energy deposition simulations and thermal analysis were performed to estimate the cooling efficiency, and preliminary results indicate that the temperature rise of the resonator corresponds to values predicted with MARS. Anomalous gain drift is nevertheless observed even with an active cooling system. A drift compensation scheme using a pilot signal 600 kHz off the designed resonator frequency is being presently tested and the preliminary results are encouraging.

INTRODUCTION

A new proton beam current monitor called "MHC5" has been installed in the PSI 590 MeV proton cyclotron. The current monitor is located approximately 8 m behind a 4 cm thick graphite target used for muon and pion production. As a consequence, the monitor is exposed to scattered particles and their secondaries from this target. The resulting thermal load is the main concern for this monitor. This problem will be even acuter for future high intensity beam operation (3 mA, 1.8 MW). Thus the main improvements of the new monitor were an active water cooling system and a surface blackening to improve the radiation cooling.

MAIN FEATURES

Measurement Principle

The current monitor consists of a TM₀₁-mode coaxial resonator, coaxially symmetric with the round proton beam pipe. The resonator is modelled as a quarter-wave transmission line, the open-end gap in the beam pipe couples some of the wall current into the resonator. The cavity is tuned at 101.26 MHz, the 2nd harmonic of the proton beam pulse frequency. This frequency is used because of the better signal-to-noise ratio, the RF noise components from the generator being mainly at the odd harmonics. No significant shape dependency of the 2nd harmonic amplitude for relative small beam pulses is expected [1]. The oscillating magnetic field in the resonator is used to measure the beam current.

Resonance Condition

For a given resonant frequency, using an external capacitor shunt reduces the physical length of the resonator. The corresponding resonance condition is given by:

$$\tan\left(\frac{2\pi L}{\lambda_m}\right) = \frac{\lambda_m}{2\pi c C Z_0}$$

with L the resonator length, C the capacitor shunt, Z_0 the characteristic impedance of the transmission line, and λ_m the resonant wavelength.

Mechanical Design

The monitor is made of aluminium (anticorodal 110), with a 10 μ m coating layer of silver to improve the electrical conductivity. Compared to the monitors already into operation, the thermal coupling conductance was increased to improve the efficiency of the active water cooling. The monitor itself being in vacuum, the external surfaces have been chemically blackened to increase the emissivity of the monitor to provide an additional cooling. Four type K thermocouples monitor the resonator temperature.

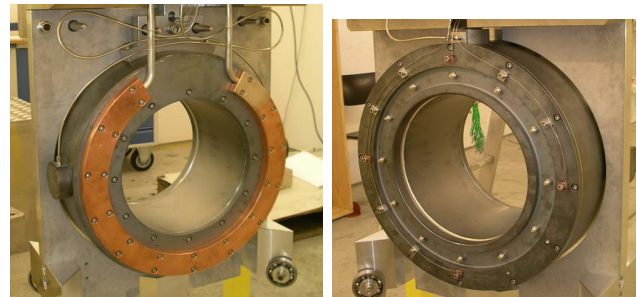


Figure 1: The new current monitor, showing the water cooling circuitry at the beam entry side (left). The four thermocouples are installed on the beam exit side (right).

Temperature Drift Compensation

Effect of temperature changes on the resonant frequency has been measured on a laboratory test bench before the installation of the monitor. External resonant circuits have been added to compensate the temperature drifts. Gain drifts smaller than 0.3dB were measured for the expected temperature variations during beam operation (30 to 70 °C).

A “NOT-INTERCEPTIVE” FARADAY CUP IN THE CNAO LOW ENERGY INJECTION LINES

G. Balbinot, J. Bosser, M. Caldara, L. Lanzavecchia, M. Pullia, A. Parravicini, Pavia, Italy
on behalf of the CNAO collaboration

Abstract

The CNAO, the first Italian synchrotron for deep hadron therapy [1, 2], is presently in its final step of installation. It will deliver beam of both Protons and Carbon ions, in three treatment rooms, in order to cure solid tumours with active scanning technique.

CNAO beams are generated by two ECR sources, able to produce both particle species, and transferred to a RFQ and a LINAC through a Low Energy Beam Transfer line (LEBT) at 8 keV/u and then accelerated up to 7 MeV/u before being injected in the synchrotron ring.

At the end of the LEBT line, just upstream the RFQ (L2-011A-IC1 in Fig. 1), an electrostatic Chopper deviates the beam on the vacuum chamber except for about 100 micro-seconds every 2 seconds, in order to shape the particles batch according to LINAC requirements and to minimize the beam losses at the RFQ entrance. An electrically insulated vacuum pipe section hit by the deviated beam allows reading the LEBT beam current: this detector is called Chopper Faraday Cup (CFC) and is based on the Faraday Cup working principle: it results a “not-interceptive” monitor that is able to measure, continuously, the source beam current ripples and stability, without affecting the beam delivered to the synchrotron. The CFC detector is presently under commissioning and preliminary results are presented.

CFC DESCRIPTION

The CFC is a detector installed in the LEBT line, devoted to monitor, continuously, source current ripples and stability, even during treatments, without affecting the beam delivered to the synchrotron: the goal is the monitoring of beam current slow variations due to sources instabilities and ripples. This implies that the system should be able, in the worst case, to have 1% resolution of the minimum nominal beam current, which corresponds to 1.5 μ A, according to LEBT beam parameters at chopper level (Table 1).

The CFC key idea (Fig. 2) consists of insulating the vacuum chamber sector downstream the chopper and measuring the collected current: the cup measures the full beam intensity while the Electrostatic Chopper is powered. The result is an on-line monitor based on the Faraday Cup (FC) principle but not interceptive for the beam directed to the synchrotron: it will be blind only when the beam is directed into the LINAC section, that is nominally 100 μ sec every 2 sec. Like a conventional Faraday Cup, the CFC is constituted by a body (A to B on Fig. 2), collecting the charge to be measured, and a repeller, aiming to push back the secondary emitted

electrons produced by the beam-to-body interaction, whose escape would affect the measurement. The CFC body is the insulated section of the vacuum chamber where the beam is bent; it is showed grounded by a “resistance” in Fig. 2. The voltage across the “resistance” is proportional to the LEBT current. It is defined by inserting two insulating gaskets at its extremities. CFC length and diameter are optimized to the Chopper kick range and to the beam rigidity (Table 2).

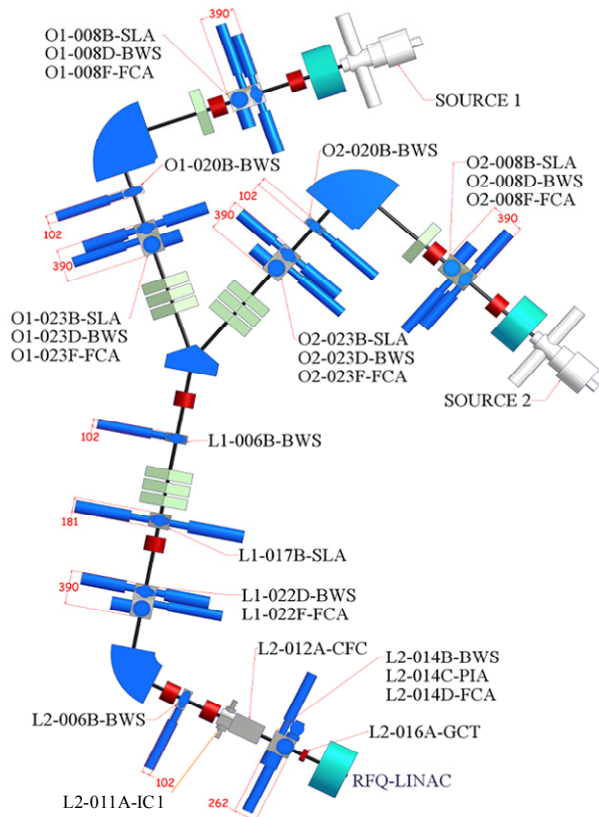


Figure 1: LEBT Instrumentation Layout with elements names. SLA are Slits, BWS are Wire Scanner in both planes, FCA is Faraday Cup, CFC is the Chopper Faraday Cup, PIA is Profile Grid, GCT is a current transformer and IC1 is the electrostatic chopper.

The repelling field, aimed to send back secondary electrons to the body, is generated by a metallic cylinder having an aperture where the beam is expected to pass (Fig. 2); this cylinder is inserted into the CFC tank and grounded, while the chamber is polarized with a positive voltage ($V_{bias} = 50\div 100V$) and so protected with a Plexiglas cover (Fig. 3) for safety.

BEAM BASED MEASUREMENTS OF THE RF AMPLITUDE STABILITY AT FLASH USING A SYNCHROTRON RADIATION MONITOR

Ch. Gerth, F. Ludwig and Ch. Schmidt

Deutsches Elektronen-Synchrotron DESY, D-22603 Hamburg, Germany

Abstract

To exploit the short radiation pulses in pump-probe experiments at single-pass free-electron lasers, stabilization of the longitudinal profile and arrival time of the electron bunches is an essential prerequisite. Beam energy fluctuations, induced by the cavity field regulation in the accelerating modules, transform into an arrival time jitter in subsequent magnetic chicanes used for bunch compression due to the longitudinal dispersion. The development of beam based monitors is of particular importance for the validation and optimization of the cavity field regulation. In this paper we present bunch-resolved energy jitter measurements that have been recorded with a synchrotron radiation monitor at the Free-electron LASer in Hamburg (FLASH). The (rms) beam energy jitter was determined to be $8.8 \cdot 10^{-5}$, and the cavity field detectors of the accelerating module have been identified as the main noise source within the cavity regulation system with an (rms) amplitude fluctuation of $6.5 \cdot 10^{-5}$. The reduction of deterministic cavity field imperfections by applying a feedforward learning algorithm for the cavity field regulation is demonstrated.

INTRODUCTION

Stable and reliable user operation of the Free-electron LASer in Hamburg (FLASH) requires precise control and stabilization of the RF accelerating amplitudes and phases. This is in particular true for RF accelerating fields prior to bunch compressors, as the ultra-short electron bunches with high peak currents are produced by off-crest acceleration in combination with magnetic dipole chicanes. Small fluctuations in the energy chirp rate may cause unacceptable peak current and bunch arrival time jitters. For instance at FLASH, RF amplitude and phase stabilization of about 10^{-4} and 0.01° are required to achieve peak current variations on a percent level.

A schematic of the FLASH injector is shown in Fig. 1. The RF photo-cathode gun is directly followed by the super-conducting 1.3 GHz accelerating module ACC1 which accelerates the electrons to a beam energy of typically 130 MeV. The module comprises eight 9-cell niobium cavities with a very high quality factor, i.e. very narrow bandwidth and very long response times. The maximum feedback gain g_0 that can be applied in the low-level RF (LLRF) system for the regulation of ACC1 is limited due to instabilities generated by the digital control loop, and, therefore, imperfect compensation of effects such as beam loading may occur.

A deviation of the beam energy $\Delta E/E$ transforms into a

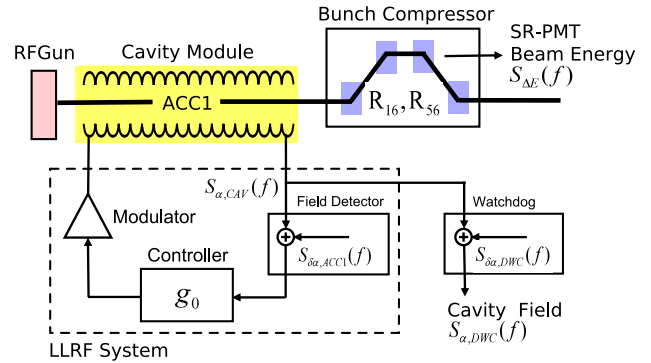


Figure 1: Schematic of FLASH injector.

horizontal beam displacement Δx in the dispersive section of the bunch compressor (BC) downstream of ACC1 and a beam arrival time difference Δt at the end of the BC given by (first order transport theory, $\beta \simeq 1$):

$$\Delta x = R_{16} \cdot \frac{\Delta E}{E} \quad \text{and} \quad \Delta t = R_{56} \cdot \frac{\Delta E}{E}, \quad (1)$$

where $R_{16} \approx 300 - 400$ mm and $R_{56} \approx 140 - 230$ mm are the the horizontal and longitudinal dispersion of the BC. The beam energy can be determined by recording the beam position Δx with a synchrotron radiation (SR) monitor.

SR MONITOR

The SR emitted in the third dipole of the first BC at FLASH is imaged by a SR monitor which comprises an intensified CCD camera (SR-Camera) and a multi-array photomultiplier tube (SR-PMT). By utilizing a beam splitter, both the SR-camera and SR-PMT can be used simultaneously.

The SR-camera [1] records the full x-y projection of the electron bunches. By adjusting the gate and delay of the camera timing, single bunches or any number of subsequent bunches can be chosen out of a bunch train. However, the readout of the CCD is too slow to resolve more than one electron bunch within a bunch train.

Two adjacent anodes of the SR-PMT [2] are used to measure the centre-of-gravity beam position which is given by the normalized difference signal s of both anodes:

$$s = \frac{I_1 - I_2}{I_1 + I_2}, \quad (2)$$

where I_1 and I_2 are the signal intensities of each anode.

DETECTORS FOR ABSOLUTE LUMINOSITY MEASUREMENT AT DAFNE

G. Mazzitelli[#], M. Boscolo, F. Bossi, B. Buonomo, F. Murtas, G. Sensolini, P. Raimondi, INFN LNF,
Frascati, Italy

N. Arnaud, D. Breton, L. Burmistrov, A. Stocchi, A. Variola, B. Viaud, LAL, Orsay, France

P. Valente, INFN Roma, Rome, Italy

P. Branchini, INFN Roma Tre, Rome, Italy

M. Schioppa, INFN Cosenza, Rende, Italy

Abstract

The Frascati electron-positron collider DAFNE is testing the crabbed waist scheme, aiming to reach a large improvement of the specific and integrated luminosity of the accelerator. In order to have a reliable, fast and accurate measurement of the absolute luminosity, a number of dedicated detectors have been designed, built, tested, calibrated and put into operation.

INTRODUCTION

At the Frascati DAFNE accelerator, running at the Φ meson peak ($\sqrt{s}=1.02$ GeV), the idea of enhancing the luminosity of an electron/positron collider with the introduction of a large Pwinski angle and low vertical beta function compensated by crab waist [1], is being tested. The accelerator has been modified to test the crab waist sextupoles compensation scheme and has restarted operations at the beginning of year 2008. Dedicated detectors have been installed for the measurement of the luminosity and the backgrounds.

Luminosity Detectors

Three different types of detectors using different physical processes are used, with different degrees of statistical and systematic accuracy:

- resonant decay $e^+e^- \rightarrow \Phi \rightarrow K^+K^-$: a set of scintillators (Kaon monitor) has been installed around the vertical axis ($\theta \sim 90^\circ$) by the SIDDHARTA collaboration to count back-to-back high-ionization tracks: a rate of about 25 Hz at 10^{32} is expected.
- The elastic (Bhabha) scattering $e^+e^- \rightarrow e^+e^-$: two calorimetric detectors have been placed on both sides of the interaction region (IR) to detect back-to-back tracks with energy deposit of about the beam energy ~ 510 MeV. Even though the polar angle is limited due to the presence of the low- β quadrupoles, the rate expected in the covered acceptance of $18^\circ \leq \theta \leq 27^\circ$ is high enough (~ 440 Hz at a luminosity of $10^{32} \text{ cm}^{-2} \text{ s}^{-1}$) to provide a clean measurement on-line.

The radiative Bhabha process: $e^+e^- \rightarrow e^+e^-\gamma$; it has the advantage of a very high rate and that the emission of highly collimated photons (95% of the signal is contained in a cone of 1.7 mrad aperture), but it is heavily affected by backgrounds. In particular beam losses due to interactions with the residual gas in the beam-pipe,

Touschek effect, and particles at low angles generated close to the IR. Very limited space is available at very small angles, close to the beam pipe, so that compact crystal calorimeters have been realized, in order to count events with a radiated photon.

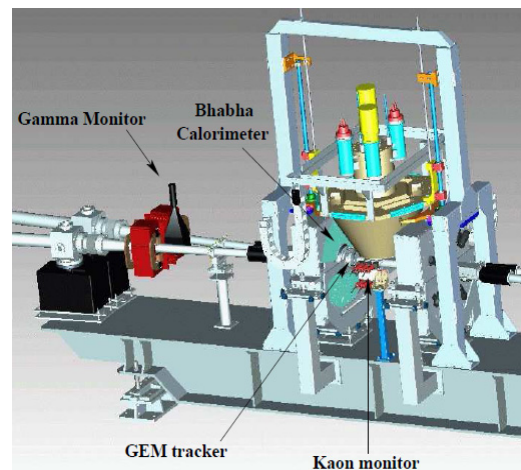


Figure 1: View of the DAFNE interaction region, with the detectors for luminosity measurement around the SIDDHARTA experiment setup.

BHABHA DETECTORS

The Bhabha monitors consist of two different detectors: a couple of calorimeters and two GEM trackers of annular shape, on either sides of the IR.

Calorimeters

Two modules of calorimeters surround each of the two final permanent quadrupole magnets, located at a distance of 32.5 cm on both sides of the IR, as shown in Fig. 1. Each of the four modules are segmented in the azimuth angle in five sectors, 30° wide. A $1/6$ of the acceptance, i.e. the $\pm 15^\circ$ region, has not been instrumented, both for leaving space for the supporting structure, and for the high rate of background events expected on the machine plane.

Each sector is a sandwich of 12 trapezoidal tiles of 1cm thick scintillator, wrapped with Tyvek, alternated with lead plates: eight 5 mm thick plates towards the interaction point and three 1cm thick plates in the back part, for a total thickness of 19 cm. This choice was

HIGH DYNAMIC RANGE SPECTRAL ANALYSIS IN THE kHz BAND

M. Gasior, A. Boccardi, CERN, Geneva, Switzerland

Abstract

Many beam instrumentation signals of large circular accelerators are in the kHz range and can thus be digitised with powerful high resolution ADCs. A particularly large dynamic range can be achieved if the signals are analysed in the frequency domain. This report presents a system employing audio ADCs and FPGA-based spectral analysis, initially developed for tune measurement applications. Technical choices allowing frequency domain dynamic ranges beyond 140 dB are summarised.

INTRODUCTION

The large market for PC sound cards and audio processing devices has resulted in the availability of excellent and inexpensive audio ADCs. Often they have two channels and are accompanied by two (or more) DACs in a single chip, commonly referred to as “codec”. Good audio ADCs have 24-bit resolution with excellent linearity given by the Σ/Δ architecture and datasheet signal-to-noise ratios (SNRs) in the order of 100-120 dB, corresponding to some 16-20 effective number of bits. The remaining bits normally contain noise, but as this is to a large extent white noise, it can be lowered by spectral analysis or time domain filtering, resulting in an increased dynamic range. Since the frequency domain SNR improves as $\sqrt{N/2}$ for an N -point FFT, for 4K-point FFT one gains some 33 dB and for 64K-point FFT the gain is about 45 dB, giving potential SNRs above 160 dB.

As illustrated in Fig. 1, the presented spectral analysis system is based on an audio codec, connected to a digital acquisition board (DAB) through an LVDS link. The DAB, hosting a large FPGA and memory, is a standard CERN acquisition/processing VME board used for most of the LHC beam instrumentation systems. In the discussed system the DAB stores the acquired data and performs FFT calculation, prior to transmitting raw data and calculated spectra to a VME front-end computer (FEC). The FEC, connected to the control infrastructure by a fast Ethernet link, makes the data available for end applications [1].

As the DAB-based real-time FFT analysis providing 180 dB dynamic range is described in [2], this paper

focuses on the remaining crucial aspects of the system, making it a powerful, inexpensive high dynamic range acquisition and spectral analysis system.

24-BIT ADC/DAC MODULE

The system described in this paper was built primarily for the LHC tune and chromaticity measurement systems [1], which process two beam signals and provide two excitation signals that are band-limited to half the revolution frequency ($f_r \approx 11.2$ kHz for the LHC). An audio stereo codec with two ADCs and two DACs was the natural choice for the core of the system. Since system prototypes were studied at the CERN SPS ($f_r \approx 43$ kHz) and BNL RHIC ($f_r \approx 78$ kHz), the design is compatible with all these machines.

The 24-bit ADC/DAC circuit was built not as a VME module, but in a NIM format, at the expense of having an additional crate in the system. This solution offered more room to accommodate input and output insulation transformers, which have substantial dimensions as they carry low frequency signals of relatively large amplitudes. Furthermore, NIM chassis typically offer lower levels of electromagnetic interference, since they usually contain analogue electronics in shielded modules, and as they provide power supplies of good quality that are less subject to perturbations from complex digital modules rare in NIM chassis.

From the many audio codecs available in the market Cirrus Logic CS4272 was selected, a 28-pin chip containing two 24-bit ADCs and two 24-bit DACs with differential inputs and outputs. The choice was a compromise between the chip performance and complexity, mainly of the configuration protocol. Its datasheet SNR is 111 dB and the maximal sampling frequency (f_s) 200 kHz, however, its best SNR was found to be for f_s below 50 kHz.

The codec inputs and outputs allow differential architecture for the input amplifiers and low pass filters (LPFs) as well as for differential output interpolation LPFs. This increases the immunity to interference and the dynamic range.

Despite the fact that the 24-bit ADC/DAC module

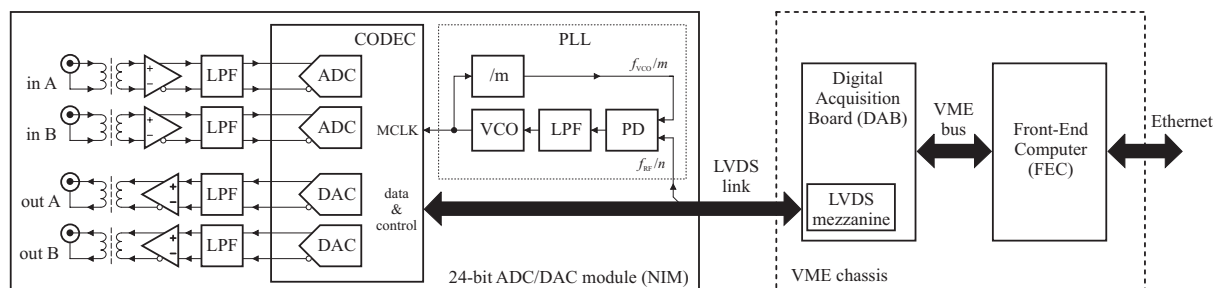


Figure 1: Block diagram of the kHz range spectral analysis system.

MACHINE PROTECTION SYSTEM FOR PETRA III

T. Lensch, M. Werner

Deutsches Elektronen Synchrotron DESY, Hamburg, Germany

Abstract

The basic design for the machine protection system (MPS) for the light-source PETRA III is discussed. High synchrotron radiation can damage absorbers and vacuum chambers. Therefore the MPS identifies alarm conditions from different systems, including the beam position monitors (BPM), temperature and vacuum systems and creates a dump command within 100µs. For diagnostic purposes a post-mortem trigger is implemented and a first alarm detection is planned. The initial commissioning of the MPS with its alarm-delivering systems is described.

INTRODUCTION

The former electron and proton preaccelerator PETRA II was reconstructed into a high brilliant X-ray source. PETRA III will operate at 6 GeV. The circumference of the accelerator is 2.3 km. In the first step a beam current of 100mA is planned, the goal is 200mA [1]. The experiments are placed behind 14 undulator beamlines. Absorbers and beam chambers in the damping wiggler section and the undulator section have to be protected against synchrotron radiation. Closed vacuum shutters in the whole storage ring have to be protected as well against the electron beam. A dump trigger from the MPS is connected to the RF system which stops delivering power to the beam. The beam will be lost within 1ms at a dedicated scraper. In addition the beam shutters will be driven into the beam.

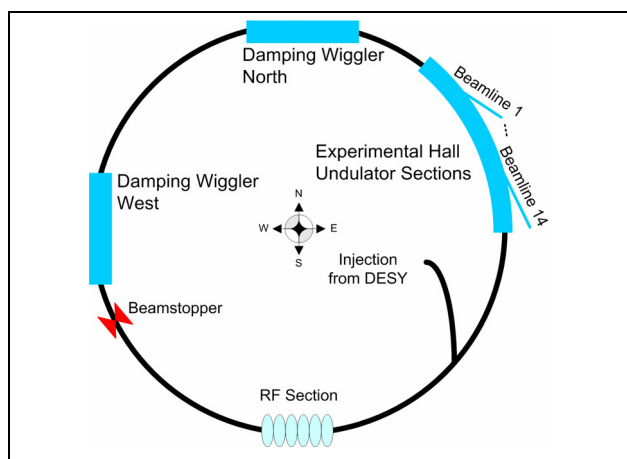


Figure 1: Overview PETRA.

MPS SPECIFICATION

The MPS should provide a dump trigger within 100µs after alarms are received. After a beam loss the MPS should provide a post mortem trigger which is delivered

04 Beam Loss Detection

to other systems. In order to locate the initial alarm which triggered the dump, a first alarm detection should also be implemented.

About 170 alarms are connected to the MPS to protect the machine against damage from synchrotron radiation or the electron beam. Further 50 alarms are connected to the MPS for optimizing the first alarm detection. The alarms are distributed over nine PETRA halls but with main contributions from the damping wiggler sections and the experimental hall. Partially alarms are merged to one alarm for the MPS. The Tables 1 - 3 give an overview of all alarms connected to the MPS.

Table 1: Dump Triggering Alarms

System	Total Count of Alarms	Inputs at MPS
Beam Position Monitors	95	95
Temperature	260	17
Vacuum Shutters	35	8
Fast Vacuum Shutters	14	14
Personnel Interlock	1	1
Getter pumps	26	13
Vacuum Hand Shutters	14	4
Water Flow	33	5
Screen Monitor	1	1
Total	479	158

Table 2: Alarms for Masking Other Inputs

System	Inputs at MPS
Undulator Gaps	14
Damping Wiggler Gaps	2
Total	16

Table 3: Alarms First Alarm Detection

System	Total Count of Alarms	Inputs at MPS
Magnet Power Supplies	700	42
RF System	8	8
Total	708	50

LHC BLM SINGLE CHANNEL CONNECTIVITY TEST USING THE STANDARD INSTALLATION

J. Emery, B. Dehning, E. Effinger, G. Ferioli, C. Zamantzas, CERN, Geneva, Switzerland
H. Ikeda, KEK, Ibaraki, Japan; E. Verhagen, IceCube, UW-Madison, USA

Abstract

For the LHC beam loss measurement system (BLM), the high voltage supply of the ionisation chambers and the secondary emission detectors is used to test their connectivity. A harmonic modulation of 0.03 Hz results in a current signal of about 100pA measured by the beam loss acquisition electronics. The signal is analyzed and the measured amplitude and phase are compared with individual channel limits for the 4000 channels. It is foreseen to execute an automatic procedure for all channels every 12 hours which takes about 20 minutes.

The paper will present the design of the system, the circuit simulations, measurements of systematic dependencies of different channels and the reproducibility of the amplitude and phase measurements.

TEST PURPOSE AND PRINCIPLE

The primary purpose of this test is to ensure the integrity of the cabling of each beam loss monitor. By adding a small harmonic modulation signal on the high voltage supply of the monitors, it is possible to detect a small current on the measurement side (Fig. 1). If anywhere in the signal chain a cable is missing, disconnected or discontinued for any reason, the measurement will not show any harmonic variation of the current.

The second goal is to survey the integrity of the components. The measured amplitude and phase of every channel (monitor or spare) is compared to a predefined threshold measured for every channel. If one of them is outside the limits, the test will fail and the beam permit [1] will not be raised.

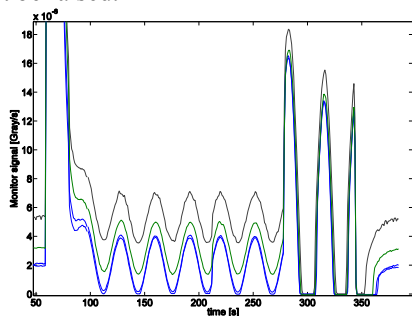


Figure 1: Four ionisation chamber signals modulated.

LHC BLM SYSTEM

The LHC BLM system is organised in eight different groups. Each group has a high voltage power supply, which covers two half arcs and one straight section. For each group, there are three or four crates, which can hold up to 256 channels each, connected to one ionisation chamber (IC) or two in certain case (IC2) or one

04 Beam Loss Detection

secondary emission monitor (SEM). Each monitor has a low pass filter with a serial resistor and a capacitor used to store charges. With this structure, the surface power supply can be small. When a beam loss or a variation of the high voltage occurs, charges are moving to the tunnel card BLECF [2]. This card integrates charges for 40 μ s and sends the result digitally to the surface electronic threshold comparators BLETC [3]. Longer integration windows (running sums) are then computed. When a connectivity test is performed, the central processing unit (CPU) sends one of the running sums every second to the combiner and survey card BLECS for analysis (Fig. 2).

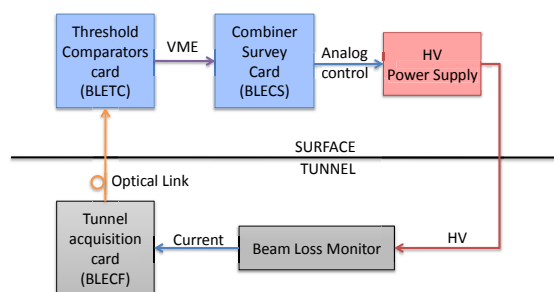


Figure 2: The LHC BLM system looped for the connectivity test.

Connection to the Beam Interlock System

The LHC BLM system is connected to the beam interlock system through the CIBUS interface [1]. There are two of these interfaces per point. One is for unmaskable and the other for maskable channels. The BLM system receives from this interface the status of the global beam permits (beam info). The BLM logic used to generate the beam permits includes the results of various system tests including the connectivity test.

Hardware Timers and Test Triggering

The LHC BLM system includes two hardware timers to ensure regular testing of the system. The first timer is linked to the "system test" which includes the connectivity test. The second one is linked to the online check [4] which ensures agreement between settings held inside the front-end and in the LSA database. If the tests are not triggered within a fixed time, the next injection will be blocked through the beam permits lines. To allow LHC operation again, the tests have to be triggered and their results need to be satisfactory.

When a test is requested by the internal timer, the BLM system raises a status bit and the LHC sequencer (or a manual operation) triggers the test. No test can start if there is beam inside the machine (hardware check of the beam info).

UPGRADE OF THE TIMING SYSTEM AT THE AUSTRALIAN SYNCHROTRON

E. van Garderen, M. ten Have, G. LeBlanc, A. Starritt, K. Zingre
Australian Synchrotron, Melbourne, Australia

Abstract

The Australian Synchrotron (AS) timing system is based on a hybrid design: an Event Generator-Event Receiver (EVG-EVR) system creates the injection trigger and various clocks, while a network of digital delay generators adjusts pulse delays and widths. This architecture, combined with a storage ring fill pattern monitor, allows the targeting of injection into specific buckets in the storage ring. Nevertheless, more demanding needs from the machine and the beamlines require an upgrade of the system. Delay generators will be removed and replaced by EVRs. This will allow fixed or variable frequency clocks to be made available to beamlines or to trigger diagnostic hardware in a flexible way, while reducing jitters to below 100 ps.

INTRODUCTION

The Australian Synchrotron is a 3rd generation light source [1]. It consists of a 100 MeV linac, a 100 MeV to 3 GeV booster synchrotron and a 3 GeV storage ring composed of 14 sectors. The storage ring can store up to 200 mA. First beam was delivered to users in 2007 and, currently, eight of the nine beamlines are in operation.

The timing system was partly commercially delivered. Its in-house design was limited to the storage ring fill pattern monitor, AC synchronization and a down-graded EVG/EVR-200 to provide just the storage ring orbit clock for diagnostics and the injection trigger.

The first improvement in 2007 included the upgrade to the EVG/EVR-230RF with Radio Frequency (RF) recovery. The event system gun transmitter (GTX) and receiver (GRX) were also added to improve jitter performance of the electron gun while replacing the original LiteLink fibre optics transmission system.

This upgrade will replace all the delay generators and other smaller parts to improve reliability and maintainability, with easy-to-program signals.

TIMING REQUIREMENTS

The AS injection process uses a static injector [2] with a repetition rate of 1 Hz. Buckets are targeted by delaying the whole injector from the gun to the injection of the electrons into the storage ring instead of just the extraction from the booster. All trigger signals are therefore fixed with respect to the gun that can be delayed in ~ 2 ns steps, given by the RF from the Master Oscillator: $f_{RF} = 499.671838$ MHz ± 20 kHz. Moreover, the injection system is synchronized

03 Time Resolved Diagnostics and Synchronization

Table 1: Summary of relevant timing requirements

Clocks	Frequency
RF	499.671 MHz
Event Clock	125 MHz
SROC	1.38 MHz
Items	Trigger Delay/Width
GUN	
Gun single-bunch	181.4 μ s / 1 ns
Gun multi-bunch	181.4 μ s / up to 150 ns
LINAC	
500 MHz pre-buncher	175 μ s / 140 ns
3 GHz electron multiplier	184 μ s / 140 ns
MAGNETS	
Booster injection septum	0 ns / 300 μ s
Booster injection kicker	175 μ s / 10 μ s
Booster ramping magnets	2 ms / 500 μ s
Booster extraction septum	601 ms / 100 μ s
Booster extraction kicker	601 ms / 5 μ s
SR injection septum	601 ms / 1 μ s
SR injection kicker	601 ms / 830 ns

to the 50 Hz mains frequency (AC sync) to minimize the influence of the AC heated linac modulator and gun.

The 90 keV gun can be run in single-bunch or multi-bunch modes. Multi-bunch mode is limited by the size of the booster ring and speed of the kicker magnets for up to a bunch train of 75 buckets. The single-bunch trigger requires a very low jitter of a few tens of picoseconds to optimize capture in the booster, whereas the multi-bunch trigger does not have those tight demands because bunches are separated by the 500 MHz modulation of the gun.

Most triggers require TTL, CML or LVPECL levels terminated into 50 Ω and a few optical links. All triggers should have low jitter performance of a few hundreds of picoseconds, as discussed further. Table 1 summarizes important trigger requirements.

PRESENT ARCHITECTURE

The current hybrid timing features the event system [3] from Micro Research Finland, including a VME-EVG-230RF, two VME-EVR-230RF, an optical fanout VME-OUT-12, a GTX VME-GUNTX-200, plus a stand-alone GRX GUNRC-202, and delay generators DG535s from Stanford Research Systems and with details shown in Fig. 1.

FIRST MEASUREMENTS OF THE LONGITUDINAL PHASE SPACE DISTRIBUTION USING THE NEW HIGH ENERGY DISPERSIVE SECTION AT PITZ*

J. Rönsch[†], G. Asova[‡], J. Bähr, C. Boulware, H.J. Grabosch, L. Hakobyan[§], M. Hänel, Y. Ivanisenko
M. Khojayan[¶], M. Krasilnikov, B. Petrosyan, S. Rimjaem, A. Shapovalov^{||}, L. Staykov^{**},
R. Spesyvtsev, F. Stephan, DESY, 15738 Zeuthen, Germany
S. Lederer, DESY, 22761 Hamburg, Germany
J. Rossbach, Hamburg University, 22761 Hamburg, Germany
D. Richter, HZB für Materialien und Energie, 12487 Berlin, Germany

Abstract

The Photo Injector Test facility at DESY, Zeuthen site, (PITZ) develops and optimizes high brightness electron sources for Free Electron Lasers (FELs) like FLASH and the European XFEL. A new multi-purpose dispersive section was designed [1, 2] and installed to characterize the momentum distribution, the longitudinal phase space distribution and the transverse slice emittance of the electron bunch for an electron energy up to 40 MeV. The spectrometer consists of a 180 degree dipole magnet followed by a slit, a quadrupole magnet and two screen stations. One of the screen stations allows the measurement of the longitudinal phase space distribution. The first measurement results and corresponding beam dynamics simulations of the momentum and the longitudinal phase space distributions will be reported in this contribution. The resolution of the system will be analysed and compared to the design expectations.

INTRODUCTION

The main goal of PITZ is to test and to optimize L-Band RF photo injectors for Free-Electron Lasers (FELs) like FLASH and XFEL at DESY in Hamburg and to study the emittance conservation by using a matched booster cavity. The demands on such a photo injector are a small transverse emittance, a charge of about 1 nC and short bunches (of about 20 ps). Besides the accelerating (gun and booster) cavities, the electron beam line of PITZ consists mainly of diagnostics elements. In 2008 a new multi-purpose dispersive section was installed downstream the booster cavity to characterize the momentum distribution, the longitudinal phase space distribution and the transverse slice emittance [3] of the electron bunch for an energy up to 40 MeV.

*This work has partly been supported by the European Community, contract numbers RII3-CT-2004-506008 and 011935, and by the 'Impuls- und Vernetzungsfonds' of the Helmholtz Association, contract number VH-FZ-005.

[†] jroensch@ifh.de

[‡] On leave from INRNE, Sofia, Bulgaria

[§] On leave from YerPhi, Yerevan, Armenia

[¶] On leave from YerPhi, Yerevan, Armenia

^{||} On leave from MEPHI, Moscow, Russia

^{**} On leave from INRNE, Sofia, Bulgaria

THE SETUP

Figure 1 shows the layout of the new installed first high-energetic dispersive arm (HEDA1). It consists of a 180 degree dipole spectrometer (deflecting in vertical direction) followed by an insertable slit, a quadrupole magnet (DISP2.Q1) and two screen stations (DISP2.Scr1&2). The first screen stations (DISP2.Scr1) is equipped with a YAG-screen imaged onto a 8-bit TV-camera¹ for momentum measurements and a Cherenkov radiator (Silica aerogel, thickness of 5 mm and a refractive index of $n = 1.05$) [4] to measure the longitudinal phase space distribution using an extended optical read-out and a streak camera [5]. All the results presented in this paper have been made using DISP2.Scr1. DISP2.Scr2 is currently mainly used for transverse slice emittance measurements [3] which are not presented in this paper.

The position where a particle hits the screen after passing the dipole magnet depends on the momentum, the transverse position and the angle of the particle before it enters the dipole spectrometer, according to the first order transport matrix:

$$y_{DA} = R_{11}y_0 + R_{12}y'_0 + R_{16}\frac{\Delta p_0}{p_0}, \quad (1)$$

where y_0 , y'_0 and $\frac{\Delta p_0}{p_0}$ are the position, divergence and relative momentum deviation of the particle at the entrance of the dipole magnet and R_{11} , R_{12} and R_{16} are the dipole matrix elements. For a 180 degree dipole spectrometer without pole face rotation these values become:

$$R_{11} = -1, \quad R_{12} = -L_{DA}, \quad R_{16} = 2r, \quad (2)$$

with L_{DA} the drift length between the dipole exit and the screen station where the measurement is performed and r the deflecting radius.

When the dipole magnet is switched off the vertical position of a particle at longitudinal position L_{drift} downstream the dipole entrance is given by:

$$y = 1y_0 + L_{drift}y'_0. \quad (3)$$

¹In the future this 8-bit camera will be replaced by a 12 bit camera with a higher sensitivity

MEASUREMENT DEVICES FOR THE SPARC SYNCHRONIZATION SYSTEM

M. Bellaveglia, D. Alesini, A. Gallo, C. Vicario,
INFN-LNF, Via Enrico Fermi 40, Frascati, Italy

Abstract

The SPARC FEL facility is under commissioning at the Frascati National Laboratories of INFN. The synchronization system is working as expected and various devices are used to monitor its performances. In particular this paper is focused on a comparison between the results obtained using different methods and instruments to perform laser, RF and beam synchronization measurements. Both electro-optical and full electrical techniques are used to obtain information about the phase noise of the RF fields inside the accelerating structures, the phase noise of the IR laser oscillator, the time of arrival of the laser UV pulse on the cathode and the time of arrival of the accelerated electron bunch at a selected reference position along the linac.

INTRODUCTION

The SPARC project is now under its commissioning phase at the Frascati National Laboratories of INFN. First FEL lasing in the SASE regime has been observed and other experimental activities are on the way [1]. The synchronization system is working as expected. Its performance has been recently upgraded using a new scheme and also new diagnostic devices have been installed, as described later in this document.

System Layout

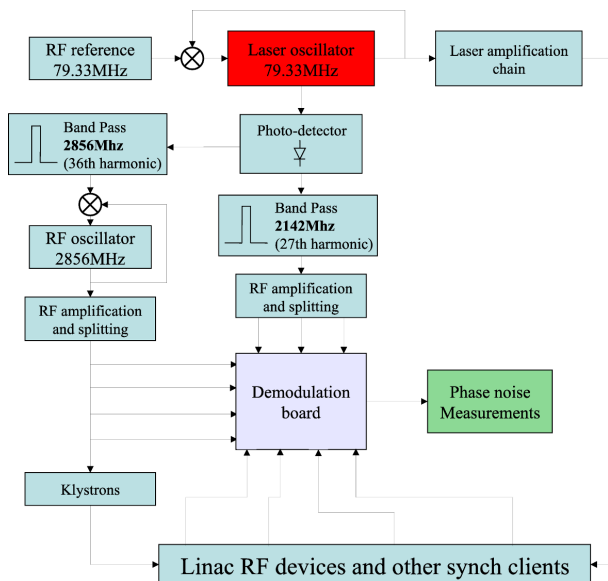


Figure 1: Layout of the synchronization system of SPARC.

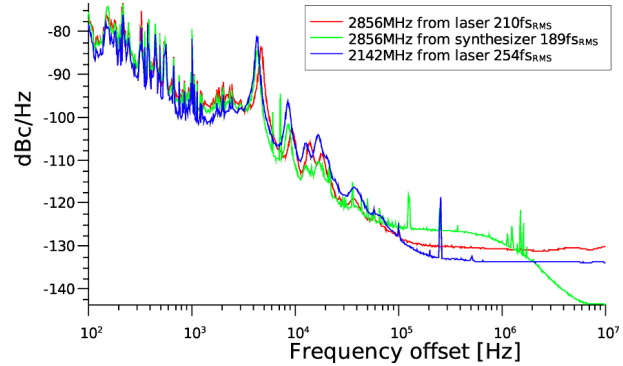


Figure 2: Phase noise spectra of the RF reference signals with integrated absolute jitter (from 100 Hz to 10 MHz).

The synchronization system has been modified and upgraded respect to the one operating during the last SPARC run [2]. We chose to use the Ti:Sa oscillator of the photocathode laser as optical master oscillator (OMO) instead of using a RF synthesizer. Doing this, we can bypass the electro-mechanical PLL used to synchronize the laser cavity oscillation to the RF reference. This loop has a bandwidth of ≈ 5 kHz and was the main limitation of the SPARC synchronization system. Using the new scheme and starting from the laser cavity frequency, we can lock the RF synthesizer to that, using a PLL with a larger bandwidth (≈ 1 MHz). Thus the RF-to-laser relative jitter results pretty much reduced, as reported later in this paper. The long term frequency stability of the laser cavity is granted by a 79.3 MHz signal coming from a RF synthesizer and squared by dedicated standard NIM electronics. The PLL around the oscillator cavity make use of both the fundamental and the 9th harmonic to lock the laser repetition rate.

Reference Generation

As described in Figure 1, the RF reference signals are obtained by the 79.3 MHz pulse train coming from a solid state 10 GHz bandwidth photodetector illuminated by the laser Ti:Sa oscillator. In particular we used two filters to isolate the 27th (2142 MHz) and the 36th (2856 MHz) harmonic of the laser repetition rate. The signal has been also pre-filtered after the photodetector to eliminate the fundamental frequency and the unwanted harmonics that could generate distortion in the RF amplification process. Actually a commercial RF synthesizer from Rhode&Schwarz is used to generate the reference sent to the RF power stations. We used its FM port to close a PLL to have a copy of

YTTERBIUM FIBER LASER FOR ELECTRO-OPTICAL PULSE LENGTH MEASUREMENTS AT THE SWISSFEL

F. Müller*, S. Hunziker, V. Schlott, B. Steffen, D. Treyer, Paul Scherrer Institute (PSI), Switzerland
T. Feurer, University of Bern, Switzerland

Abstract

Pulsed Yb fiber lasers emit at 1030 nm which provides a better phase matching in standard EO crystals (GaP, ZnTe) than the wavelength of Ti:Sa lasers (800 nm). We present a mode locked ytterbium fiber laser which is phase locked to the RF. A subsequent fiber amplifier is used to boost the power and to broaden the spectrum due to nonlinear effects. The produced pulses have a spectral width of up to 100 nm and are therefore suitable for EO bunch length measurements, especially for spectral decoding.

INTRODUCTION

In accelerator diagnostics the knowledge of the electron bunch length and the temporal structure plays an important role. Electro optical (EO) techniques offer the possibility for non destructive single shot pulse length measurements [1]. This laser based method requires an environmentally stable and robust laser system with a small jitter and a broad spectrum. Ytterbium (Yb) fiber lasers fulfill these criteria. Yb has a number of interesting properties as a small quantum defect which leads to high pump efficiencies, a long upper state lifetime, a broad gain spectrum and a good phase matching to the THz field in GaP and ZnTe crystals [2, 3]. Combined with the advantages of fiber based systems, as compactness, freedom from misalignment and robustness, Yb fiber laser systems offer an attractive alternative to Ti:Sa lasers for EO measurements. Besides, the price of an Yb laser system is only a fraction of the costs of a Ti:Sa laser system. The EO setup contains the fiber laser and a compact bunch length monitor [4].

LASERSYSTEM

Setup

The laser consists of an oscillator and a single pass amplifier. A schematic of the oscillator is depicted in Fig. 1. The ring resonator has a fiber and a free space part. The latter is basically necessary for dispersion compensation and for the mode locking mechanism, which is based on nonlinear polarization evolution (NPE) [5]. The polarization state is controlled by the three wave plates, which allow to rotate the polarization in a way, that the short and intense part of the pulse remains in the oscillator where the rest, which underwent less polarization rotation is coupled out

*felix.mueller@psi.ch

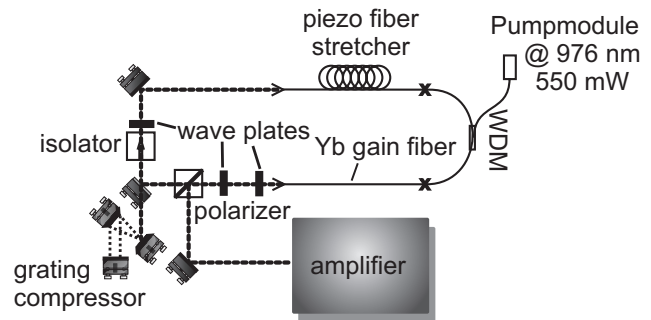


Figure 1: Scheme of the oscillator; WDM, wavelength division multiplexer

by the polarizer. This fast and passive effect is responsible for mode locking. The unidirectional way of propagation is defined by the isolator. The amplification and the pumping is done in fiber. The piezo stretcher modulates the resonator length and therefore the repetition rate, which is used to synchronize the laser to a reference signal.

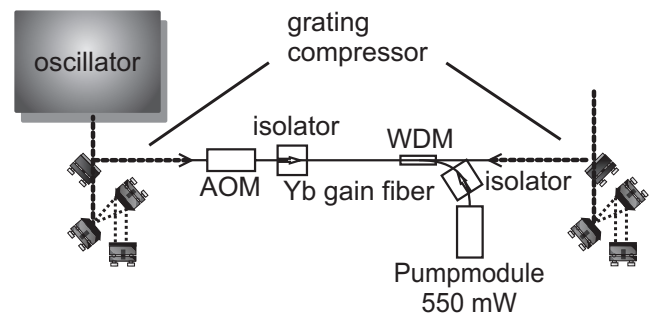


Figure 2: Scheme of the amplifier; AOM, acousto optic modulator; WDM, wavelength division multiplexer

The amplifier is shown in Fig. 2. After the oscillator a first grating compressor modulates the pulse width in order to compensate the dispersion of the following fiber section. The AOM reduces the repetition rate which allows to boost the pulse energy without increasing the average power. Near the end of the fiber, the amplified pulses become short, the intensity increases and strong nonlinear effects occur which broaden the spectrum.

The according spectra are shown in Fig. 3. In the inset plot the spectrum of the oscillator is depicted, which has a spectral width of about 40 nm. It has the typical parabolic shape of self similar pulses [6]. After amplifi-

ULTRA-FAST MM-WAVE DETECTORS FOR OBSERVATION OF MICROBUNCHING INSTABILITIES IN THE DIAMOND STORAGE RING

G. Rehm, A.F. Morgan, Diamond Light Source, Oxfordshire, U.K.

R. Bartolini, I.P. Martin, DLS, Oxfordshire and John Adams Institute at Oxford, U.K.

P. Karataev, John Adams Institute at RHUL, London, U.K.

Abstract

The operation of the Diamond storage ring with short electron bunches using low alpha optics for generation of Coherent THz radiation and short X-ray pulses for time-resolved experiments is limited by the onset of microbunching instabilities. We have installed two ultra-fast (time response is about 250 ps) Schottky Barrier Diode Detectors sensitive to radiation within the 3.33-5 mm and 6-9 mm wavelength ranges. Bursts of synchrotron radiation at these wavelengths have been observed to appear periodically above certain thresholds of stored current per bunch. The fast response allows a bunch-by-bunch and turn-by-turn detection of the burst signal, which facilitates study of the bursts structure and evolution. In this paper we present our first results for various settings of alpha and also discuss future plans.

INTRODUCTION

Diamond Light Source has recently started an experimental programme for the generation of short radiation pulses in the storage ring. Dedicated low-alpha optics[1] have been developed and tested for users providing radiation pulses as short as 1 ps r.m.s. Both X-ray time resolved experiments and THz users are expected to benefit from such operating mode. In order to study microbunching instabilities and the potential for coherent emission at mm and sub-mm wavelengths, additional diagnostic instrumentation has been installed.

EXPERIMENTAL SETUP

Schottky Barrier Diode (SBD) detectors are common devices at microwave and mm-wave applications. In com-

Table 1: Specifications of the two Schottky Barrier Diode Detectors (terminated into 50 Ω) and Connected Standard Gain Horn Antennas [2, 3]

Detector Model	DXP-22-RPFW0	DXP-12-RPFW0
Frequency range	33-50 GHz	60-90 GHz
Video sensitivity	40 mV/mW	23 mV/mW
Video bandwidth	1 GHz	1 GHz
Horn Model	SGH-22-RP000	SGH-12-RP000
Gain [dB]	24	24
Input aperture	55 mm · 42 mm	30 mm · 23 mm

03 Time Resolved Diagnostics and Synchronization

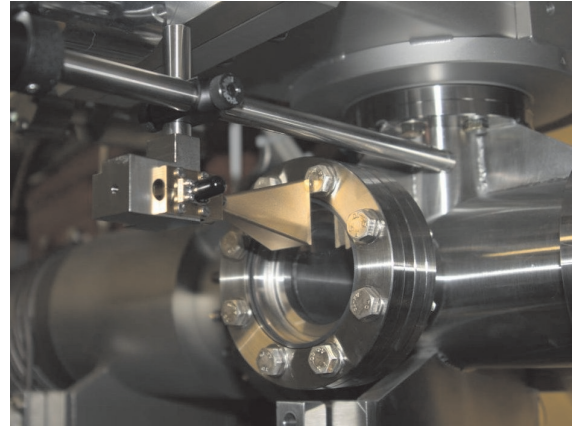


Figure 1: Photo of the 60-90 GHz detector with horn antenna mounted next to the visible light extraction.

parison to other detectors for mm and sub-mm-wavelengths like bolometers and Golay cells they have a very fast response, allowing turn by turn observation of emissions. The only alternative with similarly fast response are hot electron bolometers, which are more expensive, delicate and space consuming due to the required dewar. While at microwave frequencies SBD detectors are typically packaged with coaxial connectors, for mm-wave frequencies they are waveguide mounted, which limits their bandwidth. Coupling to free space fields is then achieved using a horn antenna, for instance of pyramidal design.

For the evaluation of SBD detectors to detect mm-wave synchrotron radiation emissions, we have mounted two types of detector with the according horn antenna near the window of the visible light extraction used for optical diagnostics (streak camera and fill pattern measurement from photon counting). The two detectors from Millitech differ in their frequency range, sensitivity and dimensions, and were mounted one at a time, as the current setup does not provide the space to mount both at the same time without interfering with the visible light transport. The frequencies of the two detectors have been chosen close to the vacuum vessel cutoff, estimated to be 54 GHz from the relation $f_c = 2h\sqrt{h/\rho}$ with our total vertical aperture $h = 38$ mm and the bending radius $\rho = 7.13$ m.

Figure 1 show the setup where the detector can be seen mounted off centre near the window, so that visible light which comes from a mirror inside the vessel [5] can still pass beneath the horn antenna. The detector is oriented to

FIRST LIGHT FOR OPTICAL TRANSITION RADIATION MONITOR AT THE J-PARC*

A. Toyoda, K. Agari, E. Hirose, M. Ieiri, Y. Katoh, A. Kiyomichi, M. Minakawa, T. Mitsuhashi, R. Muto, M. Naruki, Y. Sato, S. Sawada, Y. Shirakabe, Y. Suzuki, H. Takahashi, M. Takasaki, K.H. Tanaka, H. Watanabe, Y. Yamanoi, High Energy Accelerator Research Organization (KEK), 1-1 Oho, Tsukuba, Ibaraki, Japan

H. Noumi, Research Center for Nuclear Physics (RCNP), 10-1 Mihogaoka, Ibaraki, Osaka, Japan

Abstract

We have continuously developed the Optical Transition Radiation (OTR) monitor with optics system based on the Newtonian telescope to measure a profile for a high intensity proton beamline. Now we installed the OTR monitors of production version on the J-PARC hadron beamline, and successfully observed a first OTR light. This led to the establishment of high S/N profile measurement with minimum beam disturbance. At this commissioning stage, beam intensity is expected to be as small as 1.2 kW, but expected to increase up to 750 kW, so that maintenance work becomes important. To improve ease of maintenance, we plan to replace the focusing lens system with reflective mirror system with higher resistance to radiation. A result of beam profile measurement, an estimation of dependence of an OTR background on a beam loss, and a future plan for an upgrade of our optics system will be presented.

INTRODUCTION

We have finished constructing first stage J-PARC hadron facility to provide high intensity proton beam whose design intensity is 750 kW for various particle and nuclear physics experiments such as strangeness nuclear physics, exotic hadron physics, kaon rare decay physics, and so on. A 50 GeV proton beam is slowly extracted via switchyard (SY) section into T1 target (Ni disk; 30 % beam loss). It is crucial to minimize a beam loss to observe the beam status by various monitors for such high intensity beamline. For this purpose, the OTR monitor is one of the best solutions because the OTR is a surface phenomenon so that we can minimize a screen thickness. Thus the OTR is widely used at electron and proton facility for the profile measurement [1-3]. We have developed the OTR monitor for a profile measurement at the upstream part of the SY section.

OPTICS DESIGN AND INSTALLATION

We performed a test experiment at KEK 12-GeV PS with proto-type OTR monitor, and realized that it is important to reduce background and radiation to detector system [4]. Therefore, we prepared an OTR optics system like Catadioptric-type telescope and planned to put this system 5 m away from a beamline. Detailed design and optimization are described in Ref. [4].

After the fine tuning of each component of optics system, we installed the OTR chamber and optics system, and finely aligned them with a beamline. As shown in Fig. 1, OTR1 is installed just upstream of a q01 quadrupole magnet, OTR2 is just upstream of a q02 quadrupole magnet, and OTR3 is just upstream of a v04 vertical steering magnet.

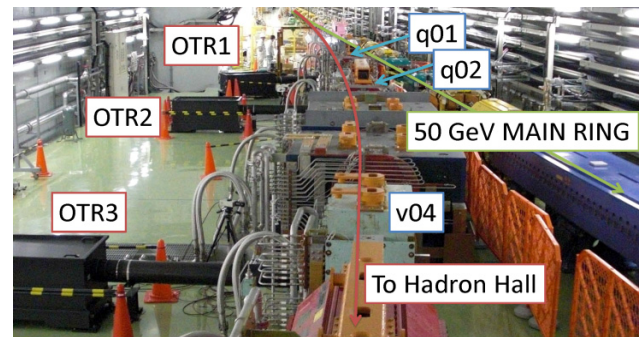


Figure 1: Layout of OTR monitors.

Figure 2 shows the OTR optics layout. There is an OTR screen (Al foil, 7 μm thickness) with rotating drive mechanism which enables to remove and install the screen remotely inside the OTR chamber. An OTR light emitted downward at the screen is first reflected by a planer mirror, and introduced into the dark box containing the OTR optics.

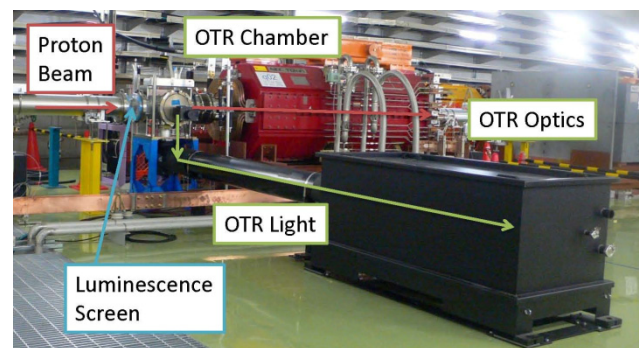


Figure 2: OTR optics installation upstream of q02.

*Work supported by Grant-in-Aid for Young Scientists (B) (20740155), and Grant-in-Aid for Scientific Research (A) (17204019)

BEAM TRANSVERSE PROFILE MONITOR BASED ON RESIDUAL GAS IONIZATION FOR IFMIF-EVEDA ACCELERATOR

J. Marroncle, P. Abbon, F. Jeanneau, J.-P. Mols, J. Pancin, CEA Saclay, DSM/IRFU, France

Abstract

Within the framework of IFMIF-EVEDA project, a high-intensity deuteron (125 mA - 9 MeV) prototype accelerator will be built and tested at Rokkasho (Japan) in order to validate the future IFMIF accelerator. One of the most challenging diagnostics is the Beam Transverse Profile Monitor (BTPM), which has to be a non-interceptive device. Two R&D programs have been initiated: one based on residual gas fluorescence developed by CIEMAT Madrid (see J. Carmona et al. contribution) and another one based on residual gas ionization developed at CEA Saclay [1]. The principle of the last one is to measure the current induced by ionization electrons, drifting under an electric field influence, towards several strips to get a one-dimension projection of the transverse beam profile. Preliminary results of a first prototype tested on the IPHI Saclay accelerator will be shown, as well as a new prototype design. In the new design several improvements have been carried out. The new detector will be tested soon with continuous and pulsed beam at higher energy.

INTRODUCTION

The International Fusion Materials Irradiation facility (IFMIF) aims at producing an intense flux of 14 MeV neutrons, in order to characterize materials envisaged for future fusion reactors. The primary mission of IFMIF is to provide a materials irradiation database for the design, construction, licensing and safe operation of the future Fusion Demonstration Reactor (DEMO) [2]. In such a reactor, high neutron fluxes may generate up to 30 dpa/fpy (displacements per atom / full power year). IFMIF facility is based on two high power continuous drivers (175 MHz) delivering 125 mA deuteron beams at 40 MeV each, colliding with a liquid lithium target.

In the framework of the “Broader Approach”, the IFMIF-EVEDA (Engineering Validation and Engineering Design Activities) project includes the construction of an accelerator prototype with the same characteristics as IFMIF, except a lower energy of 9 MeV instead of 40 MeV for the incident deuteron energy. Most of the components of the accelerator are developed by France, Italy and Spain. Accelerator parameters are

- 125 mA cw deuteron beam at 175 MHz (5.7 ns)
- Vacuum pipe pressure level: 10^{-5} mbar (at target region) and below 10^{-7} mbar elsewhere.

In such high current accelerator, non-interceptive diagnostics are required. This paper will focus on a Beam Transverse Profile Monitor (BTPM) based on beam residual gas ionization.

05 Beam Profile and Optical Monitors

Firstly, we will present the main beam test results which were obtained using a first prototype. A new prototype was designed with respect to conclusions coming from the previous test. This will be described in a second part.

FIRST PROTOTYPE

This monitor is based on the ionization induced by the beam particles on the residual gas of the accelerator beam pipe [3] (Fig. 1). An electric field is applied between two parallel plates, on which electrons and ions are collected. A high voltage is applied to the upper plate while the lower plate is grounded. The lower plate consists of 32 conductive strips covering a 4x3 cm² surface. On each side of the active area 9 thin pads are set regularly in voltage in order to insure the electric field uniformity (each resistor is 60 M Ω). This monitor is fixed on a flange (DN100), which is held on the accelerator beam pipe.

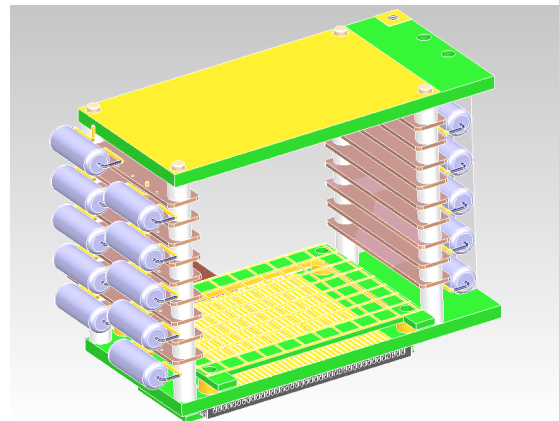


Figure 1: First prototype drawings.

Front-End Electronics

The currents induced by charges on the strips are read-out by a front-end electronic card developed in our group. The 32 channels are connected, via a kapton bus, to this card (Fig. 2).

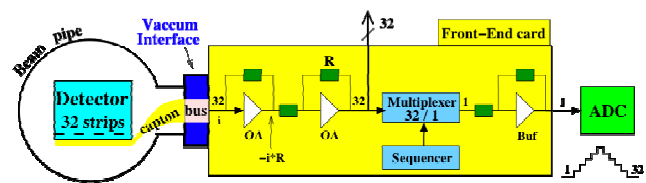


Figure 2: Front-end electronic sketch.

TARGET MATERIALS FOR A LOW ENERGY PEPPER-POT EMITTANCE DEVICE

M. Ripert, A. Peters, HIT, Heidelberg, Germany

Abstract

The ion cancer therapy facility HIT in Heidelberg [1] is producing ions (H, He, C and O) from two ECR sources at an energy of 8 keV/u with different beam currents from about 80 μ A up to 2 mA. Typical sizes for the beam in the LEBT range from are 5 – 30 mm. Matching the always slightly changing output from the ECR sources to the first accelerating structure, an RFQ, demands a periodical monitoring of the beam emittance. For that, a special pepper-pot measurement device is under design, whose most important parts are a damage-resistant pepper-pot mask and a vacuum-suitable scintillator material. The material lifetime, the list of feasible materials, the modelling of the target damage will be discussed.

PEPPER-POT SCINTILLATOR SCREEN DESIGN

As part of the ongoing development at HIT, and to provide necessary information for beam dynamics, high quality emittance and beam profile measurements are needed. A pepper-pot device is under investigation to provide a 4-D emittance measurement.

Location

The Pepper-Pot Scintillator Screen system should fit within the existing beam line components (vacuum boxes already used with beam diagnostics equipment like Faraday cups, profile grids and slits). The N1DK1 vacuum boxes will be equipped with a fast iris shutter, a pepper-pot mask and a scintillator screen. The N1DK2 vacuum boxes will contain a 45 degrees tilted mirror inside and a CCD camera outside. (Figure 1)

The Pepper-Pot Principle

The pepper-pot mask, which is perpendicular to the beam and contains a regular array of identical holes, splits the beam into beamlets. The beamlets drift toward the scintillator screen where they are imaged. The determination and the arrangements of the optical component must be designed in such a way that it meets its basic function requirements:

- The production of an image of a suitable size,
- The system should fit into the available space.

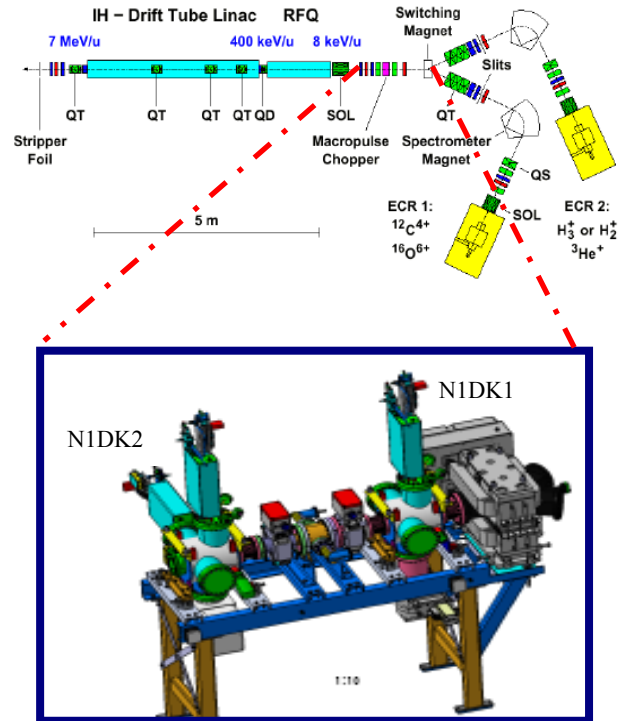


Figure 1: The Low Energy Beam Transport at HIT and the position of the Pepper-Pot Scintillator Screen device within the LEBT.

Some considerations [2] in the choice of the aperture parameters have to be followed so that:

- The beamlets images on the scintillator screen are larger than the mask aperture d ,
- The pepper-pot mask thickness, L_s , should be small enough to prevent any smearing effects due to multiple slit scattering
- The separation spacing, w , should be much larger than the mask aperture d to prevent the beamlets from overlapping at the screen.

Different optical systems have been designed along the previous set of rules [2] depending on the minimum beamlet width. From the arguments given above, a set of the pepper-pot parameters (Table1) with a 0.2 mm hole diameter, 1.5 mm separation, and 0.1 mm maximum depth was calculated.

SYNCHROTRON RADIATION MONITOR AND MIRROR AT SSRF

K.R. Ye, Y.B. Leng, J. Chen, J. Yu, G.B. Zhao, W.M. Zhou, Sinap, Shanghai, 210200, China
 T. Mitsuhashi, KEK, Japan

Abstract

SR monitor for the measurements of beam profile, sizes, and bunch length has been designed and constructed at the Shanghai synchrotron radiation Facility (SSRF). A water-cooled beryllium mirror is installed to extract the visible SR. This beryllium mirror was designed via thermal analysis based on ANSYS. The extracted visible SR is relayed to dark room by three mirrors. The measurement system includes, imaging system, SR interferometers (SRI), streak camera and fast-gated camera etc are set in the dark room. Both the horizontal and the vertical beam sizes are monitored by SRI, and bunch length and temporal profile of the beam are measured by streak camera. The existed system suffers with dynamic problem for beam physics studies. The commissioning of synchrotron radiation monitor system has been performed in SSRF since December, 2007. The results obtained at SSRF are presented.

GENERAL OVERVIEW

A diagnostics beamline has been installed in the BM02 bending magnet of the SSRF storage ring. The designed parameter of the SSRF is listed in Table1.

Table 1: Designed parameter of Storage Ring

parameters	Value
Energy (GeV)	3.5
Beam current (mA)	200-300
Critical photon energy (keV)	9.96
Emittance ϵ_x (nm.rad)	3.9
Beam profile σ_x (μm) 1% coupling	53
Beam profile σ_y (μm)	22
Bunch Length (ps)	14.4

Synchrotron radiation monitor measures beam profile and beam size of the synchrotron radiation light source for performance optimization, routine operation check and various beam physics study. The monitor should be able to measure a small transverse beam dimension and motion [1]. Using this monitor, we can characterize the electron beam size, phase-space ellipse and emittance. It is described that the general design of the SRM, extraction mirror design, and measurement equipments such as SR interferometer and streak camera in this paper.

05 Beam Profile and Optical Monitors

Instruction

The source point of for SRM is bending magnet near injecting point. The synchrotron light is extracted by a water-cooled beryllium mirror. Then three mirrors guide the light to the dark room. The synchrotron light interferometers [2] [3] is set in the dark room and they measure horizontal and vertical beam sizes. Also a focusing system is applied to obtain the image of beam profile. The result beam profile is passed on the display in the control. Bunch length measurements is performed with a streak camera (HAMAMATSU C5680) that uses a scan streaking of 125MHz (1/4 RF) and also dual time streaking is available. (Fig.1). The general arrangement of the SRM system is shown in Fig.1.

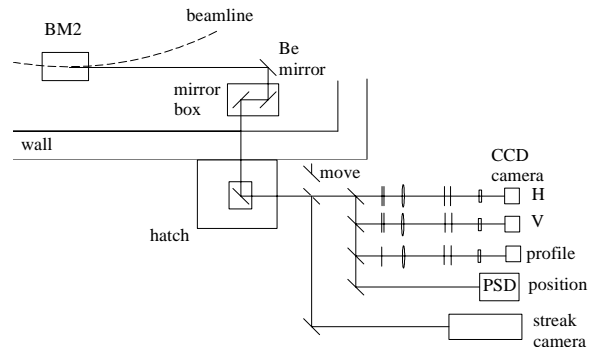


Figure 1: General arrangement of synchrotron radiation monitor.

EXTRACTION MIRROR

The vertical opening angle of visible SR is roughly 3mrad. 4mrad opening will be available in the horizontal direction. The visible part of the synchrotron radiation is reflected by water-cooled Beryllium mirror.

Water-cooled Beryllium Mirror

The first mirror is set 9m apart from the source point, which reflects the visible light by 90° downward. Thermal distortion of the Be mirror for a given absorbed heat load by X-rays is simulated using the technique of finite-element analysis. The deformation of the mirror has been studied in detail in comparison with other materials. The result shows Be is best material for the extraction mirror.

Thermal Distortion Analyse

A thermal-mechanical analysis experiments with electron beams show: the quality factor for different metals dynamic formation is indicated. The thermal distortion values for metals between 0°C to 400°C, these

TWO-DIMENSIONAL IONIZATION BEAM PROFILE MEASUREMENT*

M. Poggi, L. Boscagli, A. Dainese, R. Ponchia, INFN Laboratori Nazionali di Legnaro, Viale dell'Universita' 2, 35020, Legnaro, Padova, Italy

H.W. Mostert, J.L. Conradie, M.A. Crombie J.G. de Villiers, K.A. Springhorn, iThemba LABS, P.O. Box 722, Somerset West 7130, South Africa

Abstract

Equipment for non-destructive, two-dimensional beam profile measurement was developed for the high intensity beam project foreseen at INFN, Legnaro and the K200 variable-energy, separated-sector cyclotron at iThemba LABS. Ions, produced by the interaction of the beam with residual gas, are accelerated in an electrostatic field towards microchannel plates (MCP) for signal amplification. With the first of the two prototypes that were built, ions are accelerated in an electric field between two parallel plates and after passing through an aperture in one of the plates, move through the electric field between two curved plates and consequently bent through ninety degrees before reaching the MCP. The aperture in the plate provides one profile dimension and the spread in the energy of the produced ions the other dimension. In the second prototype two one-dimensional systems, rotated through ninety degrees with respect to each other, were installed in close proximity of each other. The beam profiles measured with both prototypes were compared with those measured with a nearby profile grid. Measurements were made on various beams and with intensities between 10 nA and 1 μ A.

BACKGROUND

One-dimensional residual gas beam profile monitors (RGBPMs) are already used successfully. Space limitations and the need to measure both dimensions of the beam at the same location, initiated the investigation of two-dimensional systems. iThemba LABS designed the first prototype, RGBPM-1, and was tested at the 6 MV Van der Graaff accelerator on site. It is based on the energy spread analyses method [1].

THE DESIGN OF RGBPM-1

In order to improve on previous designs, a different geometry, shown in Fig. 1, was developed for the analyzing field. Only electrostatic fields are used. Residual gas ions are accelerated in the collecting field and pass through a 1 mm extraction slit. The curved electrodes produce the analyzing field that bends the trajectory of the ions by approximately 90 degrees. Curved electrodes are chosen to assure that the electrostatic field remains perpendicular to the ion path. The aim is to obtain a linear projection of the two dimensional profile on the MCP surface. Ions created

further from the slit obtain additional acceleration, and because of their higher energy will be deflected less in the analyzing field. Those that are created in the collecting field at position *a* in Fig. 1 are deflected more than those created at position *c*. The vertical position information can therefore be recovered on the MCP. The horizontal information gathered in the collecting field is maintained in the analyzing field and is therefore also available on the MCP, as in the case of a one-dimensional system.

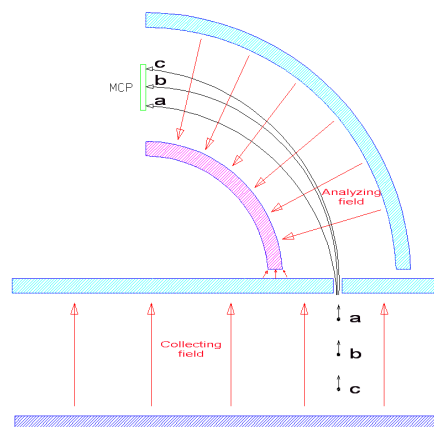


Figure 1: The electrostatic field in RGBPM-1.

Electric field calculations and particle orbit simulations were done with the program TOSCA [2], to determine the geometry as well as the potentials required on the electrodes. The calculations confirmed that beam profile information in both the horizontal and vertical directions can be obtained with this method as shown in Figures 2 and 3. For the current design, with central radius of the

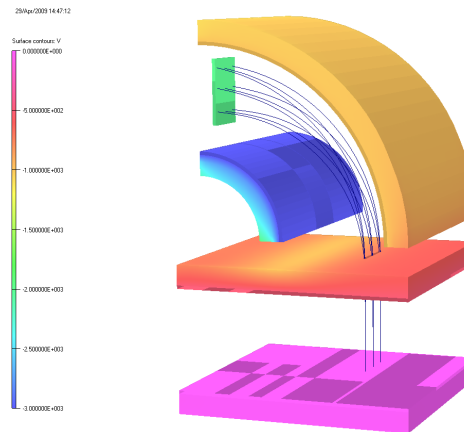


Figure 2: Calculated ion paths in the electrostatic fields of RGBPM-1.

*Supported by Istituto Nazionale di Fisica Nucleare, Italy and National Research Foundation, South Africa, project-code 15

INVESTIGATION OF THE LIGHT YIELD OF LUMINESCENT SCREENS FOR HIGH ENERGY AND HIGH BRILLIANT ELECTRON BEAMS

G. Kube, DESY, Hamburg, Germany
 W. Lauth, Institut für Kernphysik, Mainz, Germany

Abstract

Transverse beam profile diagnostics at electron accelerators is usually performed with optical transition radiation (OTR) monitors. For intense beams however, thermal load in the screen material may result in resolution degradation and even screen damage. To overcome this problem the beam can be swept over the screen, but the strong OTR light emission directivity will reduce the optical system's collection efficiency. In order to overcome these difficulties, luminescent screens can be used because of their robustness and isotropic light emission. Since only little information is available about scintillator properties for applications with high energy electrons, a test experiment has been performed in order to study the light yield of different screen materials under electron bombardment.

INTRODUCTION

For the European XFEL with a maximum beam energy of 20 GeV and an average beam power of up to 300 kW it is planned to install a beam profile monitor in the dump section in order to control beam position and size and to avoid damage of the dump window. OTR is widely used for transverse beam profile measurements with high energy electrons. Advantages of OTR are the radiation generation directly at the screen boundary in an instantaneous emission process, and the rather high light output emitted in a small lobe with an opening angle defined by the beam energy. For intense beams however, the thermal load from the particle interaction with the screen material results in a degradation of the image resolution and possible screen damage. To overcome this problem the beam can be swept over the screen, but in this case the strong OTR light emission directivity has the drawback of reducing the collection efficiency of the optical system. Therefore it is planned to use luminescent screens because of their robustness and isotropic light emission. While the use of luminescent screens at hadron machines is widespread (see e.g. Refs. [1, 2] and the references therein), there is little information about scintillator properties for applications with high energy electrons. At the SLC linac for example, screens based on phosphor ($Gd_2O_2S:Tb$ or P43) deposited on a thin aluminum foil were in use, showing no sign of damage after bombardment with up to $4 \times 10^{18} \text{ e/cm}^2$ [3]. To study the light yield of other scintillator materials, a test experiment has been performed which is described in the following.

05 Beam Profile and Optical Monitors

EXPERIMENTAL SETUP

Figure 1 shows the sketch of the experimental setup. The experiment was performed at the 855 MeV beam of the Mainz Microtron MAMI (University of Mainz, Germany) [4] in the beamline of the X1 collaboration, close to the beam dump which is located behind the vertical deflecting bending magnet BM2. The screens were mounted directly

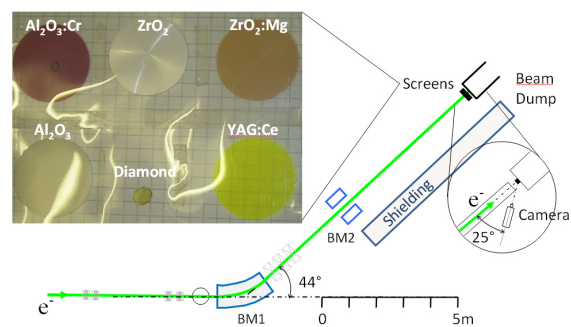


Figure 1: Screen test set-up in the X1 beamline at MAMI. The inset shows a photo of the screen materials under investigation.

in front of the dump in air. During beam exposure which lasted approximately one minute with a cw beam current of a few nA, the emitted luminescence light was observed via a standard Vidicon camera. The camera was located at a distance of about 1 m from the screens such that the loss of scintillation light intensity due to total reflection in the screen material was neglectable.

Table 1: Overview of the Screen Materials and Thicknesses Together with the Applied Beam Current

material	d / mm	current / nA
YAG:Ce	1	0.5
Diamond	0.2	1.9
Al ₂ O ₃	1	1.9
Al ₂ O ₃ :Cr (Chromox)	1	0.5
ZrO ₂ (Z700-20A)	1	32.4
ZrO ₂ :Mg (Z507)	1	32.4

Six different screens have been tested which are listed in Table 1 together with their thickness and the applied cw beam current. An industrial diamond crystal (Sumitomo Electric Industries [6]) together with four ceramic screens (BCE Special Ceramics [7]) were investigated with respect to their luminescence yield. The YAG:Ce crystal (Saint

CARBON FIBER DAMAGE IN ACCELERATOR BEAM

M. Sapinski, B. Dehning, A. Guerrero, J. Koopman, E. Metral, CERN, Geneva, Switzerland

Abstract

Carbon fibers are commonly used as moving targets in Beam Wire Scanners. Because of their thermomechanical properties they are very resistant to particle beams. Their strength deteriorates with time due to radiation damage and low-cycle thermal fatigue. In case of high intensity beams this process can accelerate and in extreme cases the fiber is damaged during a single scan. In this work a model describing the fiber temperature, thermionic emission and sublimation is discussed. Results are compared with fiber damage test performed on SPS beam in November 2008. In conclusions the limits of Wire Scanner operation on high intensity beams are drawn.

INTRODUCTION

In order to validate beam heating model [1] and to determine the breakage mechanism of the $33\ \mu\text{m}$ carbon fiber, a damage test has been performed on the SPS beam at CERN in November 2008. The final goal of the test was to verify the predictions of the limits for the wire damage in LHC beam and conclude about the specifications of the future Scanner.

EXPERIMENTAL CONDITIONS

A rotational Wire Scanner equipped with electronics which allow to measure wire resistivity and thermionic emission during the scan has been used in the experiment. The scanner contains two wires which scan the beam in horizontal and vertical directions. It can reach the scan speed of 6 m/s and performs two scans called IN and OUT. The speeds of both scans and interval between them are set independently. This interval has been set to at least 1 second to allow cooling the wire. In this test the scan IN was always performed with maximum speed and the speed of scan OUT was gradually slowed down from scan to scan in the following sequence: 6, 3, 1.5, 1, 0.8, 0.7, 0.6, 0.5 m/s. Two other Wire Scanners have been used during the test to constrain additionally the beam parameters.

A special beam cycle on CERN SPS accelerator has been prepared for this test. Beam intensity has been maximized and reached about $N_{\text{prot}} = 2.4 \cdot 10^{13}$ circulating protons. In order to diminish the effect from RF-coupling [2] the beam has been debunched. A 12-second long flat-top plateau has been kept providing enough time to perform measurements in stable beam conditions. Beam momentum was 400 GeV/c.

05 Beam Profile and Optical Monitors

WIRE BREAKAGE

The wires have been broken in conditions summarized in Table 1, where σ_1 is the beam width along and σ_t perpendicular to the scan direction (the beam is assumed to have Gaussian transverse profiles). The breakage occurred after a sequence of scans, therefore the wire has already been weakened by preceding scans. In addition the wires installed in the scanner have been used since at least a year and have performed unknown number of scans (typically a few thousand).

Table 1: Beam Conditions at Wire Breakage

scan speed	N_{prot}	σ_1 [mm]	σ_t [mm]
0.5 m/s	$2.41 \cdot 10^{13}$	0.57	0.73
0.7 m/s	$2.18 \cdot 10^{13}$	0.73	0.57

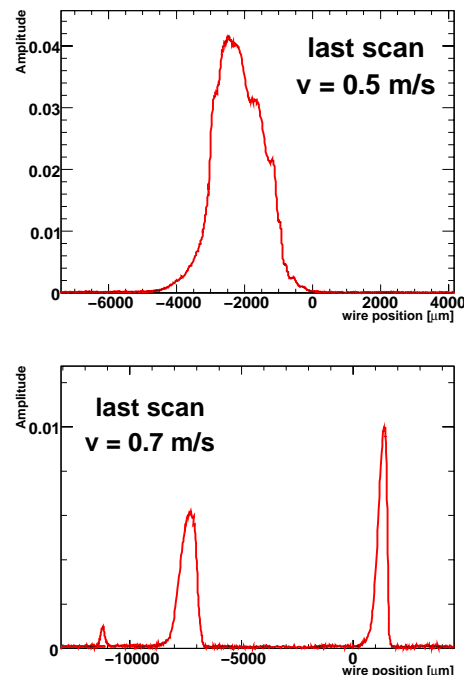


Figure 1: The last profiles after which the wire has been found broken. Upper plot shows breakage of vertical wire: deviations from Gaussian profile are visible. The bottom plot shows breakage of the horizontal wire: multiple peaks suggest that the wire has already fragmented.

In Fig. 1 the beam profiles registered during the last scans are shown. The deviations from Gaussian shape and

STATUS OF THE LASER-BASED BEAM PROFILE INSTRUMENT FOR THE RAL FRONT END TEST STAND

D.A. Lee, P. Savage, Imperial College London, U.K.
 J. Pozimski, Imperial College London U.K. / STFC/RAL, Chilton, Didcot, U.K.
 C. Gabor, STFC/RAL/ASTeC, Chilton, Didcot, U.K.

Abstract

The RAL Front End Test Stand is under construction with the aim of demonstrating production of a high-quality, chopped 60 mA H^- beam at 3 MeV and 50 pps. In addition to the accelerator development, novel laser-based diagnostics will be implemented. This paper reports on a device that will be able to measure multiple profiles of the beam density distribution in such a way that the full 2D density distribution can be reconstructed. The device is currently being commissioned. The status of the device is presented together with results of the commissioning and plans for future development.

INTRODUCTION

The Front End Test Stand is currently under construction at RAL. It will eventually consist of a high-brightness, 65 keV H^- ion source; a three solenoid Low Energy Beam Transport (LEBT); a 324 MHz, four-vane Radio Frequency Quadrupole (RFQ) that will accelerate the beam to 3 MeV; a Medium Energy Beam Transport (MEBT) section incorporating a beam chopper; and a comprehensive suite of diagnostics.

First beam was achieved from the ion source on 30 April (see Figure 1 and [1] for details). Regular operation is anticipated to begin by the end of June 2009, at which time beam commissioning of the laser-based profile monitor described in this paper will begin. A laser-based emittance monitor that will measure the emittance after the MEBT at 3 MeV is also under development; it is described in [2].

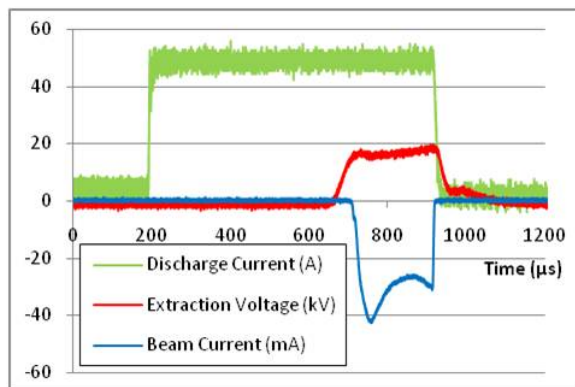


Figure 1: An oscilloscope trace of the first beam from the FETS ion source [1]

LASER-BASED H^- BEAM DIAGNOSTICS

Lasers can be used to diagnose H^- beams by the photo-detachment of the outer electron of the H^- ions, via the process $H^- + \gamma \rightarrow H^0 + e^-$. The detached electrons or neutralised H^0 atoms can then be used to diagnose the beam; in the case of the profile monitor, the electrons are used. (The emittance monitor uses the neutralised H^0 atoms.) The detached electrons are separated from the ions (and the neutralised H^0) by a dipole magnet and the number of electrons is measured by a Faraday cup. This technique is illustrated in Figure 2. For the instrument described in this paper, due to the low energy of the electrons detached from the 65 keV H^- ions, it is also necessary to accelerate the electrons (in this case by a 2 kV electric field) to reduce any possible deflection by stray fields.

By having a laser with a beam diameter significantly smaller (~ 1 mm) than the ion beam diameter (~ 50 mm), stepping the laser beam across the ion beam and counting the number of electrons detached at each laser position, a projection of the ion beam onto a plane can be built up. A series of mirrors mounted on movable stages inside the vacuum vessel be used to step the laser beam across the ion beam. Additionally, the mirrors can be rotated and so the laser beam can pass through the ion beam at a variety of angles such that a projection onto any arbitrary plane can be measured. This is illustrated in Figure 3. A series of measurements at a variety of angles can be combined tomographically to give a full, correlated 2D beam profile. For this instrument, the measurements will be combined using the Algebraic Reconstruction Technique [3, 4].

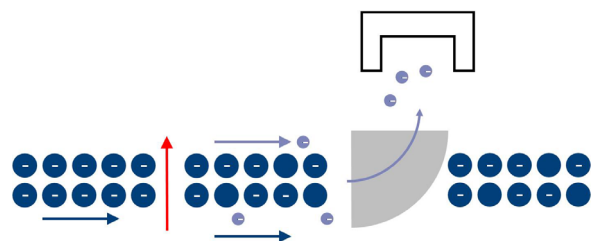


Figure 2: An illustration of the laser-based profile monitor principle. The laser (red) detaches some electrons (light blue) from the H^- ions (dark blue), which are then deflected by a dipole magnet (grey) into a Faraday cup.

DESIGN OF A NEW EMITTANCE METER FOR LINAC4

B. Cheymol, E. Bravin, C. Dutriat, T. Lefevre, CERN, Geneva, Switzerland

Abstract

LINAC4 is the first step in the upgrade of the injectors chain of the Large Hadron Collider (LHC). This Linac will accelerate H^- ions from 45 keV to 160 MeV. During the commissioning phase of LINAC4 transverse emittance measurements will be required at 45 keV, 3 MeV and 12 MeV. For this purpose a slit&grid system is currently being developed. The material and the geometry of the wires and of the slit need to be optimized in order to minimize the negative effects of the energy deposition and maximize the signals. This document describes the results of the studies carried out during the design of the emittance meter.

LINAC4

LINAC4 is an H^- linear accelerator with a maximum energy of 160 MeV intended to replace the present 50 MeV proton linac (LINAC2) as injector for the Proton Synchrotron Booster (PSB). In the present configuration the PSB represents the bottleneck in terms of beam brightness for the LHC. By injecting into the PSB a beam of higher energy and by using the phase-space painting technique, possible thanks to the use of H^- ions, the brightness and intensity of the beams produced by the PSB will double. In order to push the performances of the LHC even further additional upgrades of the injectors are foreseen. In the second step both the PSB and the Proton synchrotron (PS) will be replaced by a superconducting proton linac (SPL) and a new proton synchrotron, the PS2. [1]

EMITTANCE MEASUREMENT

The transverse phase-spaces (x and y) describe the distribution of particles in x and x' (y and y'), where x (y) is the position of the particles and x' (y') the angle between the trajectory of the particle and the longitudinal axis of the beam (z). The aim of the emittance meter is to sample the transverse phase-spaces from which the emittance can be calculated.

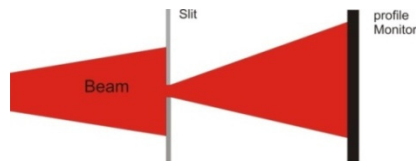


Figure 1: Slit and grid system.

As show in Fig. 1 and Fig. 2 a slit and grid system can be used to sample the transverse phase-space. In this technique the slit is used to select particles within a

narrow slice in position, then, in the following drift space, the angular distribution of the particles transmitted through the slit is transformed into a position distribution and sampled using a profile monitor, in our case a secondary emission grid. By scanning the slit across the beam, the whole phase-space is reconstructed.

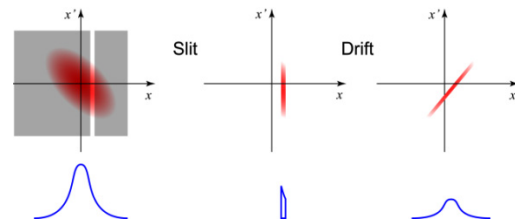


Figure 2: Phase-space sampling using a slit and grid system.

Each wire of the grid is connected to a separate acquisition channel and sampled at 250 kHz, this allows the observation of the evolution of the emittance along the linac pulse. The diameter and the material of the wires are chosen in order to reduce the thermal effects induced by the beam and provide an adequate signal.

In order to sample both transverse planes two slits and two SEM-grids are needed. (see Fig. 3)



Figure 3: The emittance meter of LINAC4.

MULTIPLE SCATTERING AND THERMAL EFFECTS ON THE SLIT

Particles scattered on the edges of the slit could perturb the measurement of the distributions and lead to errors in the calculation of the emittance. The geometry of the slit and its material must be carefully selected in order to minimize this effect.

The effect of multiple scattering on the edges has been simulated for the four slit geometries shown in Fig. 4 and for different energies using the FLUKA Monte-Carlo code [2].

SYNCHROTRON RADIATION MONITOR FOR BUNCH-RESOLVED BEAM ENERGY MEASUREMENTS AT FLASH

A. Wilhelm and C. Gerth*

Deutsches Elektronen-Synchrotron DESY, D-22603 Hamburg, Germany

Abstract

A synchrotron radiation monitor based on a multi-anode photomultiplier tube (PMT) has been installed in the first magnetic bunch compressor chicane at the Free-electron LASer in Hamburg (FLASH). The synchrotron radiation emitted in the third dipole of the magnetic chicane is imaged by a telescope onto two anodes of the PMT. In this way the horizontal beam position of the electron bunches is recorded which corresponds to the beam energy as the beam position is governed by the beam energy in the dispersive section of the magnetic chicane. The fast PMT signals are digitized by analog-to-digital converters which enables bunch-resolved beam energy measurement within the trains of the up to 800 bunches generated by the super-conducting linear accelerator of FLASH. In this paper we describe the experimental setup of the synchrotron radiation monitor and present first commissioning results for various accelerator settings.

INTRODUCTION

Various diagnostic techniques based on the detection of synchrotron radiation (SR) have been utilised for decades for the characterisation of electron and proton beams in storage rings [1, 2]. In single-pass free-electron lasers (FEL), off-crest acceleration in combination with magnetic dipole chicanes is a common scheme for longitudinal bunch compression to produce ultra-short electron bunches with high peak currents. Due to the relatively large dispersion of these magnetic chicanes, the beam energy and energy spread can directly be deduced from a beam position measurement in the dispersive section of the magnetic chicane.

In the first bunch compressor (BC) at the Free-electron LASer in Hamburg (FLASH), a SR monitor based on photomultiplier tube (SR-PMT) has been added to an existing SR monitor based on an intensified CCD camera (SR-camera) [3]. The super-conducting linear accelerator of FLASH is capable of generating trains of up to 800 bunches with a spacing of 1 μ s at a repetition rate of 5 Hz. By adjusting the gate and delay of the SR-camera, the full x-y projection of a single bunch (or any number of subsequent bunches) out of a bunch train can be recorded. However, the readout of the CCD is too slow to resolve more than one electron bunch within a bunch train. In contrast, by recording the signals of the two adjacent anodes of the SR-PMT the centre-of-gravity beam position for all individual bunches can be measured.

* christopher.gerth@desy.de

SR MONITOR SETUP

A schematic overview of the SR monitor installed in the first BC at FLASH is presented in Fig. 1. The BC, which consists of 4 horizontally deflecting dipole magnets, is located downstream of a RF photo-cathode gun and a super-conducting 1.3 GHz accelerating module (ACC1) which accelerates the electrons to a beam energy of typically 130 MeV. The large horizontal aperture of the flat vacuum chamber (200 mm \times 8 mm cross section) allows one to operate the BC at bend angles in the range 15° - 21°. The critical wavelength of the emitted SR lies in the visible at around 400 nm for a bend angle of 18°.

An Ag-coated laser mirror (Linos, 20 mm \times 30 mm) deflects the SR emitted at the entrance of the third dipole downwards by 90° (not shown in Fig. 1) onto a beam splitter. The transmitted SR is imaged by a camera lens (Sigma, $f = 180$ mm) onto an intensified CCD camera (PCO, dicam pro). The part of the SR that is reflected by the beam splitter is deflected by another mirror by 90° and then imaged by a camera lens (Tamron, $f = 300$ mm) with a teleconverter (3x) onto two anodes of a multi-anode photomultiplier tube (PMT). The PMT of type Hamamatsu R5900U-00-M4 comprises four anodes each having a size of 8 x 8 mm². The PMT was operated at a voltage of 720 V for which a linear dependence between the output signal and the electron bunch charge, i.e. SR intensity, was measured. The fast current signal of the PMT has a pulse height of about 1 V (with 50 Ohm input impedance) and a width of 4 ns (FWHM). The signals are broadened to 20 ns (FWHM) by Gauss filters with a cut-off frequency of 15 MHz to eliminate high-frequency noise and reduce the effect of timing jitter (~ 1 ns) of the 14-bit analog-to-digital converters (ADC). The ADCs are synchronised to the bunch repetition rate of 1 MHz and can be read out by the machine control system. The normalized difference signal s of both ADC channels gives then the centre-of-gravity beam position $s = (I_1 - I_2)/(I_1 + I_2)$, where I_1 and I_2 are the signal intensities of both anodes measured with the ADCs. The whole SR monitor setup is mounted on a mover which can be moved horizontally to be able to adjust to the electron beam trajectory for different bend angles of the BC.

Energy Calibration

The horizontal beam size in the BC is governed by the beam energy spread as an energy deviation $\Delta E/E$ transforms into a horizontal displacement Δx by 1st-order transport theory via $\Delta x = R_{16} \cdot \Delta E/E$ due to the large horizontal dispersion of about $R_{16} \approx 300 - 400$ mm [4].

HIGH ENERGY EMITTANCE MEASUREMENT AT SPARC*

E. Chiadroni[†], D. Alesini, M. Bellaveglia, M. Castellano, L. Cultrera, G. Di Pirro, M. Ferrario, L. Ficcadenti, D. Filippetto, G. Gatti, E. Pace, C. Vaccarezza, C. Vicario, INFN/LNF, Frascati, Italy
 A. Cianchi, B. Marchetti, University of Rome Tor Vergata and INFN-Roma Tor Vergata, Rome, Italy
 A. Mostacci, University La Sapienza, Rome, Italy
 C. Ronsivalle, ENEA C.R. Frascati, Frascati, Italy

Abstract

The characterization of the transverse phase space of electron beams with high charge density and high energy is a fundamental requirement for particle accelerator facilities. The knowledge of characteristics of the accelerated electron beam is of great importance for the successful development of the SPARC FEL, a R&D photo-injector facility for the production of high brightness electron beams to drive SASE and SEED FEL experiments in the visible and UV wavelength. Here high energy emittance measurements are discussed.

INTRODUCTION

In order to achieve the SPARC [1] goals a precise characterization of the beam phase space at high energy is needed. In this paper we present the results for both transverse and longitudinal emittance measurements, together with the slice emittance analysis. In particular we discuss systematic effects observed in the transverse emittance measurement with the quadrupole scan technique using two quadrupoles arranged as a doublet.

Typical operation energy is around 140 MeV. For this stage of commissioning we have operated with a photo-cathode driven laser pulse with gaussian longitudinal profile (6-8 ps FWHM). The bunch charge was around 200 pC. The laser spot on the cathode was around 300 μm rms. Downstream from the last accelerating section several tools for a full characterization of the beam parameters are installed (Fig. 1).

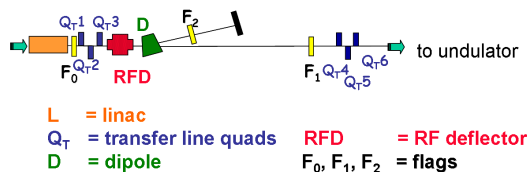


Figure 1: Layout of the high-energy experimental area.

TRANSVERSE EMITTANCE

The high energy transverse emittance measurement at SPARC is performed by means of a quadrupole scan [2]

downstream from the third accelerating section. The transverse beam size is measured on the flag F_1 for different current values of quadrupoles Q_{T1} , Q_{T2} , Q_{T3} (see Fig. 1); two quadrupoles have equal currents but opposite sign, and the third is used to control the beam spot shape. Quadrupoles are treated as thick lenses.

Typical Measurement

Usually, Q_{T1} and Q_{T3} are used with opposite polarity and Q_{T2} is set at zero current, in order to reduce the overlapping of quadrupole fields. The transverse emittance is then determined by evaluating the Twiss parameters, $\beta\varepsilon$, $\alpha\varepsilon$ and $\gamma\varepsilon$, from the χ^2 minimization. The measured beam sizes, compared to the ones retrieved from the fit, are plotted in Fig. 2 as function of the quadrupole current.

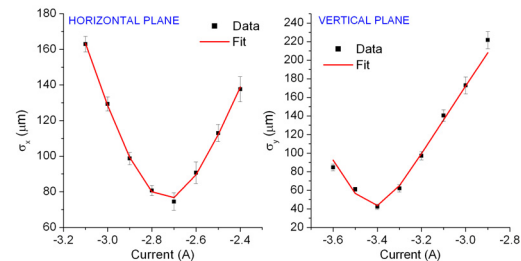


Figure 2: Comparison between the rms beam size measured at the flag F_1 (black squares) and the one retrieved from the χ^2 minimization (red curve) as function of the quadrupole current (125 pC, 140 MeV).

For a beam of 125 pC of charge and 140 MeV energy, the projected transverse emittance measured is $\varepsilon_{nx} = 1.52 \pm 0.05$ mm mrad and $\varepsilon_{ny} = 2.3 \pm 0.1$ mm mrad. The error on the emittance is estimated from the error propagation of the variance of the measurement error and accounts only for the statistical part. The high value of the projected emittance obtained with this charge is mainly due to inhomogeneities on the cathode surface.

Analysis of the Systematic Effects

The goodness of the least square fit on the experimental data is evaluated by backtracking the results in order to estimate the rms beam size on the flag F_0 at the end of the linac, where a comparison with a direct measurement can be performed.

* Work supported by MIUR Contract RBAP04XM5-001

[†] enrica.chiadroni@lnf.infn.it

SCREEN MONITOR DESIGN FOR THE SwissFEL

R. Ischebeck, B. Beutner, B. Steffen, V. Schlott, Paul Scherrer Institut, Villigen, Switzerland

Abstract

A screen monitor containing OTR foils and scintillator crystals has been designed to measure the transverse profile of electron bunches in the SwissFEL. In conjunction with quadrupole magnets in FODO cells and a transverse deflecting structure, the screen monitors will be used to measure transverse and longitudinal phase space projections of the electron pulses in the 250 MeV Injector. Tomographic methods will be used to reconstruct the phase space distributions.

INTRODUCTION

Paul Scherrer Institut is planning a free electron laser for X-Ray wavelengths, the SwissFEL [1]. The baseline design foresees to generate electron bunches with a charge between 10 and 200 pC and a normalized emittance below $0.4 \mu\text{m}$ in an RF photocathode gun. These bunches will be accelerated in a normal-conducting linear accelerator (linac) to a particle energy of up to 6 GeV and sent through one of two undulators with 15 and 40 mm period, respectively, where they radiate coherently at wavelengths between 0.1 and 7 nm. The repetition rate of this device will be 100 Hz initially, with an option to upgrade to 400 Hz. The baseline design foresees one electron bunch per RF pulse, but future extensions could allow for up to three electron bunches.

To test the feasibility of the concepts behind the generation of such high-brightness beams, their longitudinal compression and the preservation of the emittance, a 250 MeV Injector is currently being assembled. Commissioning will start early 2010, and by the end of the year PSI will submit a proposal to build the SwissFEL to the Swiss Government.

The 250 MeV Injector will have three diagnostic sections: one directly after the RF photocathode gun, at a particle energy of 7 MeV, one before and one after the bunch compressor, at an energy of 250 MeV (see Fig. 1 and Table 1). The repetition rate of this accelerator will be 10 Hz. Ideally, one would like to know the entire phase space distribution of the bunches, i.e. the phase space coordinates of each electron in the bunch. However, no method exists to measure the entire distribution directly. Instead, the distribution is projected onto sub-spaces such as the (x, y) plane which will be measured by screen monitors or the time axis which will be measured by coherent radiation and by electro-optical methods. Phase space transformations are applied to the electron beam prior to the measurements to infer the distributions in the other dimensions. If these transformations are linear, they can then be described by a matrix formalism. By scanning these transformations and measuring projections at each step, a Radon transform of the phase space distribution is acquired. Inverse Radon transformations are used to reconstruct the phase space. Maximum entropy methods [2] are particularly useful because there are often relatively few projections, which are furthermore not uniformly distributed.

SCREEN MONITORS

A total of 32 screen monitors will be built for the 250 MeV Injector. Besides measuring projected and slice emittance, they serve as prototypes for optical monitors of the SwissFEL. Screens convert the transverse electron distribution into visible light. At particle energies around 7 MeV in the gun region, scintillating crystals are used to image the beam. For higher energies, the scintillators will

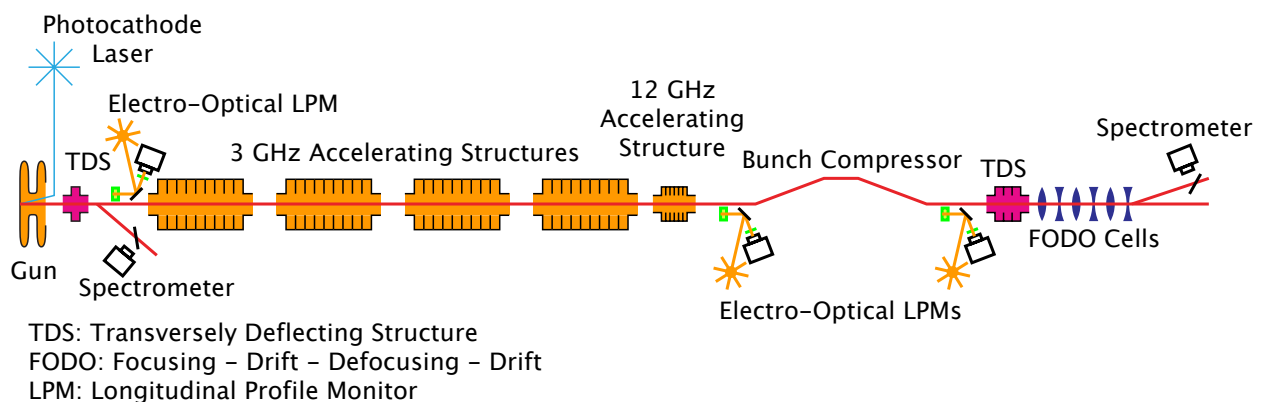


Figure 1: Schematic overview of the diagnostics for the 250 MeV Injector.

UNDULATOR RADIATION MEASUREMENTS AT LCLS USING K-EDGE X-RAY ABSORPTION TECHNIQUES*

A.S. Fisher[#], J. Frisch, R. Iverson, H. Loos and J. Welch
SLAC National Accelerator Laboratory, Menlo Park, CA, USA

Abstract

The sharp K -edge absorption energies in nickel and yttrium were exploited at LCLS to measure spectral features of spontaneous and FEL x-rays. By scanning the electron beam energy so that the first and third harmonic x-rays scanned across the nickel and yttrium K -edges, the resulting spectral features allowed the precise determination of the position of central ray and the resonant photon energy.

BACKGROUND

The LCLS is in the final stages of commissioning. We have been producing strong FEL x-ray beams with most of the complement of undulator segments installed, but the full suite of x-ray diagnostics has not yet been available. However, we are getting information about the x-ray beam properties from a temporary YAG crystal/camera combination and an insertable nickel foil. This timely information serves to confirm our expectations for the properties of the undulator radiation, provides initial photon-energy calibrations, and provides pointing data needed for precise undulator-strength comparisons to be made in coming weeks as the new x-ray diagnostics are commissioned.

THEORY AND METHOD

X-rays that have energy just sufficient to excite electrons bound in the K shell of an atom (the K -edge energy) are preferentially absorbed by the atom compared to x-rays whose energy is just below the K -edge. Figure 1 shows an example of the sharp change in transmission at the K -edge of yttrium in a YAG crystal. At the LCLS FEL facility we generate both FEL and spontaneous undulator x-rays whose energy depends on the electron beam energy. By changing the electron beam energy, the energy of the resulting x-rays can be made to sweep across the K -edge energy either of the yttrium component of a cerium doped YAG crystal, or of a nickel foil that can be inserted into the x-ray beam.

X-rays absorbed in the YAG crystal generate visible photons, detected by a camera. If the photons have energies just above the yttrium K -edge, they are preferentially absorbed in the YAG and therefore cause a brighter area. When the nickel foil is inserted in front of the YAG crystal, photons with energy above the nickel K -edge are preferentially absorbed by the nickel and leave a relatively dark area on the YAG. In either case, the K -edges provide precise x-ray energy discrimination.

Of the two sources of x-rays used, FEL radiation is much simpler in that it consists mainly of a narrow beam of x-rays, primarily at the first harmonic. The spontaneous undulator radiation is more complex: spatially broader and consisting of many comparably strong harmonics. The on-axis, fundamental photon energy is determined from the resonance equation:

$$\lambda = \frac{\lambda_u}{2\gamma^2} \left(1 + \frac{1}{2}K^2\right) \quad (1)$$

where λ is the x-ray wavelength, λ_u is the undulator period, γ is the electron energy in units of electron rest mass, and K is the undulator strength parameter (3.5, with some tunability, for LCLS). In the case of spontaneous undulator radiation, for angles small compared to K/γ , the spectrum contains many harmonics and is shifted by angle according to:

$$\lambda = \frac{\lambda_u}{2m\gamma^2} \left(1 + \frac{1}{2}K^2 + \gamma^2\theta^2\right) \quad (2)$$

Here θ is the angle from the central ray to the observation point and m is the harmonic number. From symmetry arguments, even harmonics must have no field on axis, while odd harmonics have a maximum on axis.

INSTRUMENTATION

The temporary diagnostic system shown in Fig. 2 is approximately 50 m downstream from the last undulator. This system contains, in order: a remotely controlled 1- μm -thick Be foil to block visible coherent light, a remotely controlled 10- μm Ni foil for K -edge measurements, and a fixed 100- μm -thick Ce-doped YAG crystal

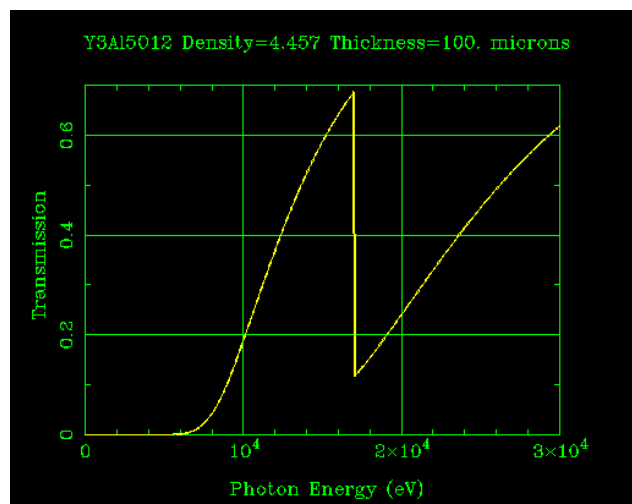


Figure 1: Transmission coefficient versus photon energy for YAG [2]. The yttrium K -edge occurs around 17 keV.

*Work supported in part by the DOE Contract DE-AC02-76SF00515, and performed in support of the LCLS project at SLAC.
[#]afisher@slac.stanford.edu

BEAM LOSS AND BEAM PROFILE MONITORING WITH OPTICAL FIBERS

F. Wulf, Helmholtz-Zentrum Berlin für Materialien und Energie, Germany

M. Körfer, DESY, Hamburg, Germany

Abstract

Beam losses and beam profiles at particle accelerators are determined by measuring the ionizing radiation outside the vacuum chamber. Four different radiation sensor systems using optical fiber will be presented. Two are based on the increase of radiation-induced attenuation of (Ge+P)-doped multimode graded index fibers, whereas the other two systems detect the Cerenkov light generated by relativistic electrons penetrating radiation hard fibers. The used fiber is an undoped multimode step-index fiber with 300 μm core diameter. Dosimetry at high dose levels uses the radiation induced Bragg wavelength shift of Fiber Bragg Gratings. The selection of a suitable fiber for the individual application is an important requirement and depends on the type, doping, used wavelength and annealing behavior. In addition, the dose range, dose rate and temperature must be considered. After an extensive selection procedure, two types of fibers for the particular application were chosen. One is used as a dosimetry sensor for the *slow* local and distributed beam loss position monitor (BLPM) and the other for *fast* beam loss monitor (BLM) as well as beam profile monitors (BPM). At six accelerators, all systems are used for in-situ particle loss control by measuring the ionization dose and/or Cerenkov light. These monitors provide a technique to improve the beam performance. This paper summarizes the basics of these measurement technologies and the experience at linear accelerators and at storage rings.

INTRODUCTION

Beam loss monitor systems (BLM systems) are an essential part of linear accelerators and storage rings. They allow the understanding of beam loss mechanisms during commissioning and operation and provide an option for an emergency shutdown. A proper understanding of beam loss events can improve machine performance, which consequently reduces also the radiation level for the used accelerator components. Well-known beam loss systems [1], like a) long and short ionization chamber, b) combination of scintillator and photomultiplier and c) PIN photo-diodes, d) scintillation counter, e) electron multipliers, f) cryogenic calorimeters have still some deficiency [2,3,4,5,6,7]. They do not cover the complete sections of the accelerator, particularly large undulator systems, and have an insufficient position and time resolution. It would be of great advantageous to monitor continuously on-line localized beam losses around the complete accelerator complex. Particular total dose measurements at the susceptible undulator magnets are desirable because they are made of radiation sensitive alloys. With in the framework of the TESLA/ILC (International Linear Collider) [8] and

FLASH (Free-Electron-Laser Hamburg) [9] design study. New concepts of BLM systems based on special types of optical fiber sensors were developed [10,11,12]. They have been tested during real operation at different accelerator facilities*.

OPTIMIZATION AND SELECTION OF OPTICAL FIBERS

Since 30 years it is well known that the radiation induced attenuation (RIA) of particular optical fibers [13,14,15,16,17,18,19] is a function of the total ionization dose (TID). This mechanism allows a reliable dose measurement up to a level of a few thousand Gray. For high dose applications the changes of the refractive index or Bragg wavelength shift (BWS) can be used. The radiation induced emission of Cerenkov light or luminescence mechanism are used for fast detection of radiation sources without calibration of TID. Fibers can also be made sensitive for thermal and fast neutrons [20,21,22]. The nonsatisfying applications in the past rely at most on insufficient knowledge and control of the producing process of the fibers. An individual characterization of each lot is therefore indispensable. This is a key function for further usage of fiber radiation sensors. The influence of core material, cladding thickness, drawing speed of the fiber and coating material of pure silica core step-index fibers have been investigated in detail [23].

CLASSIFICATION OF BEAM LOSS MONITOR SYSTEMS

As shown in Fig. 1 the BLM systems are distinguished in two categories. One system measure the TID generated by the beam losses as a function of RIA. With an optical power meter, the RIA is measured at local position along the beam line, especially at the undulator. The resolution of the absorbed dose of the so called *local sensor system* is about 60 mGy with an updating time - depending of the number of used sensors - in the range of ms [25]. The *distributed sensor system* makes use of Optical Time Domain Reflectometer (OTDR) measurements. As a result of the attenuation measurement, the position and TID along the beam line or undulators can be calculated. At FLASH, typical sensor length is less then 100 m. The update time is in the range of some seconds with a position resolution of about 1.5 m. The dose resolution for the presented measurement setup is about 3 Gy [25]. The system of the second category detects the generated Cerenkov light in the fiber over a length of about 40 m with a

* PITZ, MAX-LAB, BESSY II, DELTA, SLS

INTENSITY AND PROFILE MEASUREMENT FOR LOW INTENSITY ION BEAMS IN AN ELECTROSTATIC CRYOGENIC STORAGE RING

T. Sieber, K. Blaum, M. Grieser, F. Laux, M. Lange, D. Orlov, R. von Hahn, A. Wolf
MPI-K Heidelberg, Germany

Abstract

The cryogenic storage ring CSR is a 35 m circumference electrostatic ring, designed for molecular- and atomic physics experiments at MPI-K Heidelberg. It will operate at pressures down to 10^{-13} mbar and temperatures <10 K. The beam intensities will be in the range of 1 nA to 1 μ A, particle energies with between 20 - 300 keV.

An intensity measurement for coasting beams below 1 μ A requires magnetic field detection devices, which are much more sensitive than existing DC beam transformers. The highest sensitivity is currently achieved using DC SQUID based cryogenic current comparators (CCCs). At GSI, a prototype of such a CCC was successfully tested in the mid 90's, reaching a resolution of ~ 250 pA/Hz^{1/2}. Recently a resolution of 40 pA/Hz^{1/2} could be achieved under laboratory conditions at Jena University, however, the CCC sensitivity in an accelerator environment depends strongly on efficient shielding and mechanical decoupling.

We describe our work on adaptation and improvement of the CCC beam transformer for the CSR. Furthermore a concept for an ionisation profile monitor is discussed, which in addition to low beam intensities, has to cope with extremely low gas densities at 10^{-13} mbar.

INTRODUCTION

The CSR [1] combines a number of challenges for diagnostics development: Low currents, low ion energies, extremely low pressure, high bakeout temperatures and not least the cryogenic environment. To illustrate these boundary conditions, Table 1 shows the relevant parameters of the ring at one glance.

Table 1: Parameters of the CSR

Type	Electrostatic
Circumference	35.2 m
Corner deflectors	2x39°, 2x6°
Acceptance	100 mm mrad
Mass range	1 – 100 amu
Energy range (1 ⁺ ions)	20 – 300 keV
Intensity range	1 nA – 1 μ A
Revolution Frequency	5 - 220 kHz
Operation temperature	2 - 300 K
Bakeout temperature	$< 350^\circ\text{C}$
Vacuum pressure	1×10^{-13} mbar
Mat. cold chamber	316 L
Mat. isolation chamber	Al
Outer tank cross sect.	~ 1 m ²

The mass range of $A \leq 100$ in the table is at the moment considered a reasonable design value. Studies with much heavier molecules with $A \leq 2000$ (at much lower intensities than 1 nA) are foreseen in a later stage of CSR operation.

In the summer 2008 the setup of the CSR prototype ion trap (Cryogenic Trap for fast ions, CTF) was completed. Numerous vacuum tests have been performed with the prototype, demonstrating a pressure in the low 10^{-13} mbar range [2], which was determined by measuring the lifetimes of stored ion beams ($\tau_{\text{max}} = 320$ s for N₂⁺). The first molecular physics experiment campaign with the CTF has been successfully completed by the time of this report. For the CSR itself, the mechanical design work for the main components has been finished. The assembly of the first ring corner will start in the fall of 2009.

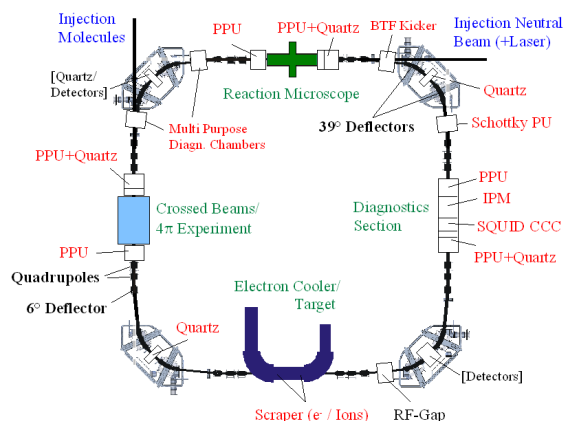


Figure 1: Layout of the CSR and diagnostics system.

The general concept for the beam diagnostics system of the CSR is shown in Figure 1. In contrast to existing or planned electrostatic rings, the CSR will have an extensive set of diagnostics devices, which is similar to the equipment of our Test Storage Ring (TSR). The four linear sections include two main experimental areas, an electron cooler/target and a section which is dedicated to beam diagnostics. Beam injection is foreseen in two corners of the ring (ions and neutral particles/laser).

For measurement of the beam intensity we have developed a mechanical and cryogenics design for a beam transformer, based on a Cryogenic Current Comparator (CCC) with a SQUID sensor, which will also be a prototype for the FAIR project at GSI.

To measure the beam profile in a non-interceptive way, we investigated the possibility of an ionisation profile monitor (IPM) at 10^{-13} mbar. At this residual gas pressure,

DATA ACQUISITION AND ERROR ANALYSIS FOR PEPPERPOT EMITTANCE MEASUREMENTS

S. Jolly, Imperial College, London, UK

J. Pozimski, STFC/RAL, Chilton, Didcot, Oxon, UK/Imperial College, London, UK

J. Pfister, IAP, Frankfurt am Main, Germany

O. Kester, NSCL, East Lansing, Michigan, USA

D. Faircloth, C. Gabor, A. Letchford, S. Lawrie, STFC/RAL, Chilton, Didcot, Oxon, UK

Abstract

The pepperpot provides a unique and fast method of measuring emittance, providing four dimensional correlated beam measurements for both transverse planes. In order to make such a correlated measurement, the pepperpot must sample the beam at specific intervals. Such discontinuous data, and the unique characteristics of the pepperpot assembly, requires special attention be paid to both the data acquisition and the error analysis techniques. A first-principles derivation of the error contribution to the rms emittance is presented, leading to a general formula for emittance error calculation. Two distinct pepperpot systems, currently in use at GSI in Germany and RAL in the UK, are described. The data acquisition process for each system is detailed, covering the reconstruction of the beam profile and the transverse emittances. Error analysis for both systems is presented, using a number of methods to estimate the emittance and associated errors.

INTRODUCTION

The use of pepperpots in measuring transverse emittance is widespread. The pepperpot is unique in providing an instantaneous measurement of the 4 dimensional emittance of a beam in a single shot. To do so the pepperpot sacrifices position resolution by measuring the beam only at discrete intervals through an intercepting screen. With suitably fast analysing software, this provides the opportunity of measuring and visualising the emittance of the beam in real time. The disadvantage of using a pepperpot is that they are highly destructive to the beam, primarily due to the intercepting screen, and the discontinuous nature of the position measurement that results from segmenting the beam.

To fully categorise emittance measurement error, a first principles analysis of the propagation of errors through the calculation of *rms* emittance has been carried out. This results in a general formula for the calculation of errors from any method of emittance measurement. This error analysis procedure is demonstrated for two contrasting pepperpot designs.

PEPPERPOT SYSTEMS

Error analysis has been carried out for two pepperpot systems: from the HITRAP project at GSI [1] and the Front End Test Stand (FETS) at RAL [2].

07 Hadron Accelerator Instrumentation

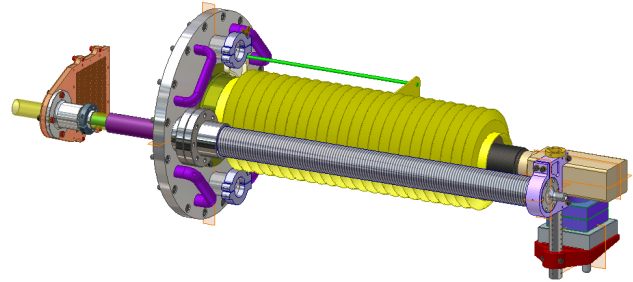


Figure 1: 3-D model of the FETS pepperpot assembly [3].

A CAD model of the FETS pepperpot assembly is shown in Fig. 1: full description of the FETS pepperpot device is given in [3]. The intercepting screen is a $100\ \mu\text{m}$ thick tungsten foil with a square array of 41×41 holes, each $50 \pm 5\ \mu\text{m}$ in diameter, on a $3 \pm 0.01\ \text{mm}$ pitch, giving a total imaging area of $120 \times 120\ \text{mm}^2$. The beam is imaged with a quartz scintillator, 10 mm from the tungsten screen, and a 2048×2048 pixel PCO 2000 high speed camera: the camera-to-screen distance of 1100 mm gives a resolution of $65\ \mu\text{m}$ per pixel and an angular resolution of 6.5 mrad. Data is recorded from the camera direct to a multi-image TIFF file and analysed with Matlab. Calibration is carried out using a series of calibration marks on the rear copper plate facing the camera: 4 lines, forming a $125\ \text{mm} \times 125\ \text{mm}$ square around the intercepting screen, provide the necessary calibration information on the size, location and rotation of the pepperpot holes.

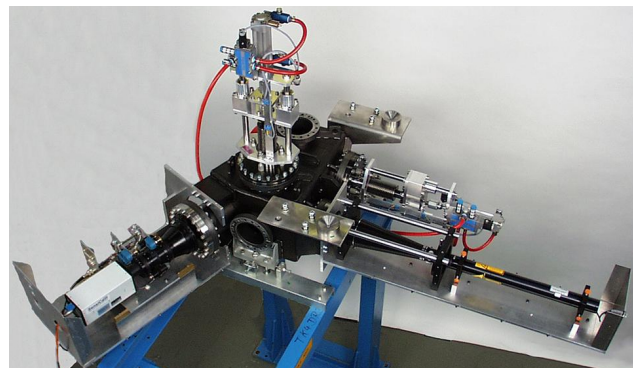


Figure 2: The HITRAP pepperpot setup (*cf.* [5]).

The setup of the GSI pepperpot system for the HITRAP

BEAM DIAGNOSTIC DEVELOPMENTS FOR FAIR*

M. Schwickert, P. Forck, P. Kowina, T. Giacomini, H. Reeg, A. Schlörit,
GSI Helmholtzzentrum für Schwerionenforschung GmbH, Darmstadt, Germany

Abstract

The FAIR (Facility for Antiproton and Ion Research) accelerator complex is currently designed and projected at GSI. The unique features of the main machine SIS100, like e.g. the acceleration of high intensity beams of 2.5×10^{13} protons and 5×10^{11} Uranium ions, the operation close to the space charge limit leading to a large tune spread and the extreme UHV conditions of the cryogenic system for fast ramped superconducting magnets, impose challenging demands on the beam diagnostic components. This contribution describes the general concept of beam diagnostics for FAIR and reports on the present status of prototype studies. Exemplarily the achievements for a novel type of dc transformer, beam position monitors and the ionization profile monitor are discussed and first measurements with prototype setups are presented.

FAIR ACCELERATOR COMPLEX

Presently GSI entered the final planning phase for the international FAIR project [1]. The existing GSI accelerators, UNILAC and SIS18, together with a new high-current proton LINAC will act as injectors. In its final stage FAIR will consist of two heavy ion synchrotrons (SIS100, SIS300) and four storage rings (CR, RESR, NESR, HESR). The main features of FAIR are: acceleration of all ion species from protons to Uranium, high currents of primary beams, generation of radioactive beams for fixed target experiments or injection in storage rings, as well as antiproton production, accumulation and storage ring experiments. For the planned large variety of physical experiments the multiplexed operation of the whole facility with different settings for ion species, energy etc. on a pulse-to-pulse basis, has been an important design criterion. In this contribution we focus on diagnostics for the fast ramped superconducting synchrotron SIS100 and the high energy beam transport section of FAIR.

REQUIREMENTS FOR DIAGNOSTICS

A set of general strategies has been considered in order to facilitate the construction of the facility with world-unique complexity. A main paradigm is the facility-wide standardization of diagnostic devices. Even though the requirements of the synchrotrons and storage rings differ, it is planned to use identical diagnostic installations wherever applicable. Standardization also covers the front-end software FESA [2] as an integrative platform for all diagnostic devices at FAIR. Concerning the hardware it is planned to use commercially available components to a maximum extent, in order to reduce manpower and spares inventory.

FAIR beam parameters impose strict requirements for all diagnostic devices. A strong constraint with regard to mechanics is the extreme UHV condition down to 5×10^{-12} mbar in SIS100. In this main synchrotron, high currents (up to the space charge limit) of primary beams in low charge states will be stored and accelerated with a large incoherent tune spread of up to $\Delta Q \approx 0.5$. An important prerequisite is the precise beam alignment since in certain locations the synchrotron acceptance is limited to 6 times the rms beam width. For the High Energy Beam Transport section of FAIR the acceptance is even lower, four times the rms beam width. The goal for diagnostics in transport lines and storage rings is to achieve a high resolution and low detection limit. Additionally, the HEBT diagnostic devices have to deal with slow and fast extracted beams, respectively. Due to the requirement for online measurements and in order to prevent device destruction at high beam intensities, non-intercepting diagnostics is preferred and focused on in this contribution.

BEAM CURRENT MEASUREMENT

Novel DC Current Transformer (NDCCT)

For the GSI-built synchrotron DCCT, it was found that at high beam currents (>70 mA) and bunch frequencies around 1.2 MHz the feedback loop of the DCCT loses control and the setting of the correct working point becomes unreliable. Therefore an alternative device based on state-of-the-art sensor technology is presently under development at GSI [3]. The NDCCT makes use of integrated GMR sensors (giant magneto-resistance) inside the gap of a split flux concentrator (amorphous alloy or ferrite toroid). The GMR signals are corrected and amplified by a differential pre-amplifier. Additionally, an AC transformer path is implemented by a secondary winding. Special requirements for the NDCCT are: low noise characteristic, high resolution (~ 100 μ A), capability to measure beam currents from 100 μ A to 150 A (2 A DC), bunch frequency up to 5 MHz, long-term zero-point stability and high absolute accuracy.

The utilized GMR sensor (AA-0002, Nonvolatile Electronics Co.) consists of 4 meandered resistors and 2 flux concentrators, building up a Wheatstone bridge. Studies on the frequency response revealed that the sensor circuitry spans inductive loops and, above a certain threshold frequency, the frequency response of the GMR sensor becomes disturbed. The upper frequency threshold was found to be a result of macroscopic effects like unwanted induced voltages in the sensor, eddy currents and skin effects in the GMR's NiFe-layer, leading to a reduced bridge voltage above the cut-off frequency of 1 MHz, as depicted in Fig. 1. The GMR frequency response is shown for different core materials (CMD5005,

*Work partly supported by EU-FP6 DIRAC-phase1, -secondary-Beams

BEAM DIAGNOSTICS AND RF SYSTEMS REQUIREMENTS FOR THE SwissFEL FACILITY

Y. Kim*, B. Beutner, H. Braun, A. Citterio, M. Dehler, A. Falone, R. Ganter, T. Garvey,
S. Hunziker, R. Ischebeck, B. Keil, M. Pedrozzi, S. Reiche, T. Schilcher, V. Schlott, B. Steffen
Paul Scherrer Institut, CH-5232 Villigen PSI, Switzerland

Abstract

In this paper, we describe four very different operating modes of the SwissFEL facility, the requirements of the challenging beam diagnostics and ultra-stable RF systems needed for two special operating modes with 10 pC, and current developments of beam diagnostics and RF systems for the PSI 250 MeV injector test facility.

INTRODUCTION

SwissFEL will supply coherent, ultra-bright, and ultra-fast XFEL photon beams covering the wavelength range from 0.1 nm to 7 nm. To build the whole facility within about 800 m, PSI will use a 2.5 cell S-band RF gun, a 530 m long normal conducting RF linac, and a 70 m long in-vacuum undulator using the NdFeB with diffused Dy for the hard X-ray beamline and a 70 m long Apple-II type undulator for the polarization controllable soft X-ray beamline [1–3]. SwissFEL will be operated with four very different operating modes according to the overall electron bunch length compression factor, which determines RF jitter tolerances. To begin with, SwissFEL will be operated with a compression factor of 75. After improving the RF systems and beam diagnostics step by step, the facility could be operated with a compression factor of about 2400 to supply a fully coherent single spike XFEL photon pulse. In this paper, we review the requirements of the beam diagnostics and RF systems for two highly challenging operating modes with 10 pC, which have compression factors of 240 and 2400, respectively.

MODES & REQUIREMENTS

To begin with, SwissFEL will be operated with three nominal modes with 10 pC and 200 pC, which have compression factors of 75, 125, and 240 [1]. In the nominal operating modes, a higher single bunch charge of 200 pC will be used to supply more photons per pulse, and a lower single bunch charge of 10 pC will be used to supply shorter photon pulses [1, 3]. For one upgraded mode with 10 pC, RF systems and beam diagnostics will be greatly improved, and attosecond XFEL photon pulses can be generated by increasing the compression factor up to about 2400. For the upgraded operating mode with 10 pC, the soft X-ray beamline will supply transversely as well as longitudinally coherent 250 as (rms) long single spike photon pulses in a

Table 1: Parameters of the SwissFEL Project.

Operating Mode Parameters	unit	Nominal		Upgraded
		long pulse	short pulse	atto pulse
beam energy E	GeV	5.8	5.8	5.8 / 3.4
single bunch charge	pC	200	10	10
core-slice emittance	μm	0.43 / 0.38	0.18	0.25
slice rms E -spread	MeV	0.35 / 0.25	0.25	1.00
peak current	kA	2.7 / 1.6	0.7	7
projected emittance	μm	0.65	0.25	0.45
rms bunch length	fs	31 / 47	6.2	2.4
compression factor	.	125 / 75	240	2400
undulator period	mm	15	15	15 / 40
undulator parameter	.	1.2	1.2	1.2 / 1.05
saturation length	m	48 / 55	50	30 / 25
shortest wavelength	nm	0.1	0.1	0.1 / 0.7
rms photon length	fs	12 / 19	2.3	0.25
number of photon	10^9	31 / 32	1.7	3.2 / 31
rms bandwidth	%	0.03 / 0.03	0.035	0.05 / 0.35
single spike pulse	.	no / no	no / no	no / yes
longitudinal coherence	.	no / no	no / no	no / yes
transverse coherence	.	yes / yes	yes / yes	yes / yes

range of wavelengths from 0.7 nm to 7 nm, while the hard X-ray beamline will supply transversely coherent 250 as (rms) long multiple spike photon pulses in a range of wavelengths from 0.1 nm to 0.7 nm. Detailed information on the four different operating modes and minimum required and expected beam parameters are summarized in Table 1 [1,3].

To check the beam quality at the entrance of the undulator for two highly challenging operating modes with 10 pC, we have optimized linac layouts for SwissFEL with the ASTRA and ELEGANT codes, and performed start-to-end (S2E) simulations as summarized in Fig. 1. Here, all key beam dilution effects such as space charge effects up to 150 MeV, short-range transverse and longitudinal wakefields in all linac structures, incoherent synchrotron radiation (ISR) and coherent synchrotron radiation (CSR) in the BC dipoles, and fringe-field and chromatic effects in all magnets are considered. From those S2E simulations, we realized that the lower charge operating modes with 10 pC can supply much better beam quality than the minimum required beam qualities, which are summarized in Table 1.

As shown in Fig. 1(top), in the case of the nominal mode with 10 pC, the rms transverse beam size, the normalized rms projected emittance, and the normalized core-slice emittance at the entrance of an undulator are about 8.5 μm ,

* Mail : Yujong.Kim@PSI.ch

RECENT RESULTS FROM THE OPTICAL REPLICA SYNTHESIZER EXPERIMENT IN FLASH

G. Angelova-Hamberg, V. Ziemann, Uppsala University, Sweden

P. van der Meulen, P. Salén, M. Larsson, Stockholm University, Sweden

H. Schlarb, J. Bödewadt, A. Winter, F. Lühl, E. Saldin, E. Schneidmiller, M. Yurkov, DESY, Germany

S. Khan, DELTA, TU Dortmund, Germany

A. Meseck, Helmholtzzentrum Berlin, Germany

Abstract

We present very promising recent results from the optical replica synthesizer experiment in FLASH where we manipulate ultrashort electron bunches in FLASH with a laser in order to stimulate them to emit a coherent light pulse from which the temporal structure of the electron bunches can be obtained using laser diagnostic (FROG) methods.

INTRODUCTION

Monitoring and tuning the bunch properties are essential for the reliable operation of linac-based SASE free-electron lasers such as FLASH [1], XFEL [2], or LCLS [3]. This need has triggered the development of new diagnostic methods based on a transversely deflecting cavity [4] or electro-optical sampling [5]. The optical replica synthesizer (ORS), a complementary scheme that was introduced in Ref. [6], is similar to an optical klystron FEL seeded by an infrared laser as is shown in Fig. 1. In the modulator the interaction of the laser with the transversely oscillating electrons causes an energy modulation. A dispersive section turns this energy modulation into a density modulation at the wavelength of the light. In a following radiator undulator the micro-bunched beam radiates coherently and the emitted light pulse allows to deduce the longitudinal profile of the electron beam. Hence the name optical replica synthesizer.

The optical replica pulse is analyzed in a FROG (frequency resolved optical gating) device [7], which is based on recording the spectrally resolved auto-correlation. Subsequent application of a pulse retrieval algorithm reveals both amplitude and phase of the incident electric field and thus of the longitudinal profile of the electron bunch. A very compact second harmonic FROG device called Grenouille [8] is available commercially and the traces are analyzed with the VideoFROG [9] software.

The complete system of seed laser, laser transport line, two undulators, the chicane and two optical stations for timing and FROG analysis was installed in FLASH during a shutdown period in spring 2007. In the remainder of this report we briefly describe the hardware components and the commissioning progress that culminated in the recent observation of FROG traces.

03 Time Resolved Diagnostics and Synchronization

HARDWARE

The laser system is located in a newly erected building next to the FLASH tunnel and connected to the accelerator tunnel by a pipe through which the laser beam is transported. The laser itself is based on a Erbium-doped fiber oscillator [10] operating at 1550 nm that is phase-locked to the radio-frequency (RF) system of the accelerator. The phase-lock is accomplished by comparing the phase of the 24th harmonic of the laser oscillator round-trip frequency at 1.3 GHz with the RF signal and adjusting the length of the optical fiber that is wound on a piezo-crystal by applying a voltage to the crystal. The timing is thus stabilized to about 50 fs. The relative timing of laser and RF can be adjusted by changing the phase of the RF signal with a vector-modulator. The stabilized pulses are amplified and frequency-doubled in a 1 mm PPLN crystal and subsequently passed to a Clark-MXR CPA-2001 regenerative Titanium-Sapphire amplifier that is based on chirped-pulse amplification and pumped by a Nd:YAG laser. This system delivers pulses with a center wavelength of 772 nm, up to 1 mJ energy per pulse and a full-width at half-maximum (FWHM) pulse length down to 150 fs.

To reach the accelerator, the laser pulse travels through a 12 m long laser transport system with remotely controlled motorized mirrors and a two-lens telescope that provides a narrow laser waist in the laser-electron interaction zone inside the modulator. For diagnostic purposes the laser beam can be reflected back to the laser building with a mirror where the position and size of the laser waist can be measured. With the mirror retracted the laser pulse is injected into the accelerator beam pipe through a back-tangent window located near the second dipole of a dog-leg chicane.

Inside the accelerator beam pipe the laser pulse co-propagates with the electron beam, passes the modulator undulator and is extracted by a silver-coated silicon OTR screen installed in the middle of the four-magnet chicane on the first optical station OS1. The optical station accommodates a camera, photo diodes with 1.5 GHz bandwidth, and a power meter in order to analyze the laser pulse and to determine the relative timing of the laser pulse and the electron beam by observing the laser pulse and the synchrotron radiation pulse from the electron beam generated in the modulator on a photo diode. The electron beam continues to propagate through the radiator undulator and pass a second optical station (OS2) where the light created at or re-

PHYSICS REQUIREMENTS FOR LINAC STABILIZATION AND TECHNICAL SOLUTIONS

J. Carwardine, Argonne National Laboratory, Argonne, IL 60439, U.S.A.

Abstract

This paper gives a general overview of active and passive stabilization systems, which are mainly required for future X-FEL and high-energy linear colliders. Key physics criteria for beam stability for X-FELs and linear colliders will be introduced and resulting technical implications discussed. New and innovative approaches to the design and development of state-of-the-art linear accelerator components and stabilization systems will be reviewed, and recent results shown from selected prototypes and new machine installations.

INTRODUCTION

Achieving performance specifications of modern accelerators places narrow tolerances on a wide range of technical parameters. The location of magnetic optics elements in space, their field strengths, and particle energy all must remain within tight bounds.

Within the context of stabilizing beams with dimensions measured in microns, there are many potential sources of drift and jitter that must be taken into account.

Sources of drift and slow changes include air and cooling water temperatures, ground motion due to settlement and lunar cycles. Medium timescale disturbances include girder vibration excited by ground motion, cooling pipes, or mechanical pumps. Faster disturbances include power supply ripple, rf jitter, switching magnet jitter, etc.

In our discussion of linac beam stabilization, we will focus on four large-scale pulsed electron linacs: LCLS and the European XFEL (both x-ray photon sources); and ILC and CLIC (both linear colliders). Table 1 lists some of their main parameters [1-4].

Table 1: Main Linac Parameters

	ILC	CLIC	EU-XFEL	LCLS	
Max. Energy	2x 250	2x 1500	20	13	GeV
ML Length	2x 12	2x 21	1.6	1	km
Cavity type	S/C	N/C	S/C	N/C	
RF Freq	1.3	12	1.3	12 + 2.8	GHz
RF source	Klystron	Drive beam	Klystron	Klystron	
Pulse rate	5	50	10	120	Hz
Pulse length	970	0.15	650	--	μs
Bunches / Pulse	2670	312	3250	1	
Bunch length	300	44	25	20	μm
Bunch size	640 nm x 5.7 nm	45 nm x 0.9 nm	20-30 μm	37 μm	

S/C: Superconducting

N/C: normal conducting

These represent the most recent generation of linacs: LCLS is in commissioning and XFEL is under construction; while ILC and CLIC remain in development and proof-of-principle stages respectively.

All four machines present significant technical challenges, in part due to their large scale and complexity. From a beam stabilization perspective, these include distribution of precision rf phase references to many locations over distances of kilometers to tens of kilometers and stabilizing beams with dimensions of nanometers.

This next section gives a brief overview of the four machines and discusses their performance and stabilization criteria. Some examples of technical solutions will also be discussed.

PHOTON SOURCES: LCLS AND EU-XFEL

For certain classes of photon user experiments, FEL-based sources such as LCLS and XFEL dramatically exceed the capabilities of storage ring light sources by:

- Peak brightness is many orders of magnitude higher than the present storage ring photon sources
- Sub-picosecond photon pulse lengths compared with 10's to 100's ps from storage rings
- Photon beams are transversally fully coherent

The ultra-short pulse lengths will make it possible to study the time evolution of chemical processes that occur in timeframes of 100's femtoseconds to picoseconds, while the high coherence will open up new classes of imaging experiments.

A comparison of peak and average brightness with other light sources is shown in Fig. 1.

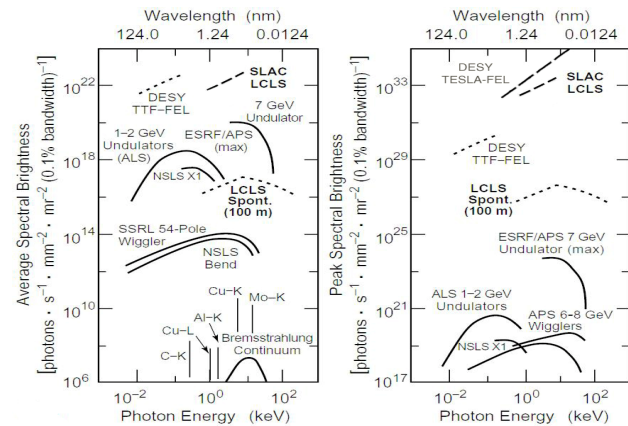


Figure 1: Average and peak brightness calculated for photon sources that are operating or under construction.